

Distribution Agreement

In presenting this thesis or dissertation as a partial fulfillment of the requirements for an advanced degree from Emory University, I hereby grant to Emory University and its agents the non-exclusive license to archive, make accessible, and display my thesis or dissertation in whole or in part in all forms of media, now or hereafter known, including display on the world wide web. I understand that I may select some access restrictions as part of the online submission of this thesis or dissertation. I retain all ownership rights to the copyright of the thesis or dissertation. I also retain the right to use in future works (such as articles or books) all or part of this thesis or dissertation.

Signature:

Jessica N. McCaffery

Date

Development of novel immunogens for malaria vaccines and serosurveillance

By

Jessica N. McCaffery
Doctor of Philosophy

Graduate Division of Biological and Biomedical Science
Immunology and Molecular Pathogenesis

Alberto Moreno, M.D.
Advisor

Rama Rao Amara, Ph.D.
Committee Member

Joshy Jacob, Ph.D.
Committee Member

Tracey J. Lamb, Ph.D.
Committee Member

Rabin Tirouvanziam, Ph.D.
Committee Member

Accepted:

Lisa A. Tedesco, Ph.D.
Dean of the James T. Laney School of Graduate Studies

Date

Development of Novel immunogens for Malaria Vaccines and Serosurveillance

By

Jessica N. McCaffery

B.S. Biochemistry, Hartwick College, 2013

Advisor: Alberto Moreno, M.D.

An abstract of

A dissertation submitted to the Faculty of the
James T. Laney School of Graduate Studies of Emory University
in partial fulfillment of the requirements for the degree of
Doctor of Philosophy

Graduate Division of Biological and Biomedical Sciences
Immunology and Molecular Pathogenesis
2019

Abstract

Development of Novel Immunogens for Malaria Vaccines and Serosurveillance

By Jessica N. McCaffery

Malaria is responsible for over 200 million cases and nearly half a million deaths annually. The successful implementation of control measures resulted in a significant reduction in transmission in the past few years. However, these epidemiological changes created a challenge for future elimination efforts because identifying areas of active transmission is more difficult due to an increase in the prevalence of asymptomatic infections and lack of treatment-seeking behavior. The increase in resistance of parasites to anti-malarial drugs and mosquitoes to insecticides have further complicated control efforts. While one malaria vaccine, RTS,S/AS01 (Mosquirix) has been approved for use in Europe, efficacy remains low at ~30%, and protection wanes rapidly. Therefore, there is a need for new vaccines and tools for determining areas of active transmission.

The failure of RTS,S to induce long-lived efficacy has been attributed to a lack of CD8⁺ T cell responses which are required for parasite clearance during the pre-erythrocytic stage. Based on the evidence that viral vectors are efficient platforms for the induction of CD8⁺ T cell-mediated immunity, we assessed the immunogenicity of a novel simian adenoviral vector (SAd36) encoding a chimeric multi-stage *Plasmodium yoelii* vaccine candidate. We demonstrate that the SAd36 vector can replace the human Ad5 vector, to which there are high levels of pre-existing immunity in adults, without compromising CD8⁺ T cell immunogenicity. The robust CD8⁺ T cell responses induced by recombinant SAd36 translated into a lower parasite load in mice following infectious challenge. Additionally, the T cell immunogenicity of the SAd36 vector can be enhanced further through the addition of a signal peptide derived from the murine IgGκ light chain in the adenoviral transgene.

Transmission-blocking vaccines (TBVs) offer an alternative strategy to achieve malaria control by eliciting antibodies that interrupt transmission in the mosquito. The post-fertilization antigen P25 is an attractive TBV target as it mediates several functions essential to parasite survival, but P25 is poorly immunogenic in humans. Here we report that a chimeric *P. vivax* Merozoite Surface Protein 1 (cPvMSP1) reported by our group is able to function as a carrier protein for *P. vivax* P25, inducing long-lived plasma cells and improving the durability and magnitude of antibody responses capable of blocking the transmission of *P. vivax* field isolates in direct membrane-feeding assays.

Serological assays can provide population-level infection history to inform elimination campaigns. Here we use multiplex antigen detection assays to evaluate cPvMSP1 for its ability to capture IgG from naturally exposed US travelers with known infection status from all four human *Plasmodium* species. We observed increased assay signals for the cPvMSP1 compared to the native recombinant PvMSP1, suggesting increased sensitivity. Regardless of infecting species, a majority of sera from malaria patients exhibited high assay signals to cPvMSP1. Therefore, a serological assay based on cPvMSP1 has a great potential for the development of sensitive surveys that may support malaria elimination efforts.

Development of Novel Immunogens for Malaria Vaccines and Serosurveillance

By

Jessica N. McCaffery

B.S. Biochemistry, Hartwick College, 2013

Advisor: Alberto Moreno, M.D.

A dissertation submitted to the Faculty of the
James T. Laney School of Graduate Studies of Emory University
in partial fulfillment of the requirements for the degree of
Doctor of Philosophy

Graduate Division of Biological and Biomedical Sciences
Immunology and Molecular Pathogenesis
2019

Acknowledgements

I first want to thank my mentor, Alberto, for guiding me to where I am today. You offered the perfect combination of support, criticism, and independence for me to find my own way. Our mutual successes and failures over the past years have helped me to improve as a scientist, a writer, and a person. Your relentless passion for malaria research continue to inspire me to be dedicated to my own research. Thank you for also going beyond your duties as a mentor by making me feel like part of your family.

I also want to thank Jairo, our former postdoc, my main co-author, and now my husband. You not only trained me in how to run the experiments I needed for our initial projects together, but you taught me the importance of good communication. I came into the lab not knowing how to handle criticism of my work; you helped me turn criticism into better protocols and into stronger and more well-thought out papers. Along with teaching me the fundamentals of scientific writing, you also provided me with support during my most difficult times. When the lab had funding issues and you had to leave to pursue your residency, you taught me how to stay focused and keep fighting. I'm happy to have had the opportunity to work with you and to celebrate our successes together. I hope we can continue to publish together for as long as we are both in research.

I also have to thank all of our amazing collaborators at the Malaria Branch of the CDC, including Eric, Doug, Kumar, and our former postdoc Balwan, for all your help in support with the serology projects. Thank you, Eric and Kumar, for giving me an opportunity to step outside my comfort zone in malaria vaccinology to work on a more epidemiological project. Thank you to Balwan for years of amazing work producing proteins for our lab and keeping me on task.

I also want to thank my committee members. Thank you to Rabin and Tracey for being tough on me in the first few years to encourage me to improve. Thank you to Rama and Rabin for allowing me to rotate in your labs and learn from your work and lab members. Thank you to Joshy for your excellent advice and conversations, as well as a paper together.

Thank you to all of my wonderful co-workers here at Yerkes. Without your support, whether it be technical or emotional, I wouldn't have been able to achieve what I have. Thanks especially to:

- Dario and Daniela for being great friends and proof-readers.
- Administrators Pearl, Maureen, Amy, Linda, and Molly.
- Ina, Mike, Gaby, Dave, Tom, and Cheryl at the café for keeping me sane, fed, and heavily caffeinated over the years.
- Paul, Anthony, Stan, Bernard, André and Brandy for making Yerkes a great place to work.
- Rachelle, Denyse, Denise, Yonas, Christie, and so many other members of the Yerkes Vet team for keeping my mice healthy during my experiments.
- Yerkes lab managers Stacey, Paul, and Hui-Mien for technical support over the years.
- Evan and Deepa for histological support.
- Lark for keeping our N₂ tank cold and chatting about our hobbies.
- Carlos for help with IT issues, particularly microscope computer troubles.

To my father, Bill, thank you for sharing your work ethic with me by teaching me what hard work really looks like. To my sister, Sarah, thank you for reminding me to hustle and never be complacent.

Thanks to my pet mice, who died of old age, for teaching me to never take any sample for granted, whether it be from a patient or a mouse.

To my cats, Earl Grey and Picasso, thanks for cheering me up when I was down and for being little alarm clocks, whether I needed it or not.

Table of Contents

Chapter 1	Introduction.....	12
Chapter 2	A prime-boost immunization regimen based on a simian adenovirus 36 vectored multi-stage malaria vaccine induces protective immunity in mice.....	61
Chapter 3	Inclusion of the murine IgG κ signal peptide increases the cellular immunogenicity of a simian adenoviral vectored <i>Plasmodium vivax</i> multistage vaccine.....	90
Chapter 4	A Multi-Stage <i>Plasmodium vivax</i> Malaria Vaccine Candidate Able to Induce Long-Lived Antibody Responses Against Blood Stage Parasites and Robust Transmission-Blocking Activity.....	124
Chapter 5	Capture of IgG Antibodies Induced during Natural Infections with Human Malaras to a Chimeric <i>Plasmodium vivax</i> Antigen.....	164
Chapter 6	Discussion and Future Directions.....	187
Chapter 7	References.....	207

Figure Index

Chapter 2

Figure 1	SAd36PyCMP elicits comparable antibody responses compared to Ad5PyCMP.....	78
Figure 2	Induction of PyCMP Antigen-Specific T cells by SAd36PyCMP and Ad5PyCMP Immunization.....	80
Figure 3	Cytokine production by CD8+ and CD4+ T cells stimulated ex vivo with the PyCMP protein.....	81
Figure 4	Cytokine production following ex vivo stimulation with PyCMP peptide pools.....	83
Figure 5	SAd36-PyCMP Protective Efficacy.....	84
Table 1	Immunization Groups.....	85
Supplementary Figure 1	Gating strategy for the definition of antigen-specific CD4 ⁺ T cells.....	86
Supplementary Figure 2	Gating Strategy for Analysis of Cytokine Production.....	87
Supplementary Figure 3	Characterization of the Infective Capacity of Ad5 and SAd36 vectors...	88

Chapter 3

Figure 1	Signal Peptide Simian Adenovirus 36 schematic and protein expression.....	107
Figure 2	Antibody response to cPvCSP and cPvMSP1 proteins.....	109

Figure 3	Immunofluorescence assays of <i>P. vivax</i> sporozoites and blood-stage schizonts.....	110
Figure 4	Cytokine-secreting T cells after <i>ex vivo</i> stimulation with cPvCSP peptide pools.....	111
Figure 5	Cytokine-secreting T cells after <i>ex vivo</i> stimulation with cPvMSP1 peptide pools.....	112
Figure 6	Frequency and total number of germinal center B cells in the draining lymph nodes nine days post priming.....	113
Supplementary Figure 1	Sample Gating Strategy.....	114
Supplementary Figure 2	Cytokine-secreting T cells after <i>ex vivo</i> stimulation with cPvCSP peptide pools.....	116
Supplementary Figure 3	Cytokine-secreting T cells after <i>ex vivo</i> stimulation with cPvMSP1 peptide pools.....	117
Supplementary Figure 4	Secretion of multiple cytokines by T cells in response to <i>ex vivo</i> stimulation with cPvCSP peptide pools.....	118
Supplementary Figure 5	Secretion of multiple cytokines by T cells in response to <i>ex vivo</i> stimulation with cPvMSP1 peptide pools.....	120
Supplementary Figure 6	Sample Gating Strategy for Germinal Center B cells.....	122
Table 1	Immunization Regimens.....	123

Chapter 4

Figure 1	cPvMSP1-Pvs25 protein structure, sequence, and characterization.....	151
Figure 2	Antibody responses to the chimeric PvMSP1-Pvs25 protein.....	153
Figure 3	Antibody responses to cPvMSP1 and Pvs25.....	154
Figure 4	Immunofluorescence assays of ookinetes and schizonts.....	155
Figure 5	IgG-producing long-lived plasma cells.....	157
Figure 6	IFN- γ production by CD4 ⁺ and CD8 ⁺ T cells following stimulation with Pvs25 and cPvMSP1 peptide pools.....	158
Table 1	Chimeric PvMSP1 and Pvs25 peptide pools.....	159
Table 2	Immunization Regimens.....	160
Table 3	Transmission Blocking Activity.....	161
Supplementary Figure 1	A full scan of the entire original Western blot.....	162
Supplementary Figure 2	Gating strategy for CD4 ⁺ and CD8 ⁺ IFN- γ -producing murine T cells.....	163

Chapter 5

Figure 1	Schematic and alignment of the PvRMC-MSP1 chimeric protein.....	180
Figure 2	Capture of rodent derived anti-PvRMC-MSP1 IgG with MSP1 antigens from all four human malarias.....	182
Figure 3	Comparison of MFI-bg assay signal for PvRMC-MSP1 and MSP1s from the four human malarias for persons with active malaria infection.....	183

Figure 4	Range of MFI-bg assay signal for PvRMC-MSP1, or the MSP1 19kD malaria antigens when grouped by active infection.....	184
Figure 5	Cross-binding of anti-PfCSP IgG with PvRMC-MSP1.....	185
Supplementary Figure 1	Recognition of recombinant PvMSP1 and PvRMC-MSP1 by individual <i>P. vivax</i> patients.....	186

Chapter 1

Introduction

Immune Responses to *Plasmodium* Infection

Jessica N. McCaffery^a, Jairo A. Fonseca^{a,b}, Alberto Moreno^{a,b}

- a. Emory Vaccine Center, Yerkes National Primate Research Center, Emory University, 954 Gatewood Road, Atlanta, GA 30329.
- b. Division of Infectious Diseases, Department of Medicine, Emory University School of Medicine, Atlanta, GA 30307.

Table of Contents - Chapter 1:

Introduction

Main Body

1. Initiation of infection of the vertebrate host and immune responses to *Plasmodium* in the dermis
 - 1.1 The infectious bite and start of migration
 - 1.2 The skin, the first line of defense
 - 1.3 Immune responses to mosquito saliva
 - 1.4 The repertoire and function of immune cells in the skin
 - 1.5 Immune sensing and parasite recognition
2. Liver Stage Infection
 - 2.1 Trafficking of the sporozoites to the liver and hepatocyte invasion
 - 2.2 *Plasmodium* liver stage forms
 - 2.3 Innate immune response to liver-stage infection
 - 2.4 Adaptive immune response to liver-stage infection
 - 2.5 Major liver-stage antigens and pre-erythrocytic vaccines
3. Blood Stage Infection
 - 3.1 Release of merozoites from the liver, erythrocyte invasion, and blood-stage infection
 - 3.2 Innate immune recognition of blood-stage infection
 - 3.3 Adaptive immune effectors during blood-stage infection
 - 3.4 Major blood-stage antigens that serve as erythrocytic vaccine targets
 - 3.5 Use of anti-*Plasmodium* antibody responses to determine population-level malaria exposure through serological assays.
4. Gametocytes and sexual maturity of *Plasmodium*
 - 4.1 Development of gametocytes
 - 4.2 Immune response to gametocytes
 - 4.3 Major gametocyte antigens and vaccine targets
5. Malaria in the Mosquito
 - 5.1 Parasite development in the midgut, movement through the peritrophic matrix, differentiation, and migration to salivary glands for transmission to the next host.
 - 5.2 Physical barriers to infection
 - 5.3 The effect of mosquito microbiota on infection
 - 5.4 Recognition of *Plasmodium* by mosquito PRRs, major immune signaling pathways, and effector mechanisms
6. Transmission Blocking Immunity
 - 6.1 Developing Transmission Blocking Vaccines
 - 6.2 Anti-parasite antibody uptake and neutralization of the parasite within the mosquito
 - 6.3 Major *Plasmodium* antigens expressed in the vector that serve as transmission-blocking vaccine targets

Conclusions

Introduction

Malaria is the infection of a host with the mosquito-borne parasite *Plasmodium*, irrespective of the symptomology. It is estimated that 3.2 billion people are currently living in areas of malaria transmission. In 2017, 219 million people were infected with *Plasmodium*, resulting in 435,000 deaths, 70% of which were in children under the age of 5 (1). The *Plasmodium* parasites responsible for malaria are members of the *Apicomplexa* phylum of parasitic protozoa, which includes other notable members such as the opportunistic pathogens *Cryptosporidium spp.*, and *Toxoplasma gondii*. Like other *Apicomplexa*, *Plasmodium spp.* are obligate intracellular organisms with a complex life cycle that comprises both mosquito and vertebrate hosts. The life cycle of *Apicomplexa* typically includes three main stages as follows: 1) infection of the host with a 'zoite' form and growth within a host cell, which also includes mitotic division for *Plasmodium spp.*; 2) sexual development which involves the production of gametes, subsequent fertilization, and formation of zygotic forms known as oocysts; and 3) sporogenesis in which new 'zoite' forms are generated that can infect the next host (2). *Plasmodium spp.* have been found to infect diverse vertebrate hosts, ranging from reptiles and birds to mammalian hosts including rodents, nonhuman primates, and humans (3).

We aim here to provide a comprehensive review of the immune responses to *Plasmodium* infections through the description of key events of each stage of the parasite life cycle. An overview of the major antigens that have been used as targets for vaccine development to prevent infection, disease, and block transmission will be discussed at the end of each section.

1. Initiation of infection of the vertebrate host and immune responses to *Plasmodium* in the dermis

1.1 The infectious bite and start of migration

Infection begins when sporozoites are injected into the dermis of the vertebrate host by a female *Anopheles* mosquito during a blood meal, with approximately 10-100 sporozoites injected per infections bite (4). Once in the dermis, the motile sporozoites must traverse through cells of multiple physical

barriers to reach their preferred developmental site, the liver. Since sporozoites lack cilia and flagella, sporozoites glide to move along solid surfaces, reaching top speeds of 10 $\mu\text{m/s}$ (5). This gliding motility is related to the immunodominant circumsporozoite protein (CSP). CSP is discharged from the apical end of the sporozoite and redistributes across the surface towards the anterior end (6) with the help of a submembranous actin-myosin motor (5), allowing the sporozoite to move forward (6) and leaving a trail of secreted CSP as it moves (7). Reverse genetic studies using thrombospondin-related adhesion protein (TRAP)-deficient *P. berghei* mutants have determined that the gliding motility and infectivity of *Plasmodium* are also dependent on TRAP (8).

To cross the physical barriers during its journey to the liver, the sporozoite migrates through cells that make up these interfaces. Sporozoite cell traversal, which was first reported in macrophages of *P. berghei* infected mice and rats (9, 10) before being reported in other cells types, involves the active penetration of sporozoites into the host cell, their subsequent cytosolic migration, and exit, often resulting in the death of the host cell. The first of the physical barriers faced by the sporozoite are the dermal phagocytes and dermal fibroblasts, which are involved in wound healing and produce the extracellular matrix that makes up the connective tissue in the skin. Next, the sporozoite must cross the endothelial cells of the skin capillaries, travel through the blood to enter the liver through the Kupffer cells to invade hepatocytes (11).

Although the majority of sporozoite development occurs in liver hepatocytes, reports in *P. berghei* infected mice indicate that ~50% of sporozoites remain in the skin immediately following an infectious bite, with 11% of those injected developing into exoerythrocytic forms in the dermis and epidermis 24 hours post-infection. These dermal exoerythrocytic forms can also generate infective merozoites (12). In addition to reports of complete exoerythrocytic schizogony outside the liver, sporozoites have been observed in the hair follicles, an immunologically privileged site due to the absence of MHC class I expression, for up to two weeks (12). Beside the ~50% of sporozoites that remain in the skin, another ~25% can be found in the proximal draining lymph node, with only 25% or less of those injected into the skin completing their migration to the liver (13). These observations may point to a secondary parasite

reservoir in the skin, which also allows for detection of the parasite by the immune cells in the dermis and their subsequent trafficking to draining lymph nodes.

1.2 The skin, the first line of defense

The skin acts as the first line of defense against infection to many pathogens, and thus, this organ harbors a variety of innate and adaptive immune cells to combat infection. The two major compartments making up the skin are the epidermis and connective tissue. The primary dendritic cell (DC) population in the epidermis and epithelium of hair follicles are Langerhans cells, which act as professional antigen-presenting cells (APCs) and perform immune surveillance functions. In addition to Langerhans cells, the epidermis is also home to skin-resident T cells in humans and dendritic epidermal T cells (DETCs) in mice. In humans, skin resident T cells are usually CD8⁺ T cells and can be activated by antigen-presenting cells within the skin (14). However, since the purpose of the mosquito bite is to obtain blood from blood vessels within the dermis, most immune sensing of invading parasites will likely occur in the dermis rather than the epidermis. The innate immune cell population of the dermis includes multiple specialized DC subsets such as dermal DCs and plasmacytoid DCs (pDCs), as well as mast cells, natural killer T cells (NKTs), and innate lymphoid cells. Cells belonging to the adaptive arm of immune responses present in the dermis include multiple T cells populations such as T_H1, T_H2, and T_H17 subsets of CD4⁺ T helper cells. Populations of $\gamma\delta$ T cells are also present in the dermis and function in both innate and adaptive immune responses (14-16).

1.3 Immune responses to mosquito saliva

Before considering the anti-parasite immune responses, we should first understand how the host responds to the mosquito saliva to appreciate the context of the response to infective mosquito bites.

During a blood meal, the female *Anopheles* mosquito uses her proboscis to puncture the dermis with the intent of rupturing a blood vessel and feeding from it directly or from the pool of blood caused by the rupture. While probing for a blood vessel, the mosquito repeatedly moves her proboscis and injects nanoliter quantities of saliva into the dermis of the host; if the mosquito is carrying a pathogen such as *Plasmodium*, this is injected into the skin as well. The injection of saliva during feeding is known to promote vasodilation, capillary extravasation, edema, hemorrhaging, and strong inflammatory responses (17), due in part to the vasoactive compounds within mosquito saliva (18). As a result, mosquito bites will usually cause local cutaneous inflammatory reactions, which include erythema, small papules, and pruritic swelling (17).

The inflammatory reactions induced by mosquito saliva vary depending on the host's exposure to previous mosquito bites and potential allergic reactions such as IgE-mediated (type I) hypersensitivity reactions (19). The type I reactions induced by mosquito saliva are caused by mast cell degranulation due to cross-linking of FcεR1 receptor-associated IgE antibodies or direct mast cell degranulation induced by salivary components. This results in further fluid extravasation and recruitment of DCs, monocytes, and polymorphonuclear leukocytes, including neutrophils from the bloodstream to respond to the injury and potential pathogen injection. In addition, the mosquito saliva dependent degranulation mast cells in the skin also result in the sequestration of DCs in the draining lymph nodes (19). Since mosquito saliva contributes to immediate hypersensitivity reactions, immune cell infiltration, and sequestration of leukocytes in the draining lymph nodes, it likely affects the resulting adaptive response to sporozoites.

1.4 The repertoire and function of immune cells in the skin

Assuming the mosquito bite described resulted in the intradermal inoculation of sporozoites, which cells would be most likely to sense the parasite first? As noted in the description of immune responses to mosquito saliva, mast cells are tissue-resident innate immune cells that function as first responders within

the tissue, releasing inflammatory mediators and cytokines upon interaction with pathogens. TNF- α and IL-8 released by mast cells promote vasodilation and recruitment of neutrophils, while TNF- α also functions in driving IL-1 production by classical M1 macrophages (14).

As with many infections and injuries, neutrophils are often the first immune cell recruited to infected tissue. The chemokines that attract neutrophils to the mosquito bite site will also upregulate endothelial adhesion molecules, allowing neutrophils to undergo extravasation into the affected tissue. Once at the site of the mosquito bite, neutrophils will engage in the killing of the sporozoites they encounter through the release of peroxidases, proteases, and can also extrude their own DNA and histones forming neutrophil extracellular traps (NETs) to immobilize the migrating sporozoite (20). A recent study by MacDaniel et al. found that intradermal injection of C57BL/6 mice with either wild-type *P. berghei* sporozoites or salivary gland extract induced similar levels of local inflammation and neutrophil infiltration at 2 hours post-inoculation, but by 4 hours the neutrophil infiltration continued to rise in the mice inoculated with sporozoites and decreased in mice receiving only mosquito salivary gland extracts. This suggests that although mosquito saliva can contribute to an inflammatory response, the parasite presence is necessary to maintain immune cell recruitment (21). This study also reported the association of neutrophils and resident myeloid cells with sporozoites in the skin and draining lymph nodes, resulting in a Th1 cytokine profile in the draining lymph nodes 24 hours post-inoculation with *P. berghei* sporozoites (21). However, it is important to note that due to the tendency of C57BL/6 mice to have skewed T_H1 responses that these results may differ in other mouse strains, such as T_H2 skewed BALB/c mice (22).

In addition to the recruitment of neutrophils by chemokine secreting mast cells, the release of TNF- α by mast cells immediately following the mosquito bite results in activation of M1 macrophages. Activation of these classical macrophages promotes their increased phagocytosis, production of inflammatory cytokines, the killing of pathogens or infected cells via NO release, expression of MHC

class I molecules and costimulatory molecules CD80/86 (23). These responses improve the ability of M1 macrophages to take up material in the tissue, including inoculated sporozoites, and present the encountered antigens to T cells in the draining lymph node leading to their subsequent activation. However, since sporozoites are known to traverse phagocytic cells in both the dermis and liver, traversal activity can also prevent the destruction of sporozoites by these cells (24). This effect has been confirmed in recent studies which demonstrated the ability of *P. berghei* sporozoites to invade and survive within CD11b+ cells, which correspond to dendritic cells, monocytes, and macrophages in mice (21).

As previously noted, dendritic cells are also resident in the dermis and will secrete cytokines and chemokines in response to infection or tissue damage. Dermal DCs also have the ability to produce inducible nitric oxide synthase (iNOS) and subsequent nitric oxide (NO) production from L-arginine within macrophages or infected cells (25). The short-lived free radical NO has multiple activities which include antimicrobial functions resulting in the killing or reduced infectivity of pathogens such as protozoa, and immunoregulatory functions that may either promote or decrease inflammation and affect the differentiation of T cells (26). Dermal DCs are known to rapidly migrate to the lymph nodes following pathogen inoculation, where they function as efficient antigen-presenting cells, activating both CD4+ T cells through presentation of antigen in the context of MHC class II, and activating CD8+ T cells through cross-presentation of antigens derived from ingested pathogens in the context of MHC class I (15). The cytokines produced by these dendritic cells will also influence the subsequent development of the T cells, driving them to differentiate into one of several cellular subsets, including T_H1, T_H2, or T_H17 for CD4+ T cells depending which cytokines are produced (15). Furthermore, studies using *P. yoelii* infected BALB/c mice have demonstrated that the DCs that pick up sporozoites inoculated by an infectious mosquito bite travel to the skin-draining lymph nodes where they prime the first cohort of CD8+ T cells to be activated in response to *Plasmodium* infection (27).

1.5 Immune sensing and parasite recognition

Although we have identified which immune cells are involved in the recognition of the sporozoite in the dermis, we should also understand the mechanisms by which dermal cells respond to the mosquito bite and injected sporozoites. Immune cells and somatic cells alike possess external and internal receptors that allow them to identify common features of pathogens and evidence of tissue damage that may correspond to injury or infection, these receptors are known as pattern recognition receptors (PRRs). PRR expression varies depending on the cell type, allowing for infected cells to recognize that they have been infected and antigen-presenting cells to recognize a wider range of molecular patterns to differentiate between tissue damage and pathogen presence so that they can respond accordingly. The two major classes of molecular patterns identified by PRRs are damage-associated molecular patterns (DAMPs) and pathogen-associated molecular patterns (PAMPs) (28). Several major classes of PRRs have been identified including Toll-like receptors (TLRs), which can detect certain PAMPs and DAMPs (29). Of the 13 TLRs identified, humans express TLRs 1-10, with TLRs 1, 2, 4, 5, and 6 being expressed as transmembrane receptors on the cell surface and TLRs 3, 7, 8, 9 found within exosomes and at the endoplasmic reticulum (30). TLRs are known to be found on professional APCs like dendritic cells and macrophages, and the role of these TLRs has also been extensively studied in the context of neutrophil activation (31). Furthermore, the expression of mRNA encoding TLRs 1-10 has been observed in mast cells in the skin (32). Certain non-immune cell subsets, such as the fibroblasts which reside in the dermis and are characterized by their production of extracellular matrix components, express TLRs 1-10 as well (30).

As noted, PRRs identify PAMPs and DAMPs following infection and injury, with the molecules that act as DAMPs sequestered away from their corresponding receptor under normal conditions, however, upon injury, these molecules are exposed. DAMPs are therefore perceived as danger signals since they are released by damaged and dying cells. Receptor triggering by DAMPs alerts the immune system of

damage, causing the cells involved to promote wound healing and recruit other immune cells that can help eliminate potential intruders (30). Although production of DAMPs as the result of mosquito bites has not been explicitly studied, we know that the mosquito bite and migration of the sporozoite in the dermis results in tissue damage, hemorrhaging, and inflammation (17) and therefore DAMPs are likely released in the process. Furthermore, the cell traversal used by sporozoites to move through various physical barriers is known to result in cell death (9-11), and the molecular components of these dead cells may also include DAMPs.

Despite the lack of knowledge of DAMP production following a mosquito bite and *Plasmodium* sporozoite inoculation, we can infer which innate signaling events may be conserved from studies examining innate immune responses in the skin. The nuclear high-mobility box group protein HMGB1, heat shock proteins 60 and 70, oxidized LDL, extracellular matrix component hyaluronic acid, fibrinogen, and fibronectin are all DAMPs released from damaged or dying cells in humans which have been identified as TLR ligands (30, 33). Specifically, HMGB1 has been demonstrated to be recognized by TLR4 (34). Studies conducted in TLR4 deficient mice have found that these mice displayed prolonged wound healing compared to their wild type counterparts (35). Based on these and similar observations of TLR associated wound healing (30), it is likely that the human host has evolved to respond to damage signals in a manner that promotes immune cell infiltration to clear any potential pathogens at the site of injury and healing of skin wounds as well to prevent any further introduction of pathogens, however these responses are not specific to mosquito bites or *Plasmodium* infection.

In addition to DAMPs that may be generated as the result of an infectious bite, *Plasmodium* sporozoites may also contain PAMPs. However, there have been no studies published which report PRR ligands derived from sporozoites present in the skin. Despite the lack of knowledge about innate immune sensing of sporozoites in the skin, studies of sporozoite invasion of hepatocytes have revealed that *Plasmodium* RNA is capable of triggering melanoma differentiation-associated protein 5 (MDA5)

activation leading to signaling through the mitochondrial antiviral signaling protein (MAVS) which induces type I interferon production (28). If sporozoite RNA is detected by dermal cells, it is likely that this pathway may also play a role in innate sensing of sporozoites in the dermis. However, future studies to confirm this are required.

Aside from the PRR signaling described, it appears that the bulk of immune cell recognition of free sporozoites includes neutrophils recruitment by chemokine secreting mast cells, classical macrophage activation which increases phagocytosis, and dendritic cell sampling of foreign matter present in the dermis (19). In addition, indiscriminate mechanisms of matter uptake by APCs, such as pinocytosis, allow for the ingestion of pathogens that do not trigger any of the receptors described and may also contribute to the sporozoite uptake in the dermis.

2. Liver Stage Infection

2.1 Trafficking of the sporozoites to the liver and hepatocyte invasion

Plasmodium sporozoites that reach the blood vessels following injection travel to the liver to initiate the next stage of their life cycle. To enter the hepatocytes, sporozoites must first traverse the sinusoidal epithelium, which forms a barrier between the blood and hepatocytes. The liver sinusoid contains endothelial cells interspersed with specialized liver resident macrophages known as Kupffer cells. Though we do not have a complete understanding of all the factors involved in the migration of the sporozoite from the blood into the liver, several key proteins involved in this process have been identified.

CSP, which was discussed briefly in the previous section due to its contribution to the gliding motility of sporozoites, also contributes to cell transversal of sporozoites into the liver as CSP has been found to bind to heparan sulfate proteoglycans (HSPGs) on liver cells. This binding is a critical step for the arrest of the sporozoite at the liver sinusoid. Although CSP has been found to be essential for this process, it is yet to be determined if the amino-terminus domain or the thrombospondin type I repeat domain of the

carboxy-terminal are involved in binding to the liver sinusoid (36). Nonetheless, antibodies directed against the cell adhesive motif present in the region I of CSP, located at the amino-terminal end of the protein, are capable of inhibiting invasion of HepG2 cells by multiple *Plasmodium spp.* (37), indicating that this region may be necessary for binding. In addition, it has been demonstrated that CSP is proteolytically cleaved by parasite-derived cysteine proteases following contact with hepatocytes, and inhibiting this cleavage prevents the invasion of hepatocytes by the sporozoite without affecting its migration (38).

Following attachment of the sporozoite to the liver sinusoidal barrier via CSP, TRAP and its related family of proteins appear to be involved in the gliding motility of the sporozoite at the sinusoid surface and mediate entry into the target cells (39). Most reports indicate that sporozoites cross into the liver through Kupffer cells (40, 41), but evidence of endothelial cell transversal has also been reported (36). Once in the liver parenchyma, sporozoites traverse several hepatocytes before ultimately arresting their migration to begin their differentiation into the next stage of their life cycle (42).

In addition to the highly conserved *Plasmodium* proteins CSP and TRAP, at least five other proteins have been found to be essential for in sporozoite cell traversal into the liver. These include the sporozoite microneme protein essential for cell transversal (SPECT 1), SPECT 2, cell traversal protein for ookinetes and sporozoites (CeITOS), phospholipase (PL), and gamete egress and sporozoite traversal protein (GEST), whose functions are reviewed by Sinnis et al. (43) and Cowman et al. (44).

2.2 *Plasmodium* liver-stage forms

After migration through several hepatocytes, the sporozoite invades and forms a parasitophorous vacuole within the hepatocyte in which it will differentiate into an exoerythrocytic form (EEF) (39). During its development in the hepatocyte, the parasite undergoes transformation into a spherical liver-stage form that increases in size, known as the large exoerythrocytic form (LEF) (2). In *P. vivax*, *P. ovale*,

and *P. cynomolgi* infections, some sporozoites invade hepatocytes without developing into the LEF and instead form dormant hypnozoites, which are resistant to treatment with all anti-malarial drug treatments except primaquine and the recently introduced tafenoquine. In addition, the hypnozoite can become activated weeks to months following the initial infection, being responsible for relapse infections.

As a LEF, the parasite undergoes karyokinesis without cytokinesis, resulting in the formation of up to 30,000 nuclei in a period of ~30 hours (36). This process of nuclear fission without cell division is referred to as exoerythrocytic schizogony (28) and culminates with the budding of merozoites which are contained within a vesicle known as the merosome. Over a period of 7-10 days in humans (2, 36) or ~48 hours in mice (45), between 10,000 and 30,000 merozoites are produced from a single sporozoite, which then rupture from the merosome into the bloodstream to go on to infect red blood cells (2, 28). It is also important to note that the pre-erythrocytic *Plasmodium* infection of the dermis and liver is clinically silent, with the period before the release of merozoites into the bloodstream known as the prepatent period.

2.3 Innate immune response to liver-stage infection

The concept of pathogen and damage-associated molecular patterns (PAMPs and DAMPs) that are recognized by pattern recognition receptors of the innate immune system were discussed above, but these immune sensing mechanisms apply to liver-stage *Plasmodium* infection as well.

One of the main PAMPs associated with liver-stage *Plasmodium* infection is glycosylphosphatidylinositol (GPI) anchors, which link many of the surface proteins to the plasma membrane. Protozoan derived GPI anchors have been found to be potent stimulators of macrophages, resulting in subsequent cytokine synthesis (28, 46). The PAMP activity of these GPI anchors seems to be dependent on their specific structure, which includes a longer glycan core and lipid component that differs from that of mammals, and two or three fatty acyl chains for *P. falciparum* merozoites. These features

allow the differentiation of *Plasmodium*-derived GPI anchors and recognition by TLR1/2 or TLR2/6 heterodimers, as well as lower levels of TLR4 homodimer stimulation (46). Activation of these TLRs results in phosphorylation of inhibitor of nuclear factor- κ B (I κ B) and mitogen-activated protein kinases (MAPK) family members and typical downstream signaling associated with these pathways, culminating in the synthesis of pro-inflammatory cytokines, such as TNF- α (46).

As described in the previous section, *Plasmodium* RNA present within infected hepatocytes is capable of activating MDA5 and subsequent MAVS signaling, resulting in the production of type I IFNs (28). In addition, reports from studies in wild-type and TLR7 deficient mice have demonstrated that in the first 24 hours following infection, the host immune response to *Plasmodium* is highly dependent on TLR7 signaling (47). This report indicates a role for TLR7 in the detection of *Plasmodium* RNA as TLR7 is typically associated with the recognition of single-stranded RNA internalized in phagosomes within APCs.

In addition to the limited understanding of the PRRs capable of recognizing liver stage infection, the innate immune mechanisms involved in targeting infected hepatocytes is also an area of ongoing research. In the liver, $\gamma\delta$ T cells, NK cells, and NKT cells have been implicated in contributing to IFN- γ secretion and targeting of LEF within infected hepatocytes (2). IFN- γ also promotes the production of IL-12 and IL-18 by phagocytes and helps in boosting NK cell activation. NK cells, $\gamma\delta$ T cells, as well as any previously activated CD8⁺ cytotoxic T cells, produce granzymes and perforin in addition to IFN- γ to further promote the killing of infected hepatocytes, thereby preventing the development of merozoites and their release into the blood (2). Studies of irradiated *P. berghei* infected mice have shown that the induction of iNOS, and resulting NO production can protect mice from challenge with viable sporozoites. This study highlights the importance of IFN- γ production by CD8⁺ T cells and other cell types as described above, and subsequent iNOS induction and NO production by hepatocytes or Kupffer as a means of killing liver stage parasites and infected hepatocytes (47). However, further studies are required to determine if other innate immune cells or mechanisms are involved in targeting infected hepatocytes.

Sporozoites arrive to the liver through the bloodstream after exiting the inoculation site. The route taken through the liver by the blood travels through the portal vein or the hepatic artery, and ultimately into the liver sinusoids, which due to a fenestrated endothelium reduce the speed of the blood through the sinusoids. This reduction in speed allows for the immune cells within the liver to detect pathogens within the blood, but at the same time provides an opportunity for hepatotropic pathogens to invade hepatocytes (48-50). As was mentioned above, sporozoites most frequently cross from the bloodstream through Kupffer cells in order to enter the liver. Kupffer cells are considered one of the largest populations of tissue-resident macrophages and are responsible for clearing substances identified as foreign, such as bacteria, or altered-self, such as endotoxins from the liver. A pro-inflammatory cytokine response in these cases would result in a continuous inflammatory environment that could cause liver damage (40); as a result, the liver is considered to be immunologically tolerant to protect against uncontrolled inflammation in response to the foreign and gut-derived antigens that pass through regularly (51). Instead, Kupffer cells have been reported to secrete anti-inflammatory cytokines, a phenomenon described as portal vein tolerance. However, pro-inflammatory responses initiated by Kupffer cells do occur but lead to liver fibrosis and cirrhosis (40). Interactions between Kupffer cells and sporozoites have been reported to cause suppression of antigen presentation by Kupffer cells and downregulation of MHC class I expression (16).

In addition to the tolerogenic phenotype of Kupffer cells, sporozoite interaction has been reported to further downregulate immune responses to *Plasmodium* infection. Studies have demonstrated that sporozoite-Kupffer cell interactions are capable of inducing cAMP signaling, which results in decreased phagocytosis (16). It has also been reported that CSP can inhibit respiratory burst, and production of reactive oxygen species (ROS), by Kupffer cells (52). Studies in which C57BL/6 mice received either infection with *P. berghei* sporozoites or immunization with irradiated *P. berghei* sporozoites found differences in MHC class I expression (53). This study found that mice receiving the sporozoite infection

showed no IL-12p40 production and reduced expression of MHC class I, while irradiated sporozoite-immunized mice upregulated MHC class I and costimulatory molecules, and produced IL-12p40 (53).

2.4 Adaptive immune response to liver-stage infection

As previously noted, a subset of the sporozoites injected into the dermis will either migrate via the lymphatics to draining lymph nodes or will be phagocytosed by APCs present in the skin which subsequently migrate to the draining lymph node. DCs in particular, play a crucial role in priming CD8+ T cells with *Plasmodium* antigens through cross-presentation of sporozoite antigens (27). The importance of DC cross-presentation of sporozoite antigens has been demonstrated through studies in which DCs were pretreated with TLR ligands, resulting in pre-maturation and inhibition of cross-presentation to CD8+ T cells (27, 54). However under conditions mimicking natural infection, the migration of APCs carrying sporozoite antigens to draining lymph nodes ultimately results in the priming of the first cohort of CD8+ T cells to be activated in response to *Plasmodium* infection in mouse models (27). Although these cells have been detected in draining lymph nodes as early as 48 hours post-immunization with irradiated *P. yoelii* sporozoites, significant CD8+ T cell responses are not detected in the liver and liver draining lymph nodes until 72 hours (55). This experimental evidence is consistent with the epidemiological observation that multiple *Plasmodium* infections are required to obtain immunity to the infection since the anti-sporozoite CD8+ T cells induced can only reach the liver after sporozoites have begun the liver stage development. Also, prolonged antigen exposure may be necessary to promote optimal liver-stage-specific CD8+ T cells (56).

Following trafficking of anti-sporozoite CD8+ T cells to the liver, two effector mechanisms capable of killing of *Plasmodium*-infected hepatocytes are the production of granzyme and perforin, and Fas/FasL interactions (55). However, CD8+ T cells that lack one or both of these mechanisms are still capable of eliminating *Plasmodium* liver stage forms (57). Instead, production of IFN- γ by activated CD4+ and

CD8⁺ T cells, as well as by NK cells, $\gamma\delta$ T cells, and NKT cells, contributes to the immune responses against hepatic *Plasmodium* infection in a number of ways. These responses include the induction of nitric oxide synthase production and subsequent nitric oxide production capable of killing infected hepatocytes as mentioned earlier, canonical activation of macrophages to become M1/classical macrophages which display increased phagocytosis and cytokine production, and the induction of isotype switching in B cells resulting in the production of cytophilic IgG2a antibodies (58). Despite this diversity of effector mechanisms, extremely high percentages of anti-sporozoite specific CD8⁺ T cells are required to provide protection. It has been estimated that sterilizing immunity against *P. berghei* in BALB/c mice was associated with a population of memory T cells of a single antigenic-specificity that exceeded 8% of the total population of CD8 T cells (59). Due to this requirement for very high numbers of circulating CD8⁺ T cells to maintain protection, the focus has shifted to define tissue-specific immune responses capable of providing protection from liver-stage malaria.

Recently the roles of CD8⁺ tissue-resident memory cells, T_{RM}, in the liver have been revealed to be essential for protection against liver-stage malaria (60). T_{RM} responses were first identified as CD8⁺ memory populations in the liver that contributed to immunity following studies with radiation attenuated sporozoites (61, 62). T_{RM} cells are differentiated from early effector T cells by IL-15 and TGF- β signaling (49, 63), while differentiated circulating effector T cells have been found to be incapable of migrating to tissues. The CD8⁺ T_{RM} cells display high expression of CXCR6 (62), which allow these cells traffic to and stay in the liver due to the production of CXCR6 ligands by liver sinusoidal epithelial cells and hepatocytes (64). As a result, CXCR6 expression is required for the maintenance of liver T_{RM} cells and loss of CXCR6 results in loss of liver-associated memory and anti-sporozoite immunity (64). Protection by CD8⁺ T_{RM} cells is mediated by the production of cytokines including IFN- γ and TNF- α , as well as the production of granzyme B (60), allowing the direct and immediate killing of sporozoites and infected hepatocytes. Recent studies have shown that T_{RM} cells patrol the liver sinusoids, with an approximate

half-life of 36 days (65). Due to the loss of protection when T cells lack CXCR6 (64), and that strategies capable of reliably inducing sporozoites-specific T_{RM} cells are capable of providing sterile protection from malaria, it is likely that immunizations capable of inducing these cells display improved efficacy.

Recent studies by two different groups were able to identify that the immunization route, adjuvant, and a prime-boosting strategy could be used to specifically enhance liver T_{RM} responses (60, 66). Improved induction of liver T_{RM} responses compared to radiation attenuated sporozoite immunization could be obtained through immunization regimens designated prime and trap (60), or prime and target (66). The prime and trap strategy employs DC targeting through Clec9A monoclonal antibodies to deliver a peptide antigen intravenously (60). This is then followed up by an adeno-associated viral boost, as this vector targets hepatocytes and expresses the antigen encoded within the transgene (60, 67). In contrast, the prime and target method uses an adenovirus intramuscular prime, followed by a boosting immunization with a poly(lactic-co-glycolic acid) (PLGA) protein-loaded nanoparticles delivered intravenously. The PLGA-nanoparticles were found to be taken up by Kupffer cells following concentration within the liver (66). Both of these methods rely on generating a robust CD8⁺ T cell response that is then directed to the liver through a boosting immunization that specifically targets liver cells. While no difference was found between adjuvanted and unadjuvanted immunization regimens in the prime and target studies when the adjuvants Remiquimod and monophosphoryl A were tested (66), the prime and trap strategy found that the use of the anti-TLR3 agonist poly(I:C) or the TLR9 agonist CpG were able to further enhance the formation of T_{RM} cells in response to vaccination (60).

Besides the contribution of CD8⁺ T cells, humoral immune responses are a major contributor to anti-sporozoite immunity and protection against liver-stage infection. Anti-CSP monoclonal antibodies have been known to block infection *in vivo* since the 1980s (68, 69). Mathematical modeling of results from the Phase IIb clinical trial of the *P. falciparum* CSP based vaccine candidate RTS,S suggests that high levels of anti-CSP repeat antibodies, ranging between 100-200 µg/ml, are required for protection (70). In

addition to anti-CSP antibody responses, there have also been reports from *P. falciparum* endemic areas that anti-TRAP antibodies are associated with protection from infection (71). Interestingly, anti-parasite antibodies can be downregulated during the infection, as it has been reported in *P. yoelii* infected mice that *Plasmodium* blood-stage infection may contribute to a loss of antibody-producing plasma cells by induction of apoptosis of the blood-stage antigen Merozoite Surface Protein-1 (MSP-1)-specific plasma cells and memory B cells and induced apoptosis of other bystander plasma cells (72).

Based on these observations, it is apparent that high levels of CD8+ T cells and antibodies are needed to provide protection from liver infection or progression of the parasite to the blood stage. However, it should be noted that a single infected hepatocyte able to avoid destruction by these immune mechanisms can produce ~10,000-30,000 infectious merozoites that can produce the full blood-stage infection.

2.5 Major liver-stage antigens and pre-erythrocytic vaccines

Due to the protective effects mediated by IFN- γ secreting CD8+ T cells and anti-sporozoite antibody responses, induction of these cells has become a goal of many pre-erythrocytic vaccines and vaccine candidates.

One of the first models of vaccination against malaria was the use of irradiated sporozoites. In the initial studies carried out by Nussenzweig et al. in 1967, A/J mice immunized with 5,000-75,000 irradiated *P. berghei* sporozoites displayed different levels of protection from challenge with 1,000 viable sporozoites two weeks post-immunization, with the average protective efficacy of this method around 37% (73). This concept was later applied to humans in 1973 using mosquitoes irradiated at 15,000 rads carrying *P. falciparum* as the mode of immunization. Upon the experimental challenge of the volunteers with non-irradiated mosquitoes, it was observed that one of these four volunteers was protected from infection (74). Clinical trials carried out in the 1980-1990s revealed that over 1,000 bites from irradiated

mosquitoes carrying *P. falciparum* sporozoites were necessary to protect against challenge by nine weeks post final exposure and this protection lasts for 23-42 weeks (75). More recently, radiation-attenuated *P. vivax* sporozoites were used for seven immunizations of 89 adults at ~65 infectious bites each, following controlled human malaria infection at eight weeks post final immunization a 42% protective efficacy was observed (76).

Although irradiated mosquito and sporozoite-based vaccination methods have revealed a great deal about the mechanisms of protection against *Plasmodium* infection, immune responses against pre-erythrocytic stage antigens need to be very robust to prevent blood-stage infection given that a single infected hepatocyte can release up to 30,000 infectious merozoites. This may explain why it is difficult to produce sterilizing immunity based on radiation attenuated sporozoites unless a high number are used for immunizations. As a result of the requirement for a high number of radiation attenuated sporozoites or high bite counts by irradiated mosquitoes, this immunization method will likely be difficult to administer to large numbers of people, especially in endemic areas where the equipment required to either irradiate or store sporozoites is scarce. Looking at examples of successful disease eradication measures as a guide for malaria vaccination, one of the factors contributing to the reduction of polio cases in the developing world was the use of oral administration of the attenuated oral poliovirus vaccine (77). Therefore it is likely that a vaccine that is easier to administer will be more successful at reducing the disease burden of malaria. However, Sanaria has recently conducted clinical trials using isolated irradiated sporozoites delivered intravenously (PfSPZ vaccine) in several African countries including Mali, Tanzania, Kenya, Burkina Faso, Ghana, and Equatorial Guinea (78), demonstrating that although difficult, malaria eradication using this immunization method may be feasible.

Another promising vaccination strategy has been the use of CSP and CSP subunit vaccines. One of the most notable examples is the *P. falciparum* CSP based subunit vaccine candidate RTS,S/AS01, as it is the most advanced malaria vaccine candidate, having completed Phase III clinical trials (79), and received

approval in 2015 by the European Medicines Agency for use outside the European Union in malaria-endemic areas (80). Despite this significant step in the development of malaria vaccines, there is still room for improvement as the vaccine efficacy of RTS,S/AS01 is between 28-32% (81). Relevantly, vaccine efficacy induced by RTS,S/AS01 has been found to wane over time with children in the fifth year of follow-up displaying negative efficacy due to higher than average exposure to malaria parasites (79). Similar results have recently been reported for the *P. vivax* CSP-based vaccine candidate VMP001, as this candidate was unable to induce sterile protection and only 59% of the vaccinees displayed delayed onset of parasitemia compared with unvaccinated controls (82).

In addition to the challenge of eliminating every infected hepatocyte to prevent blood-stage infection, the genetic variability of *Plasmodium* isolates and subsequent vaccine failure should be of major concern as vaccine candidates based on a single strain risk promoting the selection of strains not represented in the formulation (83, 84). Using the example of polio eradication efforts again, characterization of the circulating polio was carried out before three strains were selected to be included in the inactivated polio vaccine (77). In contrast RTS,S/AS01 was designed based on the sequences of a single African-derived strain of *P. falciparum* designated 3D7 (85). To account for strain variability, our group has designed several experimental CSP-based vaccine candidates including a *P. vivax* CSP recombinant protein chimera (PvRMC-CSP), which includes sequences representing the VK247 strain repeat region and two different VK210 type I repeat variants. We observed that immune responses elicited in mice against this chimeric protein were not genetically restricted, and all six mouse strains tested elicited robust antibody responses as well as multi-functional PvRMC-CSP-specific CD4⁺ and CD8⁺ T cells (86). However, further pre-clinical studies in non-human primates and clinical trials are required to determine the protective efficacy of this novel candidate against *P. vivax* challenge.

Vaccines targeting the thrombospondin-related adhesion protein (TRAP) have also shown promise in clinical trials. Clinical trials of a heterologous prime-boost regimen that includes a multiple epitope TRAP

protein delivered by the chimpanzee adenovirus 63 (ChAd63) and the modified vaccinia Ankara (MVA) viral vectors have been recently reported. These trials showed 13% sterile protection in malaria-naïve adults, and of those that did develop an infection, 33% displayed a delayed time to treatment (87).

There are currently no published studies on Cell-traversal protein for ookinetes and sporozoites (CelTOS) based vaccine candidates. However, a clinical trial of a falciparum malaria protein FMP012 (Clinical Trial Identifier NCT01540474), based on *E. coli* expressed *P. falciparum* CelTOS was conducted by the Walter Reed Army Institute of Research (WRAIR) and the United States Army Medical Research and Development Command (USAMRMC) in thirty malaria naïve volunteers, but this work remains unpublished. Since CelTOS is highly conserved among *Plasmodium spp.*, it is likely that this protein may serve as the target of future preclinical and clinical studies. This high level of conservation translates into cross-species protection as mice immunized with *P. falciparum* CelTOS are protected from heterologous challenge with *P. berghei* sporozoites (88).

Although there are many pre-erythrocytic malaria vaccine candidates under development, it is still debated whether multiple pre-erythrocytic antigens should be used to improve sterilizing immunity (89). As an alternative, multiple stages would be targeted to eliminate any merozoites that escape destruction by vaccine-induced responses in the liver (90, 91). Finally relevant for pre-erythrocytic vaccines a robust vaccine platform should be considering including human adenoviruses (92, 93), simian adenovirus (87), modified vaccinia viruses (87), or virus-like particles (94).

3. Blood Stage Infection

3.1 Release of merozoites from the liver, erythrocyte invasion, and blood-stage infection

Following the release of tens of thousands of merozoites from each infected hepatocyte into the hepatic circulation, merozoites immediately begin the invasion of erythrocytes. Erythrocyte invasion is a

multi-step process in which merozoites engage in pre-invasion interactions with the red blood cell before actively invading and once inside, the infection with merozoites causes morphological changes in the erythrocyte membrane in a process known as echinocytosis. Despite the complexity of this process, the invasion of erythrocytes by merozoites occurs within 2 minutes (44).

The pre-invasion stage comprises the low-affinity interactions between the merozoite surface coat proteins and the erythrocyte, which mediates the first contact between the two cells. One of the major surface proteins involved in this process is the merozoite surface protein 1 (MSP1) which is attached to the plasma membrane of the merozoite via glycosylphosphatidylinositol (GPI) and one of the most abundant proteins of the surface coat of merozoites (95). MSP1 binding of the erythrocyte surface is known to be blocked by binding of exogenous heparin sulfate and considering that human erythrocytes possess heparin-like molecules on their surface, these heparin proteins likely act as receptors for merozoite binding (96). Evidence also suggests that MSP1 serves as a platform for three or more large protein complexes that exhibit erythrocyte binding capabilities (97). *P. falciparum* MSP1 is synthesized during schizogony and is expressed as a complex on the surface of the merozoite. The ~200 kDa MSP1 precursor that appears on the surface of newly released schizonts is cleaved into four fragments, of approximately 83, 30, 38, and 42 kDa each, with the MSP1 42 kDa fragment (MSP1₄₂) attached to the surface via the GPI anchor at the C-terminus (98, 99). Upon erythrocyte invasion, MSP1₄₂ is cleaved into a ~ 33 and 19 kDa fragments, with the MSP1₁₉ kDa fragment remaining on the merozoite surface during the invasion process (98, 100). Notably, antibodies targeting MSP1₁₉ can inhibit merozoite invasion of erythrocytes in humans (101).

In addition to merozoite binding of erythrocytes mediated by MSP1 and related complexes, alternative pathway ligands, which exhibit redundant erythrocyte binding functions, are involved in the pre-invasion process (102). These ligands include reticulocyte-binding homologs, such as the *P. falciparum* PfRh2a, PfRh2b, PfRh4, and PfRh5. A class of proteins known as erythrocyte binding

antigens, which include EBL-1, EBA-140, EBA-175, and EBA-181, also function as alternative pathway ligands (102). The functions of members of both ligand families are reviewed in Tham et al. (103). Overall these ligands bind to receptor proteins on the erythrocyte surface, including the complement receptor CR1, and glycophorin A, B, and C (44).

In *P. falciparum*, binding of PfRh5 to basigin is essential for merozoite invasion and results in an influx of Ca^{2+} ions into the erythrocyte (102). This influx then allows for the deposition of the apical membrane antigen-1 (AMA1) and the rhoptry neck (RON) protein complex into the plasma membrane of the erythrocyte, resulting in irreversible attachment of the erythrocyte and merozoite (44). The influx of Ca^{2+} ions into the erythrocyte is also thought to contribute to the echinocytosis that occurs after PfRh5 binding, which includes erythrocyte shrinkage and appearance of spiky protrusions on the erythrocyte surface (44, 102). The force of the merozoite's actomyosin motor then pushes the parasite into the erythrocyte as the lipid-rich rhoptry proteins form the parasitophorous vacuole, followed by fusion of the erythrocyte membrane and parasitophorous vacuole at the posterior end of the merozoite (44).

Although the process of erythrocyte invasion for *P. vivax* is not as well characterized as that of *P. falciparum*, several major proteins and receptors critical for this process have been identified. However, one major difference from *P. falciparum* blood-stage infection is that *P. vivax* preferentially binds and invades reticulocytes, the immature red blood cells. Similar to other *Plasmodium spp.*, *P. vivax* merozoites express three major surface proteins, MSP1, MSP3 (variants MSP3.10 and MSP3 α), and MSP9, which can be targeted by naturally acquired immunity to provide protection from blood-stage infection (104). Other merozoite surface proteins including MSP4, MSP5, MSP7, and MSP10 have also been examined to determine potential protein-protein interactions which mediate merozoite invasion, which may make these proteins logical targets for vaccination (105).

In *P. vivax*, MSP1 the processing of the ~200 kDa fragment first into the 42 kDa surface fragment, then into the 19 kDa fragment occurs in a similar process to that observed for *P. falciparum* (98), leaving

MSP1₁₉ on the surface just before the invasion. In addition to MSP1 binding to the reticulocyte surface, invasion of *P. vivax* is for the most part dependent on the expression of the Duffy blood group antigen, also known as the Duffy antigen receptor for chemokines (DARC), on erythrocytes. The *P. vivax* Duffy binding protein 1 (PvDBP1) is responsible for the interaction between the merozoite and the reticulocyte via DARC (106). Lack of the Duffy blood group, known as Duffy-null, is a common phenotype in Africa and confers resistance of Duffy-null individuals to *P. vivax* (106). However, it has recently been documented that Duffy-null individuals throughout Africa and South America are capable of being infected with *P. vivax*, which may be the result of a DNA expansion of DBP1 that allow DBP1 to bind with low affinity to an alternate receptor based on parasites isolated from Duffy-null *P. vivax* infections (106). Additional *P. vivax* proteins capable of interactions with reticulocytes have also been identified, including MSP6, reticulocyte binding proteins (PvRBP1 and 2), and AMA1, whose functions are reviewed in Li and Han (107).

Once infection of the red blood cell has been established, *Plasmodium* begins an ~48-hour cycle of erythrocyte invasion, replication, and erythrocyte rupture resulting in the release of 16-32 more merozoites from each infected erythrocyte into the blood (44, 108). The egress of merozoites is a highly regulated process involving multiple protein kinases, including cGMP protein kinase (PfPKG) and the calcium-dependent protein kinase (PfCDPK5). MSP1 also plays a role in merozoite egress from erythrocytes by processing subtilisin 1 on the merozoite surface, allowing it to bind to the spectrin protein on the erythrocyte membrane (44). Due to the erythrocyte damage caused by merozoite egress and the appearance of variant surface antigens on the erythrocyte membrane the blood stage of *Plasmodium* infection is responsible for the clinical symptoms which include fever, malaise, anemia and chills and in severe cases renal failure, cerebral malaria, seizures, and coma. Placental malaria is also a risk for pregnant women infected with *Plasmodium* (108).

3.2 Innate immune recognition of blood-stage infection

Multiple innate immune cells are involved in the response to blood-stage malaria infection. Macrophages play an essential role in blood-stage immunity as they can phagocytose infected erythrocytes in a cytophilic antibody or opsonin-independent manner through the use of scavenger receptors such as CD36 (109). NK cells in the peripheral blood are considered necessary for elimination of infected red blood cells (iRBCs) as depletion of NK cells in *P. chabaudi* infected mice results in a sharp increase in parasitemia (110). IFN- γ production by NK cells is also essential for the activation of macrophages and isotype switching of B cells to produce IgG2a cytophilic antibodies (109). NKT cells and $\gamma\delta$ T cells are also considered to aid in the immune response to blood-stage infection through similar methods as NK T cells (108). In addition, dendritic cells are one of the earliest responders to blood-stage *Plasmodium* infection due to their expression of various pattern recognition receptors (109).

Of the *Plasmodium* pathogen-associated molecular patterns identified, most are associated with blood-stage infection (28). GPI-anchored proteins, including MSP1, have been found to activate TLR1/2 heterodimers, TLR4 homodimers, and TLR2/6 heterodimers with GPI anchors containing three fatty acid chains preferentially activating TLR1/2 and those containing two fatty acid chains activating TLR2/6 (28). Activation of these TLRs within macrophages causes the release of cytokines, including TNF, and nitric oxide production (28).

Nucleic acids derived from *Plasmodium* have also been found to stimulate several different classes of PRRs. Due to the high number of AT-rich motifs present in both *P. falciparum* and *P. vivax*, which contain ~6000 and ~5000 AT-rich motifs respectively, these motifs have been found to cause downstream PRR signaling through STING-IRF3, which induces the production of type I IFNs, IFN- α and IFN- β (28, 111). Although *P. falciparum* and *P. vivax* both possess AT-rich genomes, the accumulation of *Plasmodium* DNA within macrophages involved in phagocytosis of iRBCs allows for the activation of TLR9 by immunostimulatory CpG motifs since ~300 CpG motifs are present within *P. falciparum* and

~2500 CpG motifs are present in *P. vivax*. Recognition of CpG motifs by TLR9 results in the secretion of pro-inflammatory cytokines from TLR9 stimulated macrophages and DCs (28). In addition, *Plasmodium* DNA has also been found to stimulate AIM2 signaling, which results in caspase 1 activation and release of active IL-1 β (28, 112). As mentioned previously, *Plasmodium* RNA has also been found to activate TLR7 and MDA5 signaling (28).

Hemoglobin is the main energy source for *Plasmodium* during blood-stage infection, and digestion of hemoglobin by *Plasmodium* is associated with the production of toxic protoporphyrin metabolites, including heme. The heme molecules are then polymerized via parasite associated enzymes to ensure parasite survival within the iRBC and result in the production of hemozoin crystals. Upon ingestion of iRBCs by macrophages and DCs, these hemozoin stimulate multiple PRRs (28). TLR9 has been found to be activated by hemozoin associated with *Plasmodium* DNA, resulting in the production of pro-inflammatory cytokines (28). AIM2 and NLRP3 are also stimulated by the presence of hemozoin, which again promotes the production of type I IFNs, production of active IL-1 β , and causes caspase 1 activation (28). In addition to the multiple PAMPs produced during blood-stage infection, the destruction of erythrocytes during merozoite release from iRBCs produces three major damage-associated molecular patterns (DAMPs), which include heme, microvesicles, and uric acid.

Besides the production of heme by the parasite as a byproduct of hemoglobin digestion, heme is also produced via the oxidation of free hemoglobin released from RBCs. Free heme triggers TLR4 present on the surface of multiple APCs and endothelial cells. In macrophages and DCs, TLR4 activation causes the release of pro-inflammatory mediators. However, activation of TLR4 on endothelial cells promotes the surface expression of adhesion molecules, such as ICAM-1 (108), causing increased vascular permeability and infiltration of leukocytes into the tissues. This process ultimately results in membrane damage, necrotic cell death, and further inflammation (28). Heme is degraded by heme oxygenase 1,

without TLR4 activation, it results in anti-inflammatory effects and tissue repair that antagonize the effects of heme-associated TLR4 activation (28).

Host cells, including infected red blood cells, platelets, endothelial cells and leukocytes, use microvesicles for intracellular communication. These microvesicles can also contribute to inflammation through the delivery of TLR agonists. In malaria, microvesicles have been found to activate TLR4 on macrophages resulting in the release of inflammatory mediators, and TLR4 on endothelial cells, causing the expression of adhesion molecules (28).

The degradation product of nucleic acids derived from dying host cells also produces pro-inflammatory responses. Uric acid is produced as a byproduct of purine metabolism, and when present in sufficient quantities in the blood or other body fluids will form monosodium urate crystals. During *Plasmodium* infection, the buildup of uric acid and urate crystals has been found to activate the cytosolic receptor NLRP3 when internalized by phagocytes, resulting in caspase 1 activation and release of IL-1 β (28).

3.3 Adaptive immune effectors during blood-stage infection

Due to the importance of IFN- γ in the immune response to blood-stage infection, IFN- γ producing Th1 CD4⁺ T cells are an essential part of the adaptive immune response to iRBCs. Th1 CD4⁺ T cells promote improved humoral responses by providing B cell help, while the secretion of IFN- γ promotes B cell isotype switching to produce cytophilic IgG2a antibodies (108) and optimally activates CD8⁺ T cells (58).

Cytotoxic CD8⁺ T cells have also recently become appreciated for their role in protection against blood-stage malaria in *P. yoelii* infected mice, although iRBCs lack MHC class I molecules required to be recognized by the TCRs of CD8⁺ T cells (113). Instead, CD8⁺ T cell-mediated anti-blood stage immune

responses are Fas ligand (FasL) dependent, with iRBCs expressing the death receptor Fas on their surface. Fas-FasL interactions between the iRBC and the CD8⁺ T cell, respectively cause the infected erythrocyte to externalize phosphatidylserine, thereby allowing the infected cell to be more easily phagocytosed (113). In addition to this function, production of IFN- γ and inducible nitric oxide synthase production by CD8⁺ T cells has also been observed to promote improved immune responses toward *Plasmodium* as well as the direct killing of parasites and iRBCs (58).

The cytophilic anti-merozoite antibodies produced in response to IFN- γ secretion and Th1 mediated B cell help facilitate anti-blood stage immunity through three main actions. Antibody binding to free merozoites prevents the invasion of new red blood cell and recruitment of complement, which further prevents invasion as well as parasite killing by antibody-dependent cell-mediated cytotoxicity (ADCC) (114). The binding of antibodies to free parasites also acts as an opsonin, improving their uptake by macrophages and other phagocytic cells (58). The antibodies bound to iRBCs also act as opsonins and result in enhanced phagocytosis of these cells (58).

3.4 Major blood-stage antigens that serve as erythrocytic vaccine targets

Due to the numerous antigens involved in the invasion of erythrocytes by merozoites and the expression of variant surface antigens on the erythrocyte during blood-stage infection, there are a variety of antigens that have been targeted by erythrocytic vaccines. We will, therefore, focus on the antigens targeted by several vaccine candidates that have advanced to clinical trials.

Merozoite surface protein 1 (MSP1) has been a frequent target of blood-stage malaria vaccines, often in combination with other antigens. A recent phase I clinical trial of a combination *P. falciparum* MSP1 and EBA175 vaccine tested in healthy malaria naïve volunteers from India found that while the vaccine was well tolerated, that antibodies generated primarily against the EBA175 antigen PfF, while eliciting a

poor immune response to PfMSP1, likely due to antigen interference (115). Clinical trials conducted using a simian adenovirus ChAd63 and MVA vectored vaccine targeting the *P. falciparum* blood-stage antigens MSP1 and the apical membrane antigen 1 (AMA1) found that although the induction of strong cellular immune responses against these antigens was safe, that it did not affect blood-stage parasite growth (116). Also, immune interference was observed as anti-MSP1 responses were dominant over anti-AMA-1 responses (116). Later clinical trials of this vaccine noted that although the antibody response was not able to protect vaccinees against controlled human malaria infection, serum IgG levels against both antigens were boosted post-infection (117). These studies highlight the importance of considering antigen interference of dual or combination antigen vaccines.

Clinical trials of a vaccine candidate known as JAIVAC-1, which used mixture of recombinant *P. falciparum* blood-stage proteins targeting the 19kDa domain of MSP1 and the F2 domain of the erythrocyte binding antigen 175 (EBA175), demonstrated that this vaccine-elicited antibody responses against the EBA175 F2 domain, but not against MSP1 (115). Safety and immunogenicity testing has also been carried out using the *P. falciparum* region II of EBA175 delivered in aluminum phosphate antigen and has shown this vaccine to be well tolerated and capable of eliciting antibody responses in young adults (118).

AMA1 has also been a frequent target of single-antigen blood-stage malaria vaccines. A phase Ia clinical trial of the *P. falciparum* 3D7 blood-stage antigen AMA1 delivered as a recombinant protein formulated in the adjuvant Alhydrogel, with or without CPG 7909, or delivered using the ChAd63 and MVA vectors showed that IgG responses elicited by ChAd63 priming could be boosted by immunization with the recombinant protein, independent of the inclusion of CPG 7909 (119). This work also highlights the promise of heterologous prime-boost vaccinations including an adenoviral prime and protein boost, however further studies are required to determine if these responses can provide significant protection.

Phase 1 clinical trials of the FMP2.1/AS02 vaccine which uses the recombinant protein FMP2.1 targeting the protein AMA1 derived from the *P. falciparum* strain 3D7 formulated in the AS02 adjuvant found that the vaccine was well tolerated in children living in the endemic malaria nation of Mali and capable of inducing high antibody responses that were sustained by the one year follow-up (120).

Although there have been numerous erythrocytic vaccine clinical trials for *P. falciparum* derived antigens, there have been relatively fewer trials targeting *P. vivax*, and a distinct lack of anti-erythrocytic stage antigens. However, a further description of multiple pre-erythrocytic and erythrocytic *Plasmodium* spp. vaccine clinical trials have been reviewed by Moreno and Joyner (121). Additionally, many of the *P. falciparum* variant surface antigens that serve as immune targets and malaria vaccine candidates are reviewed in Chan et al. (122).

3.5 Use of anti-*Plasmodium* antibody responses to determine population-level malaria exposure through serological assays.

While repeat exposure to *Plasmodium* is required for individuals living in malaria-endemic regions to develop antibody responses capable of providing protection (123-125), the presence of anti-*Plasmodium* antibodies can be detected after a single infection (126). Serological assays can take advantage of the presence of these antibodies to indirectly measure malaria transmission intensity, a useful tool for determining malaria transmission in a large population where nucleic acid studies would be too costly (127). This method is especially advantageous in regions entering or undergoing elimination campaigns, as the reduction in malaria transmission has been found to result in increased numbers of sub-patent and sub-microscopic asymptomatic infections (128). In addition to the skilled staff required for detection of malaria by microscopy, the use of microscopy for detection of the level of exposure in the population is unfeasible. Serological assays, such as multiplex, have been compared with other measures of transmission intensity, including hospital records, PCR, and entomological inoculation rates (EIR) (127),

as well as comparing longitudinal versus cross-sectional study designs (129), and have been found to be robust and provide either improved or consistent results in comparison to these other commonly used methods of transmission assessment. Hospital records have been notably unreliable as the number of malaria-infected patients could be over-inflated due to the presence of other febrile illnesses within endemic malaria regions, such as dengue virus infection (127). The entomological inoculation rate, which measures the mosquito bites per person over a period of time, has been reported to be unreliable at times due to the heterologous distribution of mosquitoes (130). Additionally, this method relies on mosquito trapping with adult volunteers, which creates practical and ethical concerns, while also making these results difficult to extrapolate to children (127), who make up more than 70% of malaria deaths annually (1).

Serological transmission assessments, including multiplex assays, offer other advantages inherent to the assay. Unlike microscopy and nucleic acid-based tests, which provide information on the presence or absence of an active infection, serology relies on antibody detection, which provides a history of infection. These results can be used to determine the seroconversion, or when an individual becomes positive for a particular antibody response, and mapping seroconversion by age can be used to inform the distribution of resources for elimination campaigns. Conversely, the drop off in antibody-positive individuals can be used to determine historical changes in strains or species within a region (131). Furthermore, serological assays can use dried blood spot samples, which are relatively easy to collect, store, and process (132). Additionally, because bead-based multiplex assays have the ability to use antigens linked to microbeads associated with unique fluorescent dyes, this method can be used to detect multiple antigens within a single sample (132). Serological methods for malaria antibody detection have frequently been used by the CDC to aid in malaria elimination efforts in countries including Haiti (128, 129) and Mali (133). Due to the unique features of serological based assays, it is likely that these assays

will continue to see increased use to aid in elimination campaigns as we approach the goals set out by the WHO for reducing malaria transmission (134).

4. Gametocytes and sexual maturity of *Plasmodium*

4.1 Development of gametocytes

The study of gametocytes has been challenging as gametocytes are difficult to detect in the human host by routine microscopy since their numbers are below the threshold of detection. Furthermore, many epidemiological studies neglect the study of these forms as they are not related to symptomatology (135). Recent studies of malaria transmission using molecular tools to increase the gametocyte detection threshold have demonstrated that the carriers of submicroscopic gametocyte parasitemias are still able to infect mosquitoes and constitute a disease reservoir.

Gametocytes develop from the asexual blood-stage forms and appear between 7 and 15 days after the emergence of the blood forms (136). Studies in *P. falciparum* have shown that the decision to convert into gametocytes is taken before the production of merozoites since all of the merozoites from a single schizont will progress either to the asexual stages or to gametocytes (137, 138). In *P. berghei*, there is evidence that liver schizonts can produce gametocytes directly without the need for a blood-stage cycle (138). This can explain the early gametocytemia seen in *P. vivax*, as gametocytes appear almost simultaneously during *P. vivax* infection (139). So far, it is considered that gametocyte production is species and strain-specific. Studies based on the gene *Pfgig*, located on chromosome 9 has been related to the production of gametocytes, observed that culture of parasites with a disrupted *Pfgig* gene produce five times fewer gametocytes than wild-type controls (140).

Although it has been considered that the gametocytogenesis is a stress response to survive a hostile environment, the fact that progression to a sexual stage occurs early in the parasite life cycle seems to

contradict that idea (138). However, it appears that a variety of environmental stimuli (e.g., immune responses, the presence of reticulocytes or mammalian hormones) also induces the production of gametocytes (138) making it a response to environmental changes, guaranteeing the transmission to the mosquito which is the definitive host.

During gametocyte development, approximately 250 to 300 genes have shown to be upregulated at the mRNA level in transcriptomic studies (141, 142), with proteomic studies showing 350 gametocyte specific proteins in *P. falciparum* (143). The gametocytes exhibit 5 developmental stages within the vertebrate host and remain inside the host erythrocytes. In stage I and II of development, erythrocytes have a round appearance while taking the crescent shape of the parasite adjacent to the outer side of the gametocytes pellicle in latter stages. In the mature gametocyte, iRBC is a small cytoplasmic cover (136). Also, male and female gametocytes can only be differentiated morphologically from stage IV onwards. Giemsa stain allows for the differentiation of these parasites as female gametocytes have a small nucleus with a nucleolus and concentrated pigment resulting in violet color, while male gametocytes have a large nucleus with diffuse pigment giving a pink coloration (138). Stage I-IV gametocytes are sequestered in the bone marrow and the spleen, presumably to avoid immune clearance while stage V gametocytes are released into the bloodstream and only become infectious to the mosquito after 2 or 3 days of circulation (136, 138).

In the bone marrow CD36 appears to be the main ligand for the stage I-II gametocytes adherence, while ICAM-1, CD49c, CD166, and CD164 have been suggested as ligands for later stages (138). The expression of PfEMP-1 (*Plasmodium falciparum* Erythrocyte Membrane Protein – 1) in knob structures in erythrocytes infected with early-stage gametocytes suggest that this protein, which is the primary mechanism for cytoadherence and sequestration of asexual parasites, also plays a role in the bone marrow sequestration of early gametocytes, as later gametocyte stages do not express adhesive knobs expressing PfEMP-1 (138). It is not yet known which signals cause gametocytes to change their adhesion motifs

through their development, as the main proteins mediating the cytoadherence and sequestration in the late gametocyte stages have not been identified. The transcription profile of two proteins STEVOR (Sub-Telomeric Variant Open Reading frame) and RIFIN (Repetitive Interspersed family) suggest these proteins as possible adhesive proteins, but their role remains to be confirmed (138).

Following these processes, remaining development occurs within the mosquito midgut after gametocytes are taken up by a female *Anopheles* mosquito during a blood meal.

4.2 Immune response to gametocytes.

Epidemiological studies have demonstrated that there are host immune factors controlling gametocyte populations, as gametocytemia is higher in infants and non-immune population and gametocytemia decreases with the number of experienced infections (135). It also appears that areas with a low prevalence of malaria exhibit higher gametocyte loads (135). Although it can be considered that the reduction in gametocyte numbers are related to the control of asexual forms, the immune targeting of gametocyte proteins expressed in the red blood cell membrane has been described, and studies have demonstrated that gametocytes decrease faster than the asexual forms (135).

There are two main ways that the host immune system can attack the gametocytes: 1) inhibition of the sequestration, allowing the clearance of immature gametocytes before they become infectious, and 2) active clearance of circulating gametocytes. (138).

It is considered that the immune responses against PfEMP-1 are directed to both asexual stages and gametocytes and can, therefore, control these forms of the parasite through ADCC (138, 144). CD36, which is an early gametocyte ligand, also promotes the uptake of gametocyte-infected erythrocytes by monocytes and macrophages (138). Molecules in the surface of gametocyte-infected erythrocytes may

also induce immune responses which then promote the clearance of the circulating gametocytes, but so far no evidence of an antigen or a mechanism has been elucidated (138).

4.3 Major gametocyte antigens and vaccine targets

From the early studies of Gwardz and Carter using *P. gallinaceum*, antibodies within the host able to recognize gametocytes were described. These antibodies targeted the gametocyte proteins P48/45 and P230 but did not exert an effect in the human host. However, they were able to kill the gametes in the mosquito after they emerged from the red blood cell (145). Later epidemiological studies have shown naturally occurring antibodies against these targets (146-148). Importantly, these proteins do not show immune selection, with P48/45 and P230 exhibiting a limited level of antigenic polymorphism (145).

The P48/45 and the P230 proteins belong to a family of proteins denominated the six-cys motif protein family. These proteins contain 2 to 14 copies of a structurally similar domain characterized by conserved cysteine residues forming disulfide bonds (145). Several studies have shown that the characteristic of the disulfide bonds and structure are critical to maintaining the functionality of these proteins.

Both the P48/45 and the P230 proteins are present in the micro and the macrogametes. Studies with the *P. berghei* orthologous proteins have demonstrated that P48/45 is necessary for the fertility of microgametes, as P48/45 knockout macrogametes can be fertilized by wild-type microgametes, while knockout microgametes cannot fertilize wild-type macrogametes (145). P230 knockouts have also shown a reduction of the fertilization capacity of the gametocytes by reducing the binding of microgametes to the red blood cells to form fertilization centers (145). Further studies with monoclonal antibodies showed that the targeting of cells with monoclonal antibodies against P48/45 inhibits fertilization by blocking the macrogamete, while monoclonal antibodies against P230 were not able to block transmission (149).

Nevertheless, it has been demonstrated that for the antibodies against P230 to be effective, complement is needed (150). With this information, it can be inferred that a synergistic approach targeting both P48/45 and P230 is preferable than to target P230 alone as this protein does not seem essential for the fertilization process.

Early studies with P48/45 defined three separate, non-repeated, epitope regions on the P48/45 structure, all of which were conformation-dependent. Using monoclonal antibodies, Carter et al. demonstrated that the infectivity of the mosquitoes was significantly reduced with the antibodies that targeted epitope I, but not those that target of epitope II or III. However, further studies with combinations of monoclonal antibodies demonstrate that the simultaneous targeting of epitopes II and III could reduce the transmission (151). This suggests that a vaccine based on P48/45 should either include the whole protein structure or maintain the structure of these three epitopes for a subunit vaccine.

Another gametocyte protein that mediates gamete-gamete interactions is the HAP2 protein; this protein was first described in *Chlamydomonas* and is highly expressed in several species, including *Plasmodium* (152). Studies have shown that the disruption on HAP2 blocks the fertilization process by inhibiting the fusion of the gametes membranes (152). In addition, pre-clinical studies of a *P. berghei* HAP2 based vaccine showed promising results by reducing the *in vivo* mosquito infection by 34% (153).

5. Malaria in the Mosquito

5.1 Parasite development in the midgut, movement through the peritrophic matrix, differentiation, and migration to salivary glands for transmission to the next host

During its lifetime, a female mosquito must repeatedly take blood meals as a protein source to complete its egg development. This feature makes mosquitoes ideal transmitters of many blood-borne pathogens, including yellow fever, dengue, and Zika viruses, as well as the apicomplexan protozoa *Plasmodium* responsible for malaria (154). One of the difficulties of studying *Plasmodium* infections is the complex life cycle in both the host and the vector. Since sexual stage development and fertilization take place within the midgut lumen of the mosquito, the parasite is obligated to carry out its life cycle in the mosquito (154). The *Plasmodium* infection is also a challenge for the vector innate immune responses which must respond to the multiple stages and the anatomical locations of the parasite throughout the infection.

Infection begins upon ingestion of male and female gametocytes present in the blood of the vertebrate host from which the mosquito takes a blood meal (155). Over a period ranging from 18-24 hours, the male and female gametocytes undergo gametogenesis to develop into gametes. The mature gametocytes start developing in the mosquito midgut inside the red blood cells taken in the *Anopheles* blood meal after receiving environmental cues present in the midgut including 1) the change from a warm-blooded host to the mosquito, which includes a temperature reduction of approximately 5 °C, 2) a pH increase, and 3) xanthurenic acid a byproduct of the mosquito eye pigment synthesis (136). These mature gametocytes can follow one of two pathways, female macrogametes or male microgametes (136). When the male microgametes fertilize the female microgamete in the midgut lumen, a diploid zygote is formed (156). The zygote then divides via meiosis to develop into a motile form known as the ookinete (157). From the tens of thousands of gametocytes ingested initially, typically 50-100 ookinetes are produced (155). Ookinetes then travel to the peritrophic matrix that lines the midgut lumen and traverses this barrier to

invade a single midgut epithelial cell. After entry into the epithelial cell, the ookinete must travel to the basal lamina to differentiate into an oocyst before the infected cell is extruded from the epithelial layer. Typically between 5-200 oocysts are produced (158). Over the next ten days, the oocysts further develop into approximately 50,000 sporozoites that are released into the hemolymph of the open circulatory system of the mosquito known as the hemocoel, at approximately two weeks after the initial blood meal (154, 157). These sporozoites then migrate to the salivary glands and traverse the salivary gland epithelium to arrive at the salivary gland lumen, allowing the sporozoites to be mixed with the saliva to be injected into the next host during a blood meal (154, 157). Of the thousands of sporozoites released into the hemolymph, approximately 11,000 sporozoites successfully make the journey to the salivary gland lumen and between 10 and 100 sporozoites are injected into the next host during a single blood meal (155).

5.2 Physical barriers to infection

Infection of *Anopheles* by *Plasmodium* also poses a threat to the vector, which in response has evolved a variety of innate immune defense mechanisms to combat the infection. As noted in the previous section, the parasite must traverse, the peritrophic matrix, the midgut epithelium, and the salivary gland epithelium during its development and migration process. Thus, the *Plasmodium* parasite experiences major survival bottlenecks, which can be observed as a substantial stage-specific reduction in parasite numbers during these events. Luminal and epithelial innate immune responses account for the majority of parasite reduction (157). However, humoral immune responses also play a major role in this reduction and will be discussed in detail in later sections.

The first physical barrier faced by the *Plasmodium* parasite within the mosquito is the chitinous peritrophic matrix. The peritrophic matrix is composed of polymers secreted by cells of the midgut epithelium which surround the bolus of blood ingested by the mosquito and serves as another layer of

protection from bacteria, parasites, and other pathogens that were also taken up during the blood meal (159, 160). This is evidenced by reports that infectivity is reduced in *P. gallinaceum* infected *Aedes aegypti* when the thickness of the peritrophic matrix is increased (161).

After crossing the peritrophic matrix, the next barrier faced by the parasite is midgut epithelium, which separates the hemocoel from the digestive enzymes and potential pathogens within the midgut lumen (160). This barrier is made up of polarized epithelial cells that possess microvilli on the apical surface facing the lumen and are responsible for the secretion of enzymes that aid in digestion and nutrient absorption (160). The basolateral membrane of the midgut epithelial cells contains complex convolutions which create increased surface area to allow for the transport of water, ions, and other molecules (160, 162). The epithelial cells are connected via the basal membrane to the basal lamina, which separates hemolymph and other hemocoel contents from the midgut, while still allowing for the entry of soluble immune factors from the hemocoel (160, 162). The midgut cells also possess rigid junctional complexes at the apical region that mechanically link the cells together or allow for intracellular communication (160). Due to the rigid nature of this junction, the route through the epithelial cells may be the less challenging route for the parasite to take to reach the basal lamina. Outside the basal lamina is a layer of muscle encases the midgut and allows for the distension of the midgut during a blood meal (160).

Similar to the process of hepatocyte invasion by the sporozoite, the cell-traversal protein for ookinetes and sporozoites (CeTOS) has been found to be essential for infectivity of the mosquito as targeted disruption of CeTOS in *P. berghei* reduces the infectivity of *Anopheles stephensi* mosquitoes 200-fold compared to wild-type parasites (163). This is due to the role of CeTOS in ookinete traversal of the midgut epithelium (163).

Finally, in order to be transmitted to the next host, the sporozoites that are released into the hemolymph during their development in the mosquito must enter the mosquito salivary glands. The mosquito proteins saglin and circumsporozoite binding protein (CSPBP) act as receptors for the

thrombospondin-related adhesion protein (TRAP) and circumsporozoite protein (CSP), respectively. The interaction between these receptors and the proteins on the surface of the invading sporozoite allows the parasite to bind and penetrate the cells of the mosquito salivary gland (164). The importance of TRAP in sporozoite entry of the salivary gland has been demonstrated, as studies of TRAP deficient mutant sporozoites were reduced in the salivary gland, although they were abundant in the hemolymph (8).

5.3 The effect of mosquito microbiota on infection

Like humans, mosquitoes are host to communities of diverse bacteria which concentrate in the digestive tract. In recent years, the effect of the mosquito microbiota on survival and development of pathogens, including *Plasmodium*, has come to be more greatly appreciated, although this area is still under investigation (165). Several reports indicate that the presence of certain species of Gram-negative bacteria within mosquito midguts are associated with inhibition of the development of *Plasmodium* parasites within the midgut (165-168). In addition, it has been observed that the majority of bacteria that make up the microbiota of the mosquito are Gram-negative (165), which serves an advantage to the mosquito if they offer protection from more harmful pathogens. The microbiota has also been found to reduce mosquito permissiveness to infection, as antibiotic treatment of *An. gambiae* allowed for increased *P. falciparum* oocysts numbers following infection (165).

Several mechanisms may contribute to the modulation of *Plasmodium* infection by the microbiota. One explanation is that following a blood meal, bacteria populations increase by 70-16,000 fold in the midgut (169) and as a result, there is increased production of anti-microbial peptides by the mosquito (154). As a result, this increase in antimicrobial peptide production may enhance the ability of the mosquito to eliminate or interrupt parasite growth. Another possible explanation is that bacteria-derived factors may also kill off *Plasmodium* parasites within the midgut (170). This second hypothesis has recently been supported by studies on *Enterobacter* populations within *An. gambiae* which demonstrated

that *Enterobacter* derived reactive oxygen species are capable of preventing the infection of the mosquito by *P. falciparum* and that this interaction was also mosquito-independent (171).

5.4 Recognition of *Plasmodium* by mosquito PRRs, major immune signaling pathways, and effector mechanisms

Although as invertebrates, mosquitoes lack an adaptive immune system, there are multiple innate immune mechanisms, including pattern recognition receptors, with which the mosquito can recognize *Plasmodium* parasites during infection. PRRs that have been identified in *An. gambiae* include C-type lectins, thioester containing proteins (TEPs), peptidoglycan recognition proteins (PGRPs), scavenger receptors (SCRs), galactoside-binding lectins (GALE), Gram-negative binding proteins (GNBPs), and fibrinogen-like domains (FBNs) (172).

In addition to the recognition of Gram-negative bacteria, GNBPs have been found to be upregulated following *Plasmodium* infection (173, 174). GGBP4 has been demonstrated to participate in the killing of *P. berghei*, but not *P. falciparum*, while GGBP2 can kill *P. falciparum* but is less effective against *P. berghei* (174). The fibrinogen-related protein FBN9 has also been shown to bind to ookinetes during their invasion of the midgut epithelium (175), and may likely contribute to the killing of *Plasmodium*, as they are essential for killing bacteria and maintaining homeostasis of the mosquito immune system (174).

The recognition of *Plasmodium* by peptidoglycan recognition proteins and dGNBP1 has been found to activate the mosquito Toll pathway (157), which signals via receptor homologs of the human Toll pathway. Upon recognition of *P. berghei* derived molecules by PGRPs, a serine protease cascade is activated and causes the binding of the signaling molecule Spätzle to the mosquito Toll receptor. This binding initiates downstream signaling through MyD88, which recruits the protein Tube, which then

recruits Pelle and TRAF (157). TRAF activation causes the transcription factor Rel1 to translocate to the nucleus of the mosquito cell and upregulate transcription of immune genes, including antimicrobial effectors and genes responsible for microbial killing (157). Antimicrobial peptides expressed as the result of Toll signaling in mosquitoes include defensins and cecropins (176).

Another major immune signaling pathway in mosquitoes is the IMD pathway, which results in downstream signaling via the JNK and NF κ B pathways. Following the recognition of *P. falciparum* by the transmembrane PGRP-LC receptor, IMD is recruited to the cytosolic domain, leading to recruitment and activation of FADD and subsequently Dredd. Activation of these molecules leads to signaling via the NF κ B pathway and cleavage of the transcription factor Rel2, allowing for its translocation into the nucleus. Once in the nucleus, Rel2 causes the upregulation of anti-*Plasmodium* anti-microbial effectors (157) such as gambicin and attacin (176).

Although the thioester-containing proteins (TEPs) of mosquitoes have pattern recognition function, these hemolymph proteins also share structural similarities with vertebrate complement components. Early studies in *An. gambiae* demonstrated that the TEP1 gene has been found to be upregulated following *P. berghei* infection (177). However, this protein is also present in the mosquito hemolymph prior to *Plasmodium* infection (178). Structurally similar to the complement protein C3 in humans (178), TEP1 was later identified as a hemocyte produced opsonin which is secreted into the hemocoel as an inactive form that requires proteolytic cleavage to mediate its function (174). The cleaved TEP1 protein is then stabilized by the leucine-rich repeat proteins LRIM1 and APL1C prior to binding ookinetes in the midgut, leading to their destruction by phagocytic cells (174).

Additional humoral responses to *Plasmodium* include melanization. In this pathway, serine protease cascade is activated in response to the recognition of the pathogen. This pathway activates pro-phenoloxidasases which generate a second cascade, ultimately resulting in the generation of melanin and free radicals. The free radicals produced help to directly kill pathogens, while melanin is deposited on the

surface of the pathogen resulting in its encapsulation (154, 157, 174). The biochemical signaling pathways involved in the melanization immune response is reviewed in Christensen et al. (179).

6. Transmission Blocking Immunity

6.1 Developing Transmission Blocking Vaccines

The main objective of Transmission Blocking Vaccines (TBV) for malaria is to prevent the infection in the mosquito and therefore reduce the disease burden in a population (135). This concept of protection is different from liver or blood-stage disease vaccines which offer individual protection against the infection or the disease manifestations (135). Instead, the main benefit of TBVs is reducing the number of cases of malaria over time as an eradication measure. Furthermore, TBVs will increase the efficiency and sustainability of other control tools (135). As mentioned before, malaria is transmitted by mosquitos from the *Anopheles* genus, and transmission intensity depends on the number of *Anopheles* mosquitos in a given area and the prevalence of gametocytes in the peripheral blood of the population. It is important to mention that in an endemic area, more than half of the population carries malaria parasites in the blood as an asymptomatic infection. As a result, these individuals constitute one of the main reservoirs for malaria transmission and are the target of TBV (135).

The main concept of TBVs is to induce antibodies in the human host which will be taken up by female *Anopheles* mosquitoes during a blood meal and block the development of the mature parasite forms in the mosquito midgut, thereby rendering the mosquitoes unable to infective more individuals (135, 145). There are several controversies concerning the use of transmission-blocking vaccines. First, TBVs will not protect the vaccinated persons but reduce transmission, which will make them only effective in endemic areas (180). Second, the general opinion is that unless there is a population coverage

between 80 and 100% of the gametocyte carriers, the beneficial effects will not be seen (135, 145). In addition, TBVs could be dangerous if they delay or prevent the acquisition of naturally acquired immunity (135). Nonetheless, studies evaluating the impact of vector control measures have demonstrated that the reduction of transmission in medium to high transmission areas induces a significant reduction in all-cause mortality, with the youngest age groups of the population receiving the most benefit (181-183).

6.2 Anti-parasite antibody uptake and neutralization of the parasite within the mosquito

After induction of antibodies against mosquito stage antigens in the mammalian host, how do these antibodies exert their transmission-blocking functions in the vector? Since the parasites emerge into the mosquito midgut after the female *Anopheles* mosquito ingests the infected red blood cell, these forms are exposed to multiple plasma elements present in the mosquito blood meal including complement, granulocytes and most importantly the host-derived antibodies (135, 145). These components play a role affecting the normal development of the parasite sexual forms within the mosquito and ultimately reducing the transmission. Studies have shown that if the Fab fragments of monoclonal anti-P28 antibodies are active, complement is not required for the killing of the parasite (145). Nonetheless, human sera with anti-Pvs25 (*P. vivax* P25) antibodies loses its killing activity after heat inactivation, indicating that complement is necessary to block transmission with P25 vaccine-induced antibodies (184). If the ookinetes are incubated with anti-P28 antibodies both in culture or through membrane feeding assays, they show extensive damage in the plasmalemma and the cytoplasm, suggesting a killing mediated by the complement (185).

Antibodies against the P25 protein can also block the migration of the ookinete through the mosquito midgut, as anti-P25 antibodies in *P. gallinaceum* block the passage of the ookinete through the peritrophic membrane secreted by the mosquito midgut to containing the blood meal (186). It can be therefore considered that the antibodies against P28 and P25 affect both the zygote and the ookinete during the first hours after the blood meal as these antibodies can promote an antibody-dependent cytotoxicity

mechanism in the presence of host complement and immune cells in the midgut. However, after complement is degraded, these antibodies show a neutralization function which prevents the migration of parasite forms that were not killed previously.

6.3 Major *Plasmodium* antigens expressed in the vector that serve as transmission-blocking vaccine targets

The *Plasmodium* parasite must complete the sexual stage of its development in the mosquito before it can be transmitted to the vertebrate host. Two major classes of antigens are present in the vector, 1) the pre-fertilization antigens that are expressed in the gametocyte in the human and the gametes in the mosquito, which are described in the gametocyte section and 2) the post-fertilization antigens which are only expressed in the mosquito. The post-fertilization antigens are present in the zygotes and ookinetes, and antibodies recognizing these forms prevent the invasion of the mosquito midgut (156, 187). Under natural conditions, the human host is not exposed to the post-fertilization antigens. Therefore there would not be a natural boosting effect during infection and which may result in a short-lived response. Therefore, highly immunogenic formulations able to produce long-lasting, effective antibody levels are necessary (145).

Of the post-fertilization antigens, the best characterized is the P25 protein. P25 mRNA is present in the gametocytes, but the protein appears after the gametes emerge from the red blood cell in the mosquito midgut (136, 145). P25 is present on the surface of the zygotes and the ookinetes and mediates several functions including promoting the clustering of the ookinetes thereby allowing them to survive the midgut proteolytic environment (188). P25 also mediates the attachment and invasion of the mosquito midgut by damaging the midgut epithelium (189-191) and posteriorly binding to laminin and collagen IV in the basal membrane. The attachment of the oocyst to the basal membrane is the starting signal for the

development from ookinete to oocyst (192, 193) and therefore P25 is essential for the parasite to complete its life cycle.

P28 is a paralog of P25 present in several *Plasmodium* species and is speculated that this protein arose as a product of gene duplication (194). Studies in *P. berghei* have shown that deleting either P25 or P28 has a significant effect in transmission, while deletion of both proteins leads to complete prevention of midgut infection (195). Nonetheless, it has been demonstrated that sufficient antibody titers against one of these proteins can effectively block transmission (196).

Phase I clinical trials using Pvs25 have shown that humans can produce anti-P25 antibodies. Nevertheless, an ideal vaccine and adjuvant formulation has not been obtained. The first reported clinical trial of a protein-based Pvs25 vaccine candidate adjuvanted with alum showed poor immunogenicity with antibodies elicited unable to block transmission (184). A subsequent clinical trial using a protein-based Pvs25 in Montanide ISA 51 adjuvant, demonstrated that low doses of the formulation were able to induce transmission-blocking immunity, but higher doses were associated with systemic adverse effects (197).

After the completion of both the *P. falciparum* and *P. berghei* genomes, a family of secreted proteins consisting of multiple adhesive “animal-like” domains present in the gametocytes was described (136). This protein family known as the PfCCp (*P. falciparum* *Limulus* coagulation factor C domain-containing proteins) in *P. falciparum* (198) or as PbLAP (*P. berghei* LCCL-Lectin adhesive like proteins) in *P. berghei* (199) is expressed in the gametocytes at stage II of their maturation, but expression stops following fertilization and development of the zygote. Knockout studies have demonstrated that these proteins do not affect the gamete fertilization or the normal maturation of the zygote into the oocyst but reduce the formation of sporozoites from the midgut oocyst and block the transition of the oocyst sporozoites into the mosquito salivary glands.

Another family of proteins with adhesive functions is the protein family comprising the von Willebrand factor-like A domains and thrombospondin type 1-like domains. Members of these protein

family include CSP and TRAP Related Protein (CTRP), Membrane Attack Ookinete Protein (MAOP), Secreted Ookinete Adhesive Protein (SOAP) and Willebrand factor A domain Related Protein (WARP). Gene disruption studies with the members of these protein families have demonstrated that these proteins mediate ookinete infectivity in the midgut (136). These examples make the adhesive domains and adhesive function proteins an attractive target for a transmission-blocking vaccine, as they mediate critical steps in the development and maturation of the parasite oocysts.

Conclusions

In summary, the complexity of the *Plasmodium* life cycle requires that vaccinologists have an in-depth understanding of the major events of that occur at each stage of the parasite life cycle in order to successfully halt the parasite development. After the completion of the RTS,S/AS01, the field of malaria vaccinology came to appreciate that a second generation of malaria vaccine would be required to target this disease effectively.

Based on the results of clinical trials of malaria vaccines, it seems that a multi-stage approach is necessary to prevent disease and eradicate malaria as the complexities of the life cycle and diverse antigenic profile in each stage requires multiple targets to control parasites that can escape responses against the previous stage. This is evidenced by the high levels of anti-pre-erythrocytic immunity required to prevent a blood-stage infection. Therefore, a combined pre-erythrocytic and erythrocytic stage vaccines may be necessary to prevent illness. It should also be noted that both cellular and humoral adaptive immune responses are required to control both the liver and the blood-stage parasite forms. This suggests that a combination of vaccine platforms, such as heterologous vaccination regimens, able to induce both arms of the immune system in a high magnitude (i.e. heterologous vaccination regimens) may be essential for an effective malaria vaccine.

Furthermore, transmission-blocking candidates would be necessary in endemic areas as a part of an eradication campaign that includes vector control, active surveillance, chemotherapy of infected individuals irrespective of their symptomatology, in addition to vaccination.

Chapter 2

A prime-boost immunization regimen based on a Simian Adenovirus 36 vectored multi-stage malaria vaccine induces protective immunity in mice

Jairo A. Fonseca^{a,b,1}, **Jessica N. McCaffery**^{a,1}, Elena Kashentseva^c, Balwan Singh^a, Igor Dmitriev^c,
David T. Curiel^c, Alberto Moreno^{a,b*}

- c. Emory Vaccine Center, Yerkes National Primate Research Center, Emory University, 954 Gatewood Road, Atlanta, GA 30329.
- d. Division of Infectious Diseases, Department of Medicine, Emory University School of Medicine, Atlanta, GA 30307.
- e. Cancer Biology Division, Department of Radiation Oncology, Washington University School of Medicine 660 S. Euclid Ave., 4511 Forest Park Blvd, St. Louis, MO 63108.
- 1. These authors contributed equally to this publication.

Originally published in Vaccine:

Fonseca JA, McCaffery JN, Kashentseva E, Singh B, Dmitriev IP, Curiel DT, Moreno A. (2017). A prime-boost immunization regimen based on a simian adenovirus 36 vectored multi-stage malaria vaccine induces protective immunity in mice. *Vaccine*. 2017 May 31;35(24):3239-3248. PMID: 28483199.

doi: 10.1016/j.vaccine.2017.04.062.

Copyright © 2017, Elsevier.

Abstract

Malaria remains a considerable burden on public health. In 2017, the WHO estimates there were 219 million malaria cases causing nearly 435,000 deaths globally. A highly effective malaria vaccine is needed to reduce the burden of this disease. We have developed an experimental vaccine candidate (PyCMP) based on pre-erythrocytic (CSP) and erythrocytic (MSP1) stage antigens derived from the rodent malaria parasite *P. yoelii*. Our protein-based vaccine construct induces protective antibodies and CD4⁺ T cell responses. Based on evidence that viral vectors increase CD8⁺ T cell-mediated immunity, we also have tested heterologous prime-boost immunization regimens that included human adenovirus serotype 5 vector (Ad5), obtaining protective CD8⁺ T cell responses. While Ad5 is commonly used for vaccine studies, the high prevalence of pre-existing immunity to Ad5 severely compromises its utility. Here, we report the use of the novel simian adenovirus 36 (SAd36) as a candidate for a vectored malaria vaccine since this virus is not known to infect humans, and it is not neutralized by anti-Ad5 antibodies. Our study shows that the recombinant SAd36PyCMP can enhance specific CD8⁺ T cell response and elicit similar antibody titers when compared to an immunization regimen including the recombinant Ad5PyCMP. The robust immune responses induced by SAd36PyCMP are translated into a lower parasite load following *P. yoelii* infectious challenge when compared to mice immunized with Ad5PyCMP.

Introduction

Malaria remains a considerable burden on public health. In 2017, there were an estimated 219 million cases of malaria and 435,000 deaths, most of which occurred in children under 5 years of age, being a leading cause of death in this population (1). A vaccine against malaria is a research priority and an essential tool for control and elimination efforts.

The development of an effective malaria vaccine has been a challenge due to the complex *Plasmodium* life cycle (108). The pre-erythrocytic stage is initiated by the injection of sporozoites into the dermis by *Anopheles* spp mosquitoes. The sporozoites then travel via the circulatory system to invade hepatocytes, where the parasite then differentiates and produces tens of thousands of infectious merozoites per infected hepatocyte that burst to release the parasites into the circulatory system where they invade erythrocytes. Within the erythrocyte, the parasite again undergoes a cycle of growth and proliferation, ultimately resulting in the bursting of the erythrocyte and the release of new infectious merozoites to continue the erythrocytic stage of infection, and the clinical symptomatology associated with malaria.

Several key proteins are responsible for the motility and invasion of the infectious forms into their respective target cells. During the pre-erythrocytic stage, the circumsporozoite protein (CSP) and the thrombospondin-related adhesive protein (TRAP) are responsible for the gliding motility and infectivity of the sporozoite (5, 8). Similarly, the merozoite surface protein 1 (MSP1) is involved in the invasion of the merozoite into the erythrocyte, and antibodies targeting MSP1₁₉ have been found to inhibit merozoite invasion of erythrocytes in humans (101).

Many malaria vaccine candidates have therefore aimed to target the pre-erythrocytic antigens to prevent hepatocyte infection and the erythrocytic antigens to prevent clinical manifestations. Radiation-attenuated sporozoites have been used to produce sterilizing immunity, but this method remains impractical for widespread use due to logistical constraints (108). Furthermore, the most advanced malaria vaccine candidate, RTS,S/AS01, has failed to produce long-lived efficacy (200, 201), likely due

to lack of CD8⁺ T cell responses induced and its design based on a single pre-erythrocytic stage antigen target, CSP (202), as a single sporozoite that evades immune responses induced against CSP can produce tens of thousands of blood stage merozoites (51, 70, 108). Moreover, preclinical murine studies on a vaccine candidate based on two pre-erythrocytic-stage antigens, CSP and the thrombospondin-related adhesive protein (TRAP), have not shown increased efficacy compared to single antigen vaccines (89). Therefore, we hypothesize that a malaria vaccine targeting multiple *Plasmodium* stages is necessary for optimal induction of protective immunity.

We have designed *P. yoelii* chimeric recombinant protein-based vaccines, constructed by binding of cognate promiscuous T cell epitopes (i.e. capable of binding to 10 or more MHC class II molecules) to well characterized B-cell epitopes, representing CSP and the erythrocytic-stage antigen merozoite surface protein 1 (MSP1) (203, 204). We also have expressed a hybrid protein by genetic fusion of the chimeric CSP and MSP-1 proteins (90), designated *P. yoelii* Chimeric Multistage Protein (PyCMP). This vaccine protected mice from experimental challenge through induction of CD4⁺ T cells and antibodies (90). However, the lack of induction of protective CD8⁺ T cells led us to pursue an adenovirus-vectored malaria vaccine, and we reported that an Ad5 prime and two proteins boosts significantly increased the PyCMP protective effect (93).

Despite the relevance of the Ad5-based vector as promising vaccine platform, adult populations exhibit a high prevalence of pre-existing anti-Ad5 neutralizing antibodies, limiting the effectiveness (205, 206). Simian adenoviruses provide a promising alternative, as they maintain the same safety profile as Ad5 (205, 207) and the level of anti-vector neutralizing activity of human sera has been found to be low (208). In addition, the use of simian adenoviruses in Ebola Virus (209, 210), HIV (207), HCV (211), and malaria (116, 212-214) vaccine candidates provides further support for the safety and utility of these vectors.

Here we evaluated the immunogenicity and protective efficacy of a heterologous Ad prime – protein boost vaccination regimen, testing three different doses of the simian adenovirus 36 (SAd36), a vector

resistant to neutralizing anti-Ad5 antibodies (208). This vector was engineered to express the synthetic PyCMP gene. We show that immunization regimens including SAd36PyCMP improves immunogenicity and efficacy in comparison to Ad5 vectored PyCMP, making SAd36 a promising vector for the development of an effective malaria vaccine.

Materials and Methods

Viral Vectors. The replication incompetent Ad5PyCMP vector was constructed using the E1-deleted Ad5 backbone as we previously described (93, 215). To construct the genome of simian adenovirus 36 SAdV-36 from species E containing the PyCMP transgene cassette in place of the deleted E1A/B genes we used the strategy originally described by Roy et al. (208). We employed the E1-deleted molecular clone pC36.000.CMV.PI.EGFP.BGH (p1411) of an SAd36 vector expressing eGFP and a pShuttle plasmid that were kindly provided by Dr. James M. Wilson (Penn Vector Core – Gene Therapy Program, University of Pennsylvania). The PyCMP-coding sequence was cloned into the pShuttle plasmid between the CMV promoter and BGH polyadenylation signal. The expression cassette was excised with I-CeuI and PI-SceI restriction enzymes and ligated to plasmid DNA containing the SAd36 genome, which was linearized using unique I-CeuI and PI-SceI restriction sites introduced in place of E1 region. The ligated DNA was transformed into *E. coli* strain, XL10-Gold (Stratagene), to select the plasmid containing viral genome carrying the CMV-driven PyCMP transgene. The constructed genome was released from plasmid DNA by digestion with PacI and transfected into HEK293 cells to rescue the replication incompetent SAd36PyCMP vector. Both SAd36PyCMP and SAd36-GFP vectors were upscaled in HEK293 cells and then purified using double cesium chloride gradient centrifugation as described (216). The purified vector preparations were dialyzed against PBS containing 10% glycerol, and viral particle (vp) titers were determined based on absorbance at 260 nm as described by Maizel et al. (217).

Chimeric Vaccine, Immunization Regimens, and Parasites. The *PyCMP* gene is a 1242bp gene encoding a chimeric antigen based on the *P. yoelii* CSP genetically linked to a chimeric *P. yoelii* MSP1. The transgene expression and purification have been previously described (90, 92).

Female CB6F1/J (H-2^{db}) mice, 6 to 8 weeks of age, were purchased from Jackson Laboratory. This strain was selected based on the response of syngeneic mice to chimeric antigens (218) and to characterize T cells response via the H-2K^d/SYVPSAEQI/APC tetramer (Tetramer Core Facility, Emory University) which includes the CTL epitope of the *P. yoelii* CSP included in *PyCMP*. Mice (n= 10 per group) were primed intramuscularly at day 0 with recombinant SAd36 at a dose of 10⁶ (Low dose), 10⁷ (Intermediate dose), or 10¹⁰ v.p. (High dose), or the previously protective recombinant Ad5 10⁷ v.p. dose (92, 93). All mice received two boosting immunizations with 20 µg of *PyCMP* emulsified in Montanide ISA 51 (Seppic, Fairfield, NJ) at days 30 and 60. Naïve mice (n=10) were used as a control (Table 1). Mice were bled 20 days after each immunization for assessment of antibody titers via ELISA. PBMCs were obtained from mouse whole blood samples at days 10, 20, 40, 50, and 70 post-priming and were processed for flow cytometry.

Anopheles stephensi P. yoelii 17XNL infected mosquitoes were obtained from the NYU School of Medicine insectary core facility. At day 80 after the priming immunization, experimental challenges were done intravenously using 100 freshly isolated sporozoites. Follow-up of parasitemia and hemoglobin (Hb) was performed as previously reported (90). Hemoglobin levels below 5 g/dl were considered severe anemia and animals with this condition were euthanized. All procedures were approved by Emory University's IACUC and followed accordingly.

ELISA assays. The antibodies elicited by immunization with the hybrid protein and their IgG isotype profiles were determined by ELISA as described (204). The avidity of antibodies was assessed by a thiocyanate elution ELISA as described previously (92, 219, 220) and calculated as described by Perciani et al. (221).

Flow cytometry assays. To measure PyCMP-specific CD8⁺ and CD4⁺ T cells, peripheral blood was collected into 3.7% sodium citrate tubes at days 10, 20, 40, 50, and 70 post priming. Erythrocytes were lysed with ACK buffer (Life Technologies). After washing, the cells were incubated with LIVE/DEAD fixable yellow stain (Life Technologies) per the manufacturer's protocol. PBMCs were then incubated with the following antibodies for 30 minutes for analysis by flow cytometry: α -CD3 ϵ -PerCP, α -CD4-Alexa Fluor 700 (eBioscience), α -CD11a-PerCP-Cy5.5, α -CD49d-FITC, α -CD8-APC-Cy7, and the H-2Kd/SYVPSAEQI/APC tetramer. All antibodies were from Biolegend unless noted otherwise. The cells were initially gated on SSC/FSC, and the frequency of tetramer-positive cells was determined on the gated CD11a⁺CD8⁺ population. The co-expression of CD11a and CD49d were used to identify antigen-specific effector CD4⁺ T cells as previously described (Supplementary Figure 1) (222).

Cellular immune responses in the spleen were measured by ICS to simultaneously analyze IL-2, IFN- γ , and TNF- α at the single-cell level in T cells 5 days after the final boosting immunization as described (92). Cells were stimulated with either PyCMP or one of three peptide pools of 15-mer synthetic peptides overlapped by 10 amino acids peptides representing PyCMP. Pool 1 contained 14 peptides representing the PyCSP chimeric antigen (203); pool 2 contained 24 peptides representing the MSP1 derived promiscuous T-cell epitopes, and pool 3 contained 20 peptides representing the PyMSP1₁₉ sequence (90). Cells were stimulated for 6 hours with the protein or pools at 2 μ g/ml at 37°C in the presence of GolgiPlug (BD Biosciences). Cells were then incubated for 15 min with CD16/CD32 before surface staining for 30 min with α -CD3 ϵ -PerCP-Cy5.5, α -CD8 α -BV605, and α -CD4-Pacific Blue. Permeabilized cells were then stained intracellularly for 30 min with α -IFN- γ -FITC, α -IL-2-APC, and α -TNF- α -PE. Flow cytometry acquisition was performed using an LSRII (BD). Data were analyzed using FlowJo V10. The leukocytes were initially gated on CD3⁺CD4⁺ and CD3⁺CD8⁺; then antigen-specific cytokine-secreting T cells were identified (Supplementary Figure 2). The frequency of antigen-specific cytokine-producing cells was determined by subtracting the percentage of cytokine-producing T cells after incubation with medium alone from the percentage of cytokine-producing T cells after incubation with

PyCMP or peptide pools. A threshold for a positive cytokine response was set above the background, and samples that did not meet this requirement were set to zero. Analyses of multifunctional T cell responses were performed using a Boolean analysis in FlowJo and SPICE software (223).

Statistics. Statistical analysis and graphs were made using GraphPad Prism software. Antibody responses and tetramer staining data were log-transformed to achieve normality, permitting parametric testing and comparison using one-way ANOVA with Bonferroni's post-test. For cytokine-secreting cells, Kruskal-Wallis test with Dunns post-test was used. In experimental challenges, parasitemia differences between groups were evaluated by comparing areas under the curve of parasitemia versus time and parasitemia peak values using Kruskal-Wallis test with Dunns post-test.

Results

Infectivity of Simian Adenovirus 36 compared to Ad5

SAd36 exhibits characteristics that make it desirable as a vector beyond its resistance to anti-Ad5 antibodies (208). The AB loop within the knob domain of the SAd36 fiber, which mediates binding of CAR-binding human Ad serotypes, is identical to human Ad4 (species E) and is very similar to Ad2, Ad5 (species C) and Ad12 (species A) (224). This suggests that the fiber knob could mediate SAd36 binding to CAR similar to chimpanzee adenovirus CV-68 (species E) (225). In addition, the SAd36 penton base includes an RGD motif in one of the two surface loops, suggesting that integrins may also play a role in virus internalization giving this vector different infection routes which could potentially make it a more efficient infectious agent than Ad5.

To evaluate the infectivity of SAd36 derivatives with respect to Ad5-based vectors, we tested a generated SAd36-GFP vector along with previously described Ad5-GFP vector using gene transfer assay in human A549 and murine N2A cells. The levels of gene transfer mediated by SAd36-GFP were about

100-fold lower in both human and mouse epithelial cells when compared to the Ad5 vector.

(Supplementary Figure 3).

Immunization with SAd36 Induces Comparable Quantity and Quality of Antibodies as Ad5

We previously determined that heterologous adenoviral prime-protein boost regimens are the most efficacious where the combination of adenovirus and protein is used (92, 93). We, therefore, used one of three doses of the recombinant simian adenoviral vector at either 10^6 , 10^7 , or 10^{10} v.p for priming to determine the optimal dose to induce protective efficacy. Mice primed with recombinant Ad5 at 10^7 v.p., as well as mice receiving no immunizations, were used as controls (Table 1). Following an intramuscular adenoviral prime at day 0, mice were boosted with 20 μ g of the PyCMP protein emulsified in a 1:1 volume ratio of Montanide 51 ISA VG adjuvant subcutaneously at days 30 and 60 post priming.

To determine the effect of SAd36 prime-PyCMP protein boost regimens on antibody responses and the impact of the dosage, antibody titers were measured by ELISA against the PyCMP protein. Antibody titers determined from sera obtained at day 20 post prime revealed that immunization regimens that included a priming immunization with SAd36 at doses of 10^6 and 10^7 v.p. elicited antibody titers comparable to mice primed with 10^7 v.p. of Ad5 (Figure 1A). In addition, mice primed with SAd36 at 10^{10} v.p. had significantly higher antibody titers compared to both SAd36 10^6 and 10^7 v.p. priming groups (Figure 1A). No significant differences between groups were observed at later time points, and analysis of antibody titers 20 days after the final immunization revealed that all regimens produced over 10^5 log titers, with the SAd36 10^6 and 10^7 v.p. priming doses being the most immunogenic (Figure 1B). Although the SAd36 10^{10} regimen initially displayed the highest antibody titers at day 20 after the final immunization, by day 80 the antibody titers induced by this regimen were the lowest compared to the SAd36 10^6 and 10^7 v.p. regimen and the Ad5 regimen.

Since cytophilic antibody subclasses directed against MSP1₁₉ (226) and CSP (227) have been found to be correlated with protection against *Plasmodium* infection, we assessed the distribution of anti-PyCMP IgG1 and IgG2a induced by the immunization regimens. This approach also allows us to indirectly assess Th1 and Th2 responses as cytokines produced by Th1 cells induce antibody class switching to produce cytophilic antibodies. When titers of IgG1 and IgG2a subclasses were evaluated by ELISA 20 days after the final immunization, we observed no significant difference between IgG1 and IgG2a anti-PyCMP antibody titers within the SAd36 10⁷, SAd36 10¹⁰ or Ad5 10⁷ regimens indicating a more balanced induction of Th1/Th2 response (Figure 1C). However, we observed significantly higher IgG1 response in mice immunized with the SAd36 10⁶ regimen. When we assessed the differences in the IgG1 or the IgG2a response between the groups, we observed no significant differences suggesting that the Ad5 and SAd36 vectors elicit a similar subclass profile.

Antibody responses against PyCMP were further characterized by assessment of antibody avidity using sodium thiocyanate antibody displacement ELISAs 20 days after the final immunization. All immunization regimens induced antibodies with a mean avidity over 0.85, with the Ad5 10⁷ immunization group producing antibodies with the highest index. The only statistically significance difference observed was the higher antibody avidity of the Ad5 when compared to SAd36 at 10¹⁰ v.p. (Figure 1D).

Immunization with SAd36 is Capable of Inducing High Levels of CSP-Specific CD8⁺ T cells

To determine if the SAd36 regimens could elicit PyCMP specific-CD8⁺ T cells, the frequency of tetramer-reactive CD8⁺ T cell in peripheral blood was compared. All immunization regimens induced robust CD8⁺ T cell responses (Figure 2A). By day 40, the mice immunized with Ad5 10⁷ v.p. had the lowest numbers of PyCMP specific CD8⁺ T cells compared to the mice immunized with SAd36 at any dose, with the frequency of tetramer-positive CD8⁺ T cells induced by the Ad5 10⁷ regimen at day 40 being significantly lower than that induced by SAd36 10¹⁰ (p < 0.05). Although not significant at later

time points, lower frequencies of antigen-specific CD8⁺ T cells induced by the Ad5 10⁷ regimen were observed through day 70 (Figure 2C).

When the CD4⁺ T cell response was analyzed, the highest level of antigen-experienced CD4⁺ T cells was observed after priming and the first boosting (Figure 2B). No significant differences were observed at any time point, with all the SAd36 immunization regimens displaying ~3% or more antigen-experienced CD4⁺ T cells, similar to the levels induced by the Ad5 regimen (Figure 2B and D). Nonetheless, since this response includes both CD4⁺ T cells induced by the transgene product and the vector, the results demonstrate a higher induction of CD4⁺ T cells by SAd36 but not necessarily transgene-specific.

Multi-functionality of T cells induced by Immunization

To assess CD4⁺ and CD8⁺ T cell functionality, their ability to produce the cytokines IFN- γ , IL-2, and TNF- α was measured 5 days after the final immunization. When compared to other immunization regimens, SAd36 at 10¹⁰ v.p. produced a significantly higher proportion of triple cytokine producing CD8⁺ T cells (Figure 3A). In addition, the SAd36 10¹⁰ v.p. regimen also induced a significantly higher proportion of single producing IL-2 CD4⁺ T cells and the highest percentage of IFN- γ and TNF- α double producing, and IFN- γ single-producing CD8⁺ T cells compared to all other regimens (Figure 3A).

When the multi-functionality of CD4⁺ T cells was assessed, the SAd36 10¹⁰ regimen induced the most triple cytokine producing CD4⁺ T cells compared to all other regimens, as well as the most IFN- γ single producers followed closely by the Ad5 regimen. Furthermore, multi-functionality of CD4⁺ T cells was observed in all groups (Figure 3B).

Cytokine Production in Response to PyCMP

The breadth of the cytokine response induced by immunization was assessed in splenocytes obtained 5 days after the final immunization and stimulated with peptide pools. We observed that the SAd36 10¹⁰ immunization regimen induced the highest level of IFN- γ producing CD8⁺ T cells, and this recognition was significantly higher than that of the SAd36 10⁷ regimen for pool 1 (Figure 4A). Furthermore, the SAd36 10¹⁰ regimen induced a significantly higher IFN- γ production by CD4⁺ T cells in response to pool 3 stimulation (PyMSP1₁₉) when compared to all other immunization regimens, and higher IFN- γ production of IFN- γ by CD4⁺ T cells in response to pool 1 when compared to SAd36 10⁷ (Figure 4D).

When the IL-2 and TNF- α response was analyzed, SAd36 10¹⁰ regimen immunization also induced the highest IL-2 (Figure 4B and E) and TNF- α (Figure 4C and F) production by CD8⁺ and CD4⁺ T cells compared to all other immunization regimens, with a significantly higher CD4⁺ T cell production of IL-2 and TNF- α in recognition of the Pool 3 when compared to the Ad5 regimen (Figures 4E and 4F).

In addition to differences in cytokine production between the immunization regimens, cytokine production by CD4⁺ and CD8⁺ T cells within each immunization regimen was not significantly different in response to the three peptide pools, suggesting that there was no immunodominant epitope within the chimeric protein.

Protective Efficacy of SAd36 Prime-PyCMP Protein Boost Immunization Regimens

At day 80, mice were challenged intravenously with ~100 freshly isolated *P. yoelii* sporozoites isolated from *Anopheles stephensi* mosquitoes. All immunization regimens had significantly reduced parasitemia levels compared to naïve mice when the parasitemia kinetics were expressed as area under the curve (Figure 5A). Although not statistically significant, SAd36 10⁶ and 10¹⁰ v.p. regimens were the most protective regarding the reduction of parasitemia and all regimens that included an SAd36 prime

displayed a trend for lower parasitemia when compared to Ad5 in comparison to the naïve group (Figure 5A).

When pre-patency periods were compared, all immunization regimens showed an increased pre-patency period compared to the naïve group, indicating that all regimens reduced parasite load in the liver and delayed progression to blood stage infection. The SAd36 10^6 and 10^{10} immunization regimens displayed significantly longer pre-patency periods when compared to the Ad5 immunization regimen, however the SAd36 10^7 regimen also displayed a trend towards increased pre-patency period compared to the Ad5 regimen (Figure 5B).

Discussion

Both humoral and cellular immune responses are necessary to provide protection against *Plasmodium* infection (70, 228-230). To induce an optimal cellular response against *Plasmodium*, viral vectors have been used to increase the numbers of CD8⁺ T cells capable of recognizing *Plasmodium* antigens (92, 93, 116, 213, 214, 231). Adenoviral vectors are easily adaptable to vaccine studies because of their ability to incorporate large transgene inserts, high levels of transgene expression for periods up to one year (232), and their ability to be mass-produced at vaccine quality under good manufacturing practice (233, 234). The most commonly used adenoviral vector, Ad5, shows an excellent immunogenicity and safety profile. Nonetheless, studies of populations living in malaria endemic areas have revealed that approximately 50% of the adult population has high titers of neutralizing antibodies against this virus (235). To circumvent the pre-existing immunity to Ad5, while maintaining the many benefits of adenoviral vectors, we tested SAd36 a novel simian adenovirus vector, which is resistant to anti-Ad5 antibodies (208). We evaluated the relevance of using a recombinant SAd36 to deliver a transgene that includes chimeric *P. yoelii* CSP, and MSP1 proteins denoted PyCMP (90).

Priming with either SAd36PyCMP and Ad5PyCMP followed by two protein boosts, induced comparable antibody titers, levels of IgG1 and IgG2a subclasses, and similar antibody avidity for the SAd36 10^6 and 10^{10} regimens, indicating that SAd36 exerts effects on the humoral immune responses similar to that of the Ad5 vector. Furthermore, all immunization regimens induced antibodies with avidity indices above 0.85. These results are promising as previous reports have cited that antibody avidity above 0.80 is correlated with sterilizing immunity to *Plasmodium* infection (236).

Despite promising humoral responses, the goal of adenoviral immunization is to induce robust cellular immune responses to the transgene product. Tetramer analysis revealed that SAd36 induces more anti-CSP specific CD8⁺ T cells compared to Ad5 in response to the CTL epitope included in PyCMP. The lower induction of CD8⁺ T cells by the Ad5 10^7 regimen is consistent with previous reports that vaccination with Ad5 leads to T cell exhaustion or anergy (237). Additionally, both vectors induced comparable levels of CD4⁺ T cell activation. The ability of simian adenoviral vectors to induce more robust CD8⁺ T cells responses is a desirable feature for pre-erythrocytic malaria vaccines, as high numbers of antigen-specific CD8⁺ T cells are necessary for protection (238), while high CD4⁺ T cells levels provide protection against blood stage parasite challenge in humans (229). Furthermore, the higher immunogenicity of simian vectors has also been observed by other groups using chimpanzee-derived adenoviruses (87, 116, 212, 239, 240), making simian adenoviruses particularly attractive as rare human adenoviruses have shown lower immunogenicity than Ad5 in preclinical trials (235, 241, 242). However, despite the improved anti-CSP specific CD8⁺ T cell responses observed, analysis of memory responses following priming immunizations with either SAd36 or Ad5 is required to determine differences in long-term immunogenicity between these vectors.

The use of SAd36 as a vector for malaria vaccination is further supported by the results obtained from assessment of CD4⁺ and CD8⁺ T cells functionality in response to adenoviral prime-protein boost immunization regimens. T cell functionality was assessed as the ability of these cells to produce IFN- γ ,

IL-2, and TNF- α in response to the PyCMP recombinant protein since these cytokines have been associated with protection against malaria infection (108). We found that immunization regimens incorporating SAd36 induced equivalent, if not higher, levels of IFN- γ from both CD4⁺ and CD8⁺ T cells. IFN- γ is involved in promoting more efficient phagocytosis and presentation of foreign peptides by macrophages (108, 243). Relevantly, the protective effect of IFN- γ production was also observed during the phase IIa clinical trial of RTS,S, as prolonged IFN- γ production by CD4⁺ and CD8⁺ T cells was associated with protection (228).

In addition to T cell functionality, the breadth of the immune responses induced by vaccination must be considered since immunodominance of one or a small set of epitopes may promote the immune escape of the parasite over time. When we assessed the breadth of the immune response to three peptide pools representing the length of PyCMP, we found no indication of immunodominance. The lack of immunodominance suggests that the SAd36 vector should be considered for improving the cellular immunogenicity of protein-based malaria vaccine candidates, as immunodominance has been reported by other groups when using Simian Ad vectors and multi-antigen vaccine candidates (89, 116).

The infectious challenge with *P. yoelii* demonstrated that heterologous Ad prime-protein boost regimens including SAd36 priming provided both liver stage protection by increasing the length of the pre-patency period and blood stage protection by reducing parasitemia levels. This also further confirms the role of heterologous Ad-Protein regimens as one of the best strategies to obtain multistage malaria protection (92). Based on the similar protective efficacy of the regimens including a high and low dosage of SAd36, we can consider that the lower-dose regimen overcame the negative impact of the low adenoviral dosage on cellular immune responses through the induction of high titers of high avidity antibodies against the PyCMP transgene product, which further suggests that an effective malaria vaccine will depend on both humoral and cellular responses. However, the dosage-effect described here requires further characterization. Furthermore, it is likely that the humoral immunogenicity of SAd36 can be

improved with hexon-modifications to present T helper epitopes, as we have recently described (92, 93). It is also important to note that a lower infectivity of SAd36 compared to Ad5 can explain the capacity of SAd36 to induce protective responses in a wider dose range than Ad5, as we have demonstrated that high Ad5 doses (higher than 10^{10} v.p.) significantly reduce the protective efficacy of heterologous Ad-regimens, an event mediated by a significant reduction in antigen-specific responses (93).

In conclusion, we have found that SAd36 offers many advantages over the commonly used Ad5, beyond its resistance to anti-Ad5 antibodies, as it shows an improved humoral and cellular immune responses profile when delivered as part of an adenoviral prime-protein boost regimen that correlates with improved protection from infectious challenge in a stringent murine malaria model.

Disclosures

The authors have no relevant affiliations or financial involvement with any organization or entity with a financial interest in or financial conflict with the subject matter or the materials discussed in the manuscript.

Funding Sources

This research was supported by the National Institutes of Health, NIAID grants R56-AI103382-01A1, R21-AI095718-01, and R21-AI117459-01, and the Yerkes National Primate Research Center Base Grant No RR00165 awarded by the National Center for Research Resources of the National Institutes of Health.

Acknowledgements

The authors would like to thank Dr. James Wilson for providing the SAd36 vector, and Monica Cabrera-Mora for technical support with flow cytometry and experimental challenge.

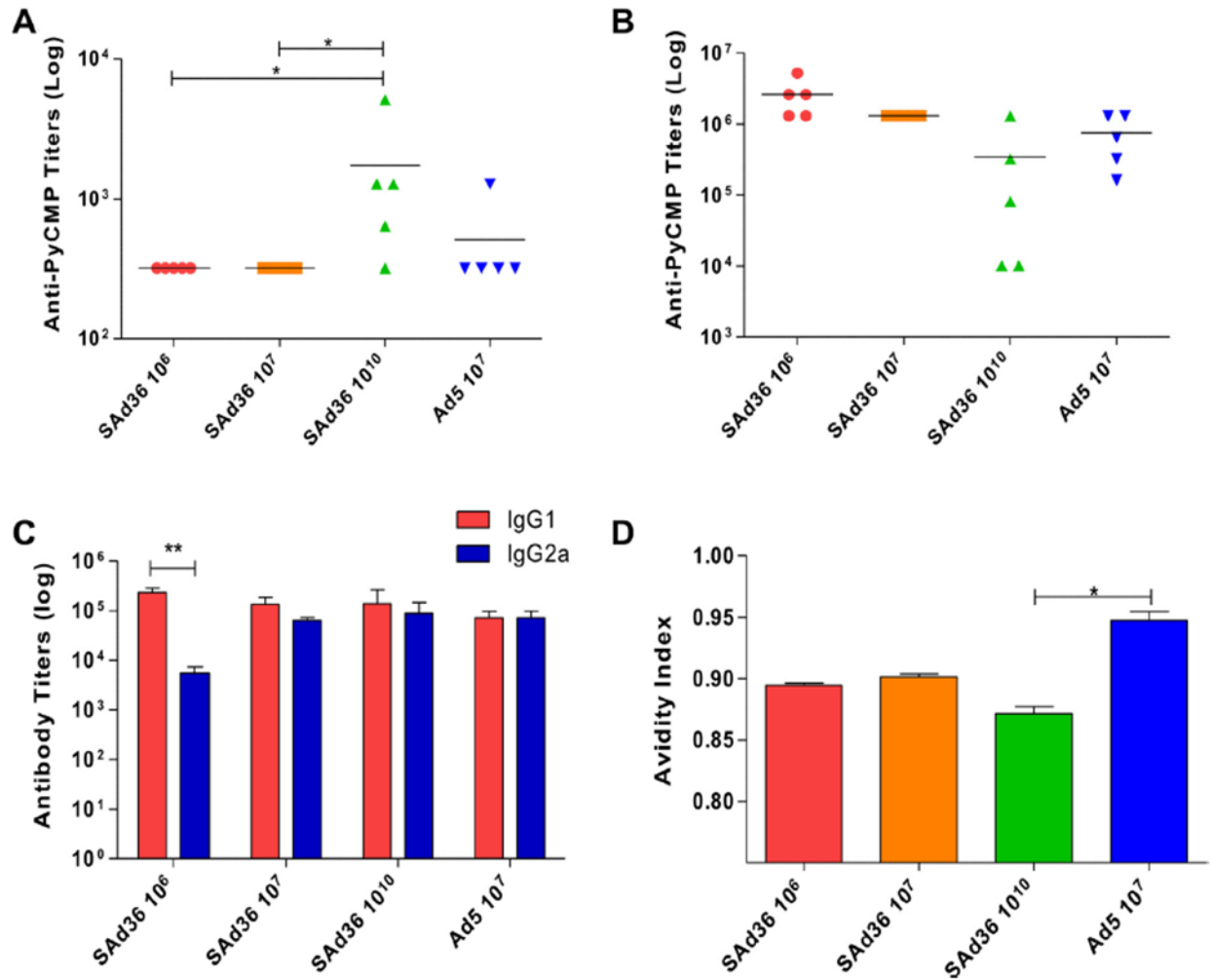


Figure 1. SAAd36PyCMP elicits comparable antibody responses compared to Ad5PyCMP. Female CB6F1/J mice (n = 5 per group) were vaccinated according to the regimens described in Table 1. (A) Anti-PyCMP antibody titers measured 20 days after the priming immunization. Each symbol represents the values for an individual mouse. The horizontal lines represent the arithmetic mean for each group. Statistical analysis was conducted using Kruskal-Wallis and Dunn's post-test, *p<0.05. (B) Anti-PyCMP antibody titers measured 20 days after the final immunization. (C) Comparative titers of IgG1 and IgG2a antibody subclasses induced by each immunization regimen measured 20 days after the final immunization. Endpoint ELISA titers were measured as the highest dilution of sera that resulted in an optical density of 0.5 (OD0.5) and were determined using the recombinant protein PyCMP and serum

from mice immunized with Ad5 or SAd36. (D) Avidity of antibodies induced by the different vaccinated groups calculated as defined by Perciani, et al. (221). Statistical analysis was conducted using Kruskal-Wallis and Dunn's post-test, * $p < 0.05$.

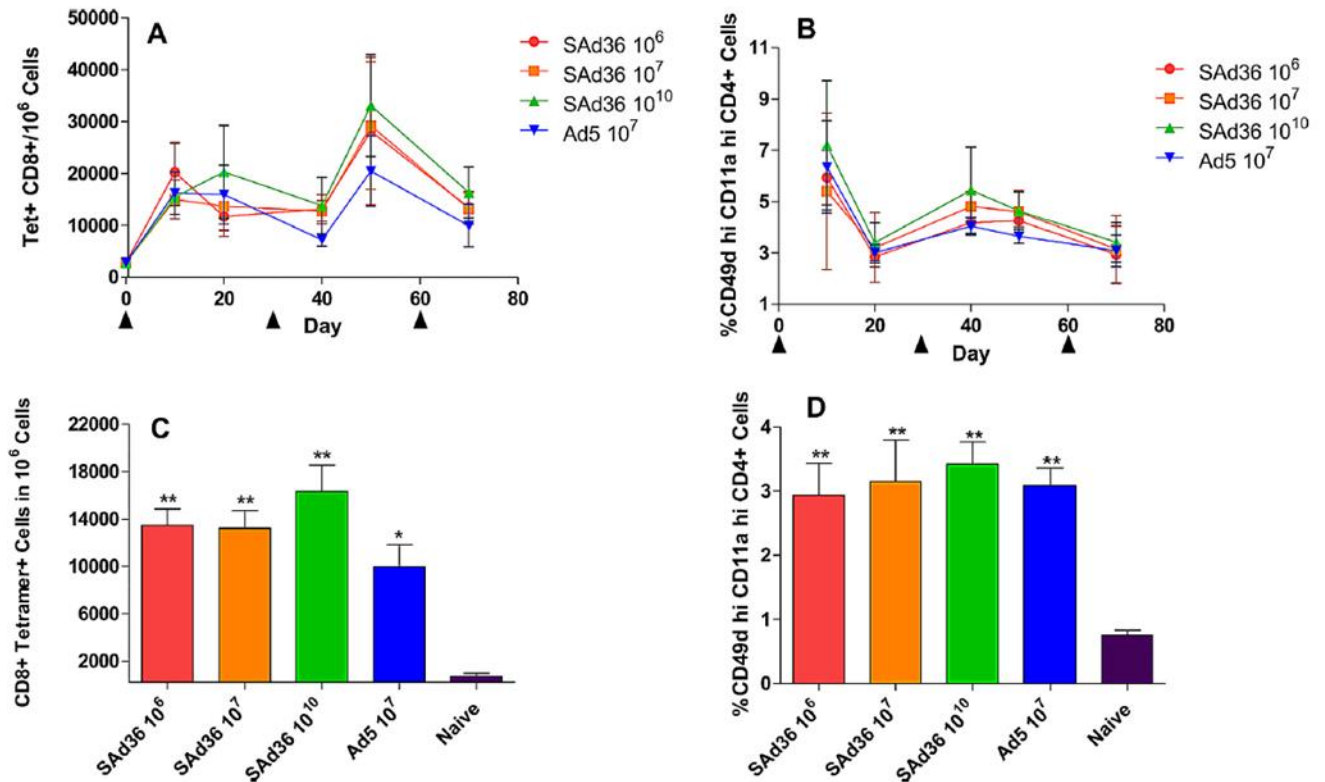


Figure 2. Induction of PyCMP-Antigen-Specific T cells by SAd36PyCMP and Ad5PyCMP

Immunization. Female CB6F1/J mice (n = 5 per group) were immunized according to the regimens described in Table 1. PBMCs were obtained from mouse whole blood samples at days 10, 20, 40, 50, and 70-post priming and were processed for flow cytometry. (A) Kinetics of CD8⁺ T cells capable of recognizing the H-2K^d/SYVPSAEQI/APC tetramer induced over the course of the immunization regimen. (B) Kinetics of the percentage of CD4⁺ T cells expressing high levels of CD11a and CD49d, indicating antigen-experienced cells, in the course of the immunizations. (C) Average number of tetramer-specific CD8⁺ T cells induced by each immunization group were determined ten days after the final immunization (day 70). (D) Percentage of activated CD4⁺ T cells, determined by high levels of expression of CD49d and CD11a, at day 70, ten days after the final immunization. Results are presented as the percentages of positive cells per 10⁶ PBMCs. Statistical analysis was conducted by Kruskal-Wallis test with Dunns post-test, statistically significant differences are denoted by *(p < 0.05) and ** (p < 0.01).

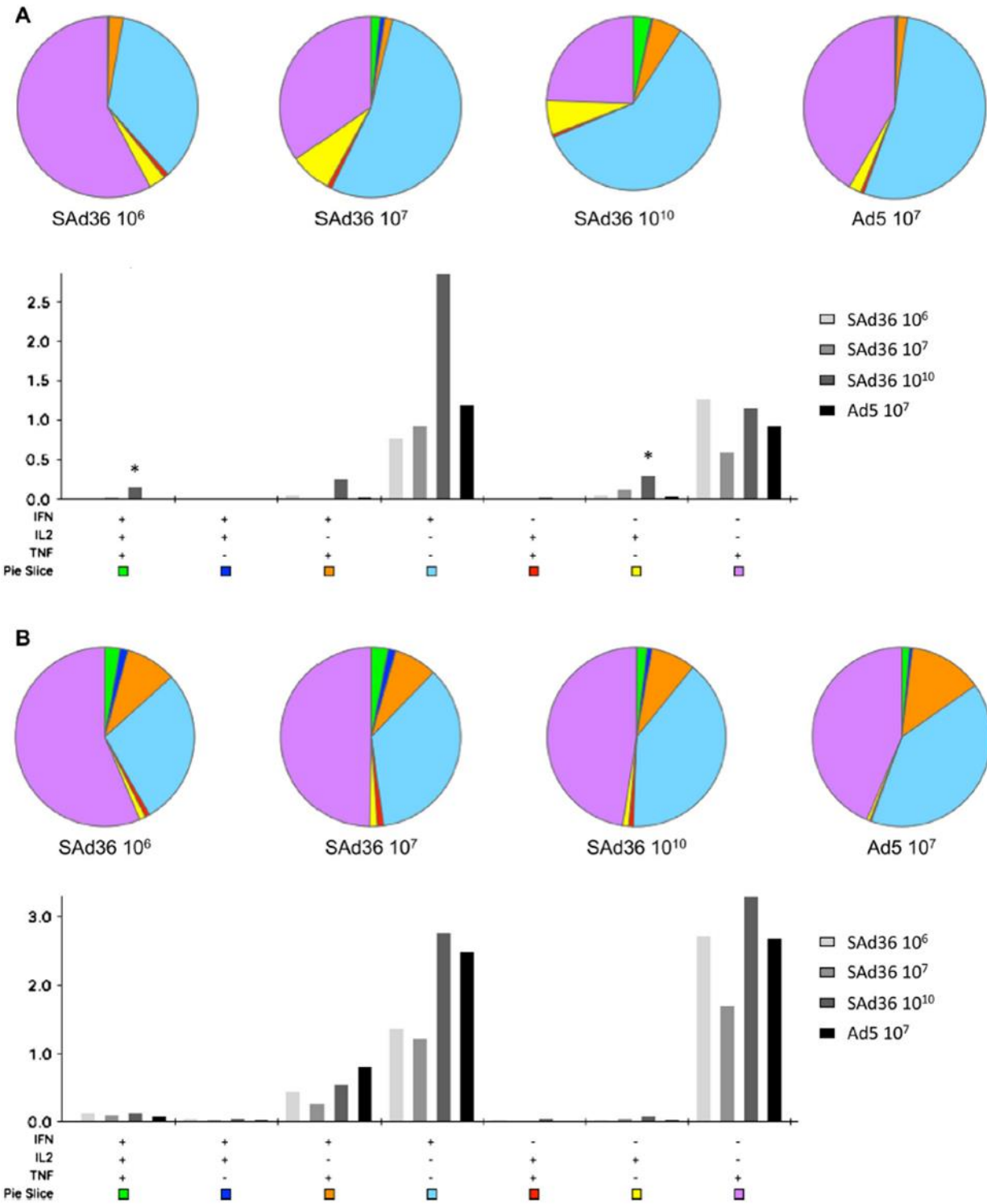


Figure 3. Cytokine production by CD8⁺ and CD4⁺ T cells stimulated *ex vivo* with the PyCMP protein. Female CB6F1/J mice (n = 5 per group) were vaccinated according to the regimens described in

Table 1. (A) Pie Charts: Percentage of multifunctional and single cytokine producing CD8⁺ T cells following *ex vivo* stimulation with PyCMP protein at day 70 post priming. Bar Graph: Percentage of total CD8⁺ T cells capable of producing one, two, or three cytokines following *ex vivo* stimulation with PyCMP protein. Results are presented as the percentages of positive cells per 10⁶ CD8⁺ T cells. (B) Pie Charts: Percentage of multifunctional and single cytokine producing CD4⁺ T cells following *ex vivo* stimulation with PyCMP protein at day 70 post priming. Bar Graph: Percentage of total CD4⁺ T cells capable of producing one, two, or three cytokines following *ex vivo* stimulation with PyCMP protein. Results are presented as the percentages of positive cells per 10⁶ CD4⁺ T cells. Graphs were produced and data was analyzed using SPICE software (223).

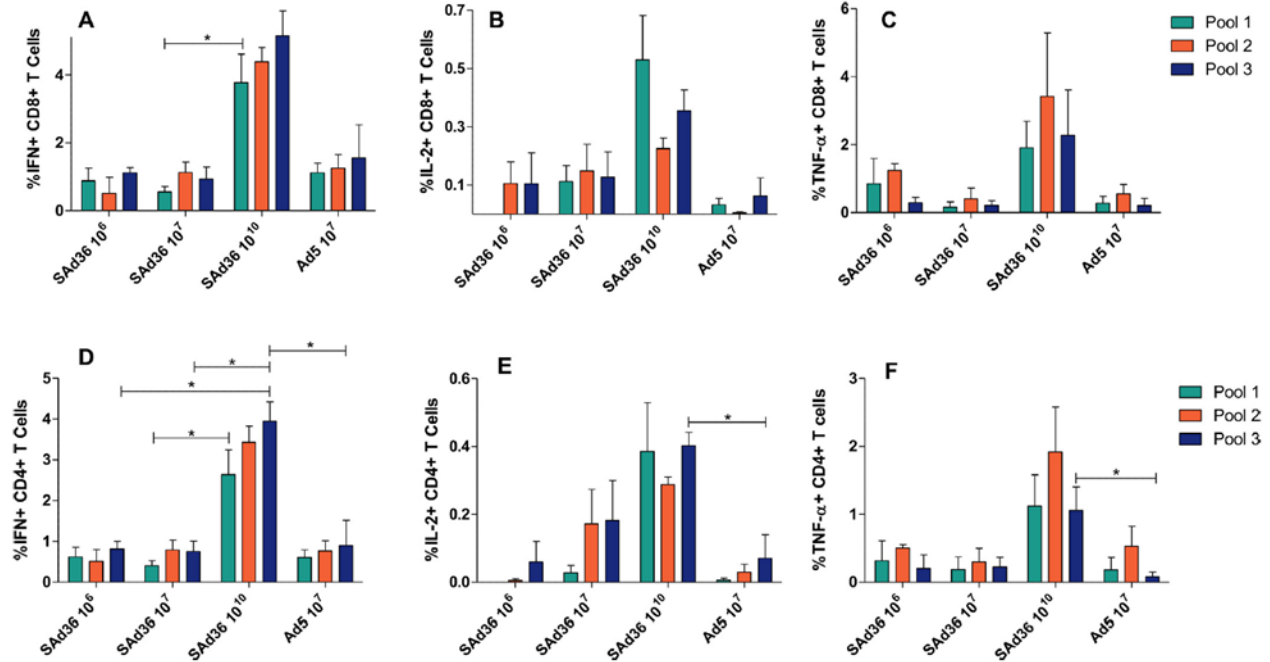


Figure 4. Cytokine production following *ex vivo* stimulation with PyCMP peptide pools. Female CB6F1/J mice (n = 5 per group) were immunized according to the regimens described in Table 1. Splenocytes were obtained five days after the final immunization and incubated with peptide pools containing pools of 15AA overlapping peptides representing PyCMP. Following 6 hours of stimulation, cells were intracellularly stained and processed for flow cytometry. Results are presented after background subtraction. Percentage of CD8⁺ T cells capable of producing IFN- γ (A), IL-2 (B), and TNF- α (C) after stimulation. Percentage of CD4⁺ T cells capable of producing IFN- γ (D), IL-2 (E), and TNF- α (F) following stimulation. Statistical analysis was conducted using Kruskal-Wallis test to determine differences between the immunization regimens. Statistically significant differences (p < 0.05) are indicated by a single asterisk.

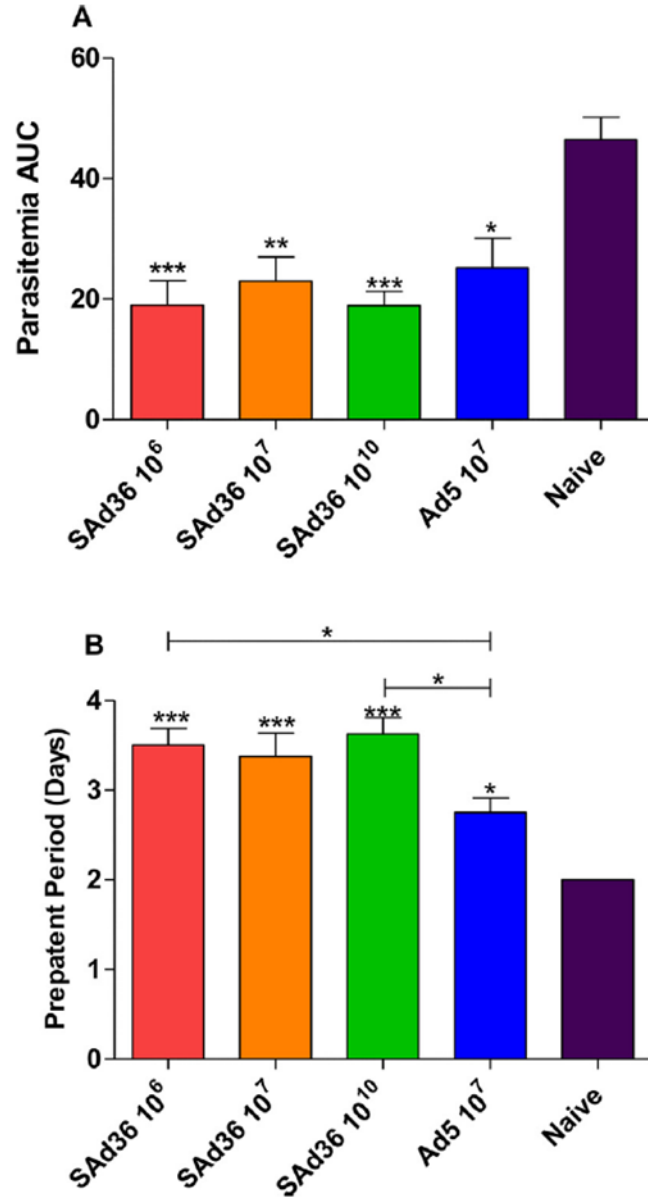
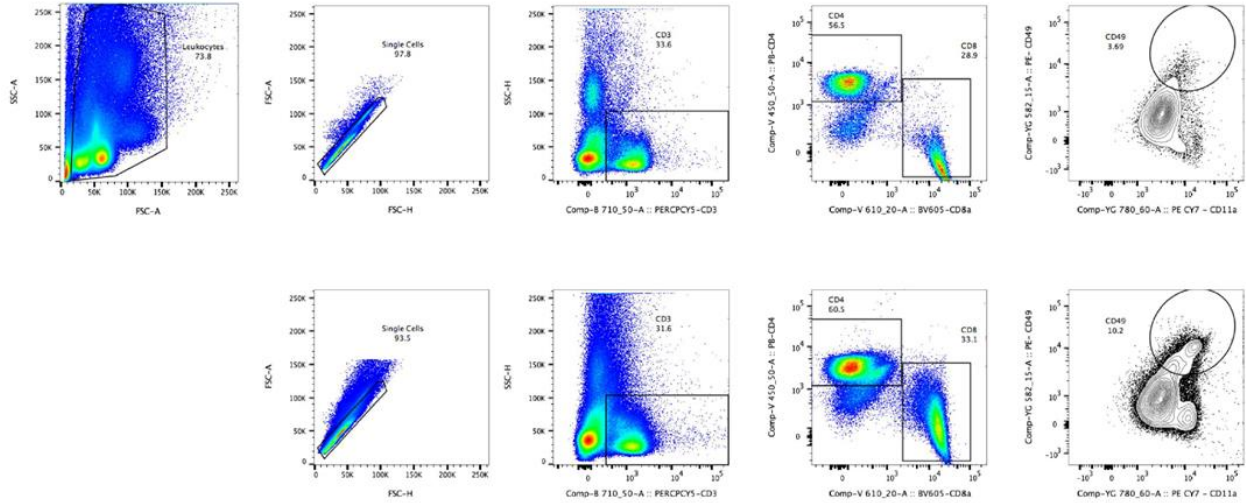


Figure 5. SAd36-PyCMP Protective Efficacy. Female CB6F1/J mice (n = 10 per group) were immunized according to the regimens described in Table 1. 30 days after the final immunization mice were challenged with 100 freshly Isolated *Plasmodium yoelii* sporozoites isolated from *Anopheles stephensi*. (A) Kinetics of parasitemia expressed as Area Under the Curve (AUC) and (B) the length of the pre-patency period were analyzed by Kruskal-Wallis test with Dunns post-test. Statistically significant differences are denoted by * (p < 0.05), ** (p < 0.01), and *** (p < 0.001).

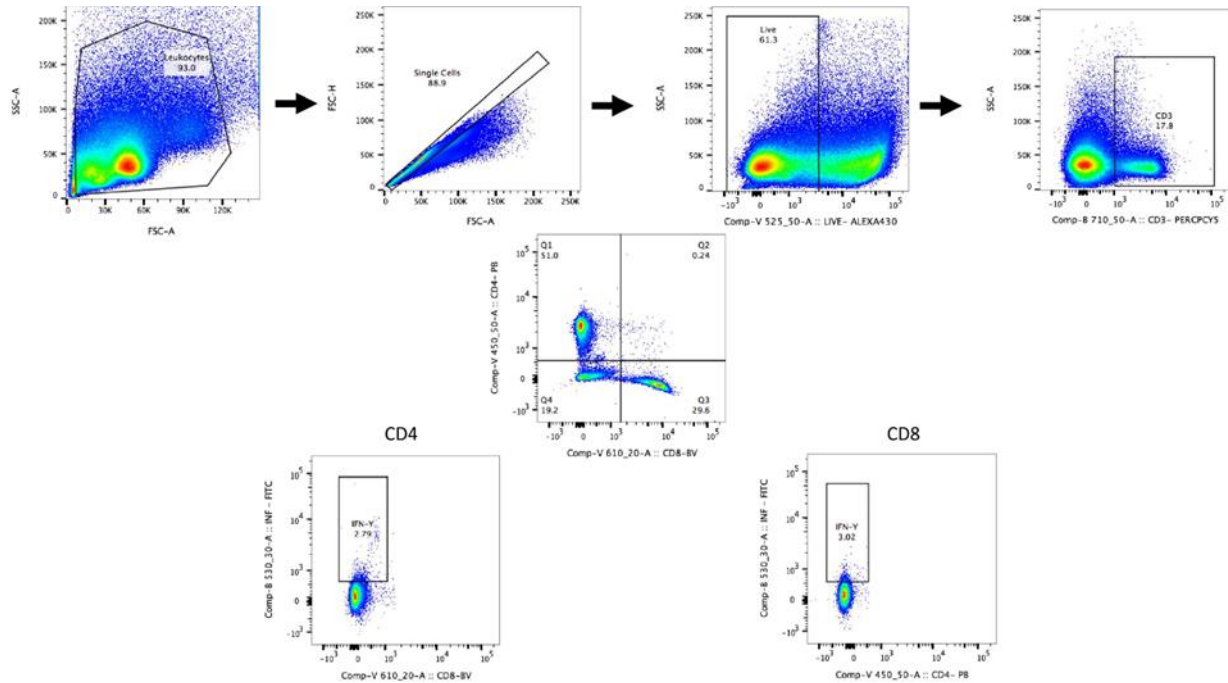
Table 1. Immunization Groups

Immunization Group	Priming, Day 0		Protein Boost 1, Day 30	Protein Boost 2, Day 60
	Ad- <i>transgene</i>	Dose		
SAd36 10 ⁶	SAd36- <i>PyCMP</i>	10 ⁶ v.p.	PyCMP	PyCMP
SAd36 10 ⁷	SAd36- <i>PyCMP</i>	10 ⁷ v.p.	PyCMP	PyCMP
SAd36 10 ¹⁰	SAd36- <i>PyCMP</i>	10 ¹⁰ v.p.	PyCMP	PyCMP
Ad5 10 ⁷	Ad5- <i>PyCMP</i>	10 ⁷ v.p.	PyCMP	PyCMP
Control	No immunization		No immunization	No immunization

Mice were immunized intramuscularly at day 0 with adenovirus in PBS at the dose corresponding to their group. Mice were then boosted subcutaneously at days 30 and 60 with 20 µg of the *P. yoelii* chimeric multistage protein (PyCMP) emulsified in Montanide ISA 51 VG in a 1:1 volume ratio. Control group mice received no immunizations. ($n = 10$ per group). Mice were bled for analysis of antibody titers via ELISA 20 days after each immunization. PBMCs were obtained from mouse whole blood samples at days 10, 20, 40, 50, and 70 post priming and were processed for flow cytometry.

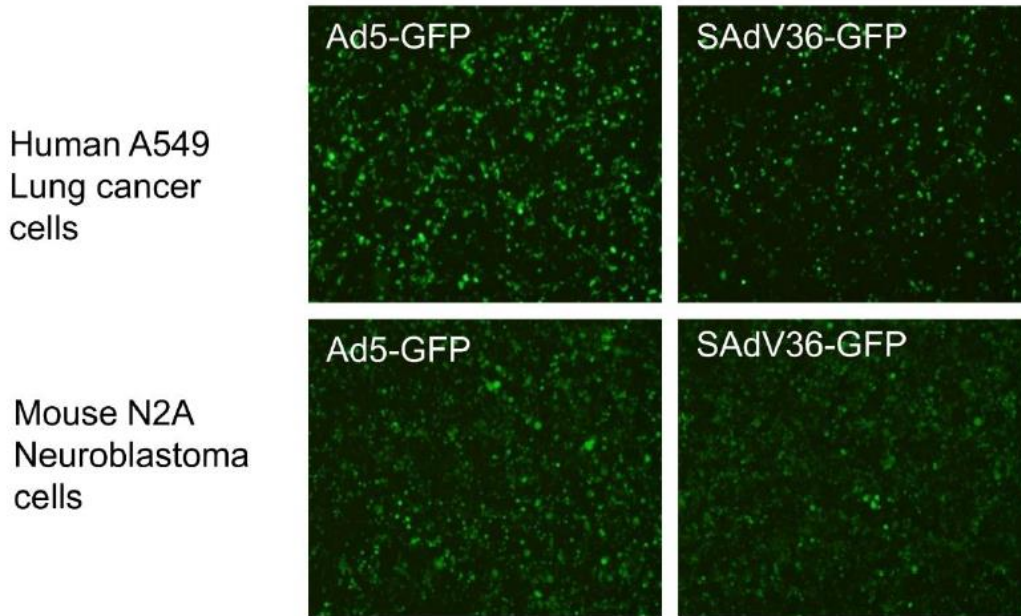


Supplementary Figure 1. Gating strategy for the definition of antigen-specific CD4⁺ T cells. In this sample gating strategy leukocytes were gated in SSC-A vs FSC-A. In the leukocyte population, CD3⁺ cells were gated to select lymphocytes, and the surface expression of CD4 and CD8 was posteriorly identified. On the CD4⁺ T cells, the expression of CD49d and CD11a was assessed as it is associated to antigen-experienced CD4⁺ T cells. The top row shows the gating of a representative naïve mouse and the bottom row shows the strategy for a mouse receiving SAd36 at 10¹⁰ dose.

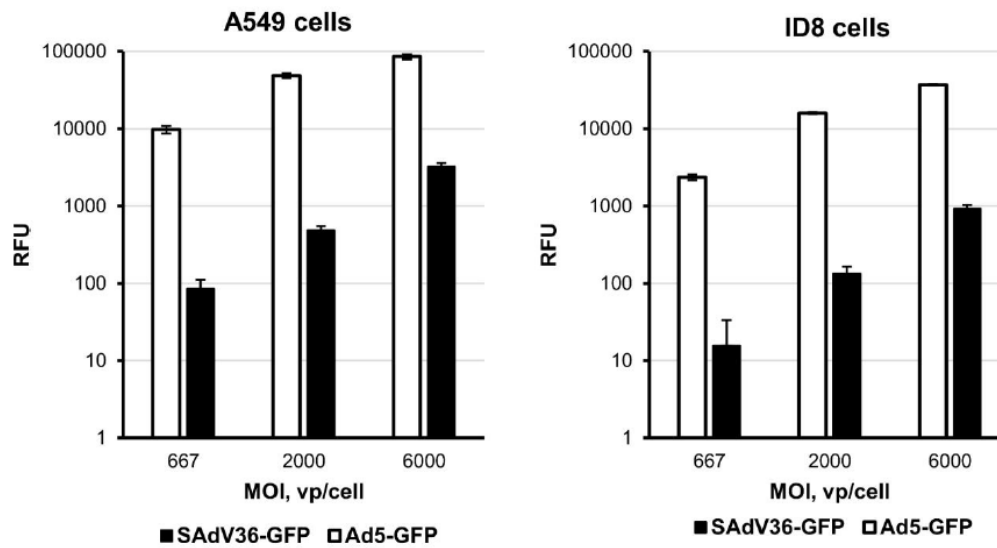


Supplementary Figure 2. Gating Strategy for Analysis of Cytokine Production. In this sample gating, cells were first gated as leukocytes (SSC-A vs FSC-A) and then for singlets (FSC-H vs FSC-A). The singlets gate was further analyzed for their uptake of the Live/Dead stain to determine live versus dead cells. After selection of the live population, the CD3 expression was then analyzed to select the T cell population. CD4 and CD8 surface expression was then determined. Intracellular expression of cytokines (IFN- γ , TNF- α , IL-2) was analyzed in each T cell subset.

A.



B.



Supplementary Figure 3. Characterization of the Infective Capacity of Ad5 and SAd36 vectors. A.

Monolayers of A549 (human epithelial lung cancer cell line) or N2A cells (mouse neuroblastoma cell

line) were incubated for 1 hour with either SAd36-GFP or Ad5-GFP at a multiplicity of infection (MOI) of 300 vp/cell. After incubation, infection medium (DMEM/F-12, 1:1) containing virus and 2% FBS was replaced with culture medium containing 5% FBS and cells were incubated at 37°C and 5% CO₂ for at least 20 hours to allow eGFP reporter gene expression. The infected cells expressing eGFP were detected using an epifluorescent microscope, and images were taken at 10X magnification. **B.** Monolayers of A549 (human epithelial lung cancer cell line) and ID8 cells (mouse epithelial ovarian cancer cell line) were infected with either SAd36-GFP or Ad5-GFP vectors using the indicated multiplicities of infection (MOI). The infection efficiencies of SAd36-GFP or Ad5-GFP vectors were determined based on the levels of fluorescent signal intensity detected with a multi-mode plate reader in infected and uninfected cells 48 hours post infection. The average values of relative fluorescent units (RFU) are presented after subtracting background signal detected in uninfected monolayers that served as negative controls. Each bar represents the cumulative mean of triplicate measurements \pm standard deviation.

Chapter 3

Inclusion of the murine IgGκ signal peptide increases the cellular immunogenicity of a simian adenoviral vectored *Plasmodium vivax* multistage vaccine

Jairo A. Fonseca^{a,b,1,2}, **Jessica N. McCaffery**^{a,1}, Juan Caceres^a, Elena Kashentseva^c, Balwan Singh^a, Igor P. Dmitriev^c, David T. Curiel^c and Alberto Moreno^{a,b,#}

- a. Emory Vaccine Center, Yerkes National Primate Research Center, Emory University, 954 Gatewood Road, Atlanta, GA 30329.
- b. Division of Infectious Diseases, Department of Medicine, Emory University School of Medicine, Atlanta, GA 30307.
- c. Cancer Biology Division, Department of Radiation Oncology, Washington University School of Medicine 660 S. Euclid Ave., 4511 Forest Park Blvd, St. Louis, MO 63108.

1. These authors contributed equally to this work.

Originally published in: Vaccine

Fonseca JA, McCaffery JN, Caceres J, Kashentseva E, Singh B, Dmitriev IP, Curiel DT, Moreno A. (2018). Inclusion of the murine IgGκ signal peptide increases the cellular immunogenicity of a simian adenoviral vectored *Plasmodium vivax* multistage vaccine. *Vaccine*. 2018 May 11;36(20):2799-2808.

PMID: 29657070. doi: 10.1016/j.vaccine.2018.03.091.

Copyright © 2018, Elsevier.

Abstract

Introduction: Cellular and humoral immune responses are both involved in protection against *Plasmodium* infections. The only malaria vaccine available, RTS,S, primarily induces short-lived antibodies and targets only a pre-erythrocytic stage antigen. Inclusion of erythrocytic stage targets and enhancing cellular immunogenicity are likely necessary for developing an effective second-generation malaria vaccine. Adenovirus vectors have been used to improve the immunogenicity of protein-based vaccines. However, the clinical assessment of adenoviral-vectored malaria vaccines candidates has shown the induction of robust *Plasmodium*-specific CD8⁺ but not CD4⁺ T cells. Signal peptides (SP) have been used to enhance the immunogenicity of DNA vaccines but have not been tested in viral vector vaccine platforms.

Objectives: The objective of this study was to determine if the addition of the SP derived from the murine IgGκ light chain within a recombinant adenovirus vector encoding a multistage *P. vivax* vaccine candidate could improve the CD4⁺ T cell response.

Methods: In this proof-of-concept study, we immunized CB6F1/J mice with either the recombinant simian adenovirus 36 vector containing the SP (SP-SAd36) upstream from a transgene encoding a chimeric *P. vivax* multistage protein or the same SAd36 vector without the SP. Mice were subsequently boosted twice with the corresponding recombinant proteins emulsified in Montanide ISA 51 VG. Immunogenicity was assessed by measurement of antibody quantity and quality, and cytokine production by T cells after the final immunization.

Results: The SP-SAd36 immunization regimen induced significantly higher antibody avidity against the chimeric *P. vivax* proteins tested and higher frequencies of IFN-γ and IL-2 CD4⁺ and CD8⁺ secreting T cells, when compared to the unmodified SAd36 vector.

Conclusions: The addition of the murine IgGκ signal peptide significantly enhances the immunogenicity of a SAd36 vectored *P. vivax* multi-stage vaccine candidate in mice. The potential of this approach to improve upon existing viral vector vaccine platforms warrants further investigation.

Introduction

The life cycle of *Plasmodium* parasites is known for its complexity, and as a result, immunity to malaria infections in vertebrates relies on both humoral and cellular immune responses. Early passive transfer experiments demonstrated the protective role of IgG antibodies derived from malaria immune adults when used as a therapeutic intervention (244). Clinical trials of sporozoite inoculation have revealed that IFN- γ producing T cells are associated with the protection from malaria (230). Based on this evidence, a multistage vaccine capable of eliciting both cytophilic antibodies and antigen-specific T cells would likely enhance protective efficacy through a comprehensive vaccination strategy.

The RTS,S/AS01 vaccine represents a significant breakthrough as the first *P. falciparum* malaria vaccine that has completed Phase 3 clinical trials (80). However, RTS,S has reported low efficacy due in part to protection based primarily on antibodies against the circumsporozoite protein (CSP) central repeat region (202) present in pre-erythrocytic stage forms, which wane rapidly and require boosting immunizations to maintain efficacy (245). The inclusion of erythrocytic stage targets to control parasites that evade liver clearance and enhancing cellular immunogenicity are likely necessary for developing an effective second generation of malaria vaccines.

Adenoviral vectored malaria vaccines have been able to improve the immunogenicity of protein-based vaccines (246-249) and induce protective *Plasmodium*-specific CD8⁺ T cells in pre-clinical and clinical studies (212, 250, 251), but low induction of CD4⁺ T cell suggests further improvements to adenoviral vectors should be investigated (251). Recent studies examining the induction of CD4⁺ cells following vaccination with an Ad5 vector have shown significantly lower frequencies of antigen-specific CD4⁺ T cells are induced when compared to acute infection, an effect that could be attributed to lower IL-2 signaling (252). Increasing secretion or altering post-translational modifications of adenoviral transgene products might result in improved presentation of vaccine antigens to CD4⁺ T cells.

Signal peptides (SP), also referred to as signal sequences, are short peptides (~20-30 residues) that can influence the targeting pathway of the protein and promote protein secretion or specific post-

translational modifications such as glycosylation (253). As a result, SP from highly secreted proteins have been used to improve protein secretion levels of recombinant proteins in cell lines (254-256), as well as for ectopic expression of endogenous adenoviral genes (257). Recently, the inclusion of an SP into a DNA vaccine targeting HPV oncogenes was found to induce potent cellular and humoral immune responses that protected against tumor challenge (258). Of the signal peptides used to improve transgene expression, the sequence derived from the murine immunoglobulin kappa (IgG κ) light chain (METDTLLLWVLLLWVPGSTG), is one of the most well characterized (254-256).

We hypothesized that the addition of the signal peptide derived from murine IgG κ light chain upstream of a transgene delivered via a recombinant adenovirus vector would improve the CD4⁺ T cell response to the transgene product in comparison to vaccination with the same recombinant vector without the signal peptide (250). Here we demonstrate that the addition of the murine IgG κ SP improves the immunogenicity of an adenoviral vectored *P. vivax* multistage vaccine (86, 259) in mice by significantly increasing IFN- γ and IL-2 secretion by CD4⁺ T cells, and improving antibody avidity. To our knowledge, this is the first report of the insertion of a peptide leader sequence as part of an adenoviral transgene with the goal of improving the immunogenicity of an adenoviral vectored vaccine candidate.

Material and Methods

Viral vectors. The DNA sequence encoding the hybrid cPvCSP/cPvMSP1 protein containing the C-terminal six-His tag was codon-optimized for mammalian expression and incorporated into a pShuttle plasmid between the CMV promoter and BGH polyadenylation signal. The constructed plasmid was further modified to introduce the N-terminal SP into the hybrid cPvCSP/cPvMSP1 protein. The oligonucleotide duplex encoding IgG κ light chain SP was cloned into KpnI restriction site upstream of the cPvCSP/cPvMSP1 transgene resulting in additional three amino acids (Tyr-Pro-Thr) introduced between the signal peptidase consensus cleavage site and the first Met start codon of the cPvCSP/cPvMSP1 transgene. Both cPvCSP/cPvMSP1 or SP-cPvCSP/cPvMSP1 expression cassettes were excised with I-

CeuI and PI-SceI restriction enzymes and ligated to plasmid carrying the SAd36 genome using unique I-CeuI and PI-SceI restriction sites introduced in place of E1 region, as previously described (208, 250). The ligated DNA was transformed into *E. coli* strain, XL10-Gold (Stratagene), to select the plasmids containing viral genomes carrying the CMV-driven cPvCSP/cPvMSP1 and SP-cPvCSP/cPvMSP1 expression cassettes. The constructed genomes were released from the plasmids by digestion with PacI restriction enzyme and were then transfected into HEK293 cells to rescue the replication incompetent SAd36 vector derivatives as described elsewhere (250). Both vectors were upscaled in HEK293 cells and purified using double cesium chloride gradient centrifugation as previously described (216). The purified vector preparations were dialyzed against PBS containing 10% glycerol, and viral particle (vp) titers were determined based on absorbance at 260 nm as described by Maizel et al. (217).

***In vitro* viral vector culture and western blot analysis.** To assess the expression levels of cPvCSP/cPvMSP1 and SP-cPvCSP/cPvMSP1 transgenes, monolayers of A549 cells grown in 6-well plates were incubated for 1 hour with either vector at the multiplicity of infection (MOI) of 2,500 vp/cell. Infection medium (DMEM/F-12, 1:1) containing 2% FBS was replaced with fresh culture medium containing 5% FBS and cells were incubated at 37°C and 5% CO₂ for at least 48 hours to allow transgene expression. The samples of cell lysates and culture medium supernatants were collected and analyzed by Western blot using anti-six-His tag mAb Penta-His (QIAGEN) and polyclonal IgG purified from sera of rabbits immunized with the cPvCSP or the cPvMSP1 chimeric proteins (Convance Inc.).

Chimeric protein vaccine design and peptide pools. We have previously described the synthetic genes encoding the chimeric *P. vivax* CSP (cPvCSP) (86) and the chimeric merozoite surface protein 1 (cPvMSP1) (259). These chimeric proteins include several promiscuous T cell epitopes (PTE) capable of binding to multiple human HLA alleles and at least one B cell epitope, with each region separated by

GPGPG spacers to enhance stability. cPvCSP contains 1) two PTE from the C-terminal region of *P. vivax* CSP; 2) the conserved region I of *P. vivax* CSP; 3) VK210 type 1 repeat sequence variants, and 4) three copies of the 9-mer peptide representing the VK247 type 2 repeat sequence variant (86). cPvMSP1 includes 1) five PTE from PvMSP1; 2) an extended PvMSP1₁₉ fragment that includes two T helper epitopes derived from PvMSP1₃₃; and 3) six copies of the CSP repeat region NANP derived from *P. falciparum* included as a purification tag (259). Production of the transgenes and proteins have been described previously (86, 259).

Peptide libraries containing 15-mer synthetic peptides, overlapping by 11 residues each and spanning the complete sequence of both cPvCSP and cPvMSP1 were commercially synthesized (Sigma-Aldrich), and used to characterize T cell reactivity to specific protein regions as described (86, 259). The cPvCSP peptide library was separated into 4 pools, with pool A representing the first PTE in cPvCSP; pool B representing the second PTE and the region I; pool C representing the VK210 repeat sequences; and pool D representing the VK247 repeat sequences (86). The two cPvMSP1 peptide pools represented the cPvMSP1 PTE (pool 1) and the PvMSP-1₃₃ and the PvMSP-1₁₉ protein fragments (pool 2) (259).

Mouse immunizations. Female CB6F1/J (H-2^{db}) mice, aged 6-8 weeks were obtained from Jackson Laboratory (Bar Harbor, ME) and housed in micro-isolation cages. We have previously assessed the immune response of six different mouse strains with different H-2 alleles to the cPvCSP protein and found that PvRMC-CSP was able to induce robust antibody responses in six different inbred mouse strains (86). Similar immunogenicity was also observed in both BALB/c and C57BL/6 mice in response to the cPvMSP1 peptide in previous assessments by our group (259). The CB6F1/J mice were selected as a TH1/TH2 neutral strain to characterize the induction of CD4 response by vaccination, as the parent strains C57BL6 and BALB/c have been reported to be skewed to TH1 or TH2 responses, respectively (260). All animal experiments and procedures were performed in accordance with guidelines and approved by the Emory University Institutional Animal Care and Use Committee. Two groups of 10 mice

were primed intramuscularly with 10^8 viral particles (v.p.) of either the SAd36-cPvCSP/cPvMSP1 or the SP-SAd36-cPvCSP/cPvMSP1 vector diluted in PBS (Table 1). Mice were boosted on days 20, and 40 post-priming with 10 μ g of each protein emulsified in Montanide 51 ISA VG (Seppic) adjuvant subcutaneously. A group of 10 naïve mice was used as a control, as we have not found significant differences between naïve and adjuvant immunized mice. Mice were bled 24 hours before each immunization and 20 days after the final immunization (day 60) for determination of antibody responses. Five days after the final immunization, 5 mice per group were euthanized for flow cytometric analysis of T cell responses.

Serological Assays. Total IgG antibody titers and IgG1 and IgG2a subclass titers against cPvCSP and cPvMSP1 were determined via ELISA, as described previously (259). Antibody avidity indices were determined using ammonium thiocyanate elution ELISA for each group using pooled sera, with each sample run in quadruplicate, as described previously (259). The avidity index was calculated as the ratio between the antilog of the absorbance curves obtained with (x_1) and without (x_2) NH_4SCN , following procedures described previously (219, 259). Sera obtained at day 60 were pooled by group to evaluate antibody reactivity against native PvCSP and PvMSP1 via indirect immunofluorescence assay as described previously using pooled sera at a 1:500 dilution in PBS with 1% BSA (259).

***Ex vivo* stimulation with peptide pools and analysis of cytokine production by flow cytometry.**

CD4⁺ and CD8⁺ T cells functionality was defined as their ability to produce IFN- γ , IL-2, and TNF- α . Flow cytometry analysis of *ex vivo* stimulated T cells derived from splenocytes obtained five days after the final immunization was performed as described previously (92). Briefly, splenocytes were stimulated for 6 hours with 1 μ g/ml of a single peptide pool, with GolgiPlug (BD Biosciences). Cells were Fc blocked (BD Biosciences) and stained with Live/Dead Fixable Yellow dye (Life Technologies) and anti-CD3, CD4, CD8, IFN- γ , IL-2, and TNF- α antibodies (BioLegend) according to the manufacturers'

protocol. Flow cytometry was performed using an LSRII cytometer (BD Biosciences) and analyzed with FlowJo V10.1 software. Cytokine positive cells were identified based on gating of unstimulated cells, with the threshold set above background. Cytokine production values for all cells that did not meet the threshold were set to zero. The sample gating strategy is provided in Supplementary Figure 1.

Germinal Center B cell responses in draining lymph nodes after priming. Mice (n=6/group) were immunized intramuscularly bilaterally into the quadriceps femoris muscles with the unmodified SAd36-*cPvCSP/cPvMSP1* or Signal Peptide- SAd36-*cPvCSP/cPvMSP1* vectors at 10^8 v.p. for the assessment of germinal center B cell responses in draining lymph nodes 9 days after priming. Lymph nodes were removed (261), and one lymph node per mouse was processed for assessment via flow cytometry as described previously (262). Lymphocytes were stained for viability, Fc blocked, and surface stained with anti-CD95 BV605 (clone SA367H8), anti-GL7 PE (clone GL7), and anti-B220 Alexa Fluor 647 (clone RA3-6B2) antibodies (Biolegend) according to manufacturer's instructions. Flow cytometry was performed using an LSRII cytometer (BD Biosciences) and analyzed with FlowJo V10.1 software. The germinal center B cell populations were identified as described previously (263), with FMO samples used to set gates for positive populations for CD95, B220, and GL7. A sample gating strategy is shown in Supplementary Figure 6.

Germinal centers were also visualized via immunofluorescent assay in tissue sections prepared from inguinal lymph nodes obtained from the same cohort of mice. Briefly, lymph nodes were frozen in optimal cutting temperature compound (VWR International) as described previously (264). Frozen tissues were cut into four sections of 10 μ m. Sections were stained with unconjugated GL7 (clone GL7, Biolegend) and B220 (clone RA3-6B2, Biolegend) antibodies for chromogenic staining prior to staining of replicate sections with anti-B220 and GL7 fluorochrome-conjugated antibodies listed previously. Slides were visualized as described previously using an Olympus FV1000 confocal microscope and Olympus Fluoview V4.2 software for image capture (259, 263).

Statistics. GraphPad Prism Software V5.0 was used to perform statistical analysis and generate graphs. Mann-Whitney test was used for analysis of differences in antibody titers between the SAd36 and SP-SAd36 regimens. Unpaired t-tests were used for analysis of differences in antibody avidity. Kruskal-Wallis test with Dunn's post-test was used to determine the differences in cytokine production between the two immunization groups and the naïve mice following stimulation with the peptide pools. Analysis of the differences in triple, double, and single cytokine producing CD4 and CD8 T cells between the SAd36 and SP-SAd36 regimens was assessed using student's t-test. Statistical analysis for germinal center B cell assessment was conducted using Kruskal-Wallis with Dunn's post-test to determine differences between the immunization regimens.

Results

The impact of the murine IgG κ signal peptide on protein secretion *in vitro*. The simian adenovirus 36 (SAd36) vector was selected for assessment of the effect of the insertion of the murine IgG κ light chain derived signal peptide on the adenoviral vector immunogenicity, as we have previously found SAd36 to exhibit higher immunogenicity than the standard Ad5 vector (250). The SAd36 vector is replication deficient due to deletion of the E1 and E3 genes. A hybrid transgene encoding a chimeric *P. vivax* CSP (cPvCSP) linked to a chimeric *P. vivax* MSP1 (cPvMSP1) protein (cPvCSP/cPvMSP1), expressed under the control of the CMV promoter, was inserted in place of the deleted E1 gene. The signal peptide derived from the murine IgG κ light chain was inserted after the CMV promoter and upstream of the cPvCSP/cPvMSP1 transgene (Figure 1A).

Before determining the immunogenicity of the SAd36 vector containing the signal peptide (SP-SAd36), the expression of the cPvCSP/cPvMSP1 transgene was analyzed in the cell lysates and tissue culture medium of A549 cells collected 2 days post-infection with 2,500 v.p. of the recombinant SAd36

and SP-SAd36 via western blot. The hybrid cPvCSP/cPvMSP1 protein is expressed as a single protein with a mass of 51 kDa (Figure 1B).

When the secretion of the cPvCSP/cPvMSP1 protein was assessed via western blot, we observed a slight reduction in the amount of soluble cPvCSP/cPvMSP1 protein released into the tissue culture medium from A549 cells infected with the SP-SAd36 vector as compared to SAd36 control, appearing as a medium intensity band at 51kDa using anti-cPvMSP1 or anti-cPvCSP antibodies (Figure 1B, Left). This demonstrated that addition of signal peptide did not affect intracellular cPvCSP/cPvMSP1 transgene expression level while resulting in Therefore, the use of murine IgGκ light chain leader sequence was not able to increase either expression or secretion efficiency of our multistage *P. vivax* vaccine candidate following infection of A549 cells in vitro. However, this does not exclude possible alterations in post-translational processing of the peptides due to the SP. Assessment of protein levels within the infected A549 cell lysates revealed bands of similar intensity at ~50 kDa for cells infected with either SP-SAd36 or SAd36 vectors expressing the chimeric *P. vivax* transgene when an anti-Penta-His monoclonal antibody was used for detection (Figure 1B, Right panel), suggesting that similar levels of the protein are retained inside the cell independent of the SP.

SP-SAd36 induces high avidity antibodies. We assessed the humoral immunogenicity through the analysis of antibody kinetics induced by priming immunization with either the recombinant SP-SAd36 or unmodified SAd36 vector followed by two protein boost immunizations (Table 1). The dose of 10^8 v.p. of SAd36 was selected based on our previous studies with the recombinant SAd36-cPyCSP/cPyMSP1 vector expressing orthologous *P. yoelii* sequences (250). When antibody titers elicited by the immunization regimens was assessed, no significant differences in antibody titers against the cPvCSP protein were observed between the two regimens at any time point (Figure 2A). Assessment of the anti-cPvMSP1 antibody responses revealed similar kinetics and final antibody titers between regimens. However, mice

immunized with SP-SAd36 displayed significantly higher anti-PvMSP1 titers post-priming compared to unmodified SAd36 primed mice (Figure 2D).

The quality of the antibodies induced by immunization was assessed through the analysis of IgG subclasses since anti-CSP (227) and MSP1 (226) cytophilic antibodies, which correspond with IgG2a in mice, as they have been found to be associated with protection. Analysis of the IgG1 and IgG2a titers 20 days after the final immunization (day 60), revealed no significant differences in the subclasses elicited by either vector against the two *P. vivax* chimeric proteins (Figure 2B, E). Antibody avidity 20 days after the final immunization was assessed as another measure of antibody quality. We observed that mice immunized with the SP-SAd36 regimen produced anti-cPvCSP and anti-cPvMSP1 antibodies of significantly higher avidity than those induced by the unmodified SAd36 regimen (Figure 2C, F).

Antibodies induced by vaccination recognize *Plasmodium* native proteins. The ability of the anti-cPvCSP and anti-cPvMSP1 antibodies to recognize the native structure of CSP and MSP1 was assessed by IFA. *P. berghei* sporozoites transgenic for the *P. vivax* CSP VK210 repeat region (265) were used for the assessment of the anti-cPvCSP antibodies, as the VK210 repeat region is present within the cPvCSP protein. We observed that antibodies elicited by either immunization regimen recognized the *P. vivax* CSP VK210 transgenic sporozoites (Figure 3A). Slides prepared with blood obtained from a *P. vivax* infected *Saimiri boliviensis* monkey were used for the assessment of anti-cPvMSP1 antibodies. We observed that sera obtained from mice immunized with either regimen bound to *P. vivax* schizonts (Figure 3B). Combined, these data indicate that antibodies elicited against the cPvCSP protein and cPvMSP1 protein recognize the native structure of the *P. vivax* CSP and MSP1, respectively.

Immunization with the SP-SAd36 regimen induces higher IFN- γ and IL-2 production by CD4+ and CD8+ T cells. The cellular response against cPvCSP and cPvMSP1 was assessed by determining the frequency of IFN- γ , IL-2 and TNF- α secreting T cells following *ex vivo* stimulation with peptides pools

representing the complete amino acid sequence of the chimeric proteins (86, 259). When the frequencies of cytokine-secreting T cells obtained from mice immunized with the SP-SAd36 regimen were compared to those of naïve mice, we observed significantly higher frequencies of cytokine-secreting CD4⁺ and CD8⁺ T cells obtained from the SP-SAd36 regimen in response to all cPvCSP and cPvMSP1 peptide pools (not shown). Significantly higher frequencies of cytokine-secreting T cells in mice immunized with the SAd36 regimen in comparison to naïve mice were only observed for IFN- γ –secreting CD8⁺ T cells in response to cPvCSP pool B and cPvMSP1 pool 2; for IL-2-secreting CD8⁺ T cells in response to cPvCSP pool A; for TNF- α secreting CD4⁺ T cells in response to cPvMSP1 pool 1; and for TNF- α secreting CD8⁺ T cells in response to both cPvMSP1 pools (Supplementary Figures 2 and 3).

Analyses between the SP-SAd36 and SAd36 immunization groups revealed significantly higher frequencies of IFN- γ secreting CD4⁺ T cells from mice immunized with the SP-SAd36 regimen following stimulation with cPvCSP pools A and B (Figure 4A). Significantly higher frequencies of IL-2-secreting CD4⁺ T cells were observed in mice immunized with the SP-SAd36 regimen in response to all four cPvCSP pools (Figure 4B). Analysis of CD8⁺ T cells revealed significantly higher frequencies of IFN- γ secreting cells in response to pool D in mice immunized with the SP-SAd36 regimen (Figure 4D). We observed no differences in the frequency of TNF- α secreting T cells between the immunization regimens (Figure 4C and F). When T cell multifunctionality was assessed, we observed that mice immunized with SP-SAd36 had significantly higher frequencies of IL-2 and TNF- α co-expressing CD4⁺ T cells when stimulated with cPvCSP Pool B (Supplementary Figure 4).

When the frequencies of IFN- γ , IL-2, and TNF- α secreting CD4⁺ and CD8⁺ T cells in response to the cPvMSP1 peptide pools were assessed, we observed a significantly higher frequency of IL-2 –secreting CD4⁺ T cells obtained from the SP-SAd36 regimen mice when compared to the unmodified SAd36 regimen (Figure 5B). No other significant differences were observed in the production of cytokines by CD4⁺ or CD8⁺ T cells in response to the cPvMSP1 peptide pools (Figure 5). When T cell multifunctionality was assessed, we observed that mice immunized with SP-SAd36 had significantly

higher frequencies of IFN- γ and IL-2 co-expressing cells CD8⁺ T cells when stimulated with cPvMSP1 Pool 2 (Supplementary Figure 5).

Higher frequencies of germinal center B cells are observed in draining lymph nodes following immunization with SP-SAd36. To further understand the mechanisms involved in the increased antibody avidity and IL-2 production by CD4⁺ T cells observed following immunization with the SP-SAd36 immunization regimen, we assessed the frequency of germinal center B cells (B220+CD95+GL7⁺) in draining lymph nodes via flow cytometry analysis. The experiments were conducted nine days after priming with 10⁸ v.p. of either the SAd36-*cPvCSP/cPvMSP1* or SP-SAd36-*cPvCSP/cPvMSP1* vector intramuscularly (Figure 6). We observed significantly higher frequencies of B220+CD95+GL7⁺ germinal center B cells in the mice immunized with the SP-SAd36 vector when compared to naïve mice (Figure 6A). However, no significant differences were observed between naïve mice and SAd36 immunized mice at this timepoint. Similarly, when we compared the total number of the B220+CD95+GL7⁺ triple positive population, we observed similar differences between the groups, with significant differences between the SP-SAd36 and naïve groups (Figure 6B). To confirm these differences in the GC B cell response, we conducted immunostaining using fluorescent microscopy of LNs obtained from the same animals at day 9 post-priming with either the SAd36 or SP-SAd36 priming. The draining inguinal LN sections were stained with anti-GL7 and anti-B220 antibodies, to identify GCs and B cell follicles respectively. Germinal centers were clearly stained in the dLN sections obtained from both SAd36 and SP-SAd36 when visualized by fluorescence microscopy with a distinctly higher number of GL7⁺ cells in lymph nodes from mice immunized with SP-SAd36 and very low number of positive cells observed in lymph nodes from unvaccinated mice (Figure 6C).

Discussion

The development of an effective malaria vaccine able to induce strong and balanced CD4+ and CD8+ T cell responses, as well as cytophilic antibodies, remains elusive. At present, multiple vaccine platforms and delivery systems are being investigated to determine the optimal vaccination regimen to induce broad and long-lasting immunity to malaria. Clinical studies of the protein-based vaccine, RTS,S, have shown protective efficacy mainly mediated through the induction of antibodies (266). However, suboptimal CD8+ T cell induction has been a concern for RTS,S (202). Evidence from clinical trials has demonstrated that adenoviral vectors induce strong CD8+ T cell responses to *Plasmodium* antigens while maintaining a good safety profile (240, 267-270). However, poor induction of CD4+ T cell responses by adenoviral-vectored malaria vaccine in clinical trials indicates that improvements in CD4+ T cell induction should be investigated (251).

Here we describe a strategy to further optimize the delivery of adenoviral transgenic products through the insertion of a murine IgG κ derived signal peptide. Although we observed no differences in the secretion of the cPvCSP/cPvMSP1 transgene product into the A549 tissue culture medium between the SP-SAd36 and unmodified SAd36 vectors, signal peptides have a variety of other effects on protein synthesis which may influence the selection of protein targeting pathways within the SP-SAd36 infected cells. Interactions between the signal peptide and the translocon at the endoplasmic reticulum (ER), as well as downstream events within the ER, including the potential cleavage of the IgG κ signal peptide, may also affect antigen presentation (reviewed in (253)). Our observations of increased antibody responses are consistent with those observed in recent studies on the effect of signal peptides on the immunogenicity of the HIV glycoprotein gp120, which found that the addition of a signal peptide impacted the glycan profile of gp120 increasing the antigenicity of the mature protein (271). Additionally, the use of a signal peptide in an HPV DNA vaccine based on the protein E7 was found to significantly increase antibody titers to E7, a tumor-associated antigen which typically exhibits low immunogenicity, when compared to mice immunized with the same antigen without the signal peptide. The authors

concluded that this was due to the conserved function of the signal peptide and its ability to alter the default protein trafficking pathway; this modulation in the sorting of the heterologous protein in mammalian cells resulted in the increased humoral immune response to the DNA vaccine (272). However, the changes in immunogenicity may also vary depending on the adenoviral vector used, as comparative assessments of Ad5 and Ad26 vectored gp120 vaccinations have found that the viral vector used can skew the Fc-effector profiles of vaccine-induced antibodies and glycosylation profiles (273-276). The contribution of the murine IgG κ signal peptide on these processes as part of the SP-SAd36 vector transgene, therefore, requires further investigation.

Comparison of the antibody response induced by the SP-SAd36 and unmodified SAd36 regimens revealed that the SP-SAd36 vector induced significantly higher antibody avidity in comparison to the unmodified vector. These findings are significant as increased avidity may translate to enhanced efficacy based on observations from preclinical studies of *P. falciparum* CSP vaccines which reported that avidity indices above 0.80 provided sterilizing protection against *P. falciparum* CSP transgenic *P. berghei* challenge (236). *P. falciparum* vaccine clinical trials have also demonstrated antibody avidity to be associated with improved ability to inhibit parasite growth (277).

Assessment of differences in cellular immunogenicity revealed significantly higher frequencies of IFN- γ -secreting CD4+ T cells in response to the peptide pools representing the promiscuous T cell epitopes within cPvCSP protein chimera. This improvement is encouraging based on reports that high frequencies of IFN- γ -secreting CD4+ T cells provide protection from malaria (58, 70). Moreover, IFN- γ producing CD4+ cells play a crucial role in promoting B cell class switching activity (243) and have also been associated with protection from *P. falciparum* in clinical trials (230).

Immunization with the SP-SAd36 regimen also resulted in increased frequencies of IL-2 secreting CD4+ T cells observed in response to all peptide pools of cPvCSP and cPvMSP1. This feature may represent a significant improvement for adenoviral vectors based on a recent study by Lee et al. (252) which found that vaccination with an Ad5 recombinant vector induced significantly lower frequencies of

antigen-specific CD4⁺ TH1 cells compared to acute infection, an effect attributed low IL-2 signaling (252). The increased IL-2 production we observed also has the potential to improve the overall T cell immunogenicity, as IL-2 promotes proliferation and differentiation of naïve CD8⁺ T cells and the survival of antigen-experienced T cells (278). These improvements in the cellular immune responses are consistent with reports demonstrating enhanced immunogenicity of a DNA vaccine due to the inclusion of the IgG κ signal peptide when compared to an unmodified vaccine (258).

When we assessed germinal center B cell responses, we observed the highest frequency of germinal center B cells in mice immunized with the SP-SAd36 vector, suggesting that the improvements in antibody avidity observed for the SP-SAd36 regimen may be due to the induction of better germinal center responses. Previous studies of germinal center B cells and T follicular helper (TFH) responses in mouse models of *Plasmodium* infection have found that increased frequencies of these cell types are associated with increased titers of anti-parasite antibodies and improvements in parasite control and clearance (222, 279). Moreover, in the murine *P. chabaudi* model the germinal centers are essential for the resolution of chronic infection (280, 281).

Overall, we observed that the inclusion of a IgG κ signal in the sequence of an adenoviral vector insert, improved the functionality of CD4⁺ cells, the antibody avidity and the frequency of germinal center B cells. Our results highlight the potential of this method to improve existing viral vector vaccine platforms and warrants further investigation.

Conflicts of Interest. None.

Funding. This research was supported by the National Institutes of Health, NIAID grants R56-AI103382-01A1 and R21-AI117459-01A1, and the Yerkes National Primate Research Center Base Grant No RR00165 awarded by the National Center for Research Resources of the National Institutes of Health. This project was supported in part by ORIP/OD P51OD011132.

Acknowledgments. The authors would like to thank Dr. James Wilson for providing us with the SAd36 vector; Dr. Fidel Zavala for providing our group with *P. vivax* CSP VK210 repeat region transgenic *P. berghei* sporozoites for IFA slides; Dr. Mary Galinski for providing our group with *P. vivax* infected *Saimiri boliviensis* blood for IFA slides; Evan Dessasau III from Yerkes Histology Core for sectioning of murine lymph nodes; Dr. Deepa Kodandera from the Yerkes Molecular Pathology Core for sectioning, staining, and technical assistance with the lymph node IFA slides; Dr. April Reedy from the Emory Integrated Cellular Imaging core for assistance in fluorescence microscopy and image capture; and Monica Cabrera-Mora for technical support.

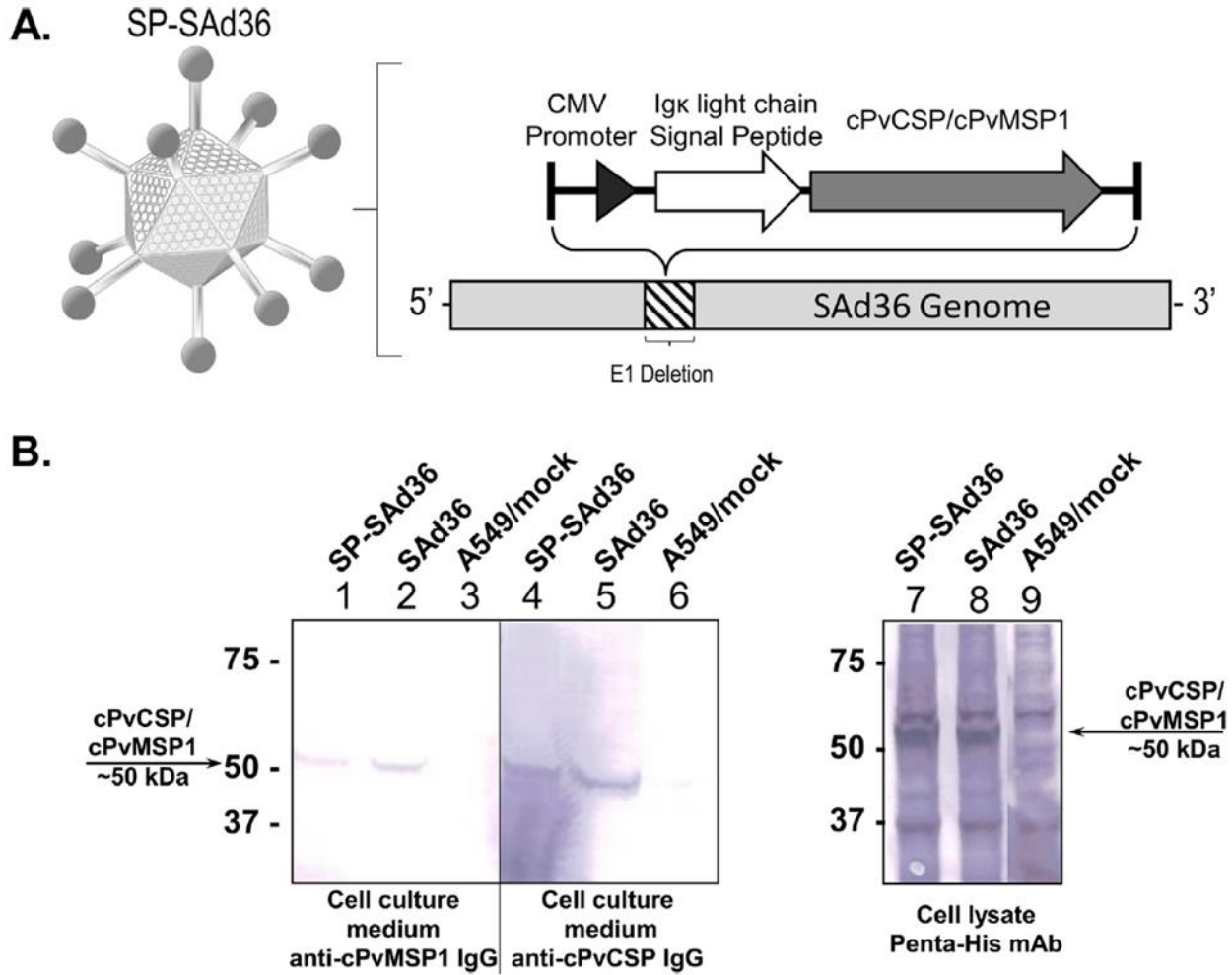


Figure 1. Signal Peptide Simian Adenovirus 36 schematic and protein expression. A) Schematic of the signal peptide simian adenovirus 36 vector (SP-SAd36-*cPvCSP/cPvMSP1*). The SP-SAd36 vector is replication deficient due to deletion of the E1 and E3 genes. Inserted in the place of the deleted E1 gene is the immunoglobulin kappa light chain signal peptide and the *cPvCSP/cPvMSP1* transgene, which is under control of the cytomegalovirus (CMV) promoter. B) Analysis of *cPvCSP/cPvMSP1* expression following Ad vector infection. Western blot analysis of A549 cells 2 days post infection with the indicated Ad vectors at the MOI of 2,500 vp/cell. The major protein bands close to 51 kDa correspond to the expected mass for *cPvCSP/cPvMSP1*. The positions of molecular weight markers (in thousands of daltons) are indicated to the left of each gel. **Left:** The secretory proteins were detected in culture medium

collected from cells infected with SP-SAd36-*cPvCSP/cPvMSP1* (lane 1) and SAd36-*cPvCSP/cPvMSP1* (lane 2) using antibodies raised against the cPvMSP1 protein in rabbits. Antibodies raised against the cPvCSP protein in rabbits were used to detect secretory proteins in tissue culture medium collected from cells infected with SP-SAd36-*cPvCSP/cPvMSP1* (lane 4) and SAd36-*cPvCSP/cPvMSP1* (lane 5). Mock-infected A549 cells (lane 3 and 6) are also shown as controls. **Right:** The hybrid cPvCSP/cPvMSP1 protein containing a 6x-His Tag, was detected in samples of cell lysates obtained from cells infected with SP-SAd36-*cPvCSP/cPvMSP1* (lane 7) and SAd36-*cPvCSP/cPvMSP1* (lanes 8) using a Penta-His mAb. The negative control sample of mock-infected A549 cells (lane 9) is also shown.

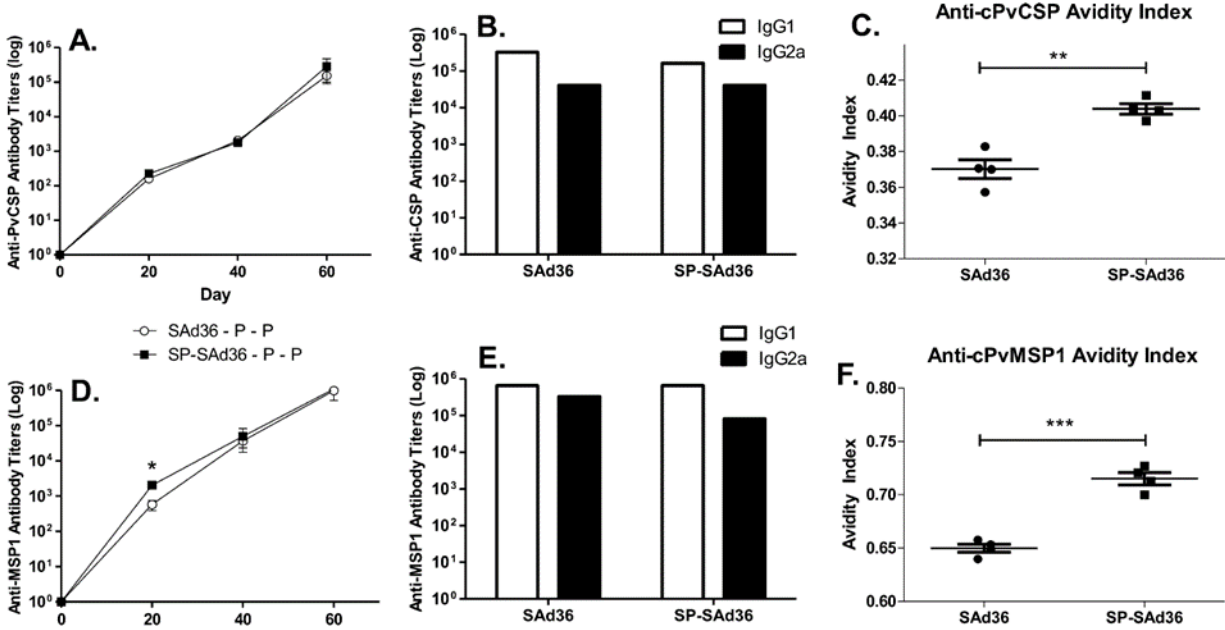


Figure 2. Antibody response to cPvCSP and cPvMSP1 proteins following priming immunization at day 0 with either the unmodified *SAd36-cPvCSP/cPvMSP1* recombinant vector or the recombinant vector including the signal peptide sequence (*SP-SAd36-cPvCSP/cPvMSP1*) and two subsequent recombinant proteins boosts at days 20 and 40. A) Kinetics of antibody titers to cPvCSP. B) IgG1 and IgG2a antibody titers elicited against cPvCSP, 20 days after the final immunization. C) Antibody avidity against cPvCSP, determined by ammonium thiocyanate ELISAs 20 days after the final immunization. D) Kinetics of antibody titers to cPvMSP1. E) IgG1 and IgG2a antibody titers elicited against cPvMSP1, 20 days after the final immunization. F) Antibody avidity against cPvMSP1, determined by ammonium thiocyanate ELISAs 20 days after the final immunization. Statistical analysis was conducted using Mann Whitney test for antibody titers, and unpaired t-test for avidity to determine differences between the immunization regimens. Statistically significant differences are denoted by *($p < 0.05$), **($p < 0.01$).

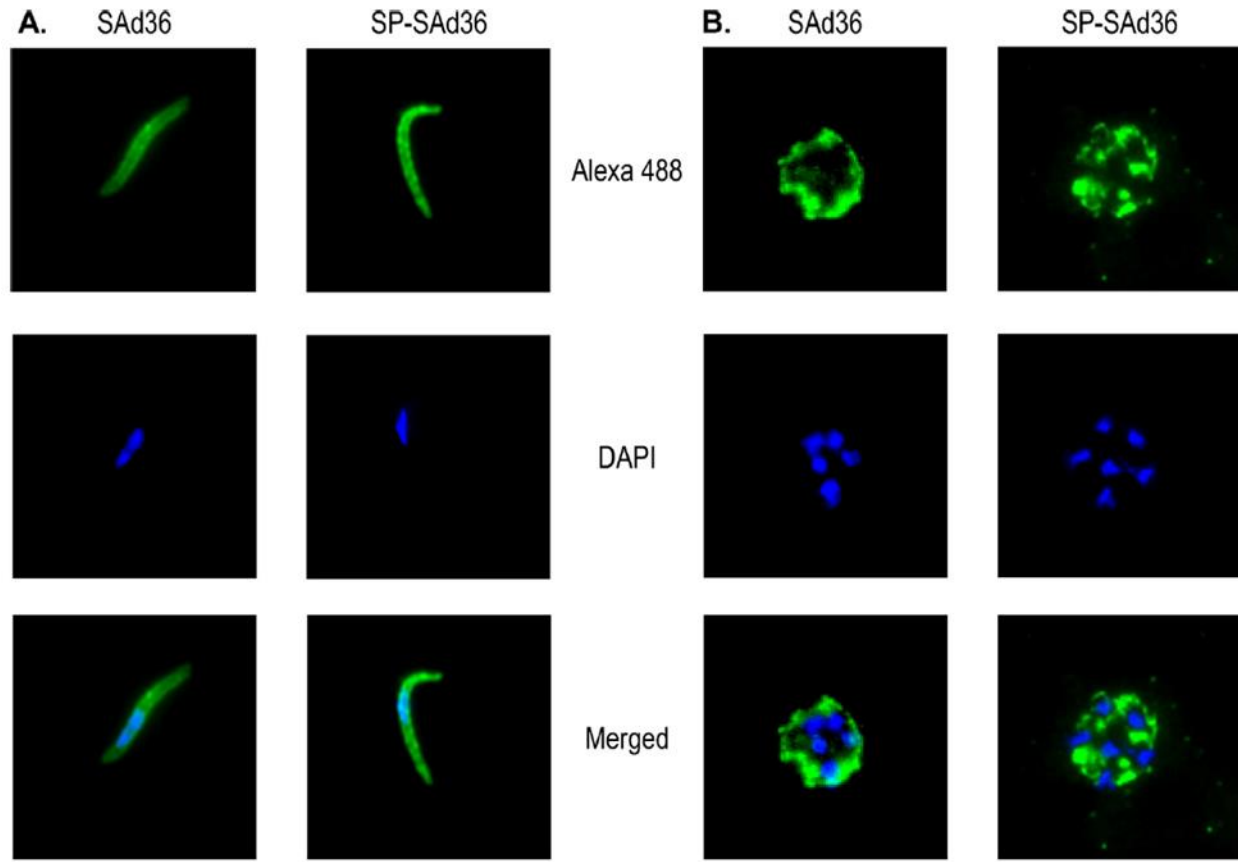


Figure 3. Immunofluorescence assays of *P. vivax* sporozoites and blood stage schizonts. Reactivity of immunized mouse sera to sporozoites (A) and blood stage schizonts (B). Top panels show Alexa 488 labeled anti-mouse IgG secondary antibodies binding to sera obtained from mice immunized with either the regimen that included priming with the unmodified SAd36-*cPvCSP/cPvMSP1* or SP-SAd36-*cPvCSP/cPvMSP1* recombinant vectors 20 days after the final immunization. Middle panels show the DAPI stained nuclei of sporozoites and blood stage schizonts. The bottom panels show the merged images.

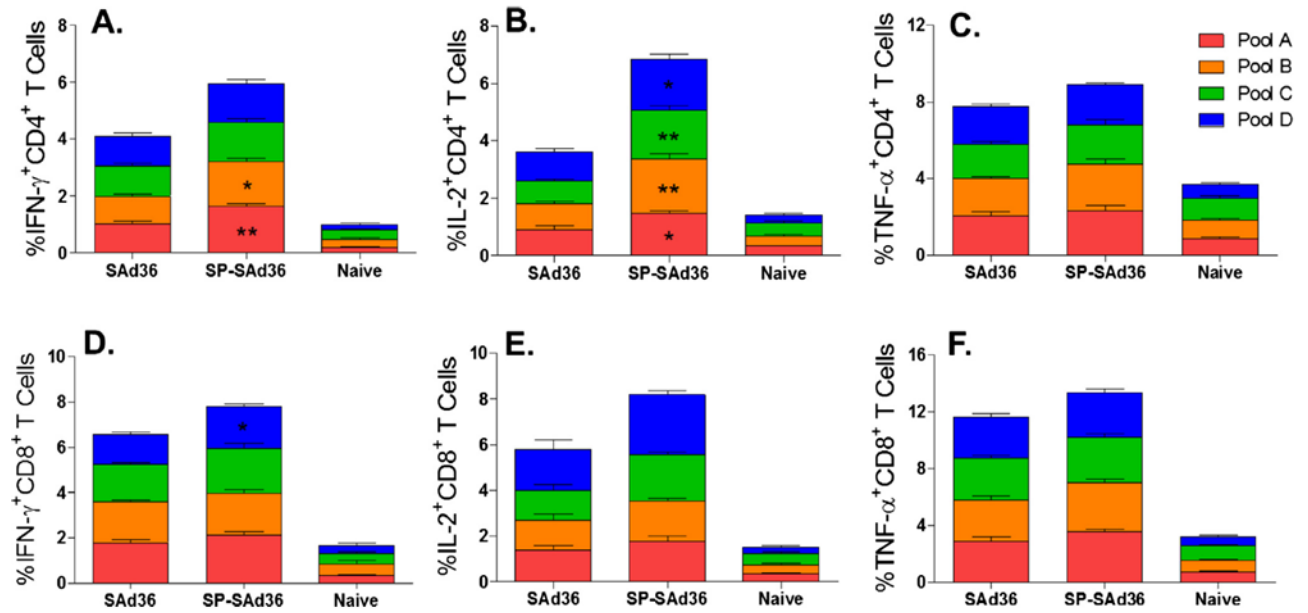


Figure 4. Cytokine-secreting T cells after *ex vivo* stimulation with cPvCSP peptide pools 5 days after the final immunization and assessed by flow cytometry. A-C) Frequency of cytokine-secreting CD4⁺ T cells following stimulation with cPvCSP peptide pools A, B, C, or D. D-F) Frequency of cytokine-secreting CD8⁺ T cells following stimulation with cPvCSP peptide pools A, B, C, or D. Interferon- γ -secreting T cells are shown in Figures A and D. Interleukin-2-secreting T cells are shown in B and E. Tumor necrosis factor- α -secreting T cells are shown in C and F. Values represent the percentage of either CD4⁺ or CD8⁺ T cells positive for the individual cytokine. Kruskal-Wallis test with Dunn's post-test was used to determine differences in the production of cytokines in response to a stimulus with an individual peptide pool between mice immunized with a regimen that included a priming with SAd36-*cPvCSP/cPvMSP1* or priming with SP-SAd36-*cPvCSP/cPvMSP1*. Statistically significant differences between the SAd36 and SP-SAd36 regimens in response to individual pools are denoted by *(p < 0.05) and **(p < 0.01) within the SP-SAd36 bar.

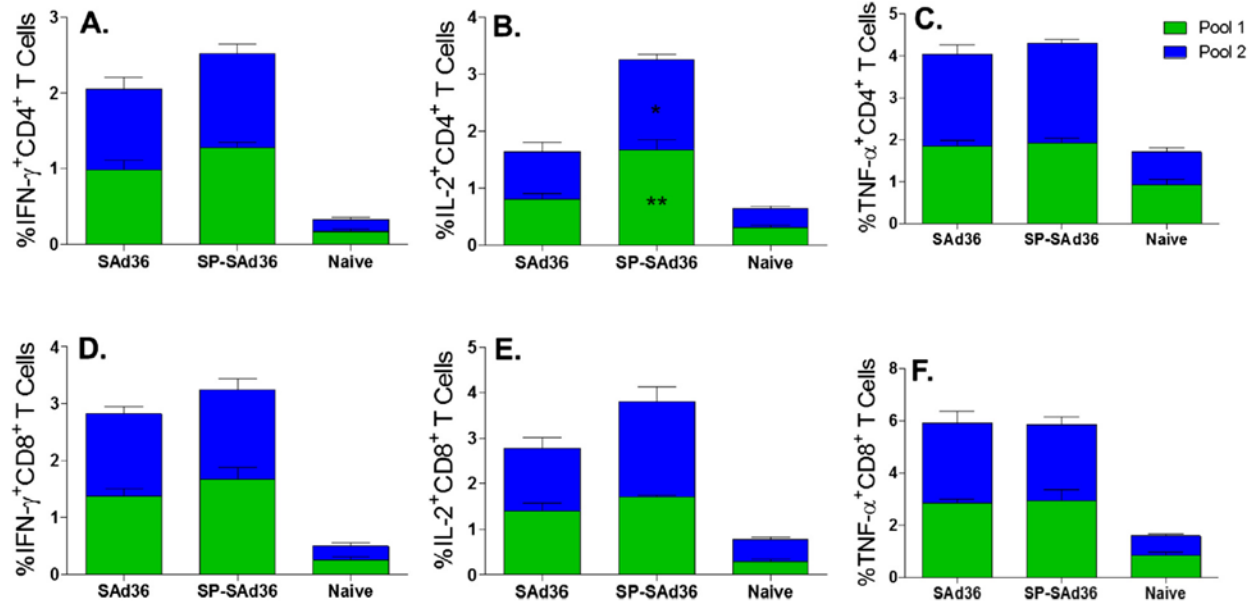


Figure 5. Cytokine-secreting T cells after *ex vivo* stimulation with cPvMSP1 peptide pools 5 days after the final immunization and assessed by flow cytometry. A-C) Frequency of cytokine-secreting CD4⁺ T cells following stimulation with cPvMSP1 peptide pools 1 or 2. D-F) Frequency of cytokine-secreting CD8⁺ T cells following stimulation with cPvMSP1 peptide pools 1 or 2. Interferon- γ -secreting T cells are shown in Figures A and D. Interleukin-2-secreting T cells are shown in B and E. Tumor necrosis factor- α -secreting T cells are shown in C, and F. Values presented represent the percentage of either CD4⁺ or CD8⁺ T cells positive for the individual cytokine. Statistical analysis was conducted using Kruskal Wallis with Dunn's post-test was used to determine differences in the production of cytokines in response to a stimulus with an individual peptide pool between mice immunized with a regimen that included priming with SAd36-*cPvCSP/cPvMSP1* or priming with SP-SAd36-*cPvCSP/cPvMSP1*. Statistically significant differences between the SAd36 and SP-SAd36 regimens in response to individual pools are denoted by *($p < 0.05$) and **($p < 0.01$) within the SP-SAd36 bar.

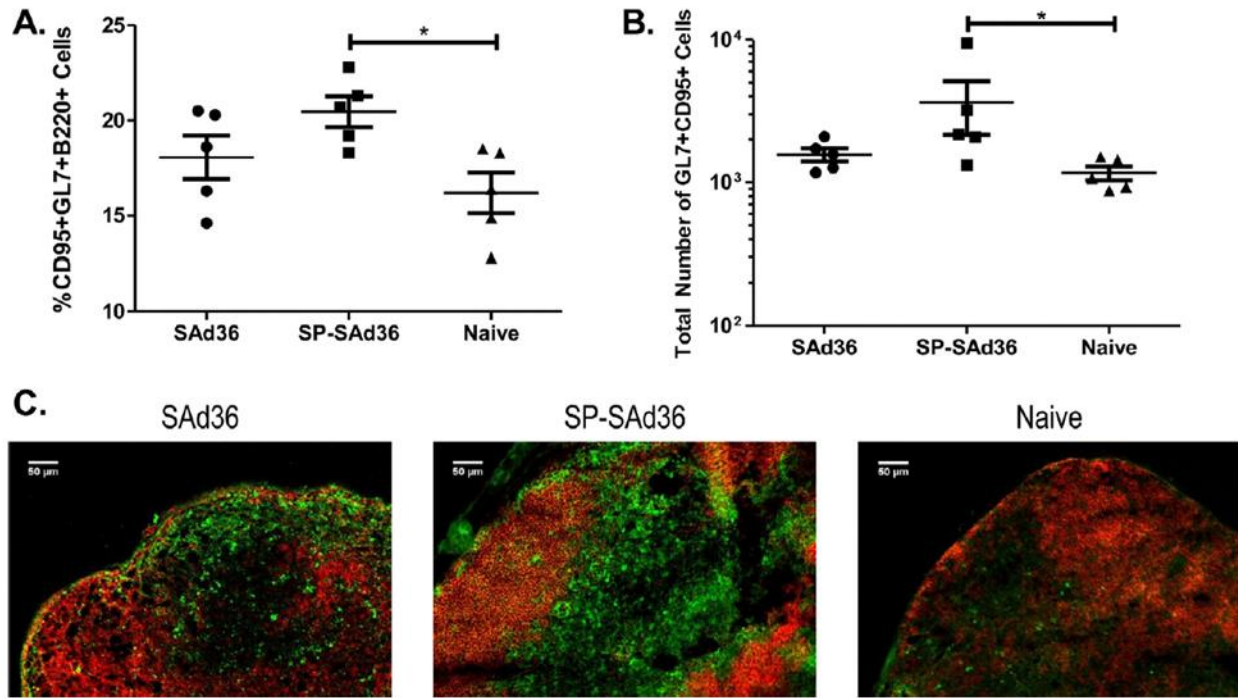
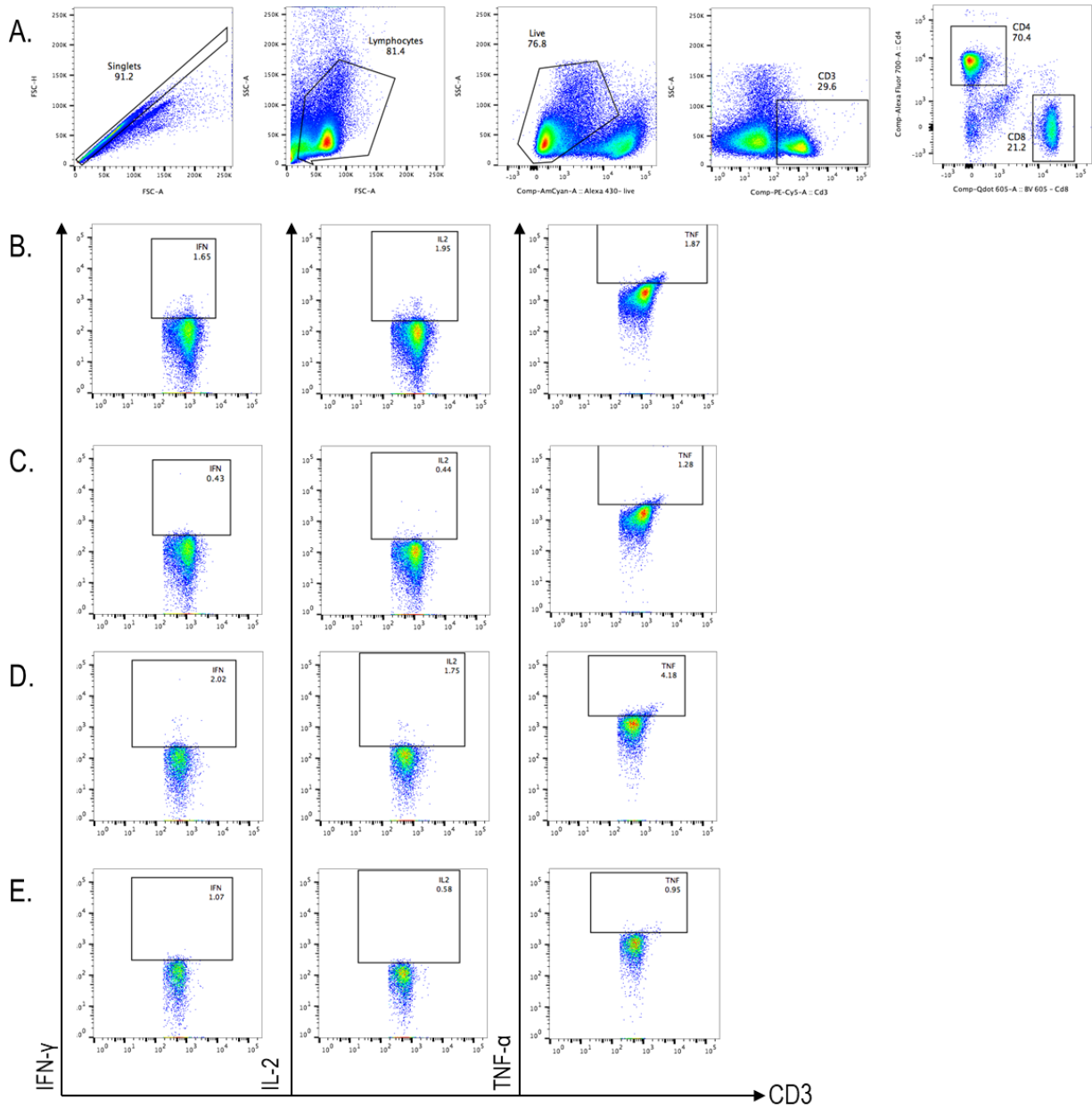
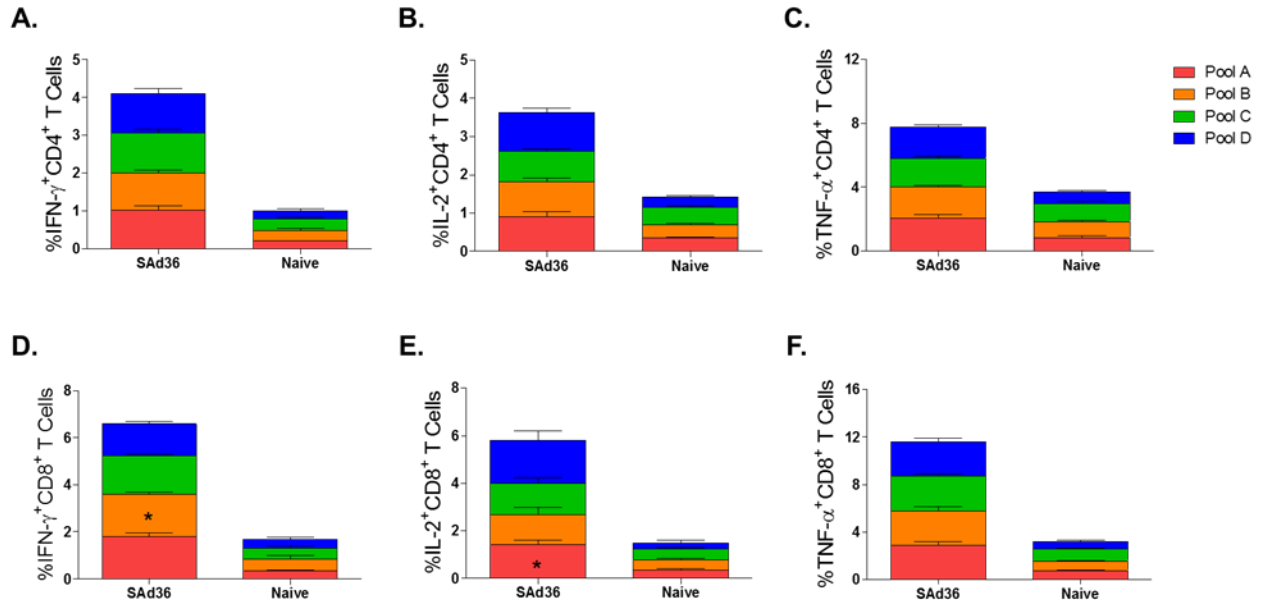


Figure 6. Frequency and total number of germinal center B cells in the draining lymph nodes nine days post priming. Frequency (A) and total number (B) of germinal center B cells, identified by positive staining with anti-B220, CD95, and GL7 antibodies via flow cytometry for the SP-SAd36-*cPvCSP/cPvMSP1* and SAd36-*cPvCSP/cPvMSP1* immunizations, and naïve mice. Statistical analysis was conducted using Kruskal-Wallis with Dunn’s post-test to determine differences between the immunization regimens. Statistically significant differences are denoted by *($p < 0.05$). C) Draining inguinal lymph node from the same mice were obtained 9 days after priming with either the SP-SAd36-*cPvCSP/cPvMSP1* or SAd36-*cPvCSP/cPvMSP1* vectors, and sectioned and stained with the same fluorochrome-conjugated anti-B220 and GL7 antibodies used for flow cytometry assessment. A representative section from each group is shown at 20x magnification.

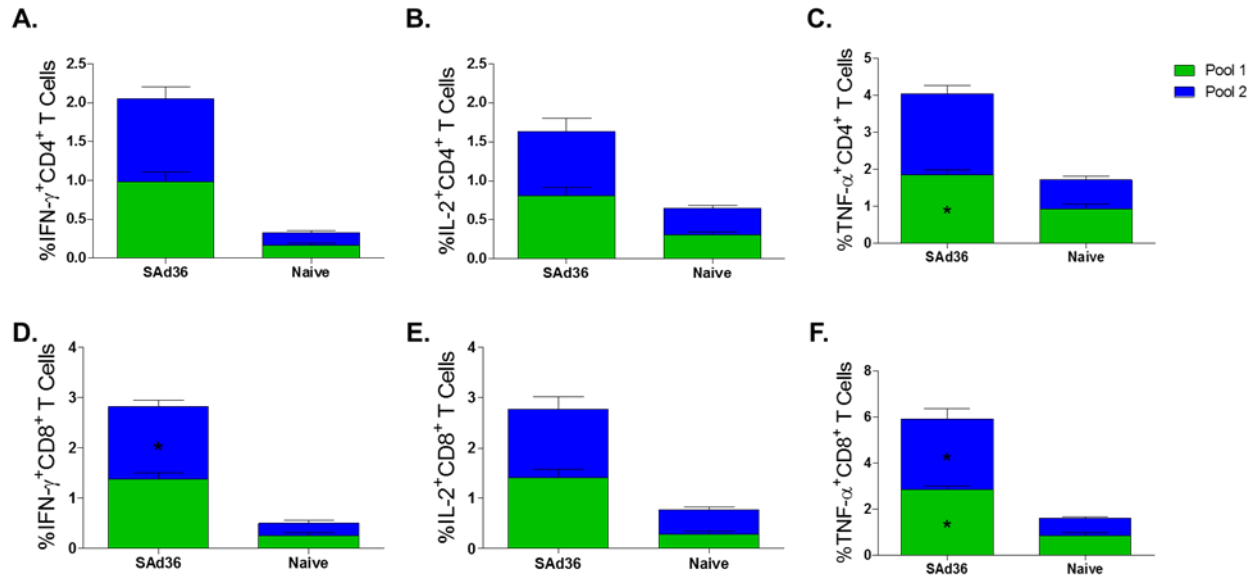


Supplementary Figure 1. Sample Gating Strategy. Splenocytes from immunized animals were obtained five days after the final immunization and stimulated with a single peptide pool from either cPvCSP or cPvMSP1. Splenocytes derived from naïve mice housed in similar conditions were used as a control. Cells were then stained with fluorescent antibodies and gated based on size for singlets and lymphocytes, then on live cells based on negative staining for viability dye. Live cells were further gated

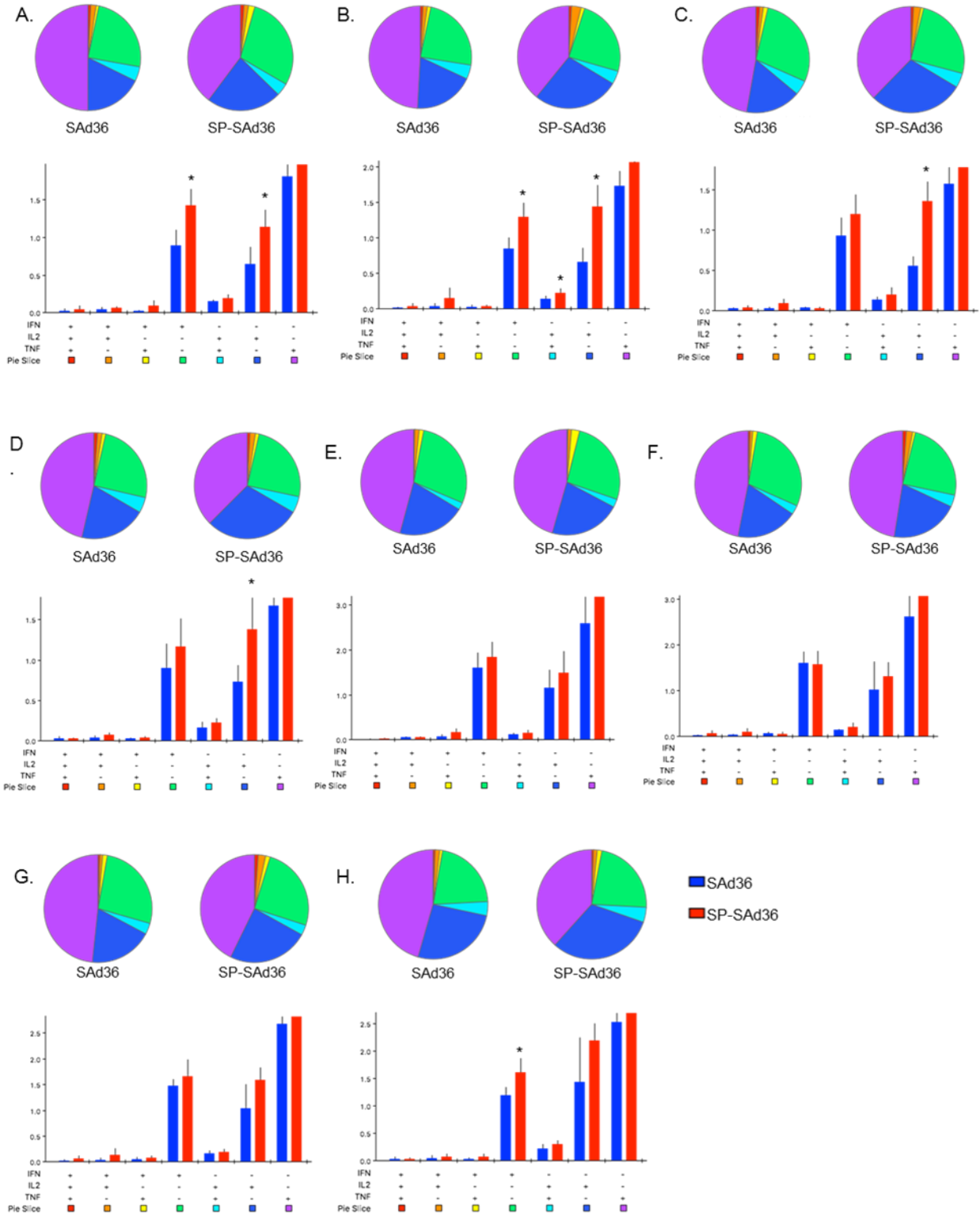
on CD3⁺, then on either CD4⁺ or CD8⁺ (A). CD4⁺ and CD8⁺ populations were then gated on interferon- γ , interleukin-2, and tumor necrosis factor- α positive populations. Plots from a representative mouse from the SP-SAd36-*cPvCSP/cPvMSP1* and naïve groups following stimulation with Pool B of cPvCSP are shown. Cytokine production by the CD4⁺ T cells from the representative SP-SAd36 mouse (B) and naïve mouse (C), and cytokine production by CD8⁺ T cells from the representative SP-SAd36 mouse (D) and naïve mouse (E).



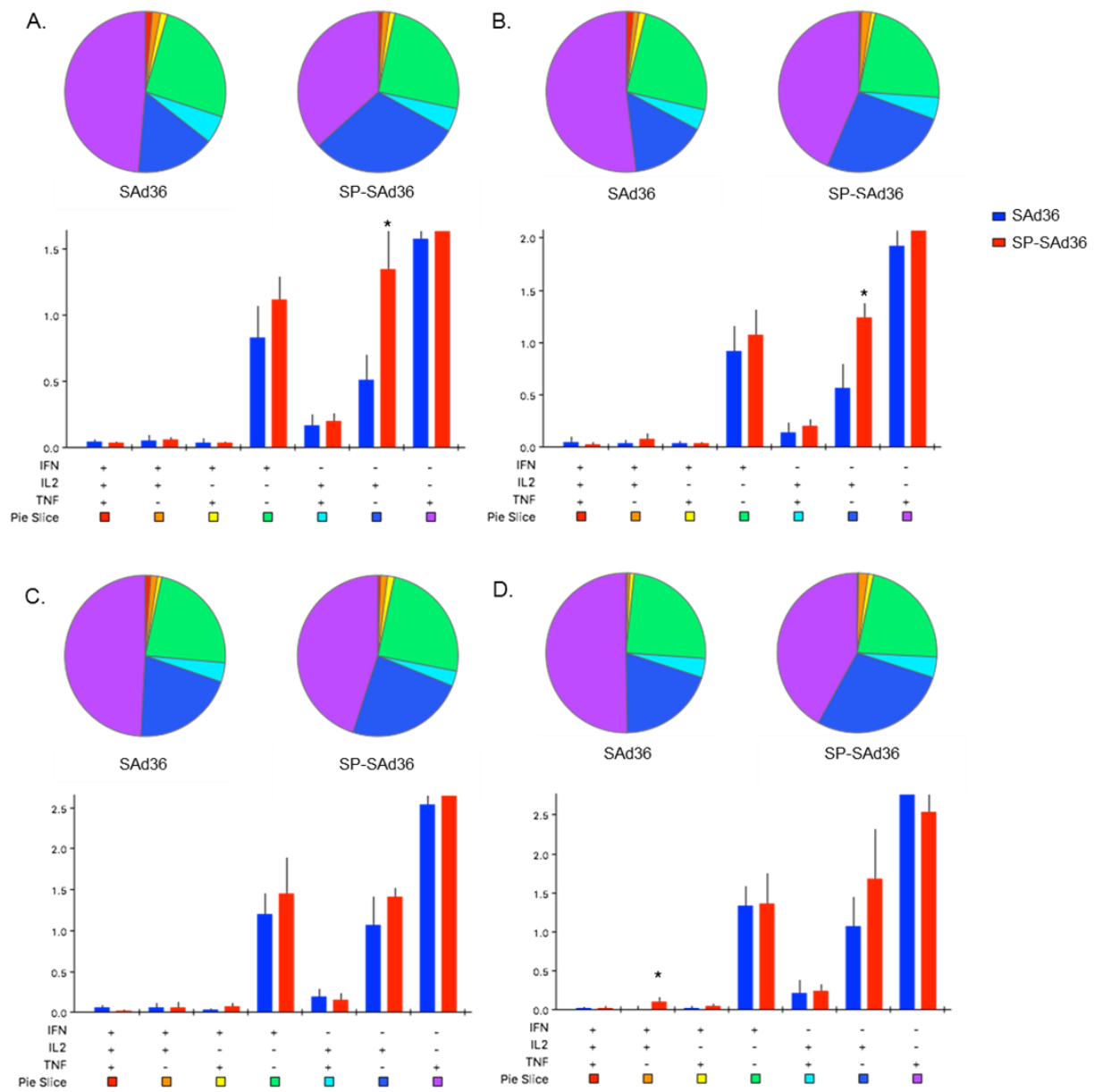
Supplementary Figure 2. Cytokine-secreting T cells after ex vivo stimulation with cPvCSP peptide pools 5 days after the final immunization of mice primed with SAD36-*cPvCSP/cPvMSP1* and assessed by flow cytometry. A-C) Cytokine responses of CD4⁺ T cells following stimulation with cPvCSP peptide pools A, B, C, or D. D-F) Cytokine responses of CD8⁺ T cells following stimulation with cPvCSP peptide pools A, B, C, or D. Interferon- γ responses are shown in figures A and D. Interleukin-2 responses are shown in B and E. Tumor necrosis factor- α responses are shown in C and F. Values presented represent the percentage of either CD4⁺ or CD8⁺ T cells positive for the cytokine. Statistical analysis was conducted using Mann Whitney test to determine differences in the production of cytokines in response to a stimulus with an individual pool between the regimen that included priming with SAD36-*cPvCSP/cPvMSP1* and naïve mice. Statistically significant differences between groups in response to individual pools are denoted by *($p < 0.05$) within the SAD36 bar.



Supplementary Figure 3. Cytokine-secreting T cells after ex vivo stimulation with cPvMSP1 peptide pools 5 days after the final immunization of mice primed with SAAd36-cPvCSP/cPvMSP1 and assessed by flow cytometry. A-C) Cytokine responses of CD4⁺ T cells following stimulation with cPvMSP1 peptide pools 1 or 2. D-F) Cytokine responses of CD8⁺ T cells following stimulation with cPvMSP1 peptide pools 1 or 2. Interferon- γ responses are shown in figures A and D. Interleukin-2 responses are shown in B and E. Tumor necrosis factor- α responses are shown in C, and F. Values presented represent the percentage of either CD4⁺ or CD8⁺ T cells positive for the cytokine. Statistical analysis was conducted using Mann Whitney test to determine differences in the production of cytokines in response to a stimulus with an individual pool between the regimen that included priming with SAAd36-cPvCSP/cPvMSP1 and naïve mice. Statistically significant differences between groups in response to individual pools are denoted by *($p < 0.05$) within the SAAd36 bar.

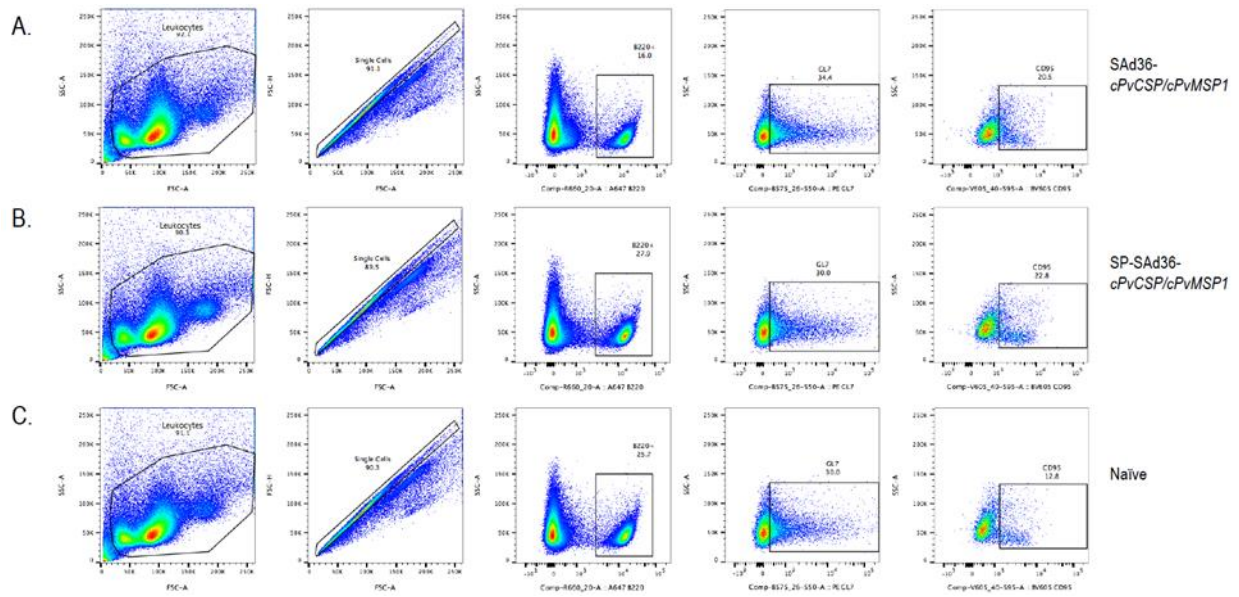


Supplementary Figure 4. Secretion of multiple cytokines by T cells in response to ex vivo stimulation with cPvCSP peptide pools 5 days after the final immunization and assessed by flow cytometry. Pies represent the percentage of multifunctional and single cytokine producing CD4+ or CD8+ T cells. Bar graphs represent the percentage of CD4+ or CD8+ T cells producing three, two or one cytokines out of the total CD4+ or CD8+ T cell population. The multifunctionality of CD4+ T in response to stimulation with cPvCSP (A) Pool A, (B) Pool B, (C) Pool C, or (D) Pool D are shown in the top four panels. The multifunctionality of CD8+ T cells in response to stimulation with cPvCSP (E) Pool A, (F) Pool B, (G) Pool C, or (H) Pool D, are shown in the bottom four panels. Statistically significant differences between mice immunized with a regimen that included priming with SAd36-*cPvCSP/cPvMSP1* (blue bars) or priming with SP-SAd36-*cPvCSP/cPvMSP1* (red bars) in response to individual pools were determined using student's T-test are denoted by *($p < 0.05$) above the SP-SAd36 bar. Graphs were produced using SPICE software (223).



Supplementary Figure 5. Secretion of multiple cytokines by T cells in response to ex vivo stimulation with cPvMSP1 peptide pools 5 days after the final immunization and assessed by flow cytometry. Pies represent the percentage of multifunctional and single cytokine producing CD4+ or CD8+ T cells. Bar graphs represent the percentage of CD4+ or CD8+ T cells producing three, two or one cytokines out of the total CD4+ or CD8+ T cell population. The multifunctionality of CD4+ T in response

to stimulation with (A) Pool 1 of cPvMSP1 and (B) Pool 2 of cPvMSP1, as well the multifunctionality of CD8⁺ T cells in response to stimulation with (C) Pool 1 of cPvMSP1 and (D) Pool 2 of cPvMSP1 are shown. Statistically significant differences between mice immunized with a regimen that included priming with SAd36-*cPvCSP/cPvMSP1* (blue bars) or priming with SP-SAd36-*cPvCSP/cPvMSP1* (red bars) in response to individual pools were determined using student's T-test are denoted by *($p < 0.05$) above the SP-SAd36 bar. Graphs were produced using SPICE software (223).



Supplementary Figure 6. Sample Gating Strategy for Germinal Center B cells. Cells from the draining lymph nodes of immunized and naïve animals were obtained nine days after priming with either the unmodified SAd36 or SP-SAd36 vector or left unvaccinated. Cells were then stained with fluorescent antibodies and gated based on size for leukocytes and singlets, then on live cells based on negative staining for viability dye. Live cells were further gated on B220+, and GL7+ and CD95+. Plots from representative mice from the SAd36-cPvCSP/cPvMSP1 (A), SP-SAd36-cPvCSP/cPvMSP1 (B), and naïve groups (C) are shown.

Table 1. Immunization Regimens

Regimen	Prime Day 0		Boost Day 20		Boost Day 40	
	Ad-transgene	Dose	Protein	Dose	Protein	Dose
Unmodified SAd36	SAd36- <i>cPvCSP/cPvMSP1</i>	10 ⁸ v.p.	cPvCSP+cPv MSP1	10 µg/each	cPvCSP+cPv MSP1	10 µg/each
Signal Peptide SAd36	SP-SAd36- <i>cPvCSP/cPvMSP1</i>	10 ⁸ v.p.	cPvCSP+cPv MSP1	10 µg/each	cPvCSP+cPv MSP1	10 µg/each
Naïve Control	No immunization		No Immunization		No Immunization	

Mice received an intramuscular prime at day 0 with the adenovirus in PBS at a dose of 10⁸ v.p.

Mice were boosted subcutaneously with a mixture of 10 µg of the individual cPvCSP and cPvMSP1 proteins emulsified in Montanide ISA 51 VG in a 1:1 volume ratio at days 20 and 40. Blood was drawn in the 24 hours preceding each immunization and 20 days after the final immunization for the analysis of antibody responses by ELISA and immunofluorescence assays (n=5). Splenocytes were obtained 5 days after the final immunization for analysis of T cell functionality in response to stimulation with cPvCSP or cPvMSP1 peptide pools (n=5).

Chapter 4

A multi-stage *Plasmodium vivax* malaria vaccine candidate able to induce long-lived antibody responses against blood stage parasites and robust transmission-blocking activity

Jessica N. McCaffery ^{1, #}, Jairo A. Fonseca ^{1, 2, a, #}, Balwan Singh ¹, Monica Cabrera-Mora ¹, Caitlin Bohannon ¹, Joshy Jacob ^{1, 3}, Myriam Arévalo-Herrera ⁴, Alberto Moreno ^{1, 2}

1. Emory Vaccine Center, Yerkes National Primate Research Center, Emory University, 954 Gatewood Road, Atlanta, GA 30329.
2. Division of Infectious Diseases, Department of Medicine, Emory University, 69 Jesse Hill, Jr. Drive, SE, Atlanta, GA 30303.
3. Department of Microbiology and Immunology, Emory University School of Medicine, 1510 Clifton Road, Atlanta, Ga 30322.
4. Caucaseco Scientific Research Center, Malaria Vaccine and Drug Development Center (MVDC), Cali, Colombia.

Originally published in *Frontiers in Cellular and Infection Microbiology*:

McCaffery JN, Fonseca JA, Singh B, Cabrera-Mora M, Bohannon C, Jacob J, Arévalo-Herrera M, Moreno A. (2019). A Multi-Stage *Plasmodium vivax* Malaria Vaccine Candidate Able to Induce Long-Lived Antibody Responses Against Blood Stage Parasites and Robust Transmission-Blocking Activity. *Front Cell Infect Microbiol.* 2019 May 1;9:135. PMID: 28483199. doi: 10.3389/fcimb.2019.00135.

Copyright © 2017, Frontiers.

Abstract

Malaria control and interventions including long-lasting insecticide-treated nets, indoor residual spraying, and intermittent preventative treatment in pregnancy have resulted in a significant reduction in the number of *Plasmodium falciparum* cases. Considerable efforts have been devoted to *P. falciparum* vaccines development with much less to *P. vivax*. Transmission-blocking vaccines, which can elicit antibodies targeting *Plasmodium* antigens expressed during sexual stage development and interrupt transmission, offer an alternative strategy to achieve malaria control. The post-fertilization antigen P25 mediates several functions essential to ookinete survival but is poorly immunogenic in humans. Previous clinical trials targeting this antigen have suggested that conjugation to a carrier protein could improve the immunogenicity of P25. Here we report the production, and characterization of a vaccine candidate composed of a chimeric *P. vivax* Merozoite Surface Protein 1 (cPvMSP1) genetically fused to *P. vivax* P25 (Pvs25) designed to enhance CD4⁺ T cell responses and assessed in a murine model. We demonstrate that antibodies elicited by immunization with this chimeric protein recognize both the erythrocytic and sexual stages and are able to block the transmission of *P. vivax* field isolates in direct membrane-feeding assays. These findings provide support for the continued development of multi-stage transmission blocking vaccines targeting the life-cycle stage responsible for clinical disease and the sexual-stage development accountable for disease transmission simultaneously.

Introduction

Malaria remains one of the most serious threats to global health. In 2017, there were an estimated 219 million malaria cases resulting in 435,000 deaths worldwide (1). Of the five *Plasmodium* species that cause malaria in humans, *P. vivax* is the most widely distributed with ~2.8 billion people at risk of infection (282). Its wide geographical range is mainly due to the ability of *P. vivax* to develop within the *Anopheles* mosquito vector at lower temperatures, allowing for its survival at higher altitudes and temperate climates (283). Furthermore, *P. vivax* has the ability to produce hypnozoites, dormant liver-stage parasites present in *P. vivax* but not in *P. falciparum* (284), causing relapse infections weeks to months after the initial infection. Effective malaria control programs, therefore, require comprehensive measures that involve targeting both of *Plasmodium* species (285, 286).

Current malaria control efforts have mainly been focused on the use of vector-based interventions, including long-lasting insecticide-treated nets (LLIN), indoor residual spraying (IRS), and preventative therapies. Preventive therapies include intermittent preventative treatment in pregnancy (IPTp) with the sulfadoxine-pyrimethamine and seasonal malaria chemoprevention (SMC) in children aged 3-59 months living in areas of high seasonal malaria transmission (1). While these interventions have resulted in a significant reduction in *P. falciparum* cases (287), *P. falciparum* vector-based interventions are less efficacious against *P. vivax* (288). Anomalous climate patterns, as well as the emergence of mosquito resistance to insecticides (289, 290) and parasite resistance to antimalarial treatments (1, 291, 292), pose additional challenges to the prevention and treatment of malaria despite improved malaria control coverage.

Due to the numerous challenges faced by traditional malaria control methods, the development of novel intervention tools is essential. One potential strategy is the use of transmission-blocking vaccines as they are considered one of the best alternatives to achieve malaria control. Since the life cycle of *Plasmodium* requires the female *Anopheles* mosquito to ingest gametocytes during a blood meal from an infected human

host to reach the mosquito midgut and begin the next stage of development outside the human red blood cells, this transition could be interrupted by anti-parasite antibodies present in the blood meal (156).

There are two kinds of transmission blocking antigens that can be targeted by vaccines: pre-fertilization and post-fertilization antigens. Pre-fertilization antigens are expressed by gametocytes and gametes; antibodies against these antigens can block the formation of zygotes by binding to the gametes (187). Post-fertilization antigens are expressed by zygotes, ookinetes, and oocysts, antibodies that recognize these forms prevent the mosquito midgut invasion (156, 187). Under natural conditions, the human host is not exposed to post-fertilization antigens. However, transmission-blocking vaccination can be used to elicit antibodies targeting post-fertilization antigens that the mosquito will be exposed to during the blood meal.

Of the post-fertilization antigens described to date, the P25 protein present on the surface of ookinetes and oocysts, first described by Tsuboi et al. (293), is one the best characterized (294). P25 mediates several functions including promoting the clustering of the ookinetes and allowing them to survive the midgut proteolytic environment (188). P25 also mediates the attachment and invasion of the mosquito midgut by damaging the midgut epithelium (189-191), and binding to laminin and collagen IV in the basal membrane which serves as the starting signal for the ookinete to oocyst development (192, 193).

While previous phase I clinical trials using the *P. vivax* P25 protein (Pvs25) have demonstrated that humans can produce antibodies against this antigen, an ideal formulation has not been reported. The first clinical trial of a protein-based Pvs25 vaccine candidate formulated with alum as an adjuvant showed poor immunogenicity and no transmission blocking effect (184). A subsequent clinical trial using a protein-based Pvs25 formulated with Montanide ISA 51 as an adjuvant, showed that low doses of the formulation were able to induce transmission blocking immunity, but higher doses were associated with systemic adverse events (197). However, pre-clinical and clinical studies aimed at improving the suboptimal immunogenicity observed by immunization with the *Plasmodium* P25 proteins, Pfs25 and Pvs25 have

suggested that the addition of a carrier protein could potentially enhance the immunogenicity of this protein (295-297).

A vaccine targeting only a transmission-blocking antigen faces challenges in maintaining an antibody response to parasite antigens to which there would be no boosting effect by natural exposure. Furthermore, this type of vaccine would not provide the human host with protection against infection and would likely have low compliance especially if multiple vaccinations were required. We hypothesize that the development of a bifunctional *P. vivax* vaccine able to target both a blood stage antigen and a sexual stage antigen could provide protection against infection to the vaccinated host as well as reduce transmission. A multi-stage transmission-blocking vaccine is particularly relevant for *P. vivax* given the fact that most relapses are asymptomatic (298), as asymptomatic patients are less likely to receive treatment to clear the infection quickly, resulting in longer periods where the parasite can be spread by mosquitoes. In addition to targeting a reservoir of malaria transmission, a *P. vivax* bifunctional blood stage and transmission blocking vaccine may also improve vaccine uptake due to its potential to provide clinical immunity, as well as a reduction in transmission.

Our group has previously defined several CD4⁺ T cell epitopes within the erythrocytic stage antigen Merozoite Surface Protein 1 (MSP1) of *P. vivax*. These epitopes contain features that define them as promiscuous T cell epitopes (i.e., able to bind a broad range of MHC class II alleles) (220). Synthetic peptides representing these *P. vivax* MSP1 T cell epitopes are recognized by lymphocytes from individuals naturally infected with *P. vivax* (220). We have designed and expressed a chimeric *P. vivax* MSP1 (cPvMSP1) by genetically linking five of these promiscuous T cell epitopes arrayed in tandem conformation to an extended version of the carboxyl-terminal 19kDa fragment of the *P. vivax* MSP1 Merozoite Surface Protein 1 (PvMSP1₁₉) (259). We have shown that immunization with cPvMSP1 induced significantly better cellular and humoral immune responses in the murine model when compared to the native protein (259). Here we report the design, production, and characterization of a chimeric bifunctional

protein composed of the previously described cPvMSP1 (259), now genetically fused to recombinant Pvs25 (cPvMSP1-Pvs25). We hypothesize that cPvMSP1 will serve both as a carrier protein that can improve Pvs25 immunogenicity while also inducing robust anti-blood stage protective immune responses. Here we assessed the cellular and humoral immunogenicity of cPvMSP1-Pvs25 in mice and its ability to induce long-lived plasma cells, as well as the ability of antibodies elicited by vaccination with cPvMSP1-Pvs25 vaccination to reduce transmission when tested in functional assays.

Methods

Ethics statements. This study including human samples was carried out in accordance with the recommendations of the ICH/GCP guidelines, Comité de Etica para Investigación con Humanos, Centro Internacional de Vacunas (CECIV) and the protocol approved by the CECIV. All subjects gave written informed consent in accordance with the Declaration of Helsinki.

All animal protocols that include experimental animal procedures using mice and NHP were carried out in accordance with the US Animal Welfare Act and approved by the Emory University's Institutional Animal Care and Use Committee and followed accordingly.

Design and biochemical characterization of the *P. vivax* chimeric Pvs25-MSP1 protein. The 861 bp synthetic gene encoding the chimeric *P. vivax* merozoite surface protein 1 protein (cPvMSP1) used for these studies has been previously described (259). A 546 bp synthetic gene encoding Pvs25 (codon optimized for expression in *E. coli*) was produced by Genart (Regensburg, Germany). The sequence for the synthetic gene was derived from the Salvador I strain (XP_001608460; A23 to L195), which does not include its signal peptide and the GPI anchor. A sequence encoding the peptide MAVD was added upstream of the amino-terminal A23 for protein expression. The synthetic gene was subcloned into a pET24d(+)

vector. For the production of the synthetic gene encoding the bifunctional chimeric protein, the chimeric PvMSP1 plasmid construct was digested with XhoI and the Pvs25 plasmid amplified by PCR using XhoI/NcoI specific primers. The fragments were annealed and then ligated with T4 DNA ligase. The proper configurations of the *Pvs25* and *cPvMSP1-Pvs25* genes were verified by enzyme restriction analysis and the sequence confirmed using an automatic sequencer. The recombinant pET plasmids were transformed into BL21 (DE3) cells with kanamycin selection. The sequence of the recombinant bifunctional erythrocytic stage-transmission blocking chimeric protein, designated cPvMSP1-Pvs25 (Figure 1A), includes: i) MAVD amino terminus to reduce degradation during synthesis in *E. coli* and to provide a start signal; ii) Five promiscuous T cell epitopes derived from *P. vivax* MSP1 capable of binding to a broad range of MHC class II alleles, arranged in tandem interspaced with GPGPG spacers: PvT4 (N₇₈-L₉₇), PvT6 (F₁₁₈-H₁₃₇), PvT8 (L₁₅₈-D₁₇₇), PvT19 (L₃₇₈-S₃₉₇) and PvT53 (S₁₀₅₈-N₁₀₇₇); iii) An extended version of the *P. vivax* MSP1₁₉ kD protein fragment, which includes two promiscuous T cell epitopes derived from MSP1₃₃ protein fragment; iv) A (NANP)₆ tag from the original chimeric PvMSP1 derived from the *P. falciparum* circumsporozoite protein included for biochemical characterization of antigenic integrity of the chimeric protein and to provide an optional affinity purification tag; and v) The Pvs25 sequence derived from the *P. vivax* Salvador I strain, without the signal peptide and the GPI anchor, but including the MAVD sequence derived from the plasmid Pvs25.

Protein expression was induced with 1 mM IPTG, and the soluble Pvs25 was purified with a Ni-NTA affinity column. cPvMSP1-Pvs25 was expressed in inclusion bodies and refolded as previously described (299) using 4M concentration of urea in the refolding solution. After refolding, the protein was purified using gel filtration chromatography. The integrity of the proteins was analyzed by western blot using the anti-Pvs25 monoclonal antibody (mAb) N1-1H10 (MRA-471, BEI Resources), anti-His tag, or the mAb 2A10 that recognize the (NANP)₆ carboxyl terminal tag of the cPvMSP1-Pvs25 (Figure 1 and Supplementary Figure 1). Additionally, endotoxin levels of the purified protein product were determined

using the E-Toxate *Limulus* amoebocyte lysate kit (Sigma), according to the manufacturer's instructions, and were determined to range between 25 and 42 EU/mg of protein.

Synthetic peptides. A library of 61 15-mer synthetic peptides overlapped by 11 residues and spanning the complete cPvMSP1-Pvs25 chimeric protein sequence was commercially synthesized by the multiple solid-phase technique (Sigma-Aldrich). Peptide pools were used to characterize cellular reactivity, with the cPvMSP1 peptide pool 1 representing the sequence of the cognate T cell epitopes derived from the MSP1 structure included in our chimeric construct and the cPvMSP1 pool 2 representing the complete amino acid sequence of the MSP1₁₉ kD protein fragment. Pvs25 pool 1 and pool 2 represent the amino acid sequence of Pvs25 (Table 1).

Mice immunizations. Groups of ten female CB6F1/J (H-2^{d/b}) mice, 6 to 8 weeks of age, were purchased from The Jackson Laboratory. The animals were immunized subcutaneously on days 0, 20 and 40, in the base of the tail and the interscapular area, using 20 µg of either the cPvMSP1-Pvs25 or Pvs25 proteins emulsified in the adjuvant Montanide ISA 51 VG (Seppic). As a control, groups of mice received PBS emulsified in the same adjuvant. A summary of the immunization regimens and groups can be found in Table 2. All animal protocols were approved by the Emory University's Institutional Animal Care and Use Committee and followed accordingly.

ELISA assays. The procedures for the assessment of IgG antibody titers, subclasses, and avidity have been previously described (259). Antibody titers elicited by immunization of mice were determined by ELISA using Immulon 4HBX plates (Thermo Scientific) coated with 1 µg/ml of cPvMSP1-Pvs25, Pvs25 or PvMSP1₁₉ diluted in carbonate buffer as described (204).

Briefly, plates were allowed to incubate overnight with 100µl of the 1 µg/ml protein solution. The solution was removed, and plates were washed three times with wash buffer consisting of PBS 1X with 0.05% Tween20. 200 µl of blocking solution, BSA (KPL) diluted 1:10 in distilled water, was added to each well and plates were incubated again for 2 hours at 37°C. Blocking solution was removed without washing. Sera were diluted in a dilution solution composed of 1:20 BSA (KPL) in distilled water at a starting dilution of 1:320. 1:320 served as the initial starting dilution for all samples. Serial dilutions were made until 1:327680, the maximum allowed in a 12 column 96 well plate, leaving one column for background. Cutoffs for positive titers were set at the highest dilution of sera where the O.D. was greater than that of the mean plus three standard deviations above the optical densities obtained using pre-immune sera. If the cutoff values were above the limit of detection of the serial dilutions allowed by the plate, the starting dilution was adjusted accordingly for repeat ELISAs until the cutoff value was reached. Following a one-hour incubation with 100 µl of the diluted mouse sera at 37°C, the plates were washed five times with wash buffer before the addition of 100 µl of peroxidase labeled goat anti-mouse IgG antibody (KPL) at 1:1000 in dilution solution. Plates were again incubated for 1 hour at 37°C before washing five times with wash buffer. ABTS solution (KPL) was used to reveal the ELISA following a one-hour incubation. Optical densities were determined using a VERSAmax ELISA reader (Molecular Device Corporation) with a 405 nm filter. Results are presented as the reciprocal of the end-point dilution.

IgG1 and IgG2a subclass profiles of vaccine-induced antibodies were also determined. ELISAs were run as described for the determination of antibody titers, except that after incubation of the plates with sera, plates were washed and incubated with biotinylated rat anti-mouse mAbs IgG1 and IgG2a, (BD Pharmingen) for 2 hours. After washing, the bound antibodies were detected using horseradish peroxidase (HRP)-streptavidin (KPL) and the SureBlue™ TMB Microwell Peroxidase Substrate (KPL). The peroxidase reaction was stopped with the TMB Stop Solution (KPL). Optical densities were determined using a VERSAmax ELISA reader (Molecular Device Corporation) with a 450 nm filter.

The avidity indices of the antibodies were assessed by ammonium thiocyanate elution-based ELISA using sera samples obtained at day 60, corresponding to 20 days after the final immunization, and day 730, (two years after the first immunization). The avidity ELISA was conducted similarly to the total IgG titer ELISA, with slight modifications. Briefly, serial dilutions of the sera were assayed in the absence and presence of 1M NH₄SCN (Sigma Aldrich) in PBS. The plates were incubated for 15 min at room temperature before washing and proceeding with the assay as described above. The avidity index was calculated as the ratio between the antilog of the absorbance curves obtained with (x_1) and without (x_2) NH₄SCN, as previously described (221).

For ELISA competition assays, purified polyclonal anti-cPvMSP1-Pvs25 and anti-Pvs25 elicited in rabbits (Covance) were used. Fixed amounts of the monoclonal antibody N1-1H10 (1 µg) were tested with 2-fold dilutions of purified rabbit IgG using the recombinant Pvs25 protein as antigen. The concentration of polyclonal antibodies required for 50% inhibition of Pvs25-N1-1H10 interaction was then estimated using linear regression.

Indirect immunofluorescence assays (IFA). Sera obtained from 10 C5B6F1/J mice after the third immunization with cPvMSP1-Pvs25 were pooled, and antibody reactivity against native Pvs25 protein was evaluated by indirect immunofluorescence. For assessment of antibody reactivity to native *P. vivax* MSP1, an aliquot of blood was collected from a *P. vivax* infected *Saimiri boliviensis* monkey (kindly provided by Dr. Mary Galinski) into CPD tubes and washed twice using RPMI 1640 medium before the cells were adjusted to 1% hematocrit. Ten microliters of the cell suspension were added to wells of 12-well slides (ICN Biomedicals Inc) and air-dried before storage at -20 °C. To evaluate reactivity, parasites slides were air-dried at RT for 30 minutes. Afterward, slides were incubated 90 min with mouse sera obtained from after the third immunization, diluted at 1:500 in PBS with 0.2% BSA in a dark, moist chamber. After the incubation, slides were washed three times with PBS containing Tween-20 (PBS-T), to minimize non-

specific binding. Parasites were stained for 30 min at RT in a dark, moist chamber with goat anti-mice Alexa Fluor 488 (Invitrogen) at a 1:500 dilution in Evans Blue 0.4% in PBS 1X. After staining, microscope slides were washed three times and allowed to dry completely. Parasite nuclei were stained using 4',6-diamidino-2-phenylindole dihydrochloride (DAPI) included in the anti-fade mounting medium Prolong (Life Technologies) before coverslips were placed.

For assessment of reactivity to Pvs25, young oocysts were derived *in vitro* as described (300) and produced using the *P. berghei* transgenic parasite expressing Pvs25 (MRA-904, pv25DR, BEI Resources). Culture smears were stored at -80°C until need. Slides were allowed to air dry at room temperature for 30 minutes before being fixed for 10 min in 4% PFA/PBS. Slides were then washed three times with PBS 1X and blocked for 1 h in blocking buffer (10% v/v FBS, 1% w/v BSA in PBS). Slides were allowed to incubate overnight with sera from individual rabbits immunized with either Pvs25 or cPvMSP1-Pvs25 at 1:500 in 1% (w/v) BSA in PBS at 4 °C in a wet chamber. The following day, slides were washed three times in PBS and then incubated with Alexa Fluor 488-conjugated goat anti-rabbit (H+L) IgG (ThermoFisher) at 1:500 in 0.4% Evans Blue in PBS 1X for 60 min. After washing three times, slides were allowed to dry completely (8 hours) and mounted with ProLong Gold anti-fade reagent with DAPI (Life Technologies) and a coverslip.

ELISpot assays. 96-well plates were coated with 5 µg/ml Pvs25, cPvMSP1-Pvs25, and cPvMSP1 and blocked with complete RPMI (10% FBS, 1% penicillin/ streptavidin, 1% HEPES, and 50 µM 2-mercaptoethanol). Bone marrow and splenic cells were then isolated from the CB6FJ/1 mice two years post-immunization with Pvs25, cPvMSP1-Pvs25, or the Montanide adjuvant control. To isolate bone marrow cells from the mice, femur bones were removed from following Emory IACUC approved euthanasia. Femurs were then placed in complete RPMI, and the ends of the bones were clipped off with sterile surgical scissors. The bone marrow was then flushed from the femur with RPMI using a syringe into

a new sterile conical tube. The bone marrow was then passed through the syringe needle several times to resuspend the cells. Similarly, spleens are removed post-mortem and then pulverized through a cell strainer using the inside of the syringe. Cells were washed and used immediately with no further processing. Cells were serially diluted on prepared plates and incubated for 16 hours at 37°C. The plates were then treated with anti-IgG-biotin (Southern Biotechnology) followed by incubation with streptavidin-alkaline phosphatase (Sigma). Plates were then developed with 5-bromo-4-chloro-3-indolylphosphate (Sigma) until spots appeared, and spots counted with CTL ImmunoSpot software. Results were then normalized to adjuvant control mice.

Flow cytometry assays. Flow cytometry analyses of cPvMSP1-Pvs25 or Pvs25 specific T cells were conducted to simultaneously analyze IFN- γ at the single-cell level in T cells derived from splenocytes obtained five days after the final boosting immunization. Mice were euthanized according to the Emory IACUC approved protocols and spleens were removed. Spleens were transferred into complete media, composed of DMEM, 1% non-essential amino acids, 2 mM L-glutamine, 5% inactivated FBS, 50 μ M 2-mercaptoethanol, 10 mM HEPES, 100 U/ml penicillin and 100 μ g/ml streptomycin. Spleens were then homogenized under sterile conditions, and the homogenized fluid was passed through 200 μ m nylon strainer to remove clumps and large pieces of tissue. Red blood cells were lysed using 2ml of BD PharmLyse buffer incubated with for 3 minutes before centrifugation at 400g for 5 minutes and washing with 5 ml of flow cytometry buffer. Cells were counted and the concentration was adjusted to 10^7 cells/ml. 100 μ l was then placed in individual round bottom tubes. Cells were stimulated for 6 hours with peptide pools at 2 μ g/ml at 37°C, in the presence of GolgiPlug (BD Biosciences). Cells were then incubated with Live/Dead Aqua Stain (Life Technologies) followed by surface staining with α -CD3 (PerCP Cy5.5), α -CD4 (Alexa Fluor 700), and α -CD8 α (APC-Cy7) for 30 min. The cells were then fixed, permeabilized and stained with antibodies against IFN- γ (APC). All the monoclonal antibodies were obtained from BioLegend. Flow

cytometry analyses were performed using an LSRII flow cytometer (BD Biosciences), and data were analyzed using FlowJo software version 10.1. The lymphocytes were initially gated on the Live/Dead channel, and then CD3⁺, and then CD4⁺ and CD8⁺ populations. Antigen-specific cytokine-secreting T cells were identified within both the CD4⁺ and CD8⁺ populations. The frequency of antigen-specific cytokine-producing cells was determined by subtracting the percentage of cytokine-producing T cells after incubation with medium alone from the percentage of cytokine-producing T cells after incubation with the peptide pools. Samples that did not meet this requirement were set to zero.

Transmission-blocking assays. The transmission-blocking activity of sera derived from rabbits immunized with Pvs25 or cPvMSP1-Pvs25 was measured by direct membrane feeding assays as described elsewhere (301-303). Briefly, 150 μ l of infected RBCs from *P. vivax* infected patients were washed twice with RPMI 1640 medium (Sigma Aldrich) and diluted in a 150 μ l of fresh sera from rabbits obtained after three immunizations with 20 μ g of cPvMSP1-Pvs25 or Pvs25 to feed 100 adult (2–3 day old) *An. albimanus* mosquitoes. Pre-immune sera from the same rabbits were used as a negative control. After 30 minutes of feeding, unfed mosquitoes were removed from the cages, and fed mosquitoes maintained at 27°C and 80–90% relative humidity. All procedures were performed at 37°C. Seven days after feeding, 30-40 mosquitoes were dissected, midguts were stained with 2% mercurochrome, and the numbers of oocysts per mosquito midgut were counted.

Statistical analysis. Statistical analysis and graphs were made using GraphPad Prism 5.0 software (GraphPad Software Inc.). For analysis of the antibody responses, all ELISA titers were log-transformed to conform to the normality and variance requirements of parametric testing and compared using Student's t-test for comparison of antibody titers between groups. Student's t-test was used for the comparison of antibody avidity between groups. Mann Whitney was used for the comparison of antibody subclass ratios

between immunization groups. Differences in the numbers of antibody secreting cells obtained via ELISpot were analyzed using the Mann-Whitney test to compare responses obtained from the Pvs25 and cPvMSP1-Pvs25 immunization groups. Levels of cytokine IFN- γ production obtained from flow cytometry were analyzed using unpaired t-tests to compare immunization groups. The transmission-blocking activity of the anti-cPvMSP1-Pvs25 or anti-Pvs25 sera compared against naïve sera or between the groups was analyzed using one-way ANOVA.

Results

Design, expression, and characterization of the chimeric protein cPvMSP1-Pvs25. The chimeric PvMSP1 protein used to create a bifunctional vaccine construct by genetic fusion to the Pvs25 protein has previously been reported by our group (259). Briefly, the protein consists of five experimentally defined promiscuous T cell epitopes (220) derived from several regions along the native *P. vivax* MSP1. These epitopes are arrayed in tandem, interspaced with GPGPG spacers, and genetically fused to an extended form of the PvMSP1₁₉ kD fragment that contains two T helper epitopes derived from MSP1₃₃ kD fragment. Initial immunogenicity studies showed that this protein was able to elicit robust cytophilic antibody and CD4⁺ and CD8⁺ T cell responses when delivered either alone as a recombinant protein formulated in water-in-oil emulsion using homologous prime-boost immunization regimens (259) or via heterologous prime-boost immunization regimens using recombinant adenoviral vectors for priming immunization (304). To test the feasibility of developing a hybrid vaccine with the potential of inducing blood and mosquito stage-specific immunity, we expressed cPvMSP1-Pvs25 and Pvs25 as recombinant proteins in *E. coli* (Figure 1A, 1B).

To confirm the biochemical identity of the cPvMSP1-Pvs25 protein, western blot analysis using monoclonal antibodies targeting specific regions of the cPvMSP1 and Pvs25 protein components was conducted (Figure 1C). The monoclonal antibody N1-1H10 was used for assessment of both the cPvMSP1-

Pvs25 and recombinant Pvs25 proteins, as it recognizes a conformational-dependent epitope (305) present in the second epidermal growth factor-like domain of Pvs25 (306) and is able to inhibit oocyst development in the vector (307). Anti-His tag antibodies were used to identify the His-tag present at the C terminal end of the Pvs25 protein segment of the cPvMSP1-Pvs25 protein and the recombinant Pvs25. The monoclonal antibody 2A10 targets the circumsporozoite (NANP)_n repeat region derived from *P. falciparum*, which is present in the cPvMSP1-Pvs25 protein at the carboxyl-terminal end of the chimeric PvMSP1 protein. We observed recognition of the cPvMSP1-Pvs25 protein as a single band with the expected size of ~52 kDa by the monoclonal antibody targeting the NANP repeats (2A10), the anti-His tag monoclonal antibody, and the monoclonal antibody targeting the Pvs25 protein (N1-1H10). As expected, we also observed binding of the anti-Pvs25 monoclonal antibody (N1-1H10) and the anti-His-tag antibody to the recombinant Pvs25 protein, shown as a ~25 kDa band. These experiments confirm that at least the epitopes of these monoclonal antibodies remained correctly folded.

To determine if the Pvs25 functional domains are conserved within cPvMSP1-Pvs25, we used ELISA competition assays (Figure 1D). Purified polyclonal antibodies elicited in rabbits by immunization with the recombinant proteins were tested at different concentrations and co-incubated with fixed amounts of the monoclonal antibody N1-1H10 (307). The polyclonal antibodies inhibited the binding of N1-1H10 with a distinct competition pattern. The concentration of the polyclonal antibodies required for 50% inhibition of antigen-monoclonal antibody interaction was estimated in 32 µg for anti-Pvs25 and 13 µg for anti-cPvMSP1-Pvs25. These results suggest that antibodies elicited by immunization with the protein expressed in *E. coli* have transmission-blocking potential.

Antibody response induced by cPvMSP1-Pvs25. Hybrid CB6F1/J mice were immunized with Pvs25 or cPvMSP1-Pvs25 on days 0, 20, and 40 (Table 2). Sera were obtained 20 days after each immunization. When we assessed the anti-cPvMSP1-Pvs25 titers at day 20 and 40, we observed significantly higher titers

in the cPvMSP1-Pvs25 immunized group than in the Pvs25 group at both time points ($P = 0.0017$ and 0.0262 , respectively). At day 60, 20 days after the last immunization, mice immunized with cPvMSP1-Pvs25 had mean antibody titers of 3.4×10^6 against the chimeric recombinant protein, significantly higher ($P = 0.0414$) than those in mice immunized with Pvs25 which had mean antibody titers of 2.4×10^6 (Figure 2). At day 730, two years after the first immunization, the group immunized with cPvMSP1-Pvs25 had mean antibody titers of 1.7×10^6 against cPvMSP1-Pvs25, a reduction of 26.8%. This observation is in sharp contrast with the group of mice immunized with Pvs25 that had mean antibody titers of 3.7×10^5 against cPvMSP1-Pvs25, a reduction of 89.2% ($P = 0.0107$, Figure 2). The data suggest that unlike Pvs25 the antibody response induced by cPvMSP1-Pvs25 is long-lasting in mice.

To assess if antigenic competition occurs in mice immunized with the chimeric protein, antibody titers against the individual components of the bifunctional chimeric protein (Pvs25 and cPvMSP1) were also measured (Figure 3). The cPvMSP1-Pvs25 immunization group was able to recognize Pvs25 at day 60 with mean antibody titers of 2.4×10^6 , which were similar to levels in mice immunized with Pvs25 ($P = 0.9617$) (Figure 3A). Assessment of anti-Pvs25 titers at day 730 in mice immunized with cPvMSP1-Pvs25 revealed a titers reduction of 47.2%, while the antibody titers in mice immunized with Pvs25 alone were reduced by 86.0%, a significant difference between the groups ($P = 0.0402$) (Figure 3A). As expected, mice immunized with Pvs25 alone did not produce antibodies against PvMSP1, showing only minimal reaction at the highest concentration of sera used. In contrast, mice immunized with cPvMSP1-Pvs25 had mean anti-PvMSP1 antibody titers of 6.6×10^6 at 20 days after the final immunization, and 1.0×10^6 two years later ($P = 0.0027$) (Figure 3D); the later titers at day 730, remained significantly higher than the Pvs25 immunized group, with a reduction of 84.8% ($P = 0.003$).

Characteristics of anti-Pvs25 and anti-MSP1 antibodies. The average avidity index of anti-Pvs25 antibodies induced by immunization with cPvMSP1-Pvs25 at 20 days after the final immunization was

significantly lower than that induced by immunization with Pvs25 (0.79 and 0.95 respectively, $P = 0.0038$) (Figure 3B). In contrast, by day 730 the respective values were 0.68 and 0.50 ($P = 0.0108$), indicating a significantly higher avidity index for antibodies induced by cPvMSP1-Pvs25 compared with Pvs25 alone.

The characteristics of the antibodies against chimeric PvMSP1 were only analyzed in the group immunized with cPvMSP1-Pvs25 since only these mice recognize this antigen. The average avidity index of the cPvMSP1-Pvs25 induced anti-MSP1 antibodies 20 days after the final immunization was 0.74 and remained similar after two years (0.71, $P = 0.6381$) (Figure 3E).

The IgG subclasses induced by vaccination with Pvs25 and cPvMSP1-Pvs25 was assessed in order to determine antibody quality, as cytophilic antibodies against MSP1, which correspond to IgG2a in mice, have previously been reported to be associated with protection (226). Measurement of the Pvs25-specific IgG2a and IgG1 subclasses, expressed as the IgG2a/IgG1 ratio, revealed a higher ratio for the cPvMSP1-Pvs25 immunized mice at both day 60 and day 730, however only at day 730 was the IgG2a/IgG1 subclass ratio of the cPvMSP1-Pvs25 group significantly higher than that of Pvs25 immunized mice ($P = 0.0131$) (Figure 3C). Assessment of the IgG subclass ratios for anti-PvMSP1 responses induced by vaccination with cPvMSP-Pvs25 revealed a different pattern, with the IgG2a/IgG1 ratio of the anti-MSP1 antibodies significantly higher at 60 days than at 730 days after the first immunization ($P = 0.0010$) (Figure 3F), showing a shift towards a Th2 phenotype over time.

Anti-cPvMSP1-Pvs25 induced antibodies recognize the native parasite proteins. The ability of the antibodies induced by vaccination with cPvMSP1-Pvs25 or Pvs25 to recognize the native antigens on the surface of oocysts and schizonts was assessed by immunofluorescence (Figure 4). Transgenic *P. berghei* parasites (MRA-904 parasites) expressing Pvs25 on the surface of oocysts were used to assess the ability of antibodies from cPvMSP1-Pvs25-immunized mice to recognize native Pvs25. As expected, pooled sera from the cPvMSP1-Pvs25-immunized group obtained at day 60 were able to bind to the surface of *P.*

berghei Pvs25 transgenic parasites (Figure 4). Thin smears made from infected red blood cells from *P. vivax* infected *Saimiri* monkeys were used to assess the ability of antibodies from cPvMSP1-Pvs25 immunized mice to recognize the native PvMSP1 protein. Pooled sera from the cPvMSP1-Pvs25 immunized group obtained at day 60 recognized *P. vivax* schizonts (Figure 4). Combined, these data indicate that chimeric cPvMSP1-Pvs25 immunization elicited antibodies capable of binding the native structure of Pvs25 and the native *P. vivax* MSP1.

cPvMSP1-Pvs25 plasma cell induction. To confirm that the long-lasting antibody responses observed at two years post-immunization were related to the induction of long-lived plasma cells (LLPCs), antigen-specific IgG plasma cells were measured in CB6F1/J mice immunized with Pvs25, cPvMSP1-Pvs25, or Montanide via ELISPOT two years post-immunization. Mice immunized with cPvMSP1-Pvs25 generated a robust, long-lived IgG plasma cell response not only to the cPvMSP1-Pvs25 protein itself but also to Pvs25 and cPvMSP1 (Figure 5). This response lasts for the lifetime of the animal. The number of long-lived IgG plasma cells in the bone marrow specific to cPvMSP1-Pvs25 was significantly higher ($P = 0.0456$) in mice immunized with cPvMSP1-Pvs25 than those immunized with Pvs25 alone (Figure 5A). Furthermore, the group immunized with Pvs25 was unable to generate a plasma cell response significantly above that of the adjuvant-only control. Mice immunized with cPvMSP1-Pvs25 also generated significantly greater numbers of IgG ASCs specific to Pvs25 (Figure 5B), and PvMSP1 (Figure 5C) compared to mice immunized with Pvs25 ($P = 0.0022$ and $P=0.0092$, respectively). This increase in long-lived IgG plasma cells was most pronounced in the bone marrow, though antigen-specific IgG plasma cells persist in the spleen at lower numbers. Overall, immunization with cPvMSP1-Pvs25 was more efficient, as it was able to stimulate long-lived, *Plasmodium*-specific IgG plasma cells when compared to standard Pvs25 immunization.

Cellular response induced by cPvMSP1-Pvs25. Following the assessment of the humoral response induced by vaccination with cPvMSP1-Pvs25 as compared to Pvs25, we sought to determine if cPvMSP1-Pvs25 was able to induce a cellular response able to recognize individual components of the bifunctional chimeric protein. CB6F1/J mice were immunized three times with 20 µg of either the chimeric cPvMSP1-Pvs25 or the recombinant Pvs25 on day 0 and 20, as described in Table 2. Mice were euthanized five days after the second immunization and splenocytes were stimulated with peptide pools representing the recombinant Pvs25 and cPvMSP1 proteins (Table 1) to analyze the production of IFN-γ by both CD4⁺ and CD8⁺ T cells (Figure 6). A sample gating strategy is shown in Supplementary Figure 2. We observed no difference in the production of IFN-γ between the immunization groups in either the CD4⁺ or CD8⁺ T cell populations in response to stimulation with the Pvs25 peptide pools (Figure 6A and 6B). Following stimulation with Pool 1 of cPvMSP1, we found that CD4⁺ T cells from mice immunized with cPvMSP1-Pvs25 produced significantly higher levels of IFN-γ than those immunized with Pvs25 (P = 0.0010) (Figure 6C). Similarly, we found that following stimulation with Pool 2 of PvMSP1, both CD4⁺ and CD8⁺ T cells from mice immunized with the cPvMSP1-Pvs25 protein produced significantly more IFN-γ than the Pvs25 immunization group (P = 0.0043 for CD4⁺, P = 0.0138 for CD8⁺, Figure 6C and 6D).

Transmission-blocking activity of anti-cPvMSP1-Pvs25 antibodies. Sera samples, obtained from rabbits after three immunizations with either cPvMSP1-Pvs25 or Pvs25, were tested for transmission-blocking activity using three different *P. vivax* isolates in independent membrane feeding assays. The transmission blocking activity and the number of oocysts counted were assessed for both groups (Table 3). The activity of immune sera was compared to pre-immune control sera (Table 3). Upon dissection of mosquitoes, we found that sera obtained from both Pvs25 and cPvMSP1-Pvs25 resulted in significantly lower percentages of infected mosquitoes when compared to the pre-immune sera samples. Similarly, we found significantly lower numbers of oocysts present in the mosquitoes that had fed on the Pvs25 and cPvMSP1-Pvs25 samples

as compared to the pre-immune rabbit sera controls. Overall, our results indicate that antibodies induced by cPvMSP1-Pvs25 are able to block the infection in 90% of exposed mosquitos, and in infected mosquitos, the parasite load is 98% lower than in mosquitoes feeding on a non-immunized source.

Discussion

Development of novel malaria intervention tools, such as transmission-blocking vaccines (TBVs), is essential to combat the increased reports of insecticide and drug resistance (289, 290), as they could increase the efficiency and sustainability of these existing malaria control methods (135). TBVs rely on the generation of antibodies that block the development of *Plasmodium* parasites within the mosquito midgut. However, under natural conditions, the human host is not exposed to the pre- and post-fertilization antigens targeted by TBVs. Since there would not be a natural boosting effect during infection, highly immunogenic formulations able to produce long-lasting, effective antibody levels are necessary (145). We propose that the ideal formulation for a transmission-blocking malaria vaccine should consist of a transmission-blocking component combined with a prophylactic vaccine in order to simultaneously provide protection against disease to the recipient and reduce transmission. Here we present evidence that a chimeric protein designed based on one of the best-characterized post-fertilization antigens, P25, conjugated to *P. vivax* MSP1 (cPvMSP1-Pvs25), elicits long-lasting antibody responses against both proteins, without immune interference, while inducing robust cellular responses to PvMSP1 in CB6F1/J, comparable to those we have previously reported for cPvMSP1 alone in BALB/c and C57BL/7 mice, which is expected as the CB6F1/J is the F1 hybrid of these two strains (259).

Assessment of the quality and longevity of the antibody response induced revealed that immunization with cPvMSP1-Pvs25, as compared to Pvs25, resulted in the induction of an antibody response against the immunogens as well as against the individual components, which lasted for the lifetime of the animal with a much lower reduction in antibody titers at two years post-immunization. Most critically, we observed a

lower reduction in anti-Pvs25 antibody titers at two years post-immunization in groups of mice immunized with the bifunctional chimeric protein as compared to the Pvs25 group. These results are significant as an ideal transmission-blocking vaccine candidate must be capable of inducing functional and long-lasting antibodies using a simplified immunization regimen for use in mass administration (308).

For the proof-of-concepts studies reported here, we selected Montanide ISA 51 VG, a water-in-oil based adjuvant (309) that has been tested before in clinical trials (310-312). Our results are consistent with the reported high efficiency of this adjuvant to induce robust antibody responses given its ability to promote polarization of naïve T cells into T follicular helper cells (313). However, safety concerns have arisen from a Phase I clinical trial of Pfs25 and Pvs25 formulated in Montanide 51 showing systemic adverse events compatible with erythema nodosum (197). Recent comparisons of *P. falciparum* Pfs25 formulated in novel oil-in-water based adjuvants compared with alum-based adjuvants found that oil-in-water-based adjuvants EM081 and EM082 were more efficient in eliciting high titers of anti-Pfs25 IgG antibodies than the alum adjuvants (314). Interestingly, this study also found that an adjuvant composed of oil-in-water-glucopyranosyl lipid A-induced high-affinity antibodies that effectively blocked infection of mosquitoes with *P. falciparum* and demonstrated that avidity could provide a surrogate measure of efficacy beyond the antibody titers (314). The strong adjuvant effect was also confirmed by a Phase I clinical trial of a Pfs25 vaccine candidate paired with the aluminum adjuvant Alhydrogel, which observed a rapid decline in antibody responses after vaccination (315). Overall, these experiments corroborate the adjuvant-dependency on the magnitude and durability of the antibody response of P25-based vaccines (295, 316). The long-lasting immunity induced by cPvMSP1-Pvs25 is therefore very encouraging compared to previous studies and warrant further investigation regarding the best adjuvant system to deliver the bifunctional chimeric protein.

Due to the importance of long-lived plasma cells (LLPC) in maintaining protective antibody levels for years (295), LLPC induced by vaccination with cPvMSP1-Pvs25 were assessed. We were able to confirm

high levels of bone marrow and spleen LLPCs at two years post-immunization. We observed that immunization with cPvMSP1-Pvs25 was more efficient at generating long-lived *Plasmodium*-specific IgG plasma cells when compared to Pvs25, with significantly more Pvs25-specific LLPCs also observed in the bone marrow. Previous assessment of the effect of different carrier proteins and adjuvants on the immunogenicity and longevity of the antibody response induced against Pfs25 in mice by Radtke et al. (295) found that both of the self-derived mouse serum albumin and the foreign tetanus toxoid carrier proteins tested generated robust humoral and cellular responses. The authors concluded that since TBVs rely on antibody responses to block transmission of the parasite, the ideal TBV should either induce a large antibody response that can diminish over time while remaining at levels high enough to provide protection or induce a durable antibody response sustained by LLPCs in order to provide lasting protection. Along with the reports by Radtke (295), subsequent studies on the effect of an MSP8 based carrier tested with Pfs25 conducted by Parzych et al. (297), both suggest that a highly immunogenic carrier protein is likely due to the presence of CD4⁺ T cell epitopes that can promote humoral responses through the recruitment of CD4⁺ T cells. Based on this we can conclude that the likely mechanism of action of the cPvMSP1 carrier protein is the improved recruitment of CD4⁺ T cells due to the five promiscuous T cell epitopes included in this chimeric protein, which ultimately promote the overall humoral response to the vaccine and induction of the anti-Pvs25 LLPC response.

Avidity of the antibodies induced by vaccination with either Pvs25 or cPvMSP1-Pvs25 was also assessed as a measure of immunogenicity. At 20 days after the final immunization, anti-Pvs25 antibody avidity indices were 0.95 for Pvs25 and 0.79 for cPvMSP1-Pvs25 immunization groups. By two years post-immunization, the anti-Pvs25 avidity index of the Pvs25 group had fallen to 0.50, significantly lower than the avidity index of 0.68 at two years induced by immunization with cPvMSP1-Pvs25. Consistent with the maintenance of antibody avidity against Pvs25 by the cPvMSP1-Pvs25 immunization regimen, the avidity indices of the anti-cPvMSP1 response were not significantly different at 60 days than at two years post-

immunization. The high avidity antibodies elicited by cPvMSP1-Pvs25 are, therefore, encouraging given their relevance as a biomarker of efficacy of TBVs beyond the antibody titers (314). We can also conclude that this is likely an effect of the improved LLPC response induced by the cPvMSP1-Pvs25 vaccination regimen, allowing for the maintenance of higher avidity antibodies over time.

Cytophilic IgG antibody subclass responses directed against MSP1₁₉, as well as other merozoite surface antigens, have previously been found to be associated with control of parasitemia and protection from symptomatic illness in children in *P. falciparum* endemic areas (226). The cytophilic antibody subclasses correspond to IgG1 and IgG3 in humans and IgG2a in mice. We observed a shift in the IgG2a/IgG1 ratio of the anti-cPvMSP1 antibody response between day 60 and two years post-prime, with a significant reduction in the IgG2a subclass response. In contrast, there was a significantly higher IgG2a/IgG1 subclass ratio for anti-Pvs25 antibodies in cPvMSP1-Pvs25 immunized mice compared to Pvs25 immunized mice at the two-year time point. Although we observed higher levels of IgG1 than IgG2a in the anti-cPvMSP1 response, the significantly higher IgG2a/IgG1 ratio observed for the anti-Pvs25 response elicited by cPvMSP1-Pvs25 vaccination is promising and may have biological significance due to differences in the ability of IgG subclasses to activate the classical complement pathway. Parasites present in the mosquito midgut after the female *Anopheles* mosquito ingests infected red blood cells are exposed to multiple plasma elements present in the mosquito blood meal including complement, granulocytes, and the host-derived antibodies (135, 145). These components can all affect parasite development within the mosquito and ultimately reduce transmission. Studies have shown that human sera with anti-Pvs25 antibodies have reduced killing activity after heat inactivation indicating that complement may be necessary to block transmission with Pvs25 vaccine-induced antibodies (184). The classical complement pathway involves the binding of complement molecule C1q to the Fc region of the antigen bound antibody. However, IgG subclasses differ in their ability to activate complement, as human cytophilic antibodies IgG3 and IgG1 have been found to more effectively activate the classical complement pathway than the IgG2 subclass.

This study suggests that cPvMSP1-Pvs25 immunization is more effective at inducing cytophilic IgG2a subclass antibodies in mice.

The ability of antibodies induced by individual components of the bifunctional chimeric protein in this study to bind the native structures expressed by ookinetes and schizonts is essential for their functional activities. We confirmed by IFAs that antibodies induced by immunization with cPvMSP1-Pvs25 recognized the native structure on the surface of transgenic oocysts expressing Pvs25 as well as the native structure of PvMSP1 in *P. vivax* blood stage schizonts. We have previously shown that passive immunization using antibodies elicited by the orthologous *P. yoelii* chimeric MSP1 protein, based on sequences from the *P. yoelii* 17X strain, protect naïve mice against heterologous challenge with *P. yoelii nigeriensis* N67 isolates (204). Although we were unable to repeat similar passive transfer experiments in this study, future studies using transgenic parasites expressing *P. vivax* MSP1 are warranted. Additionally, the binding capability of anti-cPvMSP1-Pvs25 antibodies and the robust transmission blocking activity elicited by immunization as determined by membrane feeding assays, support further studies on the functionality of the anti-Pvs25 and anti-cPvMSP1 antibodies induced by vaccination with cPvMSP1-Pvs25. Furthermore, while no differences in the IFN- γ response were observed between the immunization groups following stimulation with the Pvs25 peptide pools, as expected, stimulation with cPvMSP1 peptide pools revealed that cPvMSP1-Pvs25 induced high levels of IFN- γ CD4⁺ and CD8⁺ T cells as compared to Pvs25-immunized mice. The ability of cPvMSP1-Pvs25 to maintain robust IFN- γ responses to cPvMSP1 when conjugated to the Pvs25 protein is encouraging for the blood stage component of this vaccine candidate, as several reports have indicated that high frequencies of IFN- γ secreting CD4⁺ T cells provide protection from malaria in humans (58, 70, 230).

Direct membrane feeding assays allow the assessment of transmission-blocking activity to determine the functionality of antibodies elicited by vaccination (317). Currently, transmission-blocking assays are considered the most epidemiologically important method of evaluating transmission blocking vaccine

candidates (317). We found that sera obtained from both Pvs25 and cPvMSP1-Pvs25-immunized rabbits had significantly high transmission blocking activity, as shown by the lower percentages of infected mosquitoes and the number of oocysts compared with pre-immune sera. Unlike *P. falciparum* membrane feeding experiments, which can be done from parasite cultures, these results are promising as they came from wild *P. vivax* isolates, allowing for better prediction of the transmission blocking potential these antibodies might achieve if tested in clinical trials in endemic areas. These results support further development of cPvMSP1-Pvs25 as an effective transmission-blocking vaccine.

The leading post-fertilization transmission-blocking vaccine (TBV) candidates P25 and P28 are shown poor immunogenicity (195, 295). Chemical conjugation to carrier proteins, a strategy used for glycoconjugate vaccines to enhance the immunogenicity of bacterial polysaccharides (318), has been tested to improve the immune responses induced by post-fertilization antigens. Clinical trials of the conjugated Pfs25-exoprotein A (EPA) vaccine showed excellent safety profile, but the antibody responses induced by immunization were short lasting with poor responses elicited in volunteers living in endemic areas compared to non-endemic areas (315, 319). Using a similar approach, *P. falciparum* Merozoite Surface Protein 8 has been used as a protein carrier to improve the immunogenicity of Pfs25 taking advantage of the presence of CD4⁺ T cell epitopes reported in the protein (297).

The development of licensed vaccines that reduce malaria transmission of *P. falciparum* and *P. vivax* is one of two main strategic goals of the 2030 Strategic Goals of Malaria Vaccine Technology published by the WHO; the other is a malaria vaccine with at least 75% efficacy against clinical malaria (320). While there is controversy concerning the use of transmission-blocking vaccines, including the fact that transmission-blocking antigens alone will only reduce transmission but will not protect vaccinated populations from disease (180), the combination of transmission blocking antigens with antigens targeting the clinical stages of malaria could be used to prevent both disease and transmission. Studies evaluating the impact of vector control measures have demonstrated that the reduction of transmission in medium to high

transmission areas induces a decrease in all-cause mortality, with the youngest age groups of the population benefiting the most (181-183). We report here that the addition of an anti-erythrocytic stage antigen in the form of the chimeric PvMSP1 protein genetically conjugated to Pvs25 improves the immunogenicity of the TBV candidate while preserving the functionality of Pvs25 induced antibodies. Our results provide support for the continued development of cPvMSP1-Pvs25 and other multi-stage malaria vaccine candidates to address the need for effective vaccines targeting both the parasite stage responsible for the clinical manifestations and simultaneously the sexual stage responsible of transmission.

Conflicts of Interest

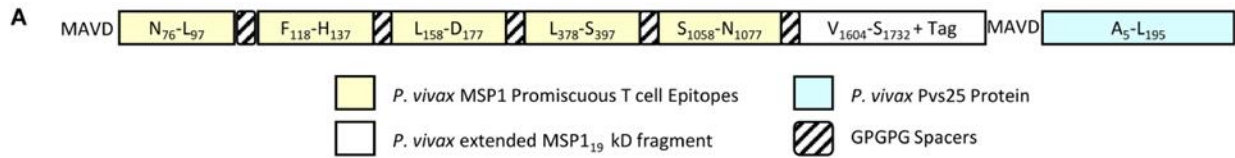
The authors declare that the research was conducted in the absence of any commercial or financial relationship that could be construed as a potential conflict of interest.

Author contributions

A.M conceived the study. J.A.F., B.S., J.J., M.A.-H., and A.M. designed the experiments. J.N.M., J.A.F., B.S., M.A.-H., M.C.-M., and C.B. performed the experiments. J.N.M, J.A.F., and A.M. performed data analysis. J.N.M., J.A.F., and A.M. wrote the manuscript. All the authors approved the final version of the manuscript.

Funding. This research was supported by the National Institutes of Health, NIAID grants R56-AI103382-01A1, R21 AI094402-01A1 and R21AI135711-01, and the Yerkes National Primate Research Center Base Grant No RR00165 awarded by the National Center for Research Resources of the National Institutes of Health. This project was supported in part by ORIP/OD P51OD011132.

Acknowledgments. The following reagents were obtained through BEI Resources Repository, NIAID, NIH: *Plasmodium berghei*, Strain pv25DR (15cy1Pb25-/PD28-), MRA-904, contributed by Robert Sinden, and Hybridoma N1-1H10 anti-*Plasmodium vivax* Ookinete Surface Protein 25 (Pvs25), MRA-471 contributed by Carole A. Long. The authors would like to thank Dr. Oskar Laur for the cloning of the hybrid *cPvMSPI-Pvs25* protein gene, Kelly Rubiano and Andres Amado from Caucaseco Scientific Research Center for supervision of *P. vivax* transmission blocking assays and Dr. Mary Galinski for providing our group with *P. vivax* infected *Saimiri boliviensis* blood aliquot for IFA slides.



B

```

1 M A V D N F V G K F L E L Q I P G H T D L L H L G P G P G F N Q L M H
1 ATGGCGGTCGACAACTTTGTGGGCAAATTTCTGGAACGTGCAGATTCGGGCCATACCGATCTGCTGCATCTGGGTCGGGTCCGGGCTTTAACCCAGCTGATGCAT
36 V I N F H Y D L L R A N V H G P G P G L D M L K K V V L G L W K P L D
106 GTGATCAACTTTCACATATGATCTGCTGCGTGCACGACGTGCATGGCCCGGGTCCGGGTCTGGATATGCTGAAAAAAGTGGTGTGGCCCTGTGGAAACCGCTGGAT
71 N I K D G P G P G L E Y Y L R E K A K M A G T L I I P E S G P G P G S
211 AACATTAAGATGGTCCAGGTCGGGCTGGAATATTATCTGCGCGAAAAAGCGAAAAATGGCGGGCACCCCTGATTATCCGGAAAAGCGGTCCGGGGCCGGGTAGC
106 K D Q I K K L T S L K N K L E R R Q N G P P G V K S S G L L E K L M
176 T N V P D N A A C Y R Y L D G T E E W R C L L T F K E E G G K C V P A
316 AAAGATCAGATCAAAAACTGACCCAGCCTGAAAAACAACCTGGAACGTGCTCAGAACGGTCCGGGTCCAGGCGTGAAAAAGCAGCGGCCTGCTGAAAAACTGATG
141 K S K L I K E N E S K E I L S Q L L N V Q T Q L L T M S S E H T C I D
421 AAAAGCAAATGATCAAAGAAAACGAAAGCAAAGAAATTCAGCCAGCTGCTGAACGTGCAGACCCAGCTGCTGACCATGAGCAGCGAACATACCTGCATTGAT
176 T N V P D N A A C Y R Y L D G T E E W R C L L T F K E E G G K C V P A
526 ACGAACGTGCGGATAACCGCGCGTCTATCGTTATCTGGATGGCAGCCGAAAGATGGCGTTGCGCTGCTGACCTTTAAAGAAGAAGCGGCAAAATCGTGCCTGGCGG
211 S N V T C K D N N G G C A P E A E C K M T D S N E I V C K C T K E G S
631 AGCAAACGTGACCTGCAAAGATAACAACCGCGCGTGTGCGCCGGAAGCGGAATGCAAAAATGACCCGATAGCAACGAAATTTGTGTCAAATGCACCAAGAAGCAGC
246 E P L F E G V F C S S S N A N P N A N P N A N P N A N P N A N P N A
736 GAACCGCTGTTGAAGCGTGTGTTGACGCTCTAGCAGCACCGCAATCCGACCGCAACCCAAATGCCAATCCGAATGCAAAATCCAAATGCTAACCCAAACGCA
281 N P M A V D A V T V D T I C K N G Q L V Q M S N H F K C M C N E G L V
841 AATCCGATGGCAGTTGATCGAGTTACCGTTGATACCATTTGCAAAAATGGTCAGCTGGTTGAGTTCAGATGAGCAATCATTTAAATGCATGTGCAATGAAGCGCTGGTT
316 H L S E N T C E E K N E C K K E T L G K A C G E F G Q C I E N P D P A
946 CATCTGAGCGAAAATACCTGTGAAGAAAAAATGAATGCAAAAAGAAAACCTGGGTAAGCCCTGGTGAATTTGGTCAGTGTATTGAAAATCCGGATCCGGCA
351 Q V N M Y K C G C I Q G Y T L K E D T C V L D V C Q Y K N C G E S G E
1051 CAGGTGAATATGTATAATGTGGTTGCATTGAGGCTATACCTGAAAGAAGATACTGCGTTCTGGATGTTGCCAGTATAAAAATTTGGTGAAGCGGTGAA
386 C I V E Y L S E T Q S A G C S C A I G K V P N P E D E K K C T K T G E
1156 TGCATTGTGAATATCTGAGTGAAACCCAGAGCGCAGTTGTAGCTGTGCAATTTGGTAAAGTTCCGAATCCGGAAGATGAAAAAATGTACCAAAAACCGGTGAA
421 T A C Q L K C N T D N E V C K N V E G V Y K C Q C M E G F T F D K E K
1261 ACCGCATGTCAGCTGAAATGTAATACCGATAATGAAGTGTGCAAAAATGTGGAAGCGGTGATAAATGTCAGTGCATGGAAGGTTTTACCTTTGTATAAGAAAAA
456 N V C L L E
1366 AATGTGTGCTGCTCGAG

```

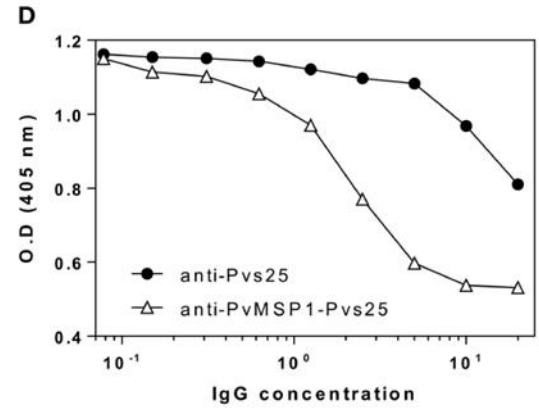
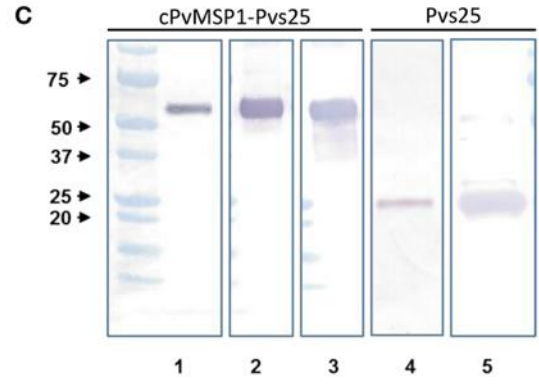


Figure 1. cPvMSP1-Pvs25 protein structure, sequence, and characterization. A) cPvMSP1-Pvs25 structure. This protein includes five promiscuous T cell epitopes of cPvMSP1 (yellow), each separated by a GPGPG spacer (diagonal lines). The promiscuous T cell epitopes are linked to a fragment derived from *P. vivax* MSP1₃₃ and the entire *P. vivax* MSP1₁₉ kD fragment (white), and the *P. vivax* Pvs25 protein (blue), with each separated by GPGPG spacers (diagonal lines). B) cPvMSP1-Pvs25 amino acid sequence is shown

in single letter code. The carboxyl-terminal (H)₆ tag provided by the vector was not included in the sequence. The yellow shaded area shows the region of the chimeric protein that contains the promiscuous T cell epitopes. The blue area shows the *P. vivax* Pvs25 protein. C) Western blot analysis of the purified cPvMSP1-Pvs25 (lanes 1-3) and the purified Pvs25 proteins (lanes 4 and 5). Each protein was run as separate PAGE gels using 1.0 µg total of purified protein under reducing conditions, and blots were stained with individual antibodies. Full uncut blots are shown in Supplementary Figure 1. Samples were incubated with following antibodies: Lane 1 and 4, the monoclonal antibody N1-1H10 which targets Pvs25; lane 2 and 5, an anti-His-Tag monoclonal antibody targeting the C terminal tags of the cPvMSP1-Pvs25 and Pvs25 proteins; lane 3, the monoclonal antibody 2A10 which targets the cPvMSP1 C terminal tag. The molecular weight markers (BioRad) are indicated. D) Polyclonal anti-cPvMSP1-Pvs25 and anti-Pvs25 elicited in rabbits compete for binding with the transmission blocking monoclonal antibody N1-1H10. Fixed amounts of N1-1H10 (1 µg) were tested with 2-fold dilutions of purified rabbit IgG using Pvs25 as antigen. O.D. values (y-axis) are shown for anti-Pvs25 in closed circles and anti-cPvMSP1-Pvs25 in open triangles using polyclonal antibodies ranging from 0.078 ng/ml to 20 µg/ml (x-axis). Data are presented as the geometric mean values.

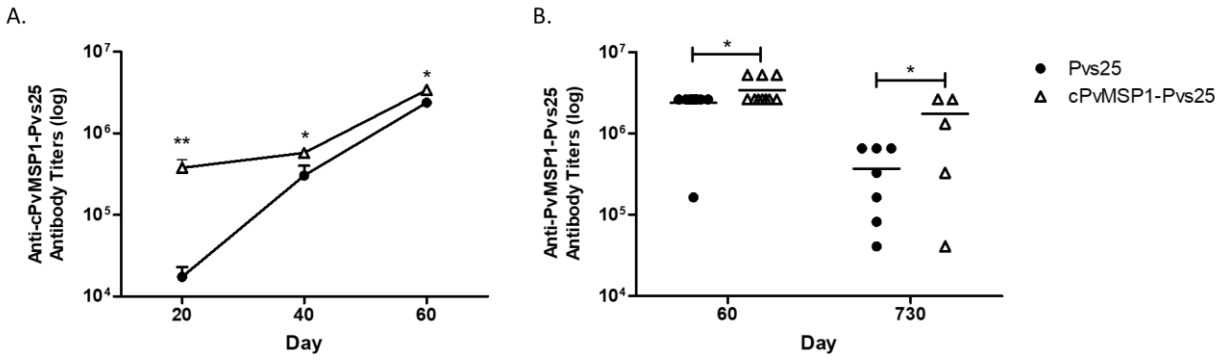


Figure 2. Antibody responses to the chimeric PvMSP1-Pvs25 protein. Antibody responses against the chimeric PvMSP1-Pvs25 protein were assessed in CB6F1/J mice following immunization with either Pvs25 (closed circles) or cPvMSP1-Pvs25 (open triangles). A) Kinetics of the antibody response against cPvMSP1-Pvs25 on days 20, 40, and 60 (n=10). B) Comparison of antibody titers between day 60 (n=10) and at 2 years (730 days after the first immunization, n=7). The titers against PvMSP1-Pvs25 are shown. Statistical analysis was conducted using Mann Whitney tests. Statistically significant differences are denoted by * ($p < 0.05$).

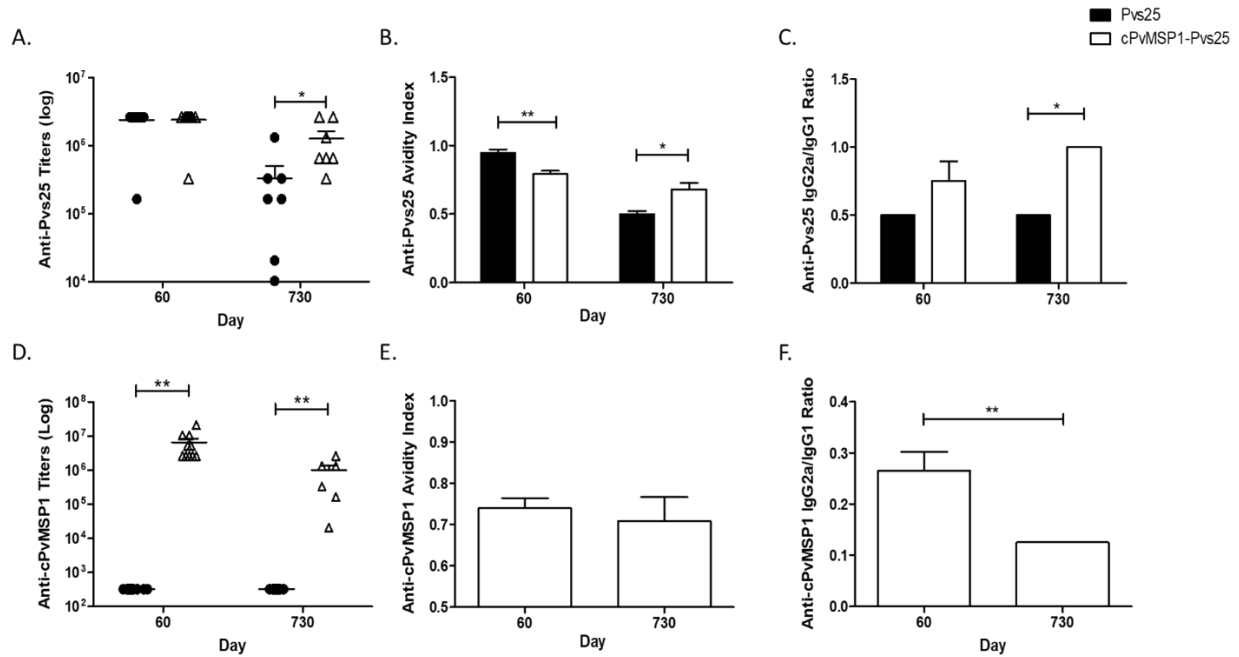


Figure 3. Antibody responses to cPvMSP1 and Pvs25. Antibody responses against the recombinant cPvMSP1 and Pvs25 proteins that form the recombinant cPvMSP1-Pvs25 protein were assessed in CB6F1/J mice following immunization with either Pvs25 (closed circles or bars) or cPvMSP1-Pvs25 (open triangles or bars) on day 60 and 730 after the first immunization. The titers against Pvs25 and cPvMSP1 are shown in A) and D), respectively. Results are presented for n=10 mice for day 60 and n=7 mice for day 730. Avidity indices for anti-Pvs25 and anti-cPvMSP1 are shown in B) and E). IgG subclass responses, displayed as the IgG2a to IgG1 ratio, are shown in C) for Pvs25 and F) for cPvMSP1. Avidity indices and subclass results are presented as the mean values obtained from sera pooled from the 10 mice at day 60 or the 7 surviving mice at day 730, responses were averaged from four technical replicates. Statistical analysis was conducted using unpaired t-tests. Statistically significant differences are denoted by * ($p < 0.05$) and ** ($p < 0.01$).

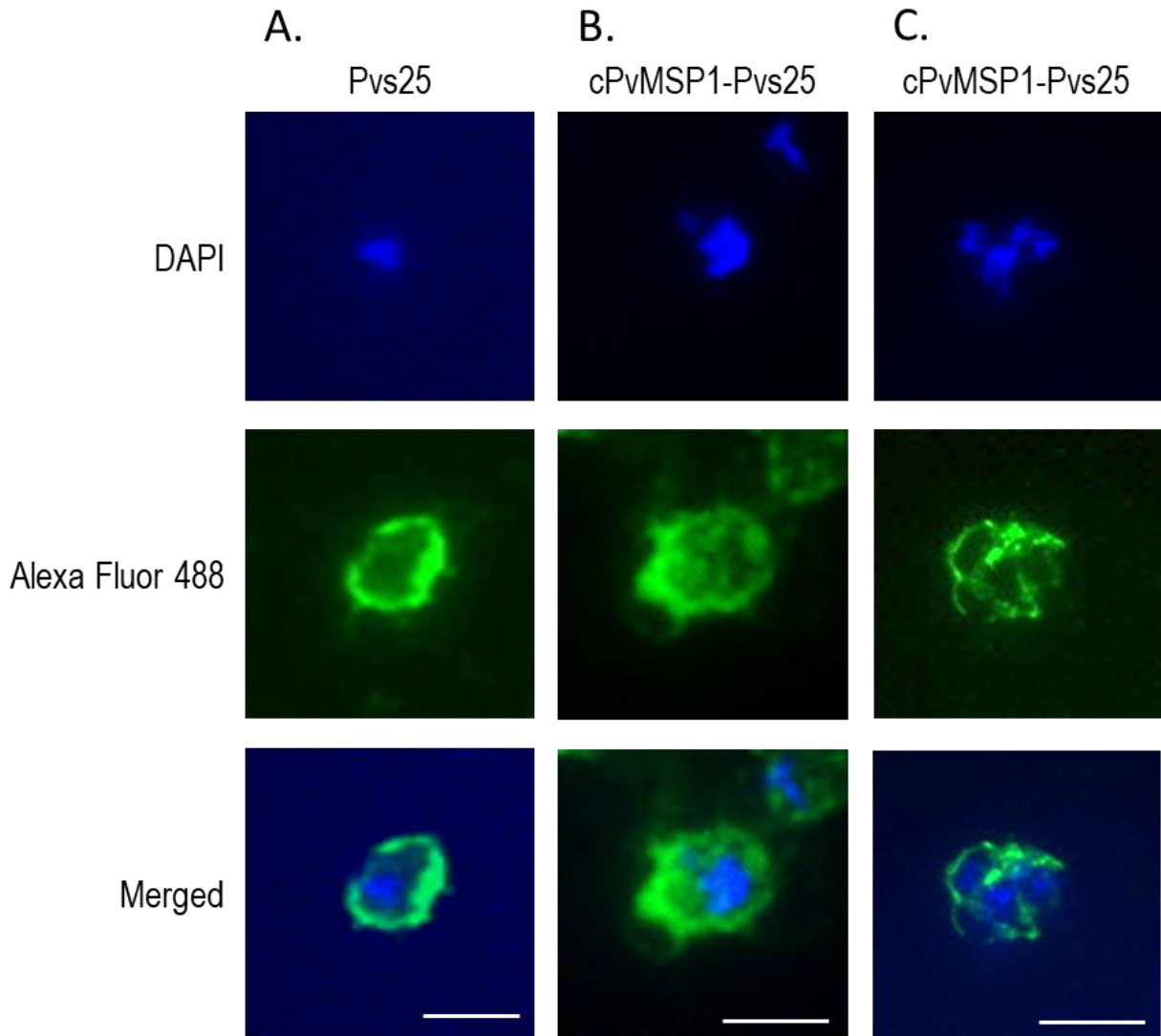


Figure 4. Immunofluorescence assays of ookinetes and schizonts. Sera from individual rabbits immunized with either Pvs25 or cPvMSP1-Pvs25 was used to assess reactivity against *in vitro* derived oocysts using the *P. berghei* transgenic parasite expressing Pvs25 (left and center columns). A pool of sera obtained from CB6F1/J mice 20 days after the final immunization with cPvMSP1-Pvs25 was used to assess reactivity against blood-stage *P. vivax* parasites (right panels). The upper panels show staining with DAPI, the middle panels show staining with a either goat-anti-rabbit or goat-anti-mouse IgG (H+L) Alexa Fluor

488 secondary antibody, and the bottom panels show the merged images. All images are shown at 100x magnification, white bars represent 5 μm in length.

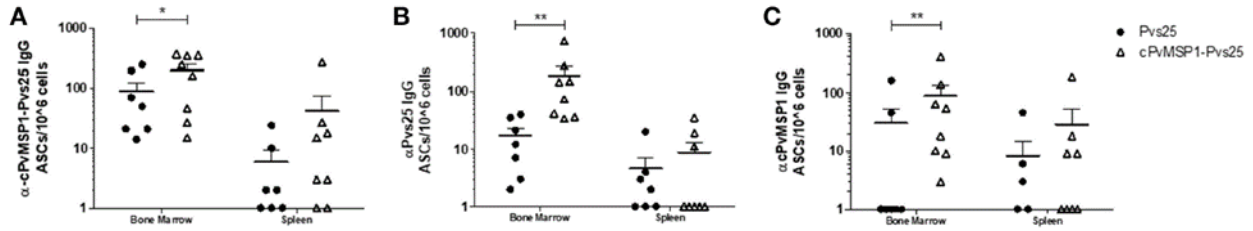


Figure 5. IgG-producing long-lived plasma cells. Antigen-specific IgG plasma cells present in the bone marrow or spleen of CB6F1/J mice immunized with Pvs25 (closed circles, n=7), cPvMSP1-Pvs25 (open triangles, n = 8) were analyzed at two years post first immunization. IgG long-lived plasma cells specific to A) cPvMSP1-Pvs25, B) Pvs25, and C) cPvMSP1 are shown. Statistical analysis was conducted using Mann Whitney. Statistically significant differences are denoted by * ($p < 0.05$) and ** ($p < 0.01$).

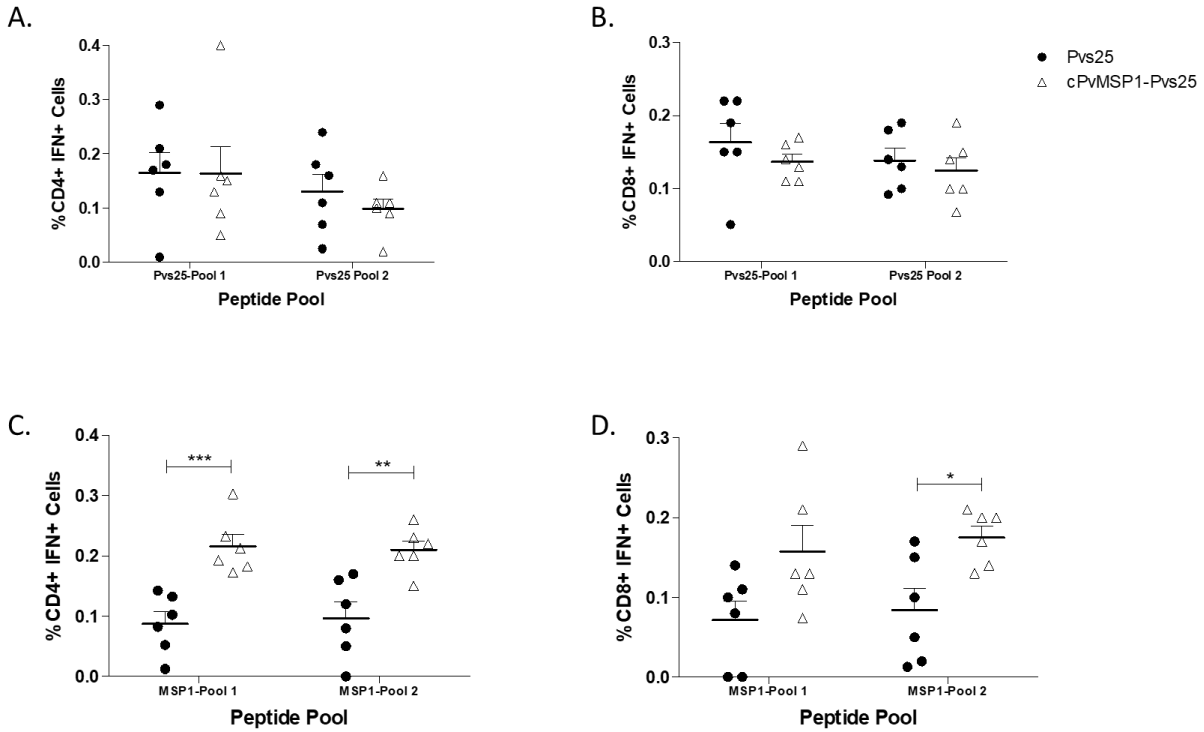


Figure 6. IFN- γ production by CD4⁺ and CD8⁺ T cells following stimulation with Pvs25 and cPvMSP1 peptide pools. Splenocytes obtained from CB6F1/J mice immunized with either Pvs25 (closed circles, n=6) or cPvMSP1-Pvs25 (open triangles, n=6) five days after the final immunization were stimulated with peptide pools representing either MSP1 or Pvs25 at 2 μ g/ml for 2 hours. Production of interferon- γ in response to stimulation with Pvs25 peptide pools by A) CD4⁺ T cells and B) CD8⁺ T cells in response to stimulation with cPvMSP1 peptide pools by C) CD4⁺ and D) CD8⁺ T cells are shown. Statistical analysis was conducted using unpaired t-tests. Statistically significant differences are denoted by * (p < 0.05) and ** (p < 0.01).

Table 1. Chimeric PvMSP1 and Pvs25 peptide pools

Peptide Pool	Sequence	Peptide Pool	Sequence
cPvMSP1 Pool 1	<p>MANFVVGKFLLELQIPG VGKFLLELQIPGHTDL LELQIPGHTDLLHLG IPGHTDLLHLGPGPG TDLLHLGPGPGFNQL HLGPGPGFNQLMHVI GPGFNQLMHVINFHV NQLMHVINFHVDLLR HVINFHVDLLRANVH FHYDLLRANVHGPGP LLRANVHGPGPGLDM NVHGPGPGLDMLKKV PPGGLDMLKKVVLGL LDMLKKVVLGLWPKL KKVVLGLWPKPLDNK LGLWPKPLDNKDGPG KPLDNKDGPGPGLE NIKDGPGPGLEYLRF GPGPGLEYLREKAK GLEYLREKAKMAGT YLREKAKMAGTLIIP KAKMAGTLIIPESGP AGTLIIPESGPGPGS IIPESGPGPGSKDQI SGPSPGSKDQIKKLT PGSKDQIKKLTSLKN DQIKKLTSLKNKLER KLTSLKNKLERRQNG LKNKLERRQNGPGPG LERRQNGPGPGVKSS</p>	Pvs25 Pool 1	<p>MAVDAVTVDTICKNG AVTVDTICKNGQLVQ DTICKNGQLVQMSNH KNGQLVQMSNHFKCM LVQMSNHFKCMCNEG SNHFKCMCNEGLVHL KCMCNEGLVHLSENT NEGLVHLSENTCEEK VHLSENTCEEKNECK ENTCEEKNECKKETL EEKNECKKETLGKAC ECKKETLGKACGEFG ETLGKACGEFGQCIE KACGEFGQCIEENPDP EFGQCIEENPDPQV CIENPDPQVNMKYK PDPQVNMKYKCGCIQ QVNMKYKCGCIQGYTL YKCGCIQGYTLKEDT CIQGYTLKEDTCVLD</p>
cPvMSP1 Pool 2	<p>QNGPGPGVKSSGLLE GPGVKSSGLEKLMK KSSGLEKLMKSKLI LLEKLMKSKLIKENE LMKSKLIKENESKEI KLIKENESKEILSQL ENESKEILSQLLNQ KEILSQLLNQVQTQLL SQLLNQVQTQLLTMSS NVQTQLLTMSSSEHTC QLLTMSSSEHTCIDTN MSSEHTCIDTNVDPN HTCIDTNVDPNAACY DTNVPDNAACYRYLD PDNAACYRYLDGTEE ACYRYLDGTEEWRC YLDGTEEWRCLLTFK TEEWRCLLTFKEEGG RCLLTFKEEGGKVP TFKEEGGKVPASN EGGKVPASNVTCKD CVPASNVTCKDNNGG SNVTCKDNNGGCAPE CKDNNGGCAPEAECK NGGCAPEAECKMTDS APEAECKMTDSNEIV ECKMTDSNEIVCKCT TDSNEIVCKCTKEGS EIVCKCTKEGSEPLF KCTKEGSEPLFEGVF EGSEPLFEGVFCSSS</p>	Pvs25 Pool 2	<p>YTLKEDTCVLDVQCQY EDTCVLDVQCQYKNCG VLDVQCQYKNCGESGE CQYKNCGESGECIVE NCGESGECIVEYLSE SGECIVEYLSETQSA IVEYLSETQSAGCSC LSETQSAGCSCAIGK QSAGCSCAIGKVPNP CSCAIGKVPNPEDEK IGKVPNPEDEKCKCT PNPEDEKCKCTGTGET DEKCKCTGTGETACQL CTGTGETACQLKCN GETACQLKCNTDNEV CQLKCNTDNEVCKNV CNTDNEVCKNVEGVY NEVCKNVEGVYKQCQ KNVEGVYKQCQMEGF GYKQCQMEGFDFDK CQCMEGFDFDKKNV EGFTDFDKKNVCLLE</p>

Peptide pools used for stimulation of T cell for assessment of cytokine production after the final immunization. cPvMSP1 Pool 1 represents MSP1 T cell epitopes present in cPvMSP1. Pool 2 represents the extended MSP1₁₉ kD protein fragment. Pvs25 pools 1 and 2 cover the full sequence of the Pvs25 protein.

Table 2. Immunization regimens

Regimen	Prime Day 0		Boost Day 20		Boost Day 40	
	Protein^a	Dose	Protein^a	Dose	Protein^a	Dose
cPvMSP1-Pvs25	cPvMSP1-Pvs25	20 μg	cPvMSP1-Pvs25	20 μg	cPvMSP1-Pvs25	20 μg
Pvs25 protein	Pvs25 protein	20 μg	Pvs25 protein	20 μg	Pvs25 protein	20 μg
Adjuvant Control	Montanide ISA 51 VG		Montanide ISA 51 VG		Montanide ISA 51 VG	

CB6F1/J mice received subcutaneous immunizations at days 0, 20, and 40 with 20 μg of either cPvMSP1-Pvs25 or Pvs25, both emulsified at a 1:1 volume ratio with the adjuvant Montanide ISA 51 VG. An equivalent volume of PBS was emulsified at a 1:1 volume ratio for subcutaneous injections in the adjuvant control group at the same intervals.

TABLE 3 | Transmission-blocking activity.

Group	Sample	Antibody titers by ELISA	Experiment 1			Experiment 2			Experiment 3			P-value ^e
			No. infected (total dissected) ^a	Average number of oocyst ^b	TBA (%) ^c	No. infected (total dissected) ^a	Average number of oocyst ^b	TBA (%) ^c	No. infected (total dissected) ^a	Average number of oocyst ^b	TBA (%) ^c	
cPvMSP1-Pvs25	Control PI 1	640	20 (36)	155 ± 7.8	85.0	23 (32)	299 ± 13	65.2	10 (30)	29 ± 2.9	100	0.01
	Immune sera 1	1310720	3 (40)	26 ± 6.8		8 (32)	13 ± 1.6		7 (30)	0		
	Control PI 2	640	17 (40)	115 ± 6.8	88.2	23 (30)	262 ± 11.4	69.6	12 (30)	35 ± 2.9	100	
Pvs25	Immune sera 2	1310720	6 (33)	2 ± 1		7 (30)	29 ± 4.14		0 (30)	0		0.01
	Control PI 1	1280	23 (40)	175 ± 7.6	100	19 (30)	262 ± 13.7	63.2	11 (30)	30 ± 2.72	100	
	Immune sera 1	1310720	0 (40)	0		7 (30)	34 ± 4.8		0 (30)	0		
	Immune sera 2 ^d	1310720	3 (30)	3 ± 1	87.0	3 (30)	8 ± 2.5	84.2	0 (30)	0	100	0.01
Negative control	AB human serum	NA	20 (36)	657 ± 17.8	NA	23 (32)	413 ± 16.5	NA	18 (30)	320 ± 10.5	NA	

NA: not applicable.

a Number of mosquitoes infected (total number of mosquitoes dissected).

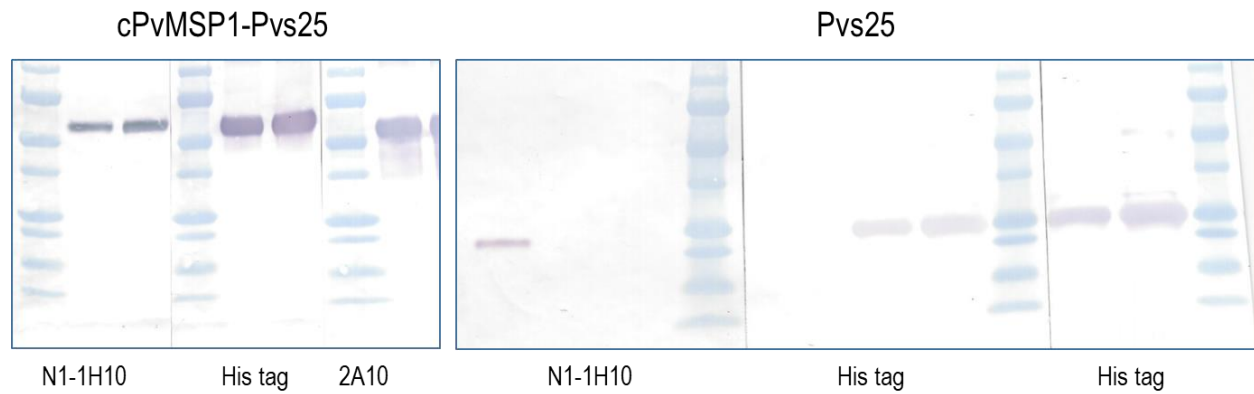
b Average calculated as total of oocyst /total of mosquitoes dissected ± standard deviation.

c Percent inhibition of mean mosquitoes post 3rd immunization sera compared to pre-immune rabbit sera in each independent assay calculated as $(1 - [\text{mean mosquitoes in normal rabbit sera}/\text{mean mosquitoes post 3rd immunization sera}] \times 100)$. A pool of AB normal human sera was used as a negative control.

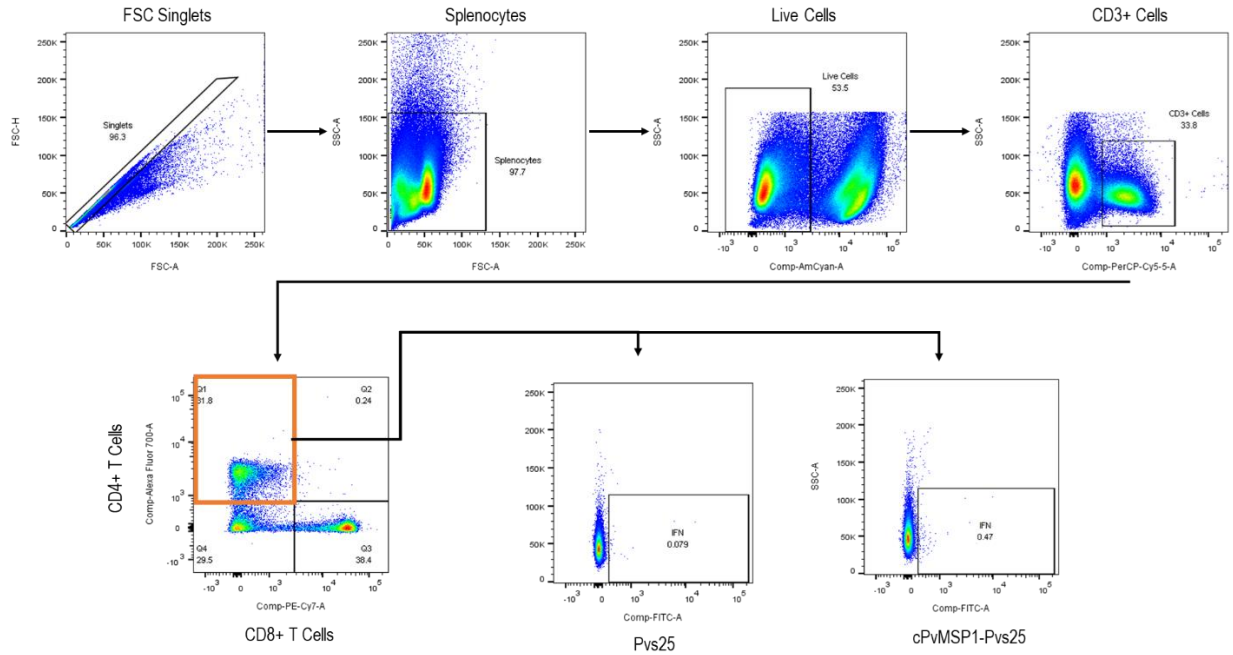
d Pre-immune sera from this rabbit was not tested, antibody titer was 1280.

e Statistical significance $P < 0.05$

Sera samples from immunized rabbits (cPvMSP1-Pvs25 and Pvs25) were tested in direct membrane-feeding assays (three different experiments) using blood samples collected from naturally infected patients as described (303).



Supplementary Figure 1. A full scan of the entire original Western blot analysis of the purified cPvMSP1-Pvs25 (left panel) and the purified Pvs25 proteins (right panel). Samples were incubated with the specified antibodies: monoclonal antibody N1-1H10 which targets Pvs25; anti-His-Tag monoclonal antibody targeting the C terminal tags of the cPvMSP1-Pvs25 and Pvs25 proteins; or the monoclonal antibody 2A10 which targets the cPvMSP1 C terminal tag. The molecular weight markers (BioRad) are included.



Supplementary Figure 2. Gating strategy for CD4⁺ and CD8⁺ IFN- γ -producing murine T cells. The gating strategy for identifying IFN- γ CD4⁺ and CD8⁺ T cells from murine splenocytes isolated 5 days post boosting includes: FSC singlets, viability gating, CD3⁺ cells, CD4⁺ versus CD8⁺ T cells, and IFN γ ⁺ cells. Data shown represent IFN- γ gating in CD4⁺ T cells of mice receiving Pvs25 or cPvMSP1-Pvs25.

Chapter 5

Capture of IgG Antibodies Induced during Natural Infections with Human Malarias to a Chimeric Plasmodium vivax Antigen

Jessica N. McCaffery¹, Balwan Singh², Doug Nace², Alberto Moreno¹, Venkatachalam
Udhayakumar², Eric Rogier²

1. Emory Vaccine Center, Yerkes National Primate Research Center, Emory University, 954
Gatewood Road, Atlanta, GA 30329.
2. Centers for Disease Control and Prevention, Center for Global Health, Division of Parasitic
Diseases and Malaria, Malaria Branch, Atlanta, GA.

Currently preparing for submission to the *Journal of Infectious Diseases*.

Abstract

As malaria incidence decreases, it becomes increasingly difficult to identify areas of active transmission due to an increase in asymptomatic infections. Serological assays can provide population-level infection history to inform elimination campaigns. Here we use multiplex antigen detection assays to evaluate a chimeric *P. vivax* MSP1 antigen (PvRMC-MSP1), initially designed to be broadly recognized for use in vaccine studies, for its ability to capture IgG from 236 naturally exposed US travelers with known infection status from all four human malarias. We observed increased assay signals for the PvRMC-MSP1 chimera vs the recombinant PvMSP1 for 89.5% (34/38) of *P. vivax* infected patients. Regardless of infecting species, we observed that a majority of sera from malaria patients provided a high assay signal to the PvRMC-MSP1 antigen. These results support further study of designed antigens as a method for increasing sensitivity or broaden binding capacity to improve existing serological tools.

Introduction

Malaria morbidity and mortality remains a major public health problem globally. According to World Health Organization (WHO) estimates, there were 219 million cases of malaria in 2017 which resulted in 435,000 deaths (1). Malaria elimination targets have been set for at least 10 countries by 2020, and by 20 countries by 2025 (134). As malaria incidence and transmission in a region decreases, it becomes increasingly difficult to identify areas of active transmission and to detect active infections partially due to an increase in the prevalence asymptomatic infections (and lack of treatment-seeking behavior) potentially contributing to further malaria transmission (127, 321-327). Therefore, improved methods for monitoring areas of active transmission in areas of low transmission intensity are required. Entomological inoculation rates, which measure the mean number of infectious mosquito bites per individual over time, remain a widely-accepted measure of transmission, but lack precision due to heterogeneous mosquito distributions (130). Furthermore, this method is not without practical and ethical considerations, as it requires mosquito trapping using adult volunteers and can be difficult to extrapolate to pediatric populations (328, 329). Co-endemic patterns of malaria also pose a problem for malaria control efforts as vector-based intervention targeted toward *Plasmodium falciparum* are less efficacious against *P. vivax* (288). In sub-Saharan Africa, *P. falciparum* is by far the most prevalent malaria, but *P. vivax*, *P. malariae* and *P. ovale* as have been identified as well (1). Human populations in many other parts of the world are also subjected to the burden of multiple *Plasmodium* species that complicates accurate diagnosis and epidemiology (330, 331).

There has been an increase in the use of serological and antibody-based detection assays as a method for measuring exposure and determining transmission intensity to aid in malaria control in regions undergoing elimination campaigns (129, 131, 332). Quantitative immunoassays offer several advantages over other platforms including more robust data generation by providing more information than only the presence or absence of an active infection. Quantitative immunoassays can also estimate individual- and

population-level malaria exposure history (127, 128, 333), and have the ability to use dried blood spot samples that are pragmatic for field and laboratory processing (334). One or multiple recombinant antigens are typically used to detect anti-malaria antibodies in patient samples, and common targets include: circumsporozoite protein (CSP), apical membrane antigen 1 (AMA1), and merozoite surface proteins (MSP1, MSP2, and MSP3) (131, 332, 333, 335, 336). IgG responses to the recombinant MSP1₁₉ isoforms for the four human malarias (*P. falciparum*, *P. vivax*, *P. malariae*, and *P. ovale*) have found to be largely specific, giving more confidence in population seroestimates even when these four *Plasmodium spp.* are co-endemic (336). Recently, the use of chimeric malaria proteins as serosurveillance tools has been explored, including a multi-epitope chimeric antigen that contained epitopes from eight *Plasmodium falciparum* antigens (337, 338). While this serological tool was well-recognized by *P. falciparum* infected patients in endemic regions along the China-Myanmar border, this antigen displayed very limited cross-reactivity with *P. vivax* infected individuals (337).

Previously, our group had developed a chimeric *P. vivax* MSP1 antigen (designated PvRMC-MSP1), intended for use in vaccine studies. This chimeric antigen was shown to bind to several MHC class II alleles (220), and was recognized by individuals living in malaria endemic areas of Brazil with no indication of genetic restriction based on HLA-DRB1 and HLA-DQB1* alleles (259). The immunological components of PvRMC-MSP1 include: an extended version of PvMSP1₁₉ containing two additional T helper epitopes present in MSP1₃₃, five promiscuous T cell epitopes (capable of binding multiple MHC Class II alleles) arrayed in tandem, and a C-terminal (NANP)₆ affinity tag (259). In this current study, we evaluate the ability of PvRMC-MSP1 to induce IgG antibodies that would bind to non-*vivax* antigenic targets, as well as the ability of the chimera to capture IgG from naturally exposed persons with known infection status to all four human malarias.

Methods

Ethics statements. All animal protocols that include experimental animal procedures using mice and rabbits were carried out in accordance with the US Animal Welfare Act and approved by the Emory University's Institutional Animal Care and Use Committee, protocol YER-2002483-092616GN and followed accordingly.

Samples with or without PCR-confirmed malaria infection were described previously (339), and determined by the CDC Human Subjects office to be research that does not involve human subjects (2017-192). No contact nor access to personal identifiers were available to laboratory staff from the Centers for Disease Control and Prevention or Emory University.

Structure of the *P. vivax* recombinant chimera, and other antigens used in the study. We have previously described the design of PvRMC-MSP1 for use as a malaria vaccine candidate (259) (Figure 1). Briefly, PvRMC-MSP1 was based on the *P. vivax* Belem sequence (GenBank: XP_001614842.1), and includes the following segments: 1) Methionine and alanine were included as the first two amino acids to provide both the start signal and decrease degradation during synthesis in *E. coli*, and valine and aspartic acid were introduced downstream as part of the cloning strategy; 2) Five promiscuous T cell epitopes (220, 259), designated PvT4 (N₇₈-L₉₇), PvT6 (F₁₁₈-H₁₃₇), PvT8 (L₁₅₈-D₁₇₇), PvT19 (L₃₇₈-S₃₉₇), and PvT53 (S₁₀₅₈-N₁₀₇₇) linked in tandem and separated by GPGPG spacers; 3) An extended version of *P. vivax* MSP1₁₉ fragment including two T helper epitopes derived from MSP1₃₃; 4) The *P. falciparum* circumsporozoite protein (NANP)₆ repeat region was included at the C-terminal end as an additional affinity purification tag. GPGPG spacers were used to separate all segments described to enhance the stability of the protein, preserve epitope conformation, and assist with antigen processing. The PfMSP1, PvMSP1, PmMSP1, PoMSP1, and CSP antigens have all been used in previous studies, and were produced as described before (336, 340).

Mouse and Rabbit Immunizations. We have previously reported on the immunogenicity of the PvRMC-MSP1 in mice and rabbits (259). Briefly, all animal experiments and procedures involving mice were performed in accordance with Emory University's Institutional Animal Care and Use Committee. Female BALB/c (H-2^d) mice aged 6-8 weeks were obtained from Charles River (Wilmington, MA). Mice were immunized at days 0, 20, and 40 with 20 µg of PvRMC-MSP1 emulsified with the adjuvant Montanide ISA 51 VG at a 1:1 volume ratio. All immunizations were administered subcutaneously at the base of the tail and in the interscapular area. Sera was collected prior to the first immunization and 20 days after the final immunization. Sera from pre-immune timepoints was used as negative controls for multiplex assays.

Similarly, rabbits were immunized four times with PvRMC-MSP1 at 20 day intervals. Sera was obtained prior to the first immunization and after the final immunization. All rabbit immunizations and sera collection was carried out by Convance (Princeton, NJ). Rabbit polyclonal IgG antibodies were purified from sera collected after the final immunization by protein A affinity chromatography using the Affi-Gel protein A MAPS II kit (BioRad) according to the manufacturer's instructions. The total IgG solution obtained from the elution was then dialyzed in PBS.

Antigen coupling to magnetic beads. All antigens were covalently linked to MagPlex (magnetic) microspheres (Luminex Corp., Austin, TX) as described previously (133). Briefly, beads were pulse vortexed before being transferred to a microcentrifuge tube and centrifuged for 90 seconds at 13,000×g. The supernatant was removed and beads were washed with 0.1M sodium phosphate, pH 6.2 (NaPO₄). Beads were activated by suspending in NaPO₄ with 5 mg/ml of EDC (1-ethyl-3-[3-dimethylaminopropyl] carbodiimide hydrochloride) and 5 mg/mL sulfo-NHS (sulfo N-hydroxysulfosuccinimide) and incubating with rotation for 20 minutes at room temperature (RT)

protected from light. After wash with 50 mM 2-(N-morpholino)ethanesulfonic acid (MES), 0.85% NaCl, pH 5.0, beads were suspended in this same buffer to a final volume of 1 ml and appropriate amount of each antigen added: PvRMC-MSP1 (20 µg), PfMSP1 (20 µg), PvMSP1 (20 µg), PmMSP1 (20 µg), PoMSP1 (20 µg), PfCSP (30 µg). Beads were rotated for 2 hours at RT protected from light, then washed and suspended in PBS with 1% bovine serum albumin (BSA) and incubated for 30 minutes at RT by rotation. Beads were washed with storage buffer (PBS, 1% BSA, 0.02% sodium azide and 0.05% Tween-20) and suspended in storage buffer containing protease inhibitors (200 µg/mL Pefabloc, 200 µg/ml EDTA, 1 µg/mL pepstatin A and 1 µg/mL leupeptin) and stored at 4°C.

Multiplex Antibody Detection Assays. All samples were diluted in blocking buffer (Buffer B: PBS, 0.05% Tween 20, 0.5% polyvinylpyrrolidone, 0.5% poly(vinyl) alcohol, 0.1% casein, 0.5% BSA, 0.05% Tween-20, 0.02% NaN₃, and 3 µg/mL *E. coli* extract to prevent nonspecific binding). All human samples were assayed at a standard 1:400x plasma dilution. The standard MBA was performed as described previously in flat bottom BioPlex Pro 96 well plates (Bio-Rad, Hercules, CA) (133). Wash steps included attaching the assay plate to handheld magnet (Luminex Corp, Austin, TX), the addition of 100 µl wash buffer PBST (PBS, 0.05% Tween-20) to each well, then gentle tapping on side of plate to facilitate magnetization of beads, and inverting the plate to evacuate the liquid. Beads (1,000 beads/antigen/well) were suspended in Buffer A (PBS, 0.5% BSA, 0.05% Tween-20, 0.02% NaN₃) and 50 µl bead master mix added to each well. Plates were washed two times with PBST and 50 µL of sample was added to each well and incubated with shaking at RT for 90 minutes. After 3 washes with PBST, beads were incubated for 45 minutes with detection antibody appropriate for the samples: biotinylated goat anti-rabbit IgG (H+L, 1:500, Zymed), biotinylated rat anti-mouse IgG (1:500, Invitrogen), or biotinylated mouse anti-human IgG (mixture of 1:500x anti-hIgG and 1:625 anti-hIgG₄, both Southern Biotech). After 3 washes, beads were incubated with streptavidin-phycoerythrin (1:200 Invitrogen, Waltham, MA) for 30min. After

3 washes, wells were incubated with Buffer A for 30 minutes under light shaking to remove any loosely bound antibodies. After 1 wash, samples were resuspended in 100 µl PBS and fluorescence data collected immediately on the MAGPIX with Bio-Plex Manager™ MP software with a target of 50 beads per region per well. Median fluorescence intensity (MFI) signal was generated for a minimum of 50 beads/region, and background MFI from wells incubated with Buffer B was subtracted from each sample to give a final value of MFI minus background (MFI-bg) for analysis.

Immunofluorescence assays. Sera obtained terminal bleeds from rabbits were used to evaluate antibody cross-reactivity against *P. falciparum* MSP1 via indirect immunofluorescence assay as described previously. *P. falciparum* NF54 thin smears were made from culture at the late schizont stage where parasitemia was determined to be 4%. Rabbit sera was diluted at 1:500 in PBS with 1% BSA, and reactivity of immunized rabbits was compared to that of rabbit sera obtained prior to immunization with PvRMC-MSP1. A human hyperimmune sera pool with high reactivity to all *Plasmodium* MSP1 antigens was created from samples previously tested by serological assays. Immunofluorescence images were captured using a Zeiss confocal fluorescence microscope with Axiovision (Zeiss, Jena, Germany) software and presented at 100x magnification.

Statistics and analyses. All graphs were made in Microsoft Excel (Redmond, WA). Protein alignments were assessed using the Clustal Omega Multiple Sequence Alignment tool available from the European Bioinformatics Institute (EMBL-EBI) using the GenBank accession numbers XP_001352170.1 for *P. falciparum* 3D7, *P. ovale* SCQ16291 for *P. ovale*, and SBS84075.1 for *P. malariae*. All sequences were compared to those reported for PvRMC-MSP1, which is based on the *P. vivax* Belem sequence, with accession number XP_001614842.1 (259).

Results

Alignment of PvRMC-MSP1 with other MSP1s from the four human *Plasmodium* species. The PvRMC-MSP1 protein has an estimated molecular mass of 31 kDa, and is shown by schematic in Figure 1A. The 5 promiscuous T cell epitopes included in the chimera ranged between 35-85% identity with other human malarias (Figure 1B), with the highest overall being PvT8 (average 81.7%) and the lowest being PvT4 and PvT19 (both average 41.7%). Accounting for all 5 T cell epitopes, *P. ovale* showed the highest alignment (59% overall) followed by *P. malariae* (52%) and *P. falciparum* (50%). Among the MSP1₁₉ fragments, *P. ovale* against showed the highest identity to PvRMC-MSP1 (51%), followed by *P. malariae* (50%) and *P. falciparum* (45%) (Figure 1C).

Assessment of PvRMC-MSP1 capacity to elicit cross-reactive antibodies. Sera or purified IgG titrations from terminal bleeds of rabbits and mice previously immunized with PvRMC-MSP1 assayed for binding to the immunogen, or the MSP1 antigen from the four human malarias. Purified total IgG from rabbits maintained a high assay signal for PvRMC-MSP1 before eventually dropping off below 1,000 pg/ml (Figure 2A). The assay signal for IgG against PvMSP1 also maintained a high signal before dropping between 100,000 and 10,000 pg/mL. In addition to IgG binding the antigens based on the *P. vivax*, we observed low-level signal at dilutions between 10⁷-10⁴ pg/ml for PfMSP1, and a very low assay signal for both PoMSP1 and PmMSP1. Assessment of immunized mouse sera resulted in a similar binding pattern, with the strongest signal elicited by PvRMC-MSP1, followed by *P. vivax* MSP1 (Figure 2B). Very low assay signals were seen for the immunized mouse sera against PfMSP1, PoMSP1, and PmMSP1, and did not appear to titrate out with further dilution. Immunofluorescence assays (IFAs) with slides fixed with parasitized red blood cells from *P. falciparum* NF54 culture showed IgG binding to *P. falciparum*-infected cells from both PvRMC-MSP1-immunized rabbit sera as well as hyperimmune

human sera (Figure 2C). We have previously reported on that anti-PvRMC-MSP1 antibodies elicited by vaccination are able to recognize *P. vivax* schizonts by IFA (259).

IgG binding to PvRMC-MSP1 and MSP1₁₉ antigens in malaria patients. A panel of 236 US travelers returning to the United States with malaria infection was chosen to assess binding to the MSP1 antigens from all 4 human malarias or PvRMC-MSP1. Irrespective of infecting species, the plots showing direct comparison of the assay signal for IgG against PvRMC-MSP1 against another MSP1 antigen typically gave four distinct quadrants of patient samples: negligible signal for both, high signal for both, or negligible signal for one but high signal for the other (Figure 3). For the relationship with PvMSP1, a dense cluster of double-positives is observed (Figure 3A), whereas many samples elicit a strong signal for PvRMC-MSP1 alone and a negligible signal for PvMSP1. As expected, no samples provided a signal for PvMSP1 only (being that this antigen is included within PvRMC-MSP1). When compared to PfMSP1, these four populations could be clearly observed, with few persons in the middle range of assay signals (Figure 3B). Comparison between PvRMC-MSP1 binding and either *P. malariae* or *P. ovale* MSP1 (Figure 3C and 3D, respectively) showed that most individuals that responded to the PmMSP1 or PoMSP1 antigen also responded to PvRMC-MSP1 resulting in many more double-positive individuals than PmMSP1 or PoMSP1 single-positive individuals alone.

To further illuminate how IgG produced during human malaria infection was able to bind PvRMC-MSP1, sera samples were categorized by species responsible for active infection (Figure 4). Of the 236 malaria patients' plasma samples, 181 were from *P. falciparum* infections, 4 from *P. malariae*, 13 were from *P. ovale*, and 38 were from *P. vivax*. Regardless of infecting species, we observed that a majority of sera from malaria patients provided a high assay signal to the PvRMC-MSP1 antigen (Figure 4A). In stark contrast to PvMSP1 alone which showed an assay signal for only 4 samples of persons with *P. falciparum* infection (Figure 4B, blue circles), IgG binding to PvRMC-MSP1 gave a range of signals for

many of the falciparum infections, with many of these approaching the maximum signal for the platform (MFI-bg of 32,000). Another observation was noted for the *P. vivax* infected plasma, with many of these samples reaching maximum signal intensity for PvRMC-MSP1, but more of a range of signals for PvMSP1 alone (green circles in Figure 4A vs Figure 4B). If assessing the MFI-bg signal between these two antigens for the 38 *P. vivax* plasma, PvRMC-MSP1 reliably provided higher IgG binding capacity when compared to PvMSP1 for a single sample (Supplementary Figure 1). As shown by high specificity estimates previously (336), IgG assay signal for the four MSP1 antigens was typically dedicated only for that particular infecting malaria species (Figure 4B,C,D,E), though heterologous signals are also observed. Life history of malaria exposure is not known for these persons, and it could not be ascertained if IgG from a previous infection would still be lingering.

Antibody binding to PvRMC-MSP1 from *P. falciparum*-infected plasma is not due to the presence of the PfCSP NANP repeat region alone. Due to the presence of the *P. falciparum* circumsporozoite protein NANP repeat region on the C-terminus of PvRMC-MSP1, we sought to determine if the PvRMC-MSP1 binding signal we observed from patients with active *P. falciparum* malaria infection was due to IgG binding the NANP region alone. A scatterplot for the PfCSP and PvRMC-MSP1 assay signals for only the 181 persons infected with *P. falciparum* showed the many persons to be double-positive for both of these antigens (Figure 5). Additionally, some plasma samples showed a correlation of assay signals between the two antigens – tracking on a $y=x$ reference line. However, some of these assay signals from falciparum infections were non-existent for PfCSP, yet showed very high PvRMC-MSP1 IgG binding. No persons were anti-PfCSP IgG positive alone.

Discussion

As the malaria community grows increasingly independent of microscopy, numerous new tools have been developed for mass screening a human population for malaria infection or exposure. In the field, these tools are typically designed to assay for some component of the *Plasmodium* parasite, and the DNA and antigens produced during the parasite life cycle are attractive targets due to their high sensitivity and specificity in detection of active infection (341, 342). However, especially in areas of low malaria endemicity, tools for detection of infection do not offer much information for residual and historical transmission outside of confirmation that infection prevalence is low in the population. By looking at history of personal (and population) exposure through host-produced antibodies, this window of time in finding a “malaria positive” is greatly augmented (127, 335). Serological studies offer numerous advantages over other measures of prevalence and transmission, including: passive surveillance which would underestimate the number of active cases occurring in a region (343), microscopy which requires skilled staff while also missing low-density infections, nucleic acid-based assays which are costly for large scale studies and detect only active infection (127, 325), and entomological inoculation rates which are laborious to collect and have shown strong biases in heterogeneous environments (130).

For malaria serological studies, tailoring the sensitivity of the assay using a highly immunogenic antigen has previously been suggested as a method to improve serological testing and estimates generated by this data (127). Recent assessment of a multi-epitope chimeric protein, initially designed as a vaccine candidate, for use as a serological marker in *P. falciparum* elimination settings in Southeast Asia demonstrated the potential of a tailored antigen in serological studies (337). An additional chimera based on the fusion of the *P. falciparum* MSP1 and MSP8 antigens has shown efficacy for induction of growth-inhibitory antibodies in animal models (344, 345), but has been yet to be used to assay human sera from naturally-exposed populations. Based on data generated using these types of unnatural antigens for malaria-based serostudies, the concept of a chimeric or some other non-naturally occurring antigen could

be of great value since the objective is anti-malarial antibody capture (and not induction of a humoral response). Using this concept, we tested a chimeric *P. vivax* MSP1 antigen for the capacity to capture naturally-induced IgG antibodies in humans with known active infection to one of the four human malarias.

For the extended 19kD fragment of the PvMSP1 antigen, we report an approximate 50% conserved amino acid identity between PvRMC-MSP1 and each of the orthologous regions from the other three human malarias. Human antibody binding to the MSP1 19kD antigen is known to have some conformational dependency, and these antibodies tend to recognize epitopes that are conserved among variant sequences (346). However, multiple motifs have been identified within the MSP1 19kD antigen which are available for antibody binding (346, 347), so sequence similarity of a single epitope would not necessarily dictate potential for cross-binding and IgG capture. Sequence identity among the five promiscuous T cell epitopes was widely varying – from 35% to 85%. This degree of conservation in the MSP1 and T cell epitopes provides a potential explanation for the assay signal for IgG capture to heterologous antigens for rabbits who had been vaccinated PvRMC-MSP1, and immunized rabbit IgG binding to *P. falciparum* blood stage schizonts by immunofluorescence assay. The sequence similarity or conformation of the 19kD fragments alone would not provide a likely explanation for this finding, as human IgG among these antigens from different human malarias has been shown to be largely specific (336). Overall, the degree of cross-binding of IgG raised against PvRMC-MSP1 in these animals appears to be very low, even at high serum and IgG concentrations.

Upon assessment of IgG capture between PvRMC-MSP1 and recombinant *P. falciparum*, *P. malariae*, and *P. ovale* MSP1 19kD antigens, we observed in *Plasmodium*-infected persons a consistent subset of individuals' plasma that contained IgG strongly recognizing both the lone MSP1 antigen and the chimeric antigen. This was seen regardless of infecting *Plasmodium* species, and this “double-positive” population of persons was much more prevalent for *P. ovale* and *P. malariae* infections when compared

to the PoMSP1 or PmMSP1 antigen “single-positives” alone. Even for active *P. falciparum* infections, the number of double positives were roughly equivalent to the PfMSP1 single positives alone. Considering the selection of promiscuous T cell epitopes within the PvRMC-MSP1 protein, which were included based on their predicted ability to multiple human MHC class II molecules, this finding may not be surprising of a broader capacity for IgG binding. An assessment of peptides from *P. vivax* MSP1 preceding the development of PvRMC-MSP1 showed a high degree of variability in the ability of peptides to bind HLA class II molecules and to be recognized by individuals from endemic areas (220), and data from the initial characterization of PvRMC-MSP1 demonstrated that 50.4% of individuals living in Brazil had antibodies able to recognize the PvRMC-MSP1, with no indication of genetic restriction based on HLA-DRB1 and HLA-DQB1* alleles (259).

An additional observation was that the majority of *P. vivax* patients carrying IgG antibodies with a higher capacity of binding PvRMC-MSP1 when compared to the recombinant PvMSP1 19kD antigen alone. Though these two antigens were coupled to the microbeads at the same concentration, the assay signal of PvRMC-MSP1 versus PvMSP1 was increased for 89.5% (34/38) of *P. vivax*-infected plasma, with some samples showing an increase of over an order of magnitude. One plasma had a decreased assay signal, and signals remained very low for three plasma. Many regions of South and central America are currently within, or approaching, the elimination phase of their national malaria programs, and *P. vivax* is the predominant residual species in some of these places (348). Having a more sensitive serological tool for detection of *P. vivax* exposure would be able to assist the Americas and other global settings in mapping out regions and populations where malaria still resides, especially when *P. vivax* is the primary human malaria.

Designed antigens with intentional broad antibody binding capacity could provide a valuable tool for use in serological assessment studies when compared to whole recombinant antigens alone which are intended to be true to the genome-encoded antigen. This current study benefitted from the use of the bead-

based multiplex system which allows simultaneous data collection of IgG presence and levels against multiple antigens (128). Including both broad-reacting, as well as *Plasmodium* species-specific, antigen coated beads in an assay panel could provide a very nuanced view of individual and population level exposure histories and provided an extensive IgG profile and detailed seroestimates (349, 350). Our study was limited by the absence of knowledge for individuals' previous *Plasmodium* exposure history outside of their current infection event. This population of US resident travelers returning with malaria infection would be more biased toward those with nascent exposure, but it would not be able to be ascertained how many previous episodes, or what species, persons would have been exposed to. This possibility of previous lifetime exposure provides a reasonable explanation for our finding of IgGs capable of binding the MSP1 antigens from the other, non-infecting, *Plasmodium* species. Beyond known active *Plasmodium* infections, future studies will work to assess antibody binding to PvRMC-MSP1 (and other chimeric antigens) to naturally-exposed human populations in different regions of the world with different transmission intensities and co-endemic patterns.

Acknowledgements

Jeffrey Priest for cloning, expression, and purification of the MSP1 antigens from the four human malarias. A portion of this research was carried out at the Yerkes National Primate Research Center and was supported in part by ORIP/OD P51OD011132.

Author Contributions

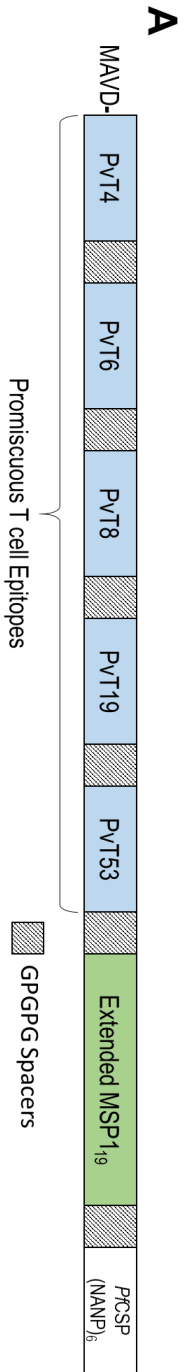
Conceived and designed experiments: E.R. Performed the experiments: J.N.M., B.S., D.N., E.R. Analyzed the data: J.N.M., E.R. Contributed reagents, materials, and analysis tools: J.N.M., B.S., A.M., V.U. Manuscript preparation: J.N.M. A.M., V.U., E.R. All authors reviewed and approved the final manuscript.

Competing financial interests

The authors declare no competing financial interests.

Disclaimer

The findings and conclusions presented in this report are those of the authors and do not necessarily reflect the official position of the Centers for Disease Control and Prevention.



B

<i>Plesiomodum</i> spp.	PvT4	Identity	PvT6	Identity	PvT8	Identity	PvT9	Identity	PvT53	Identity
PvRMG-MSP1	NEVGEFELQIEGHTDLLHT		ENQLMHVTNHFHYDLIRANVH		LIMIKKVVVIGMRFPLMINKD		LEVYIIRKARVAAGHTLIIIEES		SRDQIKRITLILKIKLERRON	
<i>P. fulvopurum</i>	SSGSTRKEVQITPSGSLIIE	35%	INELLVKINLFFPDLIRAKIN	49%	LIVVILKLVVFGYRPLDMINKD	75%	LEVYIIRKARVAAGHTLIIIEES	49%	DRMGIKRIKTLILKQLESKIN	50%
<i>P. ovule</i> (51%)	FILSRFLQNLITGSGIOLNHF	50%	FHEILVYIINLFFYDLPRAKIH	60%	LIMIKKVVVIGYRPLDMINKD	83%	LIVYIIRKARVAAGHTLIIIEES	49%	SREHIRELSLILKAOLMIRQF	55%
<i>P. mulariae</i>	NEVSKVINLNLGGYQGLPES	40%	FHEILVYIINLFFYDLPRAKIN	65%	LIMIKKVVVIGYRPLDMINKD	83%	LIVYIIRKARVAAGHTLIIIEES	35%	ITHEEGKINLALGVDLRSKLE	35%

C

Plesiomodum spp. **Extended MSP1₉ (M) Fragment**

PvRMG-MSP1	VKSGSLLERKIMRSKILIKRNSKEEILISQILANQVQ-LLMSSSEHCIDIMVVDNNAAGYVYLDGHEWRCCLAFREEGGRKCVPAISVYTCRNNNGGCAPEAFRGKMTDSNELVCKKRGSSRPLERGGVFCSSSS
<i>P. fulvopurum</i> 3D7 (45%)	KMLDGLKLSITGSLV-QVFNNTLISKLIEGRFQVMIINISQVQCVKQCPENSGCFNHLDERECCQLNLYQEGKCVENRPLTCNENNGGCDADATCTEEDSGSSRKKLTCEBTKPDQYPLFDGIFCGSSSS
<i>P. ovule</i> (51%)	IDFSNINIKLKRSGSFVDDDSKRLSELLDVDSKQLLNSGSKRCKIDITYPENAGCYEYEDREBMRCLNFKRKGETHCVFNNPFCANNGGCDPTADCAESENKRTCTCTGQ-NESTFERGGVFCGSSSS
<i>P. mulariae</i> (50%)	IASGILDLIKQKGLVNRKRSFTKILSELGLVDSNALINI SAKHACTETKYEENAGCYEYEDREKVRCLNLYKLVDECVEDQEPSCVNNNGGCAPEFANCTKGDNRKLVACNAPYSEPLFERGGVFCGSSSS

Figure 1. Schematic and alignment of the PvRMC-MSP1 chimeric protein. (A) Entire length of chimera shown with T cell epitopes represented as blue boxes with the *P. vivax* T cell epitope designation (PvT) listed inside each box. (B) Alignment of PvRMC-MSP1 T cell epitopes with orthologous regions from other human malarias. (C) Alignment of 19KD fragment within PvRMC-MSP1 with MSP1₁₉ regions in other human malarias and the partial 33kD segment.

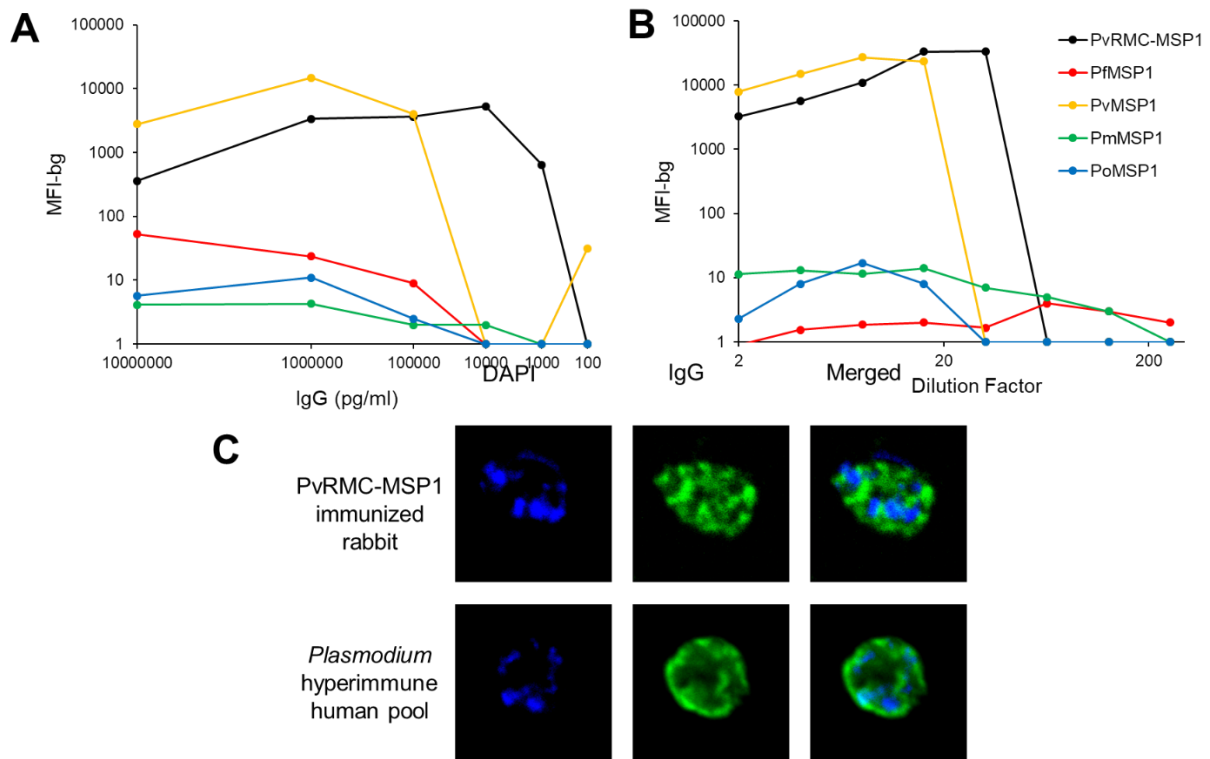


Figure 2. Capture of rodent derived anti-PvRMC-MSP1 IgG with MSP1 antigens from all four human malarias. (A) IgG assay signal for purified total IgG obtained from rabbits following four immunizations with the PvRMC-MSP1 protein. Median fluorescence intensity minus background (MFI-bg) assay signal is shown for each of the four human malaria MSP1 proteins in comparison the PvRMC-MSP1 used for immunization. (B) IgG assay signal for mouse sera obtained after three immunizations with PvRMC-MSP1 with MSP1 proteins from the four human malaria species. (C) *Plasmodium falciparum* NF54 slides incubated with sera obtained from immunized rabbits (top), and sera from persons living in *Plasmodium* endemic regions (bottom). Panels show staining for DNA (DAPI, blue), IgG (AlexaFluor 488, green), and merge. All images at 100x magnification.

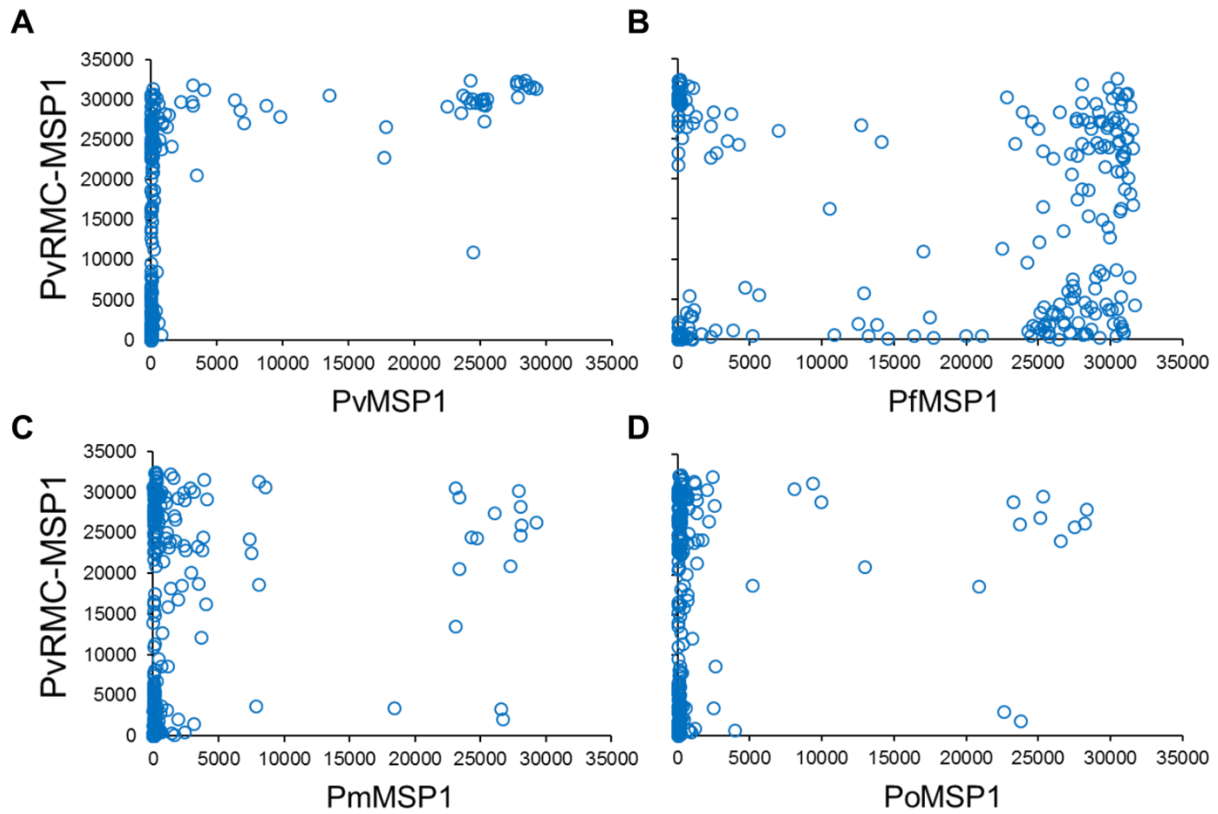


Figure 3. Comparison of MFI-bg assay signal for PvRMC-MSP1 and MSP1s from the four human malarias for persons with active malaria infection. Each point of the scatterplot displays an individual's MFI-bg IgG response against PvRMC-MSP1 (y-axis) and the MFI-bg response from the same individual against the MSP1 19kD antigens from one of the four human malarias (x-axis). Data was generated using samples obtained from 236 returning US travelers with active malaria infection.

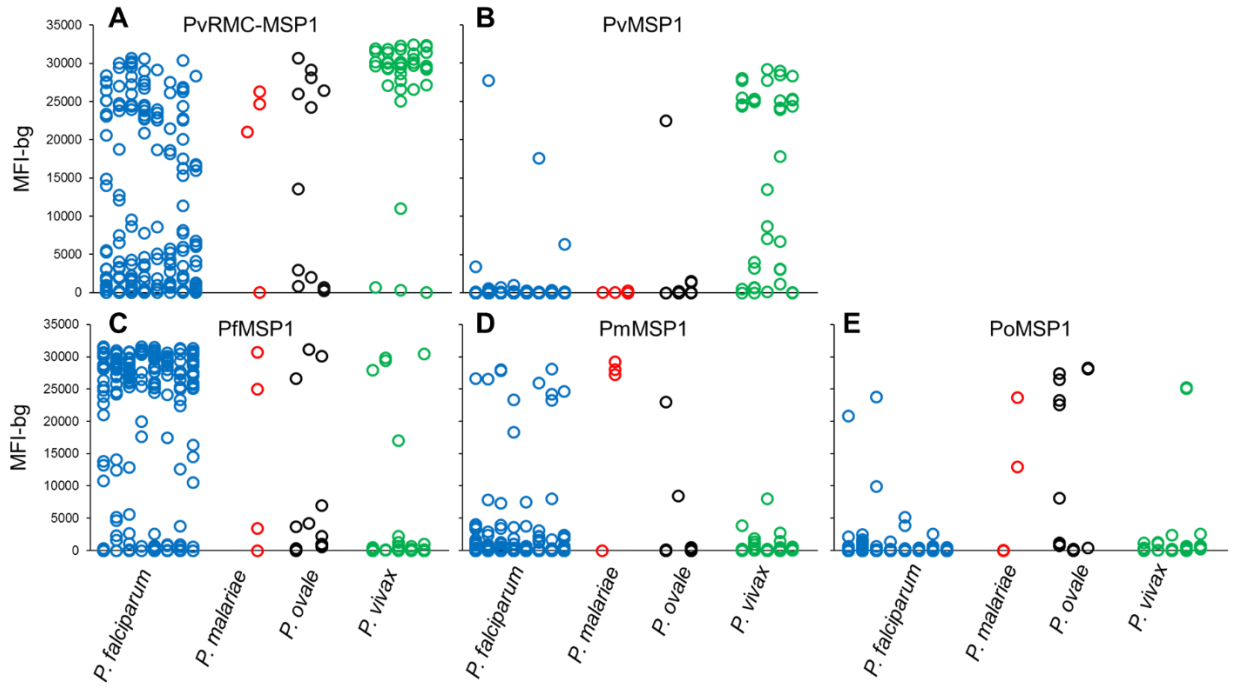


Figure 4. Range of MFI-bg assay signal for PvRMC-MSP1, or the MSP1 19kD malaria antigens when grouped by active infection. Assay signal for IgG binding to particular antigen is shown by each panel: PvRMC-MSP1 (A), PvMSP1 (B), PfMSP1 (C), PmMSP1 (D), PoMSP1 (E). Persons with active malaria infection categorized by infecting species: *P. falciparum* (n=181, blue circles), *P. malariae* (n=4, red circles), *P. ovale* (n=13, black circles), *P. vivax* (n=38, green circles).

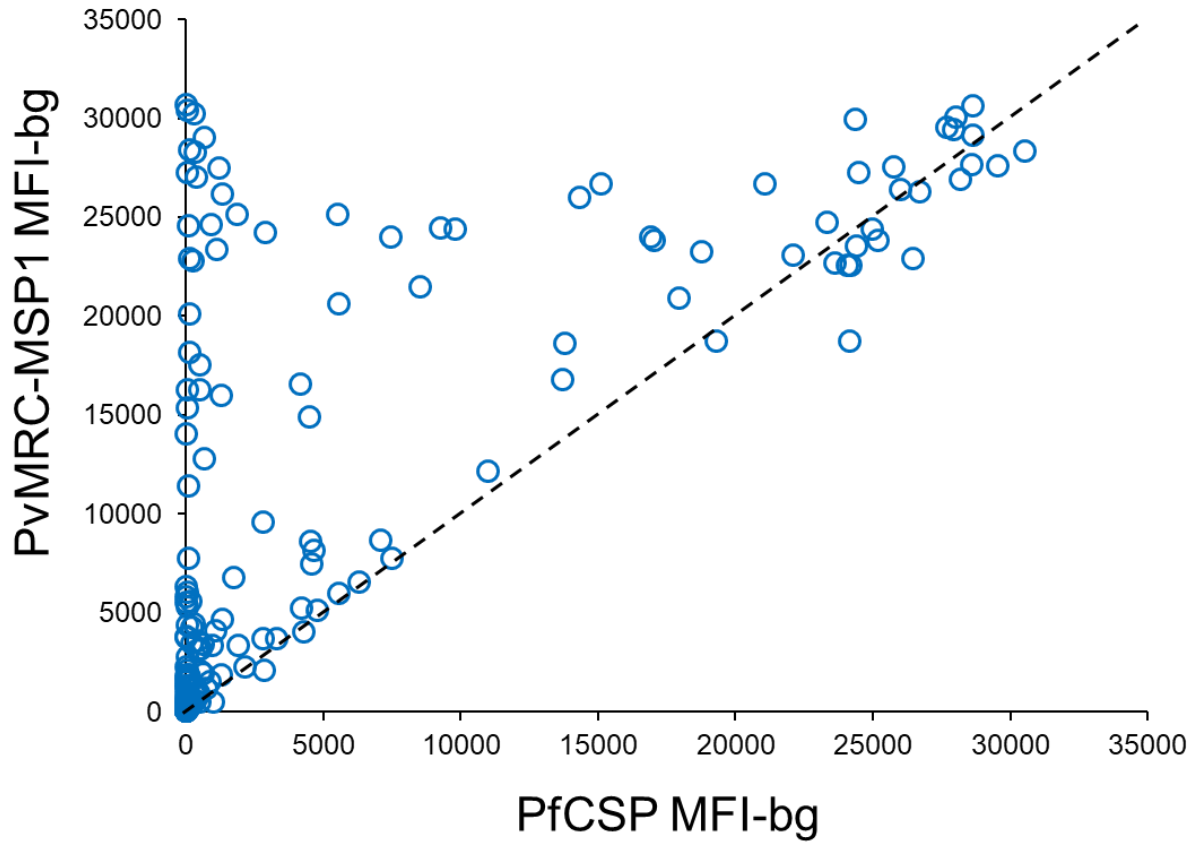
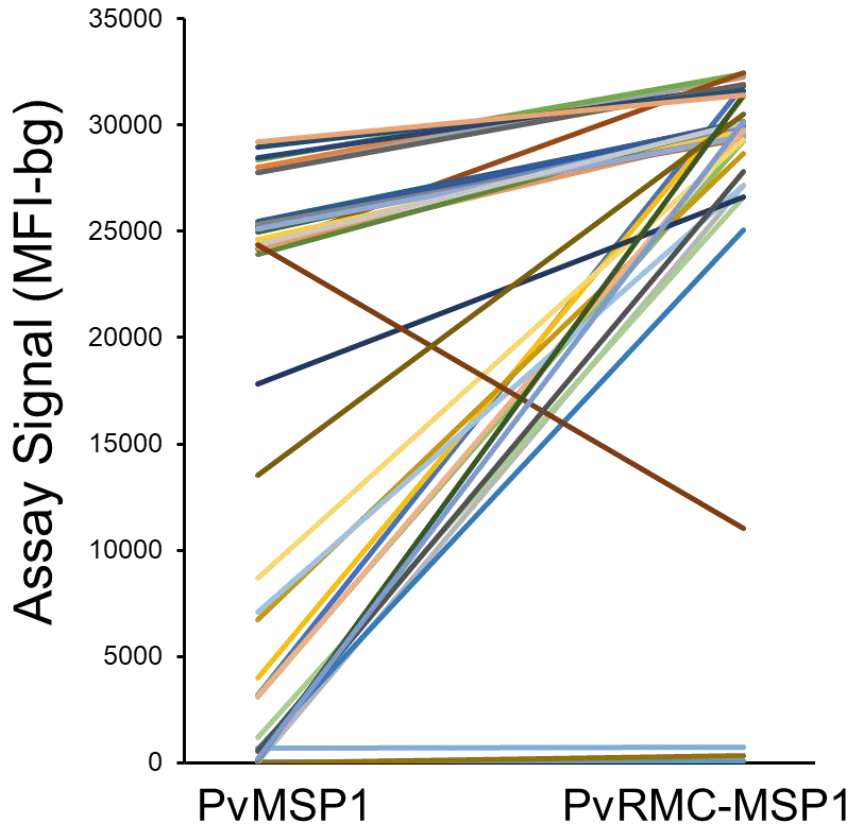


Figure 5. Cross-binding of anti-PfCSP IgG with PvRMC-MSP1. A scatterplot of PfCSP signal in comparison with PvRMC-MSP1 for the 181 persons with *P. falciparum* infection. The dashed reference line shown as $y=x$.



Supplementary Figure 1. Recognition of recombinant PvMSP1 and PvRMC-MSP1 by individual *P. vivax* patients. Assay signals for individual patients are plotted as MFI minus background for both *P. vivax* MSP1 antigens tested. Each colored line represents the change in signal between antigens for a single patient.

Chapter 6

Discussion and Future Directions

Summary of Work

The work presented in this dissertation focuses on two major areas. First, the use of a simian adenovirus vector, SAd36, to improve the immunogenicity of chimeric protein-based malaria vaccines (250, 304). Secondly, the use of a chimeric *P. vivax* MSP1 protein to act as a carrier protein for a transmission-blocking vaccine (351) and as a target for the development of a tool for serological surveys in endemic areas of malaria. Here we summarize the major findings from the work we presented here, as well highlight the progress made in these areas since our initial publications.

We conducted dose-escalation experiments in mice using the simian adenovirus 36 (SAd36) vector which included a transgene for our *P. yoelii* chimeric modular protein, consisting of a chimeric *P. yoelii* circumsporozoite protein linked to a chimeric merozoite surface protein 1 (90). Doses of 10^6 , 10^7 , and 10^{10} vp of SAd36 were compared to the recombinant human Ad5 encoding the same transgene given at a pre-standardized dose of 10^7 . Mice received priming immunizations at day 0 with one dose of either SAd36-PyCMP or Ad5-PyCMP and two protein boosts with the PyCMP protein at days 30 and 60. A control group of mice receiving no immunizations was included, as we had previously found no differences between mice receiving adjuvant or no immunization. We sought to determine if we could induce similar, or improved, immune response to the PyCMP protein using the simian adenoviral vector as previous studies have indicated that the adult human population harbor high prevalence of pre-existing immunity to Ad5 (235), which would limit the utility of this vector in future studies (208).

When we assessed the number of PyCMP-specific T cells obtained after the final immunization, we found that all immunization regimens induced significantly higher numbers of tetramer specific cells when compared to naïve animals, with the highest number of tetramer specific cells observed in the SAd36 10^{10} group. We assessed of the ability of T cells to produce cytokines after stimulation with peptide pools representing the PyCMP protein and found that T cells from mice immunized with the SAd36 10^{10} regimen produced significantly higher levels of IFN- γ in comparison with the other SAd36

immunization regimens and the Ad5 10^7 regimen. When we assessed the shift in the pre-patency period after experimental challenge, where the parasite has not yet transitioned from the liver to erythrocytic stage, we found that mice immunized with the SAd36 10^{10} regimen had significantly longer pre-patency period, suggesting that immunization was able to reduce parasite load and development prior to the erythrocytic stage. Based on these results, we continued to explore further the potential of using the SAd36 vector for malaria vaccine development.

To follow up this work, we aimed to determine if we could improve the immunogenicity of the SAd36 vector through the addition of a signal peptide derived from the murine IgG κ light chain. We compared the immunogenicity of the SAd36 vector with a Signal Peptide (SP-SAd36) at a dose of 10^8 vp, which we selected based on the previous publication to provide the optimal balance of immunogenicity (250). Both vectors included a transgene encoding a multi-stage chimeric *P. vivax* protein designated PvCMP that contains a chimeric *P. vivax* circumsporozoite protein genetically linked to a chimeric *P. vivax* merozoite surface protein 1, which is the *P. vivax* ortholog of the *P. yoelii* chimeric modular protein assessed previously (PyCMP). The signal peptide was included at the 5' end of the PvCMP protein and inserted into an E1 (replication-deficient) SAd36 genome. Mice were immunized with either the SAd36 or SP-SAd36 vectors intramuscularly at day 0 and boosted twice with the mixture of proteins at days 20 and 40. A group of unimmunized mice was included as a control.

When we compared the avidity of antibodies induced by the two vectors, we found that the SP-SAd36 vectored group induced antibodies of significantly higher avidity indices against both the cPvCSP and cPvMSP1 components of PvCMP compared to the SAd36 vectored group. Assessment of the ability of T cells obtained after the final immunization to produce cytokines was done following stimulation with peptide pools representing either cPvCSP or cPvMSP1. We found that CD4 $^+$ and CD8 $^+$ T cells obtained from mice immunized with the SP-SAd36 regimen produced higher levels of IFN- γ and IL-2 compared to the SAd36 regimen. Furthermore, we found that immunization with SP-SAd36 resulted in increased

frequency and number of germinal center B cells post priming as compared to unvaccinated mice, which we did not observe for the SAd36 primed mice. Based on this data, we have continued to include the murine IgGκ light chain signal peptide in the vectors we test for immunization.

Following this work, we tested whether the chimeric *P. vivax* MSP1 protein (cPvMSP1), which was part of the combined PvCMP protein that we assessed as part of the SP-SAd36 immunization regimen (304), could be used as a carrier protein for the transmission-blocking vaccine candidate *P. vivax* P25 (Pvs25). We compared the immunogenicity of this multi-stage transmission-blocking candidate cPvMSP1-Pvs25 to that of the recombinant Pvs25 protein alone in both mice and rabbits using the homologous prime-boost approach at 20-day intervals.

Assessment of the humoral immunogenicity of the two proteins revealed that immunization with cPvMSP1-Pvs25 resulted in significantly higher anti-cPvMSP1-Pvs25 antibody titers at days 20, 40, and 60, corresponding to twenty days after each immunization. When we assessed the longevity of the antibody responses induced by vaccination, we found that the cPvMSP1-Pvs25 group maintained significantly higher antibody titers against the immunogen at two years post-vaccination. Similarly, when we assessed the difference in the anti-Pvs25 antibody responses, we found that mice immunized with cPvMSP1-Pvs25 maintained higher antibody titers at the two-year time point, and had a lower reduction in the anti-Pvs25 antibody avidity and the ratio of cytophilic antibodies.

We further investigated the longevity of the humoral response induced by cPvMSP1-Pvs25 by assessing the number of antibody-secreting cells present in the bone marrow and spleens of mice at two years post-immunization. We observed significantly higher numbers of anti-cPvMSP1, anti-Pvs25, and anti-cPvMSP1-Pvs25 in the bone marrow of mice immunized with cPvMSP1-Pvs25 when compared to Pvs25 immunized mice.

To determine if antibodies induced by immunization with either Pvs25 or cPvMSP1-Pvs25 could block the transmission of *P. vivax* in *Anopheles* mosquitoes, rabbit sera obtained after four immunizations with either protein at 20-day intervals was used for direct membrane feeding assays. We found that sera from both Pvs25 and cPvMSP1-Pvs25 immunized rabbits resulted in significantly lower percentages of infected mosquitoes and lower oocyst numbers when compared to naïve rabbit sera.

During the assessment of the cPvMSP1 protein, we observed high levels of cross-reactivity between antibodies generated against cPvMSP1 and MSP1 proteins derived from other *Plasmodium* species. We aimed to use this feature to test the feasibility of developing a broad yet sensitive serological assay that could be used for determining population-level exposure to *Plasmodium*, providing a useful tool that may provide support for malaria elimination campaigns.

There are four main *Plasmodium spp.* that infect humans, which are *P. falciparum*, *P. vivax*, *P. malariae*, and *P. ovale*. *P. falciparum* causes the most significant number of malaria cases globally and is the predominant species in sub-Saharan Africa. However, in several African nations, including Ethiopia, *P. falciparum* and *P. vivax* are both endemic. In addition, a limited number of patients are also infected with *P. malariae* and *P. ovale*. Prevalence of exposure to these malaria parasites and parasite transmission dynamics can be determined from serological data. Together with the Malaria Branch at the CDC, we tested cPvMSP1 in multiplex assays to test the potential of using it as a biomarker to determine rates of exposure to *Plasmodium* infections. We determined that individuals infected with any of these four human *Plasmodium* species display high cross-reactivity to cPvMSP1, making it useful for surveillance in areas where multiple species are endemic.

Our lab has already reported the sequence and schematic of our chimeric *P. vivax* MSP1 protein (cPvMSP1). Alignment of the five promiscuous T cell epitopes and the *P. vivax* MSP1₁₉ kD fragment included in our chimeric protein with the orthologous sequences of the four main *Plasmodium* species revealed between 35% and 85% identity between the orthologous sequences. We observed the highest

conservation of identity between the third cPvMSP1 T cell epitope and orthologous sequences of the other *Plasmodium* species with identity values ranging between 75%-85%. Using rabbit and mouse sera raised against cPvMSP1 protein, we determined the extent of antibody cross-binding to MSP1 derived from the four *Plasmodium spp.* via a multiplex bead assay. Additional *P. falciparum* antigens other than MSP1 and several non-*Plasmodium* proteins were included to determine the specificity of the anti-cPvMSP1 antibodies. All responses were compared with the reactivity to the cPvMSP1 protein. We observed high levels of cross-reactivity with MSP1 across *Plasmodium spp.* Relevantly, we also determined that anti-cPvMSP1 antibodies were able to cross-react with *P. falciparum* parasites derived from culture via immunofluorescence assays.

Using blood spots obtained from US travelers with active malaria infection, we compared the multiplex bead assay signal against the cPvMSP1 protein against the MSP1 derived from the four human *Plasmodium* species. We observed high levels of binding to cPvMSP1 protein when compared to reactivity to all four MSP1 proteins tested. When we grouped the patients based the parasite responsible for active infection, we observed high reactivity to both the cPvMSP1 protein and the MSP1 derived from the species responsible for the active infection.

We then used this data to determine the population-level responses to the PvMSP1 protein compared to *P. falciparum* MSP1 and *P. vivax* MSP1 as a way to determine when the patients were likely to have seroconverted to produce anti-PfMSP1 or anti-PvMSP1 antibodies. Our model suggests that individuals become positive to cPvMSP1 protein sooner than they do for the native PfMSP1 and PvMSP1 proteins, suggesting that this assay may be more sensitive at detecting seroconversion in children. However, if we look at the proportion of individuals seropositive for PfMSP1, PvMSP1, and the chimeric PvMSP1, we observed higher signal for PfMSP1, which is expected given that there are higher incidences of *P. falciparum* infection in this population.

We were also able to generate additional cross-binding figures between the PfCSP NANP repeat region, which is present in cPvMSP1. We observed higher reactivity to the cPvMSP1 than to the repeat region, suggesting that the cross-reactivity we observed is to the conserved nature of the PvMSP1 T cell epitopes and not due to the presence of the *P. falciparum* NANP repeat region.

Overall, these data demonstrate that our cPvMSP1 protein may serve as a valuable tool to conduct malaria surveillance studies in areas that are endemic for multiple *Plasmodium* species due to the high levels of cross-reactivity observed and the ability to detect seroconversion in young patients sooner in comparison to assessment using the native antigens.

Overall, these results suggest that adenoviral vectors, carrier proteins, transmission-blocking vaccines, and serological means of measuring malaria transmission warrant further investigation. Numerous articles have been published in these areas since our studies were conducted. To better understand the potential of these approaches in vaccinology and malaria control, we have highlighted the most relevant findings here.

Simian adenoviral vectors, resistant to pre-existing immunity observed for the human adenovirus serotype 5 vector, elicit robust cellular immunity to malaria vaccine candidates

We have shown that a simian vector, SAd36, can be used to induce comparable or improved CD8+ T cell responses when compared to the human adenovirus serotype 5 that is often used as a standard for adenoviral vector studies. Since the publication of our findings, a number of reports have been published on adenoviral based malaria vaccine candidates have been developed, some of which have progressed to clinical trials.

The chimpanzee adenovirus serotype 63 (ChAd63) is the most closely related ape adenovirus to SAd36 (208). This vector has also frequently been used for the delivery of malaria vaccine candidates. In

a phase I study evaluating the safety and immunogenicity of a ME-TRAP (Multiple epitope thrombospondin adhesion protein) vaccine candidate delivered via ChAd63 prime and MVA boost, adjuvanted with Matrix-M (352), the authors aimed to determine if this formulation could be used to elicit humoral responses as well as T cell responses. The vaccine was reported to be safe and well-tolerated, while also eliciting high T cell responses that were durable and well maintained at six months post-immunization. Responses were found to be significantly improved with the addition of Matrix-M, suggested that an adjuvant will be required to achieve the level of CD8⁺ T cells producing IFN- γ required for protection from infection (352).

Following these reports, the ChAd63 MVA ME-TRAP vectored malaria vaccine underwent its first field assessment in the malaria-endemic nation of Burkina Faso in over 700 infants and children in a phase IIB trial (4). Previous Phase IIa trials in the UK were found to induce approximately 35% protection following sporozoite challenge. As before, a heterologous prime-boost regimen consisting of ChAd63 and MVA was used to deliver ME-TRAP. These vectors were again found to be safe and immunogenic but unfortunately were only able to induce moderate T cell responses in the children as compared to the robust responses previously observed for adults, with no efficacy observed during the trial period (4). These results highlight both the promise of simian adenoviral vectors for use in clinical trials and the importance of inducing robust immune responses in children, who account for over 70% of malaria deaths annually (1).

In addition to the assessment of ChAd63-MVA delivery of ME-TRAP alone, there have also been attempts to combine this regimen with the most advanced malaria vaccine candidate, RTS,S/AS01B (353). The ChAd63 and MVA vectors were used to assess a combined multi-stage malaria vaccine based on ME-TRAP delivered concomitantly with RTS,S/AS01B in malaria naïve adults (353). While no safety concerns arose during the study, vaccine efficacy following controlled human malaria infection (CHMI) was found to be 60% in individuals receiving three RTS,S/AS01B immunizations concomitantly with the

SAd63 prime and two MVA boosts, as compared to the 75% efficacy achieved for the standard three-dose RTS,S/AS01B regimen. The authors concluded that this reduction in immunogenicity and efficacy indicates that other immunization schedules should be tested. The authors also suggested that the decrease in efficacy may be the result of antigen interference as individuals in the concomitant vaccination group received not only the hepatitis B surface antigen and the NANP repeats and T cell epitopes of CSP included in RTS,S, but also ME-TRAP as well as the surface antigens of the ChAd63 and MVA vectors (353).

Beyond the use of ChAd63 in heterologous prime-boost regimens with MVA for delivery of ME-TRAP, ChAd63 has also been used to deliver the *P. falciparum* vaccine candidate reticulocyte-binding protein homolog 5 (RH5) in a phase IA clinical trial (354). This study found that ChAd63 induced substantial RH5-specific antibodies in malaria naïve adults, which were significantly higher than the serum antibody responses observed in African adults following years of repeated malaria exposure. These data further demonstrate the robust immunogenicity of this simian vector. In another recent murine study, ChAd63 was also recently found to induce *Plasmodium*-specific tissue-resident memory (T_{RM}) cells in the liver following intramuscular prime and intravenous boosting in mice, which conferred 100% sterilizing protection upon assessment with antigen matched transgenic sporozoite challenge (66). These results are significant as this T_{RM} cells have recently been identified as essential for protection against liver-stage malaria after vaccination protection from malaria (60, 66).

Simian adenoviruses have also been used for the assessment of immunogenicity of other *P. vivax* CSP candidates in mice. Following our report, initial immunogenicity assessment of an adenoviral prime, protein boost immunization based on *P. vivax* CSP delivered via the chimpanzee adenovirus serotype 68, was carried out in mice (355). Unlike *P. falciparum* CSP, which has one allelic variant in the central repeat region, there are three allelic variants in the CSP central repeat region of *P. vivax*. To account for these allelic differences, we have previously described the inclusion of alleles from the VK247 and

VK210 type repeat sequences into our chimeric *P. vivax* CSP construct (86, 304). The CSP candidate assessed in the AdC68 study also accounted for allelic diversity by including the VK210 and VK247, as well as the *P. vivax*-like allele into the recombinant CSP protein. This study found that when administered with the adjuvant Poly(I:C), priming with AdC68 and boosting with protein generated high titers of CSP allele-specific IgG antibodies. Upon infectious challenge with either VK210 or VK247 transgenic *P. berghei* parasites, this vaccine formulation was able to delay parasitemia in all mice (355). These results further support the use of both simian adenoviruses, as well as protein constructs accounting for *P. vivax* allelic diversity, for the generation of an efficacious universal *P. vivax* malaria vaccine.

Overall, these recent clinical trials including ChAd63 and the initial immunogenicity assessment of the AdCh68 vector to deliver a “universal” *P. vivax* CSP candidate similar to our cPvCSP protein, provide further support for the continued assessment of the SAd36 vector and similar simian adenoviral vectors to induce robust CD8+ T cell responses to malaria antigens. Furthermore, the high level of similarity between the SAd63 and SAd36 vectors (208), as well as recent reports that ChAd63 immunization can be used to elicit *Plasmodium*-specific T_{RM} responses in the liver which were found to provide sterilizing protection in mice (66) supports additional assessment of the SAd36 vector for the delivery of malaria vaccine candidates.

Adenoviral vector modifications to alter antigen processing or to target specific cells for enhancing vaccine immunogenicity

In our study on the effect of the incorporation of a murine IgG κ signal peptide into the SAd36 adenoviral transgene, we observed significantly improved cytokine production by CD4+ T cells. Although the use of signal peptides to improve viral vectored vaccines is still relatively new, there have been recent reports on the use of signal peptides to alter the post-translational processing of recombinant proteins as well as to incorporate peptides with adjuvant properties directly into the adenoviral transgene

(356, 357). Together these studies highlight the potential of further studies aimed at tailoring adenoviral vectors using exogenous peptides to produce more immunogenic and efficacious vaccines.

A recent study by Karyolaimos et al. (356) screened a panel of signal peptides to determine the optimal conditions for the production of a recombinant protein containing multiple disulfide bonds using *E. coli*. Recombinant proteins containing disulfide bonds are often targeted to the periplasm of *E. coli* for processing, but the presence of different signal peptides can affect the production rate as well as protein yields. Incorporation of a single-chain antibody fragment, BL1, or human growth hormone, hGH, were found to significantly improve yields of correctly folded and active proteins (356). These results are particularly relevant as improperly folded proteins cannot be used for vaccination studies as the conformational epitopes present in the native protein will likely be altered or absent. While incorrectly folded proteins isolated from *E. coli* can be refolded *in vitro*, adenoviral transgenes need to be able to produce high levels of correctly folded proteins. Understanding the effect of signal peptides on protein production in various systems ranging from *E. coli* to transfected mammalian cells will allow for the selection of optimal conditions for the production of recombinant proteins for vaccination.

In addition to the inclusion of signal peptides into the adenoviral transgene, it has recently been reported that adjuvants can be incorporated into the adenoviral transgenes encoding *P. falciparum* antigens (357). Fougereux et al. (357) used the MHC class II invariant chain (Ii), which has been shown to act as an adjuvant by enhancing the T cell response to tethered antigens, to enhance the immune responses to two CIDRa1.1 domain variants from *P. falciparum* erythrocyte membrane protein 1 (PfEMP1) encoded within the adenoviral transgene. Inclusion of the Ii adjuvant was found to improve antigen secretion in African green monkey cells and acted as an adjuvant for both MHC class I and II presentation to T cell hybridomas *in vitro*. When the Ii modified vectors were tested in mice, accelerated and enhanced antibody responses specific for the CIDR antigens was observed. The breadth of the antibody responses to the encoded antigens was also found to be increased (357). These data suggested

that selection of the optimal targeting molecule, such as Ii, can promote the secretion of the protein encoded by the transgene, improve both the CD4⁺ and CD8⁺ T cell response by acting as a T cell adjuvant, while also inducing robust antigen-specific antibody responses, potentially improving the protective efficacy of the vaccine.

Based on these findings, incorporation of adjuvants and signal peptides into adenoviral transgenes may offer a way to produce tailored vectors and therefore warrants further investigation.

***Plasmodium* chimeric proteins incorporating several promiscuous T helper epitopes can be used as carrier proteins to improve the immunogenicity against the linked antigen**

We have highlighted both the promise of transmission-blocking vaccines and challenges faced in the development of these vaccines previously. Briefly, transmission-blocking malaria vaccines rely on generating antibody responses to mosquito stage antigens in order to block the development and transmission of *Plasmodium* within the vector upon uptake of antibodies during a blood meal. In order for transmission-blocking vaccines to be effective, induction of long-lived plasma cells (LLPCs) to maintain protective antibody responses lasting several transmission seasons will likely be required. Currently, clinical trials of the Pfs25/Alhydrogel vaccine candidate have not been able to elicit the antibody titers to provide long-lasting transmission-blocking activity (315).

Initial studies aimed at determining the optimal carrier and adjuvant protein to induce anti-Pfs25 long-lived antibody responses found that both carrier proteins and adjuvants can influence the magnitude of the anti-Pfs25 antibody response. Using an adjuvant-carrier protein combination with either the adjuvants QS21, a liposomal adjuvant, or GLA-LSQ, a TLR4 agonist, and the carrier proteins exoprotein A or tetanus toxoid conjugated to recombinant Pfs25 resulted in the induction of T follicular helper cells and LLPCs specific for Pfs25 in immunized mice (295). Similarly, a carrier protein based on MSP8 has

also been used to improve the immune response to the *P. falciparum* transmission-blocking vaccine candidate Pfs25 (297). In this study, conjugation of recombinant MSP8 with recombinant Pfs25 induced high titers anti-Pfs25 specific IgG antibodies in rabbits. These antibodies were also able to recognize the native structure of Pfs25 and reduce transmission (297). Both of these studies suggested that the presence of CD4+ T cell epitopes within the highly immunogenic carrier proteins was responsible for promoting improved humoral responses through the recruitment of CD4+ T cells. The results of our assessment of the chimeric *P. vivax* MSP1 carrier protein linked to Pvs25 provide further support to this claim as cPvMSP1 is composed of five promiscuous T cell epitopes and the MSP1₁₉ kD fragment (351).

In a more recent report, Scaria et al. demonstrate that the outer membrane complex protein from *Neisseria meningitidis*, OMPC, can act as a carrier protein for another *P. falciparum* transmission-blocking antigen, Pfs230 (358). This combination was found to be highly immunogenic and was able to skew the T cell response to a robust Th1 phenotype, resulting in the production of high levels of IgG2 antibodies (358). This is particularly relevant for targeting Pfs230 as these antibodies can induce complement activation and contribute to the more efficient killing of *Plasmodium* parasites within the mosquito midgut.

Overall, the use of various carrier proteins has been found to improve the immune responses induced in vaccinated animals over recombinant transmission-blocking antigens alone. It is likely that similar formulations will improve the outcomes of future clinical trials of transmission-blocking vaccine candidates.

The feasibility of introducing transmission-blocking vaccines as a tool for malaria control and potential elimination

Pre-clinical studies on the effects of the use of carrier proteins to elicit improved responses to transmission-blocking antigens have shown promise. However, the success of transmission-blocking vaccine candidates depends on their ability to induce robust and durable antibodies responses with a transmission-blocking activity that reduce the transmission of malaria in the community.

Currently, the most advanced transmission-blocking vaccine candidate, Pfs25-EPA/Alhydrogel, has been tested in phase I clinical trials in malaria naïve adults (315). This vaccine was found to be safe and well-tolerated at all doses tested while also inducing higher antibody titers of higher avidity upon boosting immunizations that demonstrated transmission-blocking activity in standard membrane feeding assays. However, even at the highest dose, the mean antibody levels induced were modest after four vaccinations, and antibody titers returned to baseline levels by one year. Further improvements to transmission-blocking vaccine candidates will likely be required to induce durable high antibodies titers, and assessment of the effect of these antibodies on transmission in endemic areas (315).

Two reviews have recently discussed the feasibility of deploying a transmission-blocking vaccine in endemic areas. A recent review by Acquah et al. (359), highlights that the inability of first-line antimalarial drugs to eliminate late-stage gametocytes allows patients receiving treatment to remain infectious for more than a week post-treatment, contributing to further malaria transmission. To address this gap in malaria intervention, new tools such as transmission-blocking vaccines may offer a way to prevent transmission within a vaccinated community. The transmission-blocking antibodies induced by transmission-blocking vaccines is often measured using standard membrane feeding assays (359). However, in addition to antibodies, other immune components from the host are also taken up by the female *Anopheles* mosquito during a blood meal and remain active for several hours while in the mosquito midgut, including lymphocytes, cytokines, complement proteins, and reactive oxygen species

(360). Complement components have been found to be a critical factor of transmission reducing activity, including for anti-Pfs230 transmission-blocking antibodies (150). As a result, the role of complement needs to be considered in the search for ideal transmission-blocking antibody and accounted for *in vitro* assessments of efficacy such as membrane feeding assays.

Another recent review by Coelho et al. (361) has highlighted some of the logistical, educational, and ethical concerns that will likely be faced by transmission-blocking vaccines when they are introduced in large endemic populations. The first consideration is that a vaccine with only transmission-blocking vaccine component will be an altruistic intervention, providing a reduction in incidence to the community based on herd immunity. Due to the reliance on herd immunity, high levels of vaccine uptake will be required (361). A study conducted last year in the Peruvian Amazon in a community where over 90% of the community has had exposure to *Plasmodium*, found that 99.3% of mothers expressed willingness to be vaccinated with a transmission-blocking vaccine and 90% approved of allowing their children to receive a TBV vaccine (362). However, the authors suggest incorporating a new vaccine into existing childhood vaccine infrastructure will likely be required to reach vaccination rates high enough to reduce transmission (361).

Another issue that will hinder transmission-blocking vaccine uptake will be the price paid for vaccines. In the same study looking at the malaria-endemic region of the Peruvian Amazon, less than two-thirds of those interviewed would pay for their own vaccine if the price was less than \$2. However, according to the Vaccine Alliance partnership, the average price paid for vaccines per child by the government was between \$3.80 to \$5 (362). Based on this information, governments will need to be willing to assume the cost in order to ensure that there is sufficiently high uptake within the community. Otherwise, the transmission-blocking vaccine will not be effective. Issues such as political instability, conflict, and human migration of vulnerable populations will further complicate the task of vaccinating endemic populations (362).

While these reviews agree that transmission-blocking vaccines offer a promising strategy to achieve malaria control through interruption of transmission, their enthusiasm is tempered by the numerous challenges that face the development and deployment of future transmission-blocking vaccines. These concerns will need to be addressed by future studies in order to obtain an effective transmission-blocking vaccine.

Serological surveys to determine malaria exposure can support malaria elimination campaigns and monitor changes in transmission intensity at the population level

In this past year, there have been numerous studies employing serological assays to aid in malaria elimination efforts. An assessment of asymptomatic *Plasmodium* infections using both PCR and serological assays was recently conducted in the Atlantic Forest region of Brazil, which is considered an area of interrupted transmission as malaria cases are only occasionally reported among visitors in the area (363). Of the 324 individuals recruited for this study, only 2.8% of individuals had *Plasmodium* infections detectable by PCR. When serological assessments were carried out in 314 of these patients, 11.1% of individuals were found to be reactive to *Plasmodium* antigens (363), demonstrating how population-based studies relying on PCR miss a large number of cases in low endemic regions.

In a similar community-based study in Indonesia, a serological analysis was used to determine the heterogeneity of malaria transmission (364). Seroconversion rates were estimated for a population of 1624 individuals from 605 households in the Sabang region using filter paper blood spots and epidemiological data. In this study, the seroprevalence for *P. falciparum* antigens was determined to be 6.9%, while seroprevalence for *P. vivax* antigens was determined to be 2.0%. The authors concluded that this information could aid in malaria monitoring and surveillance in other low transmission areas of Indonesia (364).

Within the past decade, Ethiopia has completed a successful malaria control campaign and is now focusing on elimination efforts in selected low-transmission regions. To aid in these efforts, a cross-sectional study by Keffale et al. used serological assays to determine the prevalence of antibodies reactive to *P. falciparum* and *P. vivax* antigens in 1135 individuals living in the Babile district of Oromia, Ethiopia (365). They found that malaria seroconversion curves had declined from records obtained 15 and 11.5 years prior, and that antibody titers were higher in adults than in children for both *P. falciparum* and *P. vivax*. However, 5.1% and 3.6% of individuals were positive for *P. falciparum* and *P. vivax* by PCR, leading the authors to argue for continued and tailored efforts to eliminate malaria in this region (365).

In a protein microarray study by Kobayashi et al. aimed at assessing malaria transmission in low incidence settings in Zambia and Zimbabwe, it was determined that while antibody signals and transmission intensity in adults showed little correlation, children less than five years of age showed a clear correlation between these two measurements (366). The authors concluded that seroprevalence studies in children could be useful for determining malaria elimination progress as serological studies in children could provide information on recent levels of transmission activity compared to the durable antibody responses observed in adults.

In addition to determining previous malaria exposure, serological assays have also been applied to determine if serological markers are associated with functional antibodies capable of inhibiting parasite growth (367). In a study by Achan et al., two groups of adults with high or low serological evidence of exposure volunteered to undergo controlled human malaria infection with *P. falciparum* sporozoites. All ten of the volunteers with low serological evidence of exposure, and 7 out of 9 of those with high serological evidence of exposure became infected as detected by blood smear. However, individuals with high serological evidence of previous malaria exposure showed significantly higher antibody recognition of sporozoites, anti-blood stage antibodies, and growth inhibitory activity when compared to individuals with low serological evidence of exposure. Individuals with high serological evidence of exposure were

also able to control infection better, showing lower parasite counts, fewer symptoms of malaria infection, and less severe symptoms overall (367). It is possible that similar studies may be able to determine an individual's risk for developing severe disease, providing valuable information regarding correlates of protection from malaria.

Overall, serological studies have been used in a range of applications. Serological assessments have continued to be useful in different stages of malaria elimination campaigns, from studies aimed at determining transmission intensity of multiple *Plasmodium spp.* in lower endemic countries beginning elimination campaigns (364) to monitoring low transmission areas in countries that have already eliminated transmission in large portions of the respective country (365). Newer studies have recently used serology to stratify responses based on age to better determine the kinetics of recent transmission in children (366) and have demonstrated that adults with high levels of serological markers of previous malaria exposure are better protected from severe disease (367). Based on these reports, it is likely that improvements in serological studies will provide valuable information that may further aid malaria elimination campaigns.

Future Directions

In summary, we have demonstrated that the simian adenovirus 36 vector can be used in place of the human Ad5 vector to which there are high levels of pre-existing immunity without compromising T cell immunogenicity (250). Furthermore, we established that the addition of a signal peptide sequence within the adenoviral transgene can improve the CD4⁺ T cell immune responses and associated cytokine production induced by vaccination in response to the encoded antigen (304). Simian adenoviral vectors have continued to show promise for induction of protective T cell responses in preclinical studies and clinical trials, often as part of heterologous prime-boost immunization regimens consisting of two

different viral vectors (66, 352, 353, 368). Heterologous prime-boost immunization regimens are seen as attractive for malaria vaccine candidates as they can be used to improve the breadth of the T cell responses prior to protein-boosting to elicit high antibody titers that can provide further protection from malaria (93, 250). However, the use of the adenovirus vectors can lead to the induction of anti-vector antibodies that could reduce the efficiency of a subsequent boost with the same vector (93).

To further explore the ability of adenoviral vectors to induce robust T cell responses, we have begun the assessment of heterologous adenoviral immunization regimens in mice incorporating the SAd36 vector and the chimeric recombinant human Ad5/3 vector, which we have previously described (93). We sought to determine the ability of heterologous adenoviral regimens that include two different adenoviruses to induce robust T cell responses and provide protection from infectious challenge. Our initial results suggest that mice immunized with heterologous adenoviral regimens significantly improve the cytokine production by antigen-specific CD4⁺ and CD8⁺ T cells compared to protein immunized and unvaccinated mice. Relevantly, heterologous adenoviral immunized mice were also able to achieve sterilizing protection against transgenic *P. berghei* infectious challenge. Future studies will further define the effector mechanisms involved in the protection induced by this regimen, as well as the durability of protection.

In addition to our studies on heterologous prime-boost immunization regimens including SAd36, we have further explored the properties of the chimeric *P. vivax* MSP1 protein, cPvMSP1. We have already demonstrated that cPvMSP1 is able to function as an effective carrier protein for the poorly immunogenic *P. vivax* transmission-blocking antigen Pvs25, improving overall antibody responses, durability, and induction of long-lived plasma cells (351). We have shown that antibodies able to bind cPvMSP1 could be used as serological biomarkers of exposure to *P. vivax* using samples from US travelers. Due to these features, the cPvMSP1 is a potentially sensitive malaria serological tool that could be used to determine exposure history and population-level seroconversion in endemic areas. To test this hypothesis, we have

used the large dried blood spot sample bank available at the CDC to determine reactivity to cPvMSP1 using samples from two distinct populations. For these studies, 8,944 samples from Ethiopia, where all four main *Plasmodium* species are endemic, and 852 samples from Costa Rica, where *P. vivax* is endemic, and *P. falciparum* has recently been eliminated were used (manuscript in preparation). Among Ethiopian volunteers, patients below the age of 10 showed higher assay signals to cPvMSP1 than either the recombinant PfMSP1 or PvMSP1 antigens and demonstrated faster seroconversion. Additionally, the seroprevalence of antibodies that recognize cPvMSP1 remained high in adult patients, suggesting that cPvMSP1 may be able to estimate malaria transmission overall in co-endemic areas. In Costa Rica, we found a higher seroprevalence for antibodies recognizing cPvMSP1 at all age ranges. We also found that the use of recombinant PfMSP1 showed low recognition in individuals under 20 years of age, but adults above this age range had varied responses indicating historic *P. falciparum* transmission in this region. Based on our current findings, we predict that the use of tailored serological assays that improve the sensitivity of the current serological surveys could provide more accurate measurements of malaria transmission in low endemic settings and better inform future elimination campaigns.

In conclusion, the work presented here on the use of simian adenoviral vectors to induce robust antigen-specific T cell responses and the ability of a chimeric antigen to serve as both a protein carrier and a sensitive tool for the development of accurate serological marker for community-based seroepidemiological surveys have contributed to the fields of malaria vaccinology and malaria epidemiology. We hope that these findings will further support malaria elimination efforts.

Chapter 7

References

1. WHO. World Malaria Report 2018. Geneva: World Health Organization; 2018.
2. Lamb TJ. Immunity to parasitic infections. Chichester, West Sussex, UK: Wiley-Blackwell; 2012. xvi, 500 p. p.
3. Perkins SL, Schall JJ. A molecular phylogeny of malarial parasites recovered from cytochrome b gene sequences. *J Parasitol.* 2002;88(5):972-8. doi: 10.1645/0022-3395(2002)088[0972:AMPOMP]2.0.CO;2. PubMed PMID: 12435139.
4. Rosenberg R, Wirtz RA, Schneider I, Burge R. An estimation of the number of malaria sporozoites ejected by a feeding mosquito. *Trans R Soc Trop Med Hyg.* 1990;84(2):209-12. PubMed PMID: 2202101.
5. Menard R. Gliding motility and cell invasion by Apicomplexa: insights from the Plasmodium sporozoite. *Cell Microbiol.* 2001;3(2):63-73. PubMed PMID: 11207621.
6. Stewart MJ, Vanderberg JP. Malaria sporozoites release circumsporozoite protein from their apical end and translocate it along their surface. *J Protozool.* 1991;38(4):411-21. PubMed PMID: 1787427.
7. Stewart MJ, Vanderberg JP. Malaria sporozoites leave behind trails of circumsporozoite protein during gliding motility. *J Protozool.* 1988;35(3):389-93. PubMed PMID: 3054075.
8. Sultan AA, Thathy V, Frevert U, Robson KJ, Crisanti A, Nussenzweig V, Nussenzweig RS, Menard R. TRAP is necessary for gliding motility and infectivity of plasmodium sporozoites. *Cell.* 1997;90(3):511-22. PubMed PMID: 9267031.

9. Vanderberg JP, Chew S, Stewart MJ. Plasmodium sporozoite interactions with macrophages in vitro: a videomicroscopic analysis. *J Protozool.* 1990;37(6):528-36. PubMed PMID: 2086782.
10. Vanderberg JP, Stewart MJ. Plasmodium sporozoite-host cell interactions during sporozoite invasion. *Bull World Health Organ.* 1990;68 Suppl:74-9. PubMed PMID: 2094594; PMCID: PMC2393034.
11. Yang AS, Boddey JA. Molecular mechanisms of host cell traversal by malaria sporozoites. *Int J Parasitol.* 2016. doi: 10.1016/j.ijpara.2016.09.002. PubMed PMID: 27825827.
12. Gueirard P, Tavares J, Thiberge S, Bernex F, Ishino T, Milon G, Franke-Fayard B, Janse CJ, Menard R, Amino R. Development of the malaria parasite in the skin of the mammalian host. *Proc Natl Acad Sci U S A.* 2010;107(43):18640-5. doi: 10.1073/pnas.1009346107. PubMed PMID: 20921402; PMCID: PMC2972976.
13. Amino R, Thiberge S, Martin B, Celli S, Shorte S, Frischknecht F, Menard R. Quantitative imaging of Plasmodium transmission from mosquito to mammal. *Nat Med.* 2006;12(2):220-4. doi: 10.1038/nm1350. PubMed PMID: 16429144.
14. Pasparakis M, Haase I, Nestle FO. Mechanisms regulating skin immunity and inflammation. *Nat Rev Immunol.* 2014;14(5):289-301. doi: 10.1038/nri3646. PubMed PMID: 24722477.
15. Nestle FO, Di Meglio P, Qin JZ, Nickoloff BJ. Skin immune sentinels in health and disease. *Nat Rev Immunol.* 2009;9(10):679-91. doi: 10.1038/nri2622. PubMed PMID: 19763149; PMCID: PMC2947825.
16. Mac-Daniel L, Menard R. Plasmodium and mononuclear phagocytes. *Microb Pathog.* 2015;78:43-51. doi: 10.1016/j.micpath.2014.11.011. PubMed PMID: 25450889.
17. Choumet V, Attout T, Chartier L, Khun H, Sautereau J, Robbe-Vincent A, Brey P, Huerre M, Bain O. Visualizing non infectious and infectious *Anopheles gambiae* blood feedings in naive

and saliva-immunized mice. *PLoS One*. 2012;7(12):e50464. doi: 10.1371/journal.pone.0050464. PubMed PMID: 23272060; PMCID: PMC3521732.

18. Ribeiro JM, Nussenzveig RH, Tortorella G. Salivary vasodilators of *Aedes triseriatus* and *Anopheles gambiae* (Diptera: Culicidae). *J Med Entomol*. 1994;31(5):747-53. PubMed PMID: 7966179.

19. Demeure CE, Brahimi K, Hacini F, Marchand F, Peronet R, Huerre M, St-Mezard P, Nicolas JF, Brey P, Delespesse G, Mecheri S. *Anopheles* mosquito bites activate cutaneous mast cells leading to a local inflammatory response and lymph node hyperplasia. *J Immunol*. 2005;174(7):3932-40. PubMed PMID: 15778349.

20. Hopp CS, Sinnis P. The innate and adaptive response to mosquito saliva and *Plasmodium* sporozoites in the skin. *Ann N Y Acad Sci*. 2015;1342:37-43. doi: 10.1111/nyas.12661. PubMed PMID: 25694058; PMCID: PMC4405444.

21. Mac-Daniel L, Buckwalter MR, Berthet M, Virk Y, Yui K, Albert ML, Gueirard P, Menard R. Local immune response to injection of *Plasmodium* sporozoites into the skin. *J Immunol*. 2014;193(3):1246-57. doi: 10.4049/jimmunol.1302669. PubMed PMID: 24981449.

22. Watanabe H, Numata K, Ito T, Takagi K, Matsukawa A. Innate immune response in Th1- and Th2-dominant mouse strains. *Shock*. 2004;22(5):460-6. PubMed PMID: 15489639.

23. Martinez FO, Gordon S. The M1 and M2 paradigm of macrophage activation: time for reassessment. *F1000Prime Rep*. 2014;6:13. doi: 10.12703/P6-13. PubMed PMID: 24669294; PMCID: PMC3944738.

24. Amino R, Giovannini D, Thiberge S, Gueirard P, Boisson B, Dubremetz JF, Prevost MC, Ishino T, Yuda M, Menard R. Host cell traversal is important for progression of the malaria

- parasite through the dermis to the liver. *Cell Host Microbe*. 2008;3(2):88-96. doi: 10.1016/j.chom.2007.12.007. PubMed PMID: 18312843.
25. Malissen B, Tamoutounour S, Henri S. The origins and functions of dendritic cells and macrophages in the skin. *Nat Rev Immunol*. 2014;14(6):417-28. doi: 10.1038/nri3683. PubMed PMID: 24854591.
26. Bogdan C. Nitric oxide and the immune response. *Nat Immunol*. 2001;2(10):907-16. doi: 10.1038/ni1001-907. PubMed PMID: 11577346.
27. Chakravarty S, Cockburn IA, Kuk S, Overstreet MG, Sacci JB, Zavala F. CD8+ T lymphocytes protective against malaria liver stages are primed in skin-draining lymph nodes. *Nat Med*. 2007;13(9):1035-41. doi: 10.1038/nm1628. PubMed PMID: 17704784.
28. Gazzinelli RT, Kalantari P, Fitzgerald KA, Golenbock DT. Innate sensing of malaria parasites. *Nat Rev Immunol*. 2014;14(11):744-57. doi: 10.1038/nri3742. PubMed PMID: 25324127.
29. Takeuchi O, Akira S. Pattern recognition receptors and inflammation. *Cell*. 2010;140(6):805-20. doi: 10.1016/j.cell.2010.01.022. PubMed PMID: 20303872.
30. Portou MJ, Baker D, Abraham D, Tsui J. The innate immune system, toll-like receptors and dermal wound healing: A review. *Vascul Pharmacol*. 2015;71:31-6. doi: 10.1016/j.vph.2015.02.007. PubMed PMID: 25869514.
31. Prince LR, Whyte MK, Sabroe I, Parker LC. The role of TLRs in neutrophil activation. *Curr Opin Pharmacol*. 2011;11(4):397-403. doi: 10.1016/j.coph.2011.06.007. PubMed PMID: 21741310.

32. Sandig H, Bulfone-Paus S. TLR signaling in mast cells: common and unique features. *Front Immunol.* 2012;3:185. doi: 10.3389/fimmu.2012.00185. PubMed PMID: 22783258; PMCID: PMC3389341.
33. Dasu MR, Ramirez S, Isseroff RR. Toll-like receptors and diabetes: a therapeutic perspective. *Clin Sci (Lond).* 2012;122(5):203-14. doi: 10.1042/CS20110357. PubMed PMID: 22070434.
34. Park JS, Svetkauskaite D, He Q, Kim JY, Strassheim D, Ishizaka A, Abraham E. Involvement of toll-like receptors 2 and 4 in cellular activation by high mobility group box 1 protein. *J Biol Chem.* 2004;279(9):7370-7. doi: 10.1074/jbc.M306793200. PubMed PMID: 14660645.
35. Chen L, Guo S, Ranzer MJ, DiPietro LA. Toll-like receptor 4 has an essential role in early skin wound healing. *J Invest Dermatol.* 2013;133(1):258-67. doi: 10.1038/jid.2012.267. PubMed PMID: 22951730; PMCID: PMC3519973.
36. Menard R, Tavares J, Cockburn I, Markus M, Zavala F, Amino R. Looking under the skin: the first steps in malarial infection and immunity. *Nat Rev Microbiol.* 2013;11(10):701-12. doi: 10.1038/nrmicro3111. PubMed PMID: 24037451.
37. Ying P, Shakibaei M, Patankar MS, Clavijo P, Beavis RC, Clark GF, Frevert U. The malaria circumsporozoite protein: interaction of the conserved regions I and II-plus with heparin-like oligosaccharides in heparan sulfate. *Exp Parasitol.* 1997;85(2):168-82. doi: 10.1006/expr.1996.4134. PubMed PMID: 9030667.
38. Coppi A, Pinzon-Ortiz C, Hutter C, Sinnis P. The Plasmodium circumsporozoite protein is proteolytically processed during cell invasion. *J Exp Med.* 2005;201(1):27-33. doi: 10.1084/jem.20040989. PubMed PMID: 15630135; PMCID: PMC1995445.

39. Hafalla JC, Silvie O, Matuschewski K. Cell biology and immunology of malaria. *Immunol Rev.* 2011;240(1):297-316. doi: 10.1111/j.1600-065X.2010.00988.x. PubMed PMID: 21349101.
40. Frevert U, Usynin I, Baer K, Klotz C. Nomadic or sessile: can Kupffer cells function as portals for malaria sporozoites to the liver? *Cell Microbiol.* 2006;8(10):1537-46. doi: 10.1111/j.1462-5822.2006.00777.x. PubMed PMID: 16911567.
41. Baer K, Roosevelt M, Clarkson AB, Jr., van Rooijen N, Schnieder T, Frevert U. Kupffer cells are obligatory for *Plasmodium yoelii* sporozoite infection of the liver. *Cell Microbiol.* 2007;9(2):397-412. doi: 10.1111/j.1462-5822.2006.00798.x. PubMed PMID: 16953803.
42. Frevert U, Engelmann S, Zougbede S, Stange J, Ng B, Matuschewski K, Liebes L, Yee H. Intravital observation of *Plasmodium berghei* sporozoite infection of the liver. *PLoS Biol.* 2005;3(6):e192. doi: 10.1371/journal.pbio.0030192. PubMed PMID: 15901208; PMCID: PMC1135295.
43. Sinnis P, Coppi A. A long and winding road: the *Plasmodium* sporozoite's journey in the mammalian host. *Parasitol Int.* 2007;56(3):171-8. doi: 10.1016/j.parint.2007.04.002. PubMed PMID: 17513164; PMCID: PMC1995443.
44. Cowman AF, Healer J, Marapana D, Marsh K. Malaria: Biology and Disease. *Cell.* 2016;167(3):610-24. doi: 10.1016/j.cell.2016.07.055. PubMed PMID: 27768886.
45. Orban A, Rebelo M, Molnar P, Albuquerque IS, Butykai A, Kezsmarki I. Efficient monitoring of the blood-stage infection in a malaria rodent model by the rotating-crystal magneto-optical method. *Sci Rep.* 2016;6:23218. doi: 10.1038/srep23218. PubMed PMID: 26983695; PMCID: PMC4794716.

46. Gazzinelli RT, Denkers EY. Protozoan encounters with Toll-like receptor signalling pathways: implications for host parasitism. *Nat Rev Immunol.* 2006;6(12):895-906. doi: 10.1038/nri1978. PubMed PMID: 17110955.
47. Seguin MC, Klotz FW, Schneider I, Weir JP, Goodbary M, Slayter M, Raney JJ, Aniagolu JU, Green SJ. Induction of nitric oxide synthase protects against malaria in mice exposed to irradiated *Plasmodium berghei* infected mosquitoes: involvement of interferon gamma and CD8+ T cells. *J Exp Med.* 1994;180(1):353-8. Epub 1994/07/01. doi: 10.1084/jem.180.1.353. PubMed PMID: 7516412; PMCID: PMC2191552.
48. McNamara HA, Cockburn IA. The three Rs: Recruitment, Retention and Residence of leukocytes in the liver. *Clin Transl Immunology.* 2016;5(12):e123. Epub 2017/04/25. doi: 10.1038/cti.2016.84. PubMed PMID: 28435674; PMCID: PMC5384287.
49. Walk J, Stok JE, Sauerwein RW. Can Patrolling Liver-Resident T Cells Control Human Malaria Parasite Development? *Trends in Immunology.* 2019;40(3):186-96. doi: <https://doi.org/10.1016/j.it.2019.01.002>.
50. Shuai Z, Leung MW, He X, Zhang W, Yang G, Leung PS, Eric Gershwin M. Adaptive immunity in the liver. *Cell Mol Immunol.* 2016;13(3):354-68. Epub 2016/03/22. doi: 10.1038/cmi.2016.4. PubMed PMID: 26996069; PMCID: PMC4856810.
51. Bertolino P, Bowen DG. Malaria and the liver: immunological hide-and-seek or subversion of immunity from within? *Front Microbiol.* 2015;6:41. Epub 2015/03/06. doi: 10.3389/fmicb.2015.00041. PubMed PMID: 25741320; PMCID: PMC4332352.
52. Usynin I, Klotz C, Frevert U. Malaria circumsporozoite protein inhibits the respiratory burst in Kupffer cells. *Cell Microbiol.* 2007;9(11):2610-28. doi: 10.1111/j.1462-5822.2007.00982.x. PubMed PMID: 17573905.

53. Steers N, Schwenk R, Bacon DJ, Berenzon D, Williams J, Krzych U. The immune status of Kupffer cells profoundly influences their responses to infectious *Plasmodium berghei* sporozoites. *Eur J Immunol.* 2005;35(8):2335-46. doi: 10.1002/eji.200425680. PubMed PMID: 15997465.
54. Wilson NS, Behrens GM, Lundie RJ, Smith CM, Waithman J, Young L, Forehan SP, Mount A, Steptoe RJ, Shortman KD, de Koning-Ward TF, Belz GT, Carbone FR, Crabb BS, Heath WR, Villadangos JA. Systemic activation of dendritic cells by Toll-like receptor ligands or malaria infection impairs cross-presentation and antiviral immunity. *Nat Immunol.* 2006;7(2):165-72. doi: 10.1038/ni1300. PubMed PMID: 16415871.
55. Tse SW, Radtke AJ, Zavala F. Induction and maintenance of protective CD8+ T cells against malaria liver stages: implications for vaccine development. *Mem Inst Oswaldo Cruz.* 2011;106 Suppl 1:172-8. PubMed PMID: 21881772; PMCID: PMC4206913.
56. Cockburn IA, Chen YC, Overstreet MG, Lees JR, van Rooijen N, Farber DL, Zavala F. Prolonged antigen presentation is required for optimal CD8+ T cell responses against malaria liver stage parasites. *PLoS Pathog.* 2010;6(5):e1000877. doi: 10.1371/journal.ppat.1000877. PubMed PMID: 20463809; PMCID: PMC2865532.
57. Morrot A, Zavala F. Effector and memory CD8+ T cells as seen in immunity to malaria. *Immunol Rev.* 2004;201:291-303. doi: 10.1111/j.0105-2896.2004.00175.x. PubMed PMID: 15361248.
58. King T, Lamb T. Interferon-gamma: The Jekyll and Hyde of Malaria. *PLoS pathogens.* 2015;11(10):e1005118. doi: 10.1371/journal.ppat.1005118. PubMed PMID: 26426121; PMCID: PMC4591348.

59. Schmidt NW, Butler NS, Badovinac VP, Harty JT. Extreme CD8 T cell requirements for anti-malarial liver-stage immunity following immunization with radiation attenuated sporozoites. *PLoS Pathog.* 2010;6(7):e1000998. doi: 10.1371/journal.ppat.1000998. PubMed PMID: 20657824; PMCID: PMC2904779.
60. Fernandez-Ruiz D, Ng Wei Y, Holz LE, Ma Joel Z, Zaid A, Wong Yik C, Lau Lei S, Mollard V, Cozijnsen A, Collins N, Li J, Davey Gayle M, Kato Y, Devi S, Skandari R, Pauley M, Manton Jonathan H, Godfrey Dale I, Braun A, Tay Szun S, Tan Peck S, Bowen David G, Koch-Nolte F, Rissiek B, Carbone Francis R, Crabb Brendan S, Lahoud M, Cockburn Ian A, Mueller Scott N, Bertolino P, McFadden Geoffrey I, Caminschi I, Heath William R. Liver-Resident Memory CD8+ T Cells Form a Front-Line Defense against Malaria Liver-Stage Infection. *Immunity.* 2016;45(4):889-902. doi: <https://doi.org/10.1016/j.immuni.2016.08.011>.
61. Zarling S, Berenzon D, Dalai S, Liepinsh D, Steers N, Krzych U. The survival of memory CD8 T cells that is mediated by IL-15 correlates with sustained protection against malaria. *J Immunol.* 2013;190(10):5128-41. Epub 2013/04/17. doi: 10.4049/jimmunol.1203396. PubMed PMID: 23589611; PMCID: PMC3646969.
62. Tse SW, Cockburn IA, Zhang H, Scott AL, Zavala F. Unique transcriptional profile of liver-resident memory CD8+ T cells induced by immunization with malaria sporozoites. *Genes Immun.* 2013;14(5):302-9. Epub 2013/04/19. doi: 10.1038/gene.2013.20. PubMed PMID: 23594961; PMCID: PMC3722257.
63. Pallett LJ, Davies J, Colbeck EJ, Robertson F, Hansi N, Easom NJW, Burton AR, Stegmann KA, Schurich A, Swadling L, Gill US, Male V, Luong T, Gander A, Davidson BR, Kennedy PTF, Maini MK. IL-2(high) tissue-resident T cells in the human liver: Sentinels for hepatotropic

infection. *J Exp Med*. 2017;214(6):1567-80. Epub 2017/05/21. doi: 10.1084/jem.20162115.
PubMed PMID: 28526759; PMCID: PMC5461007.

64. Tse SW, Radtke AJ, Espinosa DA, Cockburn IA, Zavala F. The chemokine receptor CXCR6 is required for the maintenance of liver memory CD8(+) T cells specific for infectious pathogens. *J Infect Dis*. 2014;210(9):1508-16. Epub 2014/05/16. doi: 10.1093/infdis/jiu281.
PubMed PMID: 24823625; PMCID: PMC4207865.

65. Holz LE, Prier JE, Freestone D, Steiner TM, English K, Johnson DN, Mollard V, Cozijnsen A, Davey GM, Godfrey DI, Yui K, Mackay LK, Lahoud MH, Caminschi I, McFadden GI, Bertolino P, Fernandez-Ruiz D, Heath WR. CD8⁺ T Cell Activation Leads to Constitutive Formation of Liver Tissue-Resident Memory T Cells that Seed a Large and Flexible Niche in the Liver. *Cell Reports*. 2018;25(1):68-79.e4. doi: 10.1016/j.celrep.2018.08.094.

66. Gola A, Silman D, Walters AA, Sridhar S, Uderhardt S, Salman AM, Halbroth BR, Bellamy D, Bowyer G, Powlson J, Baker M, Venkatraman N, Poulton I, Berrie E, Roberts R, Lawrie AM, Angus B, Khan SM, Janse CJ, Ewer KJ, Germain RN, Spencer AJ, Hill AVS. Prime and target immunization protects against liver-stage malaria in mice. *Science Translational Medicine*. 2018;10(460):eaap9128. doi: 10.1126/scitranslmed.aap9128.

67. Tay SS, Wong YC, Roediger B, Sierro F, Lu B, McDonald DM, McGuffog CM, Meyer NJ, Alexander IE, Parish IA, Heath WR, Weninger W, Bishop GA, Gamble JR, McCaughan GW, Bertolino P, Bowen DG. Intrahepatic activation of naive CD4⁺ T cells by liver-resident phagocytic cells. *J Immunol*. 2014;193(5):2087-95. Epub 2014/07/30. doi: 10.4049/jimmunol.1400037. PubMed PMID: 25070847.

68. Potocnjak P, Yoshida N, Nussenzweig RS, Nussenzweig V. Monovalent fragments (Fab) of monoclonal antibodies to a sporozoite surface antigen (Pb44) protect mice against malarial infection. *J Exp Med*. 1980;151(6):1504-13. PubMed PMID: 6991628; PMCID: PMC2185881.
69. Dups JN, Pepper M, Cockburn IA. Antibody and B cell responses to Plasmodium sporozoites. *Front Microbiol*. 2014;5:625. doi: 10.3389/fmicb.2014.00625. PubMed PMID: 25477870; PMCID: PMC4235289.
70. White MT, Bejon P, Olotu A, Griffin JT, Riley EM, Kester KE, Ockenhouse CF, Ghani AC. The relationship between RTS,S vaccine-induced antibodies, CD4(+) T cell responses and protection against Plasmodium falciparum infection. *PLoS One*. 2013;8(4):e61395. Epub 2013/04/25. doi: 10.1371/journal.pone.0061395. PubMed PMID: 23613845; PMCID: PMC3628884.
71. John CC, Moormann AM, Pregibon DC, Sumba PO, McHugh MM, Narum DL, Lanar DE, Schlachter MD, Kazura JW. Correlation of high levels of antibodies to multiple pre-erythrocytic Plasmodium falciparum antigens and protection from infection. *Am J Trop Med Hyg*. 2005;73(1):222-8. PubMed PMID: 16014863.
72. Wykes MN, Zhou YH, Liu XQ, Good MF. Plasmodium yoelii can ablate vaccine-induced long-term protection in mice. *J Immunol*. 2005;175(4):2510-6. PubMed PMID: 16081823.
73. Nussenzweig RS, Vanderberg J, Most H, Orton C. Protective immunity produced by the injection of x-irradiated sporozoites of plasmodium berghei. *Nature*. 1967;216(5111):160-2. PubMed PMID: 6057225.
74. Clyde DF, Most H, McCarthy VC, Vanderberg JP. Immunization of man against sporozite-induced falciparum malaria. *Am J Med Sci*. 1973;266(3):169-77. PubMed PMID: 4583408.

75. Hoffman SL, Goh LM, Luke TC, Schneider I, Le TP, Doolan DL, Sacci J, de la Vega P, Dowler M, Paul C, Gordon DM, Stoute JA, Church LW, Sedegah M, Heppner DG, Ballou WR, Richie TL. Protection of humans against malaria by immunization with radiation-attenuated *Plasmodium falciparum* sporozoites. *J Infect Dis.* 2002;185(8):1155-64. doi: 10.1086/339409. PubMed PMID: 11930326.
76. Arevalo-Herrera M, Vasquez-Jimenez JM, Lopez-Perez M, Vallejo AF, Amado-Garavito AB, Cespedes N, Castellanos A, Molina K, Trejos J, Onate J, Epstein JE, Richie TL, Herrera S. Protective Efficacy of *Plasmodium vivax* Radiation-Attenuated Sporozoites in Colombian Volunteers: A Randomized Controlled Trial. *PLoS Negl Trop Dis.* 2016;10(10):e0005070. doi: 10.1371/journal.pntd.0005070. PubMed PMID: 27760143; PMCID: PMC5070852.
77. Orenstein WA, Committee on Infectious D. Eradicating polio: how the world's pediatricians can help stop this crippling illness forever. *Pediatrics.* 2015;135(1):196-202. doi: 10.1542/peds.2014-3163. PubMed PMID: 25548328.
78. Richie TL, Billingsley PF, Sim BK, James ER, Chakravarty S, Epstein JE, Lyke KE, Mordmuller B, Alonso P, Duffy PE, Doumbo OK, Sauerwein RW, Tanner M, Abdulla S, Kremsner PG, Seder RA, Hoffman SL. Progress with *Plasmodium falciparum* sporozoite (PfSPZ)-based malaria vaccines. *Vaccine.* 2015;33(52):7452-61. doi: 10.1016/j.vaccine.2015.09.096. PubMed PMID: 26469720; PMCID: PMC5077156.
79. Olotu A, Fegan G, Wambua J, Nyangweso G, Leach A, Lievens M, Kaslow DC, Njuguna P, Marsh K, Bejon P. Seven-Year Efficacy of RTS,S/AS01 Malaria Vaccine among Young African Children. *N Engl J Med.* 2016;374(26):2519-29. doi: 10.1056/NEJMoa1515257. PubMed PMID: 27355532; PMCID: PMC4962898.

80. Gosling R, von Seidlein L. The Future of the RTS,S/AS01 Malaria Vaccine: An Alternative Development Plan. *PLoS Med.* 2016;13(4):e1001994. doi: 10.1371/journal.pmed.1001994. PubMed PMID: 27070151; PMCID: PMC4829262.
81. White MT, Verity R, Griffin JT, Asante KP, Owusu-Agyei S, Greenwood B, Drakeley C, Gesase S, Lusingu J, Ansong D, Adjei S, Agbenyega T, Ogutu B, Otieno L, Otieno W, Agnandji ST, Lell B, Kremsner P, Hoffman I, Martinson F, Kamthunzu P, Tinto H, Valea I, Sorgho H, Oneko M, Otieno K, Hamel MJ, Salim N, Mtoro A, Abdulla S, Aide P, Sacarlal J, Aponte JJ, Njuguna P, Marsh K, Bejon P, Riley EM, Ghani AC. Immunogenicity of the RTS,S/AS01 malaria vaccine and implications for duration of vaccine efficacy: secondary analysis of data from a phase 3 randomised controlled trial. *Lancet Infect Dis.* 2015;15(12):1450-8. doi: 10.1016/S1473-3099(15)00239-X. PubMed PMID: 26342424; PMCID: PMC4655306.
82. Bennett JW, Yadava A, Tosh D, Sattabongkot J, Komisar J, Ware LA, McCarthy WF, Cowden JJ, Regules J, Spring MD, Paolino K, Hartzell JD, Cummings JF, Richie TL, Lumsden J, Kamau E, Murphy J, Lee C, Parekh F, Birkett A, Cohen J, Ballou WR, Polhemus ME, Vanloubbeeck YF, Vekemans J, Ockenhouse CF. Phase 1/2a Trial of Plasmodium vivax Malaria Vaccine Candidate VMP001/AS01B in Malaria-Naive Adults: Safety, Immunogenicity, and Efficacy. *PLoS Negl Trop Dis.* 2016;10(2):e0004423. doi: 10.1371/journal.pntd.0004423. PubMed PMID: 26919472.
83. Barry AE, Arnott A. Strategies for designing and monitoring malaria vaccines targeting diverse antigens. *Front Immunol.* 2014;5:359. doi: 10.3389/fimmu.2014.00359. PubMed PMID: 25120545; PMCID: PMC4112938.

84. Ouattara A, Barry AE, Dutta S, Remarque EJ, Beeson JG, Plowe CV. Designing malaria vaccines to circumvent antigen variability. *Vaccine*. 2015;33(52):7506-12. doi: 10.1016/j.vaccine.2015.09.110. PubMed PMID: 26475447; PMCID: PMC4731100.
85. Plowe CV. Vaccine-Resistant Malaria. *N Engl J Med*. 2015;373(21):2082-3. doi: 10.1056/NEJMe1511955. PubMed PMID: 26488465.
86. Cabrera-Mora M, Fonseca JA, Singh B, Oliveira-Ferreira J, Lima-Junior Jda C, Calvo-Calle JM, Moreno A. Induction of Multifunctional Broadly Reactive T Cell Responses by a *Plasmodium vivax* Circumsporozoite Protein Recombinant Chimera. *Infect Immun*. 2015;83(9):3749-61. Epub 2015/07/15. doi: 10.1128/IAI.00480-15. PubMed PMID: 26169267; PMCID: PMC4534670.
87. Hodgson SH, Ewer KJ, Bliss CM, Edwards NJ, Rampling T, Anagnostou NA, de Barra E, Havelock T, Bowyer G, Poulton ID, de Cassan S, Longley R, Illingworth JJ, Douglas AD, Mange PB, Collins KA, Roberts R, Gerry S, Berrie E, Moyle S, Colloca S, Cortese R, Sinden RE, Gilbert SC, Bejon P, Lawrie AM, Nicosia A, Faust SN, Hill AV. Evaluation of the efficacy of ChAd63-MVA vectored vaccines expressing circumsporozoite protein and ME-TRAP against controlled human malaria infection in malaria-naive individuals. *J Infect Dis*. 2015;211(7):1076-86. doi: 10.1093/infdis/jiu579. PubMed PMID: 25336730; PMCID: PMC4354983.
88. Bergmann-Leitner ES, Mease RM, De La Vega P, Savranskaya T, Polhemus M, Ockenhouse C, Angov E. Immunization with pre-erythrocytic antigen CelTOS from *Plasmodium falciparum* elicits cross-species protection against heterologous challenge with *Plasmodium berghei*. *PLoS One*. 2010;5(8):e12294. doi: 10.1371/journal.pone.0012294. PubMed PMID: 20808868; PMCID: PMC2924390.

89. Bauza K, Atcheson E, Malinauskas T, Blagborough AM, Reyes-Sandoval A. Tailoring a Combination Preerythrocytic Malaria Vaccine. *Infect Immun*. 2015;84(3):622-34. doi: 10.1128/IAI.01063-15. PubMed PMID: 26667840; PMCID: PMC4771343.
90. Singh B, Cabrera-Mora M, Jiang J, Moreno A. A hybrid multistage protein vaccine induces protective immunity against murine malaria. *Infect Immun*. 2012;80(4):1491-501. Epub 2012/01/19. doi: 10.1128/IAI.05980-11. PubMed PMID: 22252877; PMCID: PMC3318412.
91. Nahrendorf W, Scholzen A, Sauerwein RW, Langhorne J. Cross-stage immunity for malaria vaccine development. *Vaccine*. 2015;33(52):7513-7. doi: 10.1016/j.vaccine.2015.09.098. PubMed PMID: 26469724; PMCID: PMC4687527.
92. Fonseca JA, Cabrera-Mora M, Kashentseva EA, Villegas JP, Fernandez A, Van Pelt A, Dmitriev IP, Curiel DT, Moreno A. A Plasmodium Promiscuous T Cell Epitope Delivered within the Ad5 Hexon Protein Enhances the Protective Efficacy of a Protein Based Malaria Vaccine. *PloS one*. 2016;11(4):e0154819. doi: 10.1371/journal.pone.0154819. PubMed PMID: 27128437.
93. Cabrera-Mora M, Fonseca JA, Singh B, Zhao C, Makarova N, Dmitriev I, Curiel DT, Blackwell J, Moreno A. A Recombinant Chimeric Ad5/3 Vector Expressing a Multistage Plasmodium Antigen Induces Protective Immunity in Mice Using Heterologous Prime-Boost Immunization Regimens. *Journal of immunology*. 2016. doi: 10.4049/jimmunol.1501926. PubMed PMID: 27574299.
94. Khan F, Porter M, Schwenk R, DeBot M, Saudan P, Dutta S. Head-to-Head Comparison of Soluble vs. Qbeta VLP Circumsporozoite Protein Vaccines Reveals Selective Enhancement of NANP Repeat Responses. *PLoS One*. 2015;10(11):e0142035. doi: 10.1371/journal.pone.0142035. PubMed PMID: 26571021; PMCID: PMC4646581.

95. Holder AA, Freeman RR. The three major antigens on the surface of *Plasmodium falciparum* merozoites are derived from a single high molecular weight precursor. *J Exp Med*. 1984;160(2):624-9. PubMed PMID: 6381636; PMCID: PMC2187444.
96. Boyle MJ, Richards JS, Gilson PR, Chai W, Beeson JG. Interactions with heparin-like molecules during erythrocyte invasion by *Plasmodium falciparum* merozoites. *Blood*. 2010;115(22):4559-68. doi: 10.1182/blood-2009-09-243725. PubMed PMID: 20220119.
97. Lin CS, Uboldi AD, Epp C, Bujard H, Tsuboi T, Czabotar PE, Cowman AF. Multiple *Plasmodium falciparum* Merozoite Surface Protein 1 Complexes Mediate Merozoite Binding to Human Erythrocytes. *J Biol Chem*. 2016;291(14):7703-15. doi: 10.1074/jbc.M115.698282. PubMed PMID: 26823464; PMCID: PMC4817195.
98. Babon JJ, Morgan WD, Kelly G, Eccleston JF, Feeney J, Holder AA. Structural studies on *Plasmodium vivax* merozoite surface protein-1. *Mol Biochem Parasitol*. 2007;153(1):31-40. doi: 10.1016/j.molbiopara.2007.01.015. PubMed PMID: 17343930.
99. Holder AA, Blackman MJ, Burghaus PA, Chappel JA, Ling IT, McCallum-Deighton N, Shai S. A malaria merozoite surface protein (MSP1)-structure, processing and function. *Mem Inst Oswaldo Cruz*. 1992;87 Suppl 3:37-42. PubMed PMID: 1343716.
100. Blackman MJ, Whittle H, Holder AA. Processing of the *Plasmodium falciparum* major merozoite surface protein-1: identification of a 33-kilodalton secondary processing product which is shed prior to erythrocyte invasion. *Mol Biochem Parasitol*. 1991;49(1):35-44. PubMed PMID: 1723148.
101. Dodoo D, Aikins A, Kusi KA, Lamptey H, Remarque E, Milligan P, Bosomprah S, Chilengi R, Osei YD, Akanmori BD, Theisen M. Cohort study of the association of antibody levels to AMA1, MSP119, MSP3 and GLURP with protection from clinical malaria in Ghanaian

children. *Malar J.* 2008;7:142. doi: 10.1186/1475-2875-7-142. PubMed PMID: 18664257; PMCID: PMC2529305.

102. Weiss GE, Gilson PR, Taechalertrpaisarn T, Tham WH, de Jong NW, Harvey KL, Fowkes FJ, Barlow PN, Rayner JC, Wright GJ, Cowman AF, Crabb BS. Revealing the sequence and resulting cellular morphology of receptor-ligand interactions during *Plasmodium falciparum* invasion of erythrocytes. *PLoS Pathog.* 2015;11(2):e1004670. doi:

10.1371/journal.ppat.1004670. PubMed PMID: 25723550; PMCID: PMC4344246.

103. Tham WH, Healer J, Cowman AF. Erythrocyte and reticulocyte binding-like proteins of *Plasmodium falciparum*. *Trends Parasitol.* 2012;28(1):23-30. doi: 10.1016/j.pt.2011.10.002.

PubMed PMID: 22178537.

104. Cutts JC, Powell R, Agius PA, Beeson JG, Simpson JA, Fowkes FJ. Immunological markers of *Plasmodium vivax* exposure and immunity: a systematic review and meta-analysis.

BMC Med. 2014;12:150. doi: 10.1186/s12916-014-0150-1. PubMed PMID: 25199532; PMCID: PMC4172944.

105. Hostetler JB, Sharma S, Bartholdson SJ, Wright GJ, Fairhurst RM, Rayner JC. A Library of *Plasmodium vivax* Recombinant Merozoite Proteins Reveals New Vaccine Candidates and Protein-Protein Interactions. *PLoS Negl Trop Dis.* 2015;9(12):e0004264. doi:

10.1371/journal.pntd.0004264. PubMed PMID: 26701602; PMCID: PMC4689532.

106. Gunalan K, Lo E, Hostetler JB, Yewhalaw D, Mu J, Neafsey DE, Yan G, Miller LH.

Role of *Plasmodium vivax* Duffy-binding protein 1 in invasion of Duffy-null Africans. *Proc Natl Acad Sci U S A.* 2016;113(22):6271-6. doi: 10.1073/pnas.1606113113. PubMed PMID:

27190089; PMCID: PMC4896682.

107. Li J, Han ET. Dissection of the *Plasmodium vivax* reticulocyte binding-like proteins (PvRBPs). *Biochem Biophys Res Commun*. 2012;426(1):1-6. doi: 10.1016/j.bbrc.2012.08.055. PubMed PMID: 22925889.
108. Crompton PD, Moebius J, Portugal S, Waisberg M, Hart G, Garver LS, Miller LH, Barillas-Mury C, Pierce SK. Malaria immunity in man and mosquito: insights into unsolved mysteries of a deadly infectious disease. *Annu Rev Immunol*. 2014;32:157-87. doi: 10.1146/annurev-immunol-032713-120220. PubMed PMID: 24655294; PMCID: 24655294.
109. Stevenson MM, Riley EM. Innate immunity to malaria. *Nat Rev Immunol*. 2004;4(3):169-80. doi: 10.1038/nri1311. PubMed PMID: 15039754.
110. Mohan K, Moulin P, Stevenson MM. Natural killer cell cytokine production, not cytotoxicity, contributes to resistance against blood-stage *Plasmodium chabaudi* AS infection. *J Immunol*. 1997;159(10):4990-8. PubMed PMID: 9366426.
111. Sharma S, DeOliveira RB, Kalantari P, Parroche P, Goutagny N, Jiang Z, Chan J, Bartholomeu DC, Lauw F, Hall JP, Barber GN, Gazzinelli RT, Fitzgerald KA, Golenbock DT. Innate immune recognition of an AT-rich stem-loop DNA motif in the *Plasmodium falciparum* genome. *Immunity*. 2011;35(2):194-207. doi: 10.1016/j.immuni.2011.05.016. PubMed PMID: 21820332; PMCID: PMC3162998.
112. Kalantari P, DeOliveira RB, Chan J, Corbett Y, Rathinam V, Stutz A, Latz E, Gazzinelli RT, Golenbock DT, Fitzgerald KA. Dual engagement of the NLRP3 and AIM2 inflammasomes by plasmodium-derived hemozoin and DNA during malaria. *Cell Rep*. 2014;6(1):196-210. doi: 10.1016/j.celrep.2013.12.014. PubMed PMID: 24388751; PMCID: PMC4105362.
113. Imai T, Ishida H, Suzue K, Taniguchi T, Okada H, Shimokawa C, Hisaeda H. Cytotoxic activities of CD8(+) T cells collaborate with macrophages to protect against blood-stage murine

malaria. *Elife*. 2015;4. doi: 10.7554/eLife.04232. PubMed PMID: 25760084; PMCID: PMC4366679.

114. Boyle MJ, Reiling L, Feng G, Langer C, Osier FH, Aspelng-Jones H, Cheng YS, Stubbs J, Tetteh KK, Conway DJ, McCarthy JS, Muller I, Marsh K, Anders RF, Beeson JG. Human antibodies fix complement to inhibit *Plasmodium falciparum* invasion of erythrocytes and are associated with protection against malaria. *Immunity*. 2015;42(3):580-90. doi:

10.1016/j.immuni.2015.02.012. PubMed PMID: 25786180; PMCID: 4372259.

115. Chitnis CE, Mukherjee P, Mehta S, Yazdani SS, Dhawan S, Shakri AR, Bhardwaj R, Gupta PK, Hans D, Mazumdar S, Singh B, Kumar S, Pandey G, Parulekar V, Imbault N, Shiviyogi P, Godbole G, Mohan K, Leroy O, Singh K, Chauhan VS. Phase I Clinical Trial of a Recombinant Blood Stage Vaccine Candidate for *Plasmodium falciparum* Malaria Based on MSP1 and EBA175. *PLoS One*. 2015;10(4):e0117820. Epub 2015/05/01. doi:

10.1371/journal.pone.0117820. PubMed PMID: 25927360; PMCID: PMC4415778.

116. Sheehy SH, Duncan CJ, Elias SC, Choudhary P, Biswas S, Halstead FD, Collins KA, Edwards NJ, Douglas AD, Anagnostou NA, Ewer KJ, Havelock T, Mahungu T, Bliss CM, Miura K, Poulton ID, Lillie PJ, Antrobus RD, Berrie E, Moyle S, Gantlett K, Colloca S, Cortese R, Long CA, Sinden RE, Gilbert SC, Lawrie AM, Doherty T, Faust SN, Nicosia A, Hill AV, Draper SJ. ChAd63-MVA-vectored blood-stage malaria vaccines targeting MSP1 and AMA1: assessment of efficacy against mosquito bite challenge in humans. *Mol Ther*. 2012;20(12):2355-68. doi: 10.1038/mt.2012.223. PubMed PMID: 23089736; PMCID: PMC3519995.

117. Biswas S, Choudhary P, Elias SC, Miura K, Milne KH, de Cassan SC, Collins KA, Halstead FD, Bliss CM, Ewer KJ, Osier FH, Hodgson SH, Duncan CJ, O'Hara GA, Long CA, Hill AV, Draper SJ. Assessment of humoral immune responses to blood-stage malaria antigens

following ChAd63-MVA immunization, controlled human malaria infection and natural exposure. *PLoS One*. 2014;9(9):e107903. doi: 10.1371/journal.pone.0107903. PubMed PMID: 25254500; PMCID: PMC4177865.

118. El Sahly HM, Patel SM, Atmar RL, Lanford TA, Dube T, Thompson D, Sim BK, Long C, Keitel WA. Safety and immunogenicity of a recombinant nonglycosylated erythrocyte binding antigen 175 Region II malaria vaccine in healthy adults living in an area where malaria is not endemic. *Clin Vaccine Immunol*. 2010;17(10):1552-9. doi: 10.1128/CVI.00082-10. PubMed PMID: 20702657; PMCID: PMC2952998.

119. Hodgson SH, Choudhary P, Elias SC, Milne KH, Rampling TW, Biswas S, Poulton ID, Miura K, Douglas AD, Alanine DG, Illingworth JJ, de Cassan SC, Zhu D, Nicosia A, Long CA, Moyle S, Berrie E, Lawrie AM, Wu Y, Ellis RD, Hill AV, Draper SJ. Combining viral vectored and protein-in-adjuvant vaccines against the blood-stage malaria antigen AMA1: report on a phase 1a clinical trial. *Mol Ther*. 2014;22(12):2142-54. doi: 10.1038/mt.2014.157. PubMed PMID: 25156127; PMCID: PMC4250079.

120. Thera MA, Doumbo OK, Coulibaly D, Laurens MB, Kone AK, Guindo AB, Traore K, Sissoko M, Diallo DA, Diarra I, Kouriba B, Daou M, Dolo A, Baby M, Sissoko MS, Sagara I, Niangaly A, Traore I, Olotu A, Godeaux O, Leach A, Dubois MC, Ballou WR, Cohen J, Thompson D, Dube T, Soisson L, Diggs CL, Takala SL, Lyke KE, House B, Lanar DE, Dutta S, Heppner DG, Plowe CV. Safety and immunogenicity of an AMA1 malaria vaccine in Malian children: results of a phase 1 randomized controlled trial. *PLoS One*. 2010;5(2):e9041. doi: 10.1371/journal.pone.0009041. PubMed PMID: 20140214; PMCID: PMC2816207.

121. Moreno A, Joyner C. Malaria vaccine clinical trials: what's on the horizon. *Curr Opin Immunol.* 2015;35:98-106. doi: 10.1016/j.coi.2015.06.008. PubMed PMID: 26172291; PMCID: PMC4553069.
122. Chan JA, Fowkes FJ, Beeson JG. Surface antigens of Plasmodium falciparum-infected erythrocytes as immune targets and malaria vaccine candidates. *Cell Mol Life Sci.* 2014;71(19):3633-57. doi: 10.1007/s00018-014-1614-3. PubMed PMID: 24691798; PMCID: PMC4160571.
123. Struik SS, Riley EM. Does malaria suffer from lack of memory? *Immunological Reviews.* 2004;201(1):268-90. doi: 10.1111/j.0105-2896.2004.00181.x.
124. Triller G, Scally SW, Costa G, Pissarev M, Kreschel C, Bosch A, Marois E, Sack BK, Murugan R, Salman AM, Janse CJ, Khan SM, Kappe SHI, Adegnikaa AA, Mordmüller B, Levashina EA, Julien J-P, Wardemann H. Natural Parasite Exposure Induces Protective Human Anti-Malarial Antibodies. *Immunity.* 2017;47(6):1197-209.e10. doi: 10.1016/j.immuni.2017.11.007.
125. Langhorne J, Ndungu FM, Sponaas A-M, Marsh K. Immunity to malaria: more questions than answers. *Nature Immunology.* 2008;9:725. doi: 10.1038/ni.f.205.
126. Mathison BA, Pritt BS. Update on Malaria Diagnostics and Test Utilization. *J Clin Microbiol.* 2017;55(7):2009-17. Epub 2017/04/12. doi: 10.1128/JCM.02562-16. PubMed PMID: 28404673.
127. Corran P, Coleman P, Riley E, Drakeley C. Serology: a robust indicator of malaria transmission intensity? *Trends in Parasitology.* 2007;23(12):575-82. doi: <https://doi.org/10.1016/j.pt.2007.08.023>.

128. Rogier E, Wiegand R, Moss D, Priest J, Angov E, Dutta S, Journal I, Jean SE, Mace K, Chang M, Lemoine JF, Udhayakumar V, Barnwell JW. Multiple comparisons analysis of serological data from an area of low *Plasmodium falciparum* transmission. *Malar J*. 2015;14:436. Epub 2015/11/06. doi: 10.1186/s12936-015-0955-1. PubMed PMID: 26537125; PMCID: PMC4634594.
129. Arnold BF, Priest JW, Hamlin KL, Moss DM, Colford Jr JM, Lammie PJ. Serological Measures of Malaria Transmission in Haiti: Comparison of Longitudinal and Cross-Sectional Methods. *PLOS ONE*. 2014;9(4):e93684. doi: 10.1371/journal.pone.0093684.
130. Smith DL, Dushoff J, McKenzie FE. The Risk of a Mosquito-Borne Infection in a Heterogeneous Environment. *PLOS Biology*. 2004;2(11):e368. doi: 10.1371/journal.pbio.0020368.
131. Cook J, Reid H, Iavro J, Kuwahata M, Taleo G, Clements A, McCarthy J, Vallely A, Drakeley C. Using serological measures to monitor changes in malaria transmission in Vanuatu. *Malaria Journal*. 2010;9(1):169. doi: 10.1186/1475-2875-9-169.
132. Rogier E, Plucinski M, Lucchi N, Mace K, Chang M, Lemoine JF, Candrinho B, Colborn J, Dimbu R, Fortes F, Udhayakumar V, Barnwell J. Bead-based immunoassay allows sub-picogram detection of histidine-rich protein 2 from *Plasmodium falciparum* and estimates reliability of malaria rapid diagnostic tests. *PLoS One*. 2017;12(2):e0172139. Epub 2017/02/14. doi: 10.1371/journal.pone.0172139. PubMed PMID: 28192523; PMCID: PMC5305216.
133. Rogier E, Moss DM, Chard AN, Trinies V, Doumbia S, Freeman MC, Lammie PJ. Evaluation of Immunoglobulin G Responses to *Plasmodium falciparum* and *Plasmodium vivax* in Malian School Children Using Multiplex Bead Assay. *Am J Trop Med Hyg*. 2017;96(2):312-

8. Epub 2016/11/30. doi: 10.4269/ajtmh.16-0476. PubMed PMID: 27895279; PMCID: PMC5303029.
134. Organization WH. Global Technical Strategy for Malaria 2016-2030. 2016.
135. Sauerwein RW. Malaria transmission-blocking vaccines: the bonus of effective malaria control. *Microbes Infect.* 2007;9(6):792-5. doi: 10.1016/j.micinf.2007.02.011. PubMed PMID: 17418610.
136. Pradel G. Proteins of the malaria parasite sexual stages: expression, function and potential for transmission blocking strategies. *Parasitology.* 2007;134(Pt.14):1911-29. doi: 10.1017/S0031182007003381. PubMed PMID: 17714601.
137. Talman AM, Domarle O, McKenzie FE, Ariey F, Robert V. Gametocytogenesis: the puberty of *Plasmodium falciparum*. *Malar J.* 2004;3:24. doi: 10.1186/1475-2875-3-24. PubMed PMID: 15253774; PMCID: PMC497046.
138. Bousema T, Drakeley C. Epidemiology and infectivity of *Plasmodium falciparum* and *Plasmodium vivax* gametocytes in relation to malaria control and elimination. *Clin Microbiol Rev.* 2011;24(2):377-410. doi: 10.1128/CMR.00051-10. PubMed PMID: 21482730; PMCID: PMC3122489.
139. Olliaro PL, Barnwell JW, Barry A, Mendis K, Mueller I, Reeder JC, Shanks GD, Snounou G, Wongsrichanalai C. Implications of *Plasmodium vivax* Biology for Control, Elimination, and Research. *Am J Trop Med Hyg.* 2016. doi: 10.4269/ajtmh.16-0160. PubMed PMID: 27799636.
140. Gardiner DL, Dixon MW, Spielmann T, Skinner-Adams TS, Hawthorne PL, Ortega MR, Kemp DJ, Trenholme KR. Implication of a *Plasmodium falciparum* gene in the switch between

asexual reproduction and gametocytogenesis. *Mol Biochem Parasitol.* 2005;140(2):153-60. doi: 10.1016/j.molbiopara.2004.12.010. PubMed PMID: 15760655.

141. Silvestrini F, Bozdech Z, Lanfrancotti A, Di Giulio E, Bultrini E, Picci L, Derisi JL, Pizzi E, Alano P. Genome-wide identification of genes upregulated at the onset of gametocytogenesis in *Plasmodium falciparum*. *Mol Biochem Parasitol.* 2005;143(1):100-10. doi: 10.1016/j.molbiopara.2005.04.015. PubMed PMID: 16026866.

142. Young JA, Fivelman QL, Blair PL, de la Vega P, Le Roch KG, Zhou Y, Carucci DJ, Baker DA, Winzeler EA. The *Plasmodium falciparum* sexual development transcriptome: a microarray analysis using ontology-based pattern identification. *Mol Biochem Parasitol.* 2005;143(1):67-79. doi: 10.1016/j.molbiopara.2005.05.007. PubMed PMID: 16005087.

143. Lasonder E, Ishihama Y, Andersen JS, Vermunt AM, Pain A, Sauerwein RW, Eling WM, Hall N, Waters AP, Stunnenberg HG, Mann M. Analysis of the *Plasmodium falciparum* proteome by high-accuracy mass spectrometry. *Nature.* 2002;419(6906):537-42. doi: 10.1038/nature01111. PubMed PMID: 12368870.

144. Piper KP, Hayward RE, Cox MJ, Day KP. Malaria transmission and naturally acquired immunity to PfEMP-1. *Infect Immun.* 1999;67(12):6369-74. PubMed PMID: 10569752; PMCID: PMC97044.

145. Saul A. Mosquito stage, transmission blocking vaccines for malaria. *Curr Opin Infect Dis.* 2007;20(5):476-81. doi: 10.1097/QCO.0b013e3282a95e12. PubMed PMID: 17762780.

146. Paul NH, Vengesai A, Mduluza T, Chipeta J, Midzi N, Bansal GP, Kumar N. Prevalence of *Plasmodium falciparum* transmission reducing immunity among primary school children in a malaria moderate transmission region in Zimbabwe. *Acta Trop.* 2016;163:103-8. doi: 10.1016/j.actatropica.2016.07.023. PubMed PMID: 27491342; PMCID: PMC5007214.

147. Ateba-Ngoa U, Jones S, Zinsou JF, Honkpehedji J, Adegnika AA, Agobe JC, Massinga-Loembe M, Mordmuller B, Bousema T, Yazdanbakhsh M. Associations Between Helminth Infections, Plasmodium falciparum Parasite Carriage and Antibody Responses to Sexual and Asexual Stage Malarial Antigens. *Am J Trop Med Hyg.* 2016;95(2):394-400. doi: 10.4269/ajtmh.15-0703. PubMed PMID: 27273645; PMCID: PMC4973188.
148. Roeffen W, Lensen T, Mulder B, Teelen K, Sauerwein R, Eling W, Meuwissen JH, Beckers P. Transmission blocking immunity as observed in a feeder system and serological reactivity to Pfs 48/45 and Pfs230 in field sera. *Mem Inst Oswaldo Cruz.* 1994;89 Suppl 2:13-5. PubMed PMID: 7565122.
149. Vermeulen AN, Ponnudurai T, Beckers PJ, Verhave JP, Smits MA, Meuwissen JH. Sequential expression of antigens on sexual stages of Plasmodium falciparum accessible to transmission-blocking antibodies in the mosquito. *J Exp Med.* 1985;162(5):1460-76. PubMed PMID: 2865324; PMCID: PMC2187939.
150. Read D, Lensen AH, Begarnie S, Haley S, Raza A, Carter R. Transmission-blocking antibodies against multiple, non-variant target epitopes of the Plasmodium falciparum gamete surface antigen Pfs230 are all complement-fixing. *Parasite Immunol.* 1994;16(10):511-9. PubMed PMID: 7532850.
151. Carter R, Graves PM, Keister DB, Quakyi IA. Properties of epitopes of Pfs 48/45, a target of transmission blocking monoclonal antibodies, on gametes of different isolates of Plasmodium falciparum. *Parasite Immunol.* 1990;12(6):587-603. PubMed PMID: 1707506.
152. Liu Y, Tewari R, Ning J, Blagborough AM, Garbom S, Pei J, Grishin NV, Steele RE, Sinden RE, Snell WJ, Billker O. The conserved plant sterility gene HAP2 functions after attachment of fusogenic membranes in Chlamydomonas and Plasmodium gametes. *Genes Dev.*

2008;22(8):1051-68. doi: 10.1101/gad.1656508. PubMed PMID: 18367645; PMCID: PMC2335326.

153. Blagborough AM, Sinden RE. Plasmodium berghei HAP2 induces strong malaria transmission-blocking immunity in vivo and in vitro. *Vaccine*. 2009;27(38):5187-94. doi: 10.1016/j.vaccine.2009.06.069. PubMed PMID: 19596419.

154. Michel K, Kafatos FC. Mosquito immunity against Plasmodium. *Insect Biochem Mol Biol*. 2005;35(7):677-89. doi: 10.1016/j.ibmb.2005.02.009. PubMed PMID: 15894185.

155. Sinden RE, Billingsley PF. Plasmodium invasion of mosquito cells: hawk or dove? *Trends Parasitol*. 2001;17(5):209-12. PubMed PMID: 11323288.

156. Saxena AK, Wu Y, Garboczi DN. Plasmodium p25 and p28 surface proteins: potential transmission-blocking vaccines. *Eukaryot Cell*. 2007;6(8):1260-5. doi: 10.1128/EC.00060-07. PubMed PMID: 17557884; PMCID: PMC1951121.

157. Cirimotich CM, Dong Y, Garver LS, Sim S, Dimopoulos G. Mosquito immune defenses against Plasmodium infection. *Dev Comp Immunol*. 2010;34(4):387-95. doi: 10.1016/j.dci.2009.12.005. PubMed PMID: 20026176; PMCID: PMC3462653.

158. Espinosa DA, Vega-Rodriguez J, Flores-Garcia Y, Noe AR, Munoz C, Coleman R, Bruck T, Haney K, Stevens A, Retallack D, Allen J, Vedvick TS, Fox CB, Reed SG, Howard RF, Salman AM, Janse CJ, Khan SM, Zavala F, Gutierrez GM. The *P. falciparum* Cell-Traversal Protein for Ookinetes and Sporozoites as a Candidate for Pre-Erythrocytic and Transmission-Blocking Vaccines. *Infect Immun*. 2016. doi: 10.1128/IAI.00498-16. PubMed PMID: 27895131.

159. Lehane MJ. Peritrophic matrix structure and function. *Annu Rev Entomol*. 1997;42:525-50. doi: 10.1146/annurev.ento.42.1.525. PubMed PMID: 15012322.

160. Whitten MM, Shiao SH, Levashina EA. Mosquito midguts and malaria: cell biology, compartmentalization and immunology. *Parasite Immunol.* 2006;28(4):121-30. doi: 10.1111/j.1365-3024.2006.00804.x. PubMed PMID: 16542314.
161. Billingsley PF, Rudin W. The role of the mosquito peritrophic membrane in bloodmeal digestion and infectivity of *Plasmodium* species. *J Parasitol.* 1992;78(3):430-40. PubMed PMID: 1597785.
162. Billingsley PF. The Midgut Ultrastructure of Hematophagous Insects. *Annual Review of Entomology.* 1990;35(1):219-48. doi: doi:10.1146/annurev.en.35.010190.001251.
163. Kariu T, Ishino T, Yano K, Chinzei Y, Yuda M. CelTOS, a novel malarial protein that mediates transmission to mosquito and vertebrate hosts. *Mol Microbiol.* 2006;59(5):1369-79. doi: 10.1111/j.1365-2958.2005.05024.x. PubMed PMID: 16468982.
164. Kojin BB, Costa-da-Silva AL, Maciel C, Henriques DA, Carvalho DO, Martin K, Marinotti O, James AA, Bonaldo MC, Capurro ML. Endogenously-expressed NH₂-terminus of circumsporozoite protein interferes with sporozoite invasion of mosquito salivary glands. *Malar J.* 2016;15:153. doi: 10.1186/s12936-016-1207-8. PubMed PMID: 26964736; PMCID: PMC4785649.
165. Dong Y, Manfredini F, Dimopoulos G. Implication of the mosquito midgut microbiota in the defense against malaria parasites. *PLoS Pathog.* 2009;5(5):e1000423. doi: 10.1371/journal.ppat.1000423. PubMed PMID: 19424427; PMCID: PMC2673032.
166. Pumpuni CB, Beier MS, Nataro JP, Guers LD, Davis JR. *Plasmodium falciparum*: inhibition of sporogonic development in *Anopheles stephensi* by gram-negative bacteria. *Exp Parasitol.* 1993;77(2):195-9. doi: 10.1006/expr.1993.1076. PubMed PMID: 8375488.

167. Pumpuni CB, Demaio J, Kent M, Davis JR, Beier JC. Bacterial population dynamics in three anopheline species: the impact on Plasmodium sporogonic development. *Am J Trop Med Hyg.* 1996;54(2):214-8. PubMed PMID: 8619451.
168. Gonzalez-Ceron L, Santillan F, Rodriguez MH, Mendez D, Hernandez-Avila JE. Bacteria in midguts of field-collected *Anopheles albimanus* block *Plasmodium vivax* sporogonic development. *J Med Entomol.* 2003;40(3):371-4. PubMed PMID: 12943119.
169. Demaio J, Pumpuni CB, Kent M, Beier JC. The midgut bacterial flora of wild *Aedes triseriatus*, *Culex pipiens*, and *Psorophora columbiae* mosquitoes. *Am J Trop Med Hyg.* 1996;54(2):219-23. PubMed PMID: 8619452.
170. Azambuja P, Garcia ES, Ratcliffe NA. Gut microbiota and parasite transmission by insect vectors. *Trends Parasitol.* 2005;21(12):568-72. doi: 10.1016/j.pt.2005.09.011. PubMed PMID: 16226491.
171. Cirimotich CM, Dong Y, Clayton AM, Sandiford SL, Souza-Neto JA, Mulenga M, Dimopoulos G. Natural microbe-mediated refractoriness to *Plasmodium* infection in *Anopheles gambiae*. *Science.* 2011;332(6031):855-8. doi: 10.1126/science.1201618. PubMed PMID: 21566196; PMCID: PMC4154605.
172. Christophides GK, Zdobnov E, Barillas-Mury C, Birney E, Blandin S, Blass C, Brey PT, Collins FH, Danielli A, Dimopoulos G, Hetru C, Hoa NT, Hoffmann JA, Kanzok SM, Letunic I, Levashina EA, Loukeris TG, Lycett G, Meister S, Michel K, Moita LF, Muller HM, Osta MA, Paskewitz SM, Reichhart JM, Rzhetsky A, Troxler L, Vernick KD, Vlachou D, Volz J, von Mering C, Xu J, Zheng L, Bork P, Kafatos FC. Immunity-related genes and gene families in *Anopheles gambiae*. *Science.* 2002;298(5591):159-65. doi: 10.1126/science.1077136. PubMed PMID: 12364793.

173. Dimopoulos G, Richman A, Muller HM, Kafatos FC. Molecular immune responses of the mosquito *Anopheles gambiae* to bacteria and malaria parasites. *Proc Natl Acad Sci U S A*. 1997;94(21):11508-13. PubMed PMID: 9326640; PMCID: PMC23521.
174. Hillyer JF. Mosquito immunity. *Adv Exp Med Biol*. 2010;708:218-38. PubMed PMID: 21528701.
175. Dong Y, Dimopoulos G. *Anopheles* fibrinogen-related proteins provide expanded pattern recognition capacity against bacteria and malaria parasites. *J Biol Chem*. 2009;284(15):9835-44. doi: 10.1074/jbc.M807084200. PubMed PMID: 19193639; PMCID: PMC2665105.
176. Meister S, Koutsos AC, Christophides GK. The *Plasmodium* parasite--a 'new' challenge for insect innate immunity. *Int J Parasitol*. 2004;34(13-14):1473-82. doi: 10.1016/j.ijpara.2004.10.004. PubMed PMID: 15582524.
177. Blandin S, Shiao SH, Moita LF, Janse CJ, Waters AP, Kafatos FC, Levashina EA. Complement-like protein TEP1 is a determinant of vectorial capacity in the malaria vector *Anopheles gambiae*. *Cell*. 2004;116(5):661-70. PubMed PMID: 15006349.
178. Blandin SA, Marois E, Levashina EA. Antimalarial responses in *Anopheles gambiae*: from a complement-like protein to a complement-like pathway. *Cell Host Microbe*. 2008;3(6):364-74. doi: 10.1016/j.chom.2008.05.007. PubMed PMID: 18541213.
179. Christensen BM, Li J, Chen CC, Nappi AJ. Melanization immune responses in mosquito vectors. *Trends Parasitol*. 2005;21(4):192-9. doi: 10.1016/j.pt.2005.02.007. PubMed PMID: 15780842.
180. Jamrozik E, de la Fuente-Nunez V, Reis A, Ringwald P, Selgelid MJ. Ethical aspects of malaria control and research. *Malar J*. 2015;14:518. doi: 10.1186/s12936-015-1042-3. PubMed PMID: 26693920; PMCID: PMC4688922.

181. Smith TA, Leuenberger R, Lengeler C. Child mortality and malaria transmission intensity in Africa. *Trends Parasitol.* 2001;17(3):145-9. PubMed PMID: 11286800.
182. Larsen DA, Friberg IK, Eisele TP. Comparison of Lives Saved Tool model child mortality estimates against measured data from vector control studies in sub-Saharan Africa. *BMC Public Health.* 2011;11 Suppl 3:S34. doi: 10.1186/1471-2458-11-S3-S34. PubMed PMID: 21501453; PMCID: PMC3231908.
183. Rowe AK, Steketee RW. Predictions of the impact of malaria control efforts on all-cause child mortality in sub-Saharan Africa. *Am J Trop Med Hyg.* 2007;77(6 Suppl):48-55. PubMed PMID: 18165474.
184. Malkin EM, Durbin AP, Diemert DJ, Sattabongkot J, Wu Y, Miura K, Long CA, Lambert L, Miles AP, Wang J, Stowers A, Miller LH, Saul A. Phase 1 vaccine trial of Pvs25H: a transmission blocking vaccine for *Plasmodium vivax* malaria. *Vaccine.* 2005;23(24):3131-8. doi: 10.1016/j.vaccine.2004.12.019. PubMed PMID: 15837212.
185. Ranawaka GR, Fleck SL, Blanco AR, Sinden RE. Characterization of the modes of action of anti-Pbs21 malaria transmission-blocking immunity: ookinete to oocyst differentiation in vivo. *Parasitology.* 1994;109 (Pt 4):403-11. PubMed PMID: 7800408.
186. Sieber KP, Huber M, Kaslow D, Banks SM, Torii M, Aikawa M, Miller LH. The peritrophic membrane as a barrier: its penetration by *Plasmodium gallinaceum* and the effect of a monoclonal antibody to ookinetes. *Exp Parasitol.* 1991;72(2):145-56. PubMed PMID: 2009919.
187. Sauerwein RW, Bousema T. Transmission blocking malaria vaccines: Assays and candidates in clinical development. *Vaccine.* 2015;33(52):7476-82. doi: 10.1016/j.vaccine.2015.08.073. PubMed PMID: 26409813.

188. Gass RF, Yeates RA. In vitro damage of cultured ookinetes of *Plasmodium gallinaceum* by digestive proteinases from susceptible *Aedes aegypti*. *Acta Trop.* 1979;36(3):243-52. PubMed PMID: 43087.
189. Han YS, Thompson J, Kafatos FC, Barillas-Mury C. Molecular interactions between *Anopheles stephensi* midgut cells and *Plasmodium berghei*: the time bomb theory of ookinete invasion of mosquitoes. *EMBO J.* 2000;19(22):6030-40. doi: 10.1093/emboj/19.22.6030. PubMed PMID: 11080150; PMCID: PMC305834.
190. Vlachou D, Zimmermann T, Cantera R, Janse CJ, Waters AP, Kafatos FC. Real-time, in vivo analysis of malaria ookinete locomotion and mosquito midgut invasion. *Cell Microbiol.* 2004;6(7):671-85. doi: 10.1111/j.1462-5822.2004.00394.x. PubMed PMID: 15186403.
191. Zieler H, Dvorak JA. Invasion in vitro of mosquito midgut cells by the malaria parasite proceeds by a conserved mechanism and results in death of the invaded midgut cells. *Proc Natl Acad Sci U S A.* 2000;97(21):11516-21. doi: 10.1073/pnas.97.21.11516. PubMed PMID: 11027351; PMCID: PMC17232.
192. Arrighi RB, Hurd H. The role of *Plasmodium berghei* ookinete proteins in binding to basal lamina components and transformation into oocysts. *Int J Parasitol.* 2002;32(1):91-8. PubMed PMID: 11796126.
193. Vlachou D, Lycett G, Siden-Kiamos I, Blass C, Sinden RE, Louis C. *Anopheles gambiae* laminin interacts with the P25 surface protein of *Plasmodium berghei* ookinetes. *Mol Biochem Parasitol.* 2001;112(2):229-37. PubMed PMID: 11223130.
194. Duffy PE, Pimenta P, Kaslow DC. Pgs28 belongs to a family of epidermal growth factor-like antigens that are targets of malaria transmission-blocking antibodies. *J Exp Med.* 1993;177(2):505-10. PubMed PMID: 8426118; PMCID: PMC2190907.

195. Tomas AM, Margos G, Dimopoulos G, van Lin LH, de Koning-Ward TF, Sinha R, Lupetti P, Beetsma AL, Rodriguez MC, Karras M, Hager A, Mendoza J, Butcher GA, Kafatos F, Janse CJ, Waters AP, Sinden RE. P25 and P28 proteins of the malaria ookinete surface have multiple and partially redundant functions. *EMBO J.* 2001;20(15):3975-83. doi: 10.1093/emboj/20.15.3975. PubMed PMID: 11483501; PMCID: PMC149139.
196. Gozar MM, Price VL, Kaslow DC. *Saccharomyces cerevisiae*-secreted fusion proteins Pfs25 and Pfs28 elicit potent *Plasmodium falciparum* transmission-blocking antibodies in mice. *Infect Immun.* 1998;66(1):59-64. PubMed PMID: 9423839; PMCID: PMC107858.
197. Wu Y, Ellis RD, Shaffer D, Fontes E, Malkin EM, Mahanty S, Fay MP, Narum D, Rausch K, Miles AP, Aebig J, Orcutt A, Muratova O, Song G, Lambert L, Zhu D, Miura K, Long C, Saul A, Miller LH, Durbin AP. Phase 1 trial of malaria transmission blocking vaccine candidates Pfs25 and Pvs25 formulated with montanide ISA 51. *PLoS One.* 2008;3(7):e2636. Epub 2008/07/10. doi: 10.1371/journal.pone.0002636. PubMed PMID: 18612426; PMCID: PMC2440546.
198. Pradel G, Hayton K, Aravind L, Iyer LM, Abrahamsen MS, Bonawitz A, Mejia C, Templeton TJ. A multidomain adhesion protein family expressed in *Plasmodium falciparum* is essential for transmission to the mosquito. *J Exp Med.* 2004;199(11):1533-44. doi: 10.1084/jem.20031274. PubMed PMID: 15184503; PMCID: PMC2211786.
199. Trueman HE, Raine JD, Florens L, Dessens JT, Mendoza J, Johnson J, Waller CC, Delrieu I, Holders AA, Langhorne J, Carucci DJ, Yates JR, 3rd, Sinden RE. Functional characterization of an LCCL-lectin domain containing protein family in *Plasmodium berghei*. *J Parasitol.* 2004;90(5):1062-71. doi: 10.1645/GE-3368. PubMed PMID: 15562607.

200. Agnandji ST, Lell B, Soulanoudjingar SS, Fernandes JF, Abossolo BP, Conzelmann C, Methogo BG, Doucka Y, Flamen A, Mordmuller B, Issifou S, Kremsner PG, Sacarlal J, Aide P, Lanaspá M, Aponte JJ, Nhamuave A, Quelhas D, Bassat Q, Mandjate S, Macete E, Alonso P, Abdulla S, Salim N, Juma O, Shomari M, Shubis K, Machera F, Hamad AS, Minja R, Mtoro A, Sykes A, Ahmed S, Urassa AM, Ali AM, Mwangoka G, Tanner M, Tinto H, D'Alessandro U, Sorgho H, Valea I, Tahita MC, Kabore W, Ouedraogo S, Sandrine Y, Guiguemde RT, Ouedraogo JB, Hamel MJ, Kariuki S, Odero C, Oneko M, Otieno K, Awino N, Omoto J, Williamson J, Muturi-Kioi V, Laserson KF, Slutsker L, Otieno W, Otieno L, Nekoye O, Gondi S, Otieno A, Ogutu B, Wasuna R, Owira V, Jones D, Onyango AA, Njuguna P, Chilengi R, Akoo P, Kerubo C, Gitaka J, Maingi C, Lang T, Olotu A, Tsofa B, Bejon P, Peshu N, Marsh K, Owusu-Agyei S, Asante KP, Osei-Kwakye K, Boahen O, Ayamba S, Kayan K, Owusu-Ofori R, Dosoo D, Asante I, Adjei G, Adjei G, Chandramohan D, Greenwood B, Lusingu J, Gesase S, Malabeja A, Abdul O, Kilavo H, Mahende C, Liheluka E, Lemnge M, Theander T, Drakeley C, Ansong D, Agbenyega T, Adjei S, Boateng HO, Rettig T, Bawa J, Sylverken J, Sambian D, Agyekum A, Owusu L, Martinson F, Hoffman I, Mvalo T, Kamthunzi P, Nkomo R, Msika A, Jumbe A, Chome N, Nyakuipa D, Chintedza J, Ballou WR, Bruls M, Cohen J, Guerra Y, Jongert E, Lapierre D, Leach A, Lievens M, Ofori-Anyinam O, Vekemans J, Carter T, LeBoulleux D, Loucq C, Radford A, Savarese B, Schellenberg D, Sillman M, Vansadia P, Rts SCTP. First results of phase 3 trial of RTS,S/AS01 malaria vaccine in African children. *N Engl J Med*. 2011;365(20):1863-75. doi: 10.1056/NEJMoa1102287. PubMed PMID: 22007715.
201. Bejon P, White MT, Olotu A, Bojang K, Lusingu JPA, Salim N, Otsyula NN, Agnandji ST, Asante KP, Owusu-Agyei S, Abdulla S, Ghani AC. Efficacy of RTS,S malaria vaccines:

- individual-participant pooled analysis of phase 2 data. *Lancet Infect Dis.* 2013;13(4):319-27. doi: 10.1016/s1473-3099(13)70005-7. PubMed PMID: 23454164; PMCID: 23454164.
202. Moorthy VS, Ballou WR. Immunological mechanisms underlying protection mediated by RTS,S: a review of the available data. *Malar J.* 2009;8:312. Epub 2010/01/01. doi: 10.1186/1475-2875-8-312. PubMed PMID: 20042088; PMCID: PMC2806383.
203. Silva-Flannery LM, Cabrera-Mora M, Jiang J, Moreno A. Recombinant peptide replicates immunogenicity of synthetic linear peptide chimera for use as pre-erythrocytic stage malaria vaccine. *Microbes Infect.* 2009;11(1):83-91. doi: 10.1016/j.micinf.2008.10.009. PubMed PMID: 19015042; PMCID: 19015042.
204. Singh B, Cabrera-Mora M, Jiang J, Galinski M, Moreno A. Genetic linkage of autologous T cell epitopes in a chimeric recombinant construct improves anti-parasite and anti-disease protective effect of a malaria vaccine candidate. *Vaccine.* 2010;28(14):2580-92. Epub 2010/01/26. doi: 10.1016/j.vaccine.2010.01.019. PubMed PMID: 20097151; PMCID: PMC2844075.
205. Roy S, Zhi Y, Kobinger GP, Figueredo J, Calcedo R, Miller JR, Feldmann H, Wilson JM. Generation of an adenoviral vaccine vector based on simian adenovirus 21. *The Journal of general virology.* 2006;87(Pt 9):2477-85. doi: 10.1099/vir.0.81989-0. PubMed PMID: 16894185.
206. Chirmule N, Propert K, Magosin S, Qian Y, Qian R, Wilson J. Immune responses to adenovirus and adeno-associated virus in humans. *Gene Ther.* 1999;6(9):1574-83. doi: 10.1038/sj.gt.3300994. PubMed PMID: 10490767; PMCID: 10490767.
207. Hayton EJ, Rose A, Ibrahimsa U, Del Sorbo M, Capone S, Crook A, Black AP, Dorrell L, Hanke T. Safety and tolerability of conserved region vaccines vectored by plasmid DNA, simian adenovirus and modified vaccinia virus ankara administered to human immunodeficiency

- virus type 1-uninfected adults in a randomized, single-blind phase I trial. *PLoS One*. 2014;9(7):e101591. doi: 10.1371/journal.pone.0101591. PubMed PMID: 25007091; PMCID: 4090156.
208. Roy S, Medina-Jaszek A, Wilson MJ, Sandhu A, Calcedo R, Lin J, Wilson JM. Creation of a panel of vectors based on ape adenovirus isolates. *J Gene Med*. 2011;13(1):17-25. doi: 10.1002/jgm.1530. PubMed PMID: 21259405.
209. Kobinger GP, Feldmann H, Zhi Y, Schumer G, Gao G, Feldmann F, Jones S, Wilson JM. Chimpanzee adenovirus vaccine protects against Zaire Ebola virus. *Virology*. 2006;346(2):394-401. doi: 10.1016/j.virol.2005.10.042. PubMed PMID: 16356525.
210. Ledgerwood JE, DeZure AD, Stanley DA, Novik L, Enama ME, Berkowitz NM, Hu Z, Joshi G, Ploquin A, Sitar S, Gordon IJ, Plummer SA, Holman LA, Hendel CS, Yamshchikov G, Roman F, Nicosia A, Colloca S, Cortese R, Bailer RT, Schwartz RM, Roederer M, Mascola JR, Koup RA, Sullivan NJ, Graham BS, the VRCST. Chimpanzee Adenovirus Vector Ebola Vaccine - Preliminary Report. *N Engl J Med*. 2014. doi: 10.1056/NEJMoa1410863. PubMed PMID: 25426834.
211. Barnes E, Folgori A, Capone S, Swadling L, Aston S, Kurioka A, Meyer J, Huddart R, Smith K, Townsend R, Brown A, Antrobus R, Ammendola V, Naddeo M, O'Hara G, Willberg C, Harrison A, Grazioli F, Esposito ML, Siani L, Traboni C, Oo Y, Adams D, Hill A, Colloca S, Nicosia A, Cortese R, Klenerman P. Novel adenovirus-based vaccines induce broad and sustained T cell responses to HCV in man. *Sci Transl Med*. 2012;4(115):115ra1. doi: 10.1126/scitranslmed.3003155. PubMed PMID: 22218690; PMCID: 3627207.
212. Reyes-Sandoval A, Berthoud T, Alder N, Siani L, Gilbert SC, Nicosia A, Colloca S, Cortese R, Hill AVS. Prime-boost immunization with adenoviral and modified vaccinia virus

Ankara vectors enhances the durability and polyfunctionality of protective malaria CD8+ T-cell responses. *Infect Immun.* 2010;78(1):145-53. doi: 10.1128/iai.00740-09. PubMed PMID:

19858306; PMCID: 19858306.

213. Sheehy SH, Duncan CJ, Elias SC, Biswas S, Collins KA, O'Hara GA, Halstead FD, Ewer KJ, Mahungu T, Spencer AJ, Miura K, Poulton ID, Dicks MD, Edwards NJ, Berrie E, Moyle S, Colloca S, Cortese R, Gantlett K, Long CA, Lawrie AM, Gilbert SC, Doherty T, Nicosia A, Hill AV, Draper SJ. Phase Ia clinical evaluation of the safety and immunogenicity of the *Plasmodium falciparum* blood-stage antigen AMA1 in ChAd63 and MVA vaccine vectors. *PLoS One.*

2012;7(2):e31208. doi: 10.1371/journal.pone.0031208. PubMed PMID: 22363582; PMCID: 3283618.

214. Sheehy SH, Duncan CJ, Elias SC, Collins KA, Ewer KJ, Spencer AJ, Williams AR, Halstead FD, Moretz SE, Miura K, Epp C, Dicks MD, Poulton ID, Lawrie AM, Berrie E, Moyle S, Long CA, Colloca S, Cortese R, Gilbert SC, Nicosia A, Hill AV, Draper SJ. Phase Ia clinical evaluation of the *Plasmodium falciparum* blood-stage antigen MSP1 in ChAd63 and MVA

vaccine vectors. *Mol Ther.* 2011;19(12):2269-76. doi: 10.1038/mt.2011.176. PubMed PMID: 21862998; PMCID: 3242658.

215. Seki T, Dmitriev I, Kashentseva E, Takayama K, Rots M, Suzuki K, Curiel DT. Artificial extension of the adenovirus fiber shaft inhibits infectivity in coxsackievirus and adenovirus receptor-positive cell lines. *J Virol.* 2002;76(3):1100-8. PubMed PMID: 11773386; PMCID: PMC135866.

216. Kashentseva EA, Douglas JT, Zinn KR, Curiel DT, Dmitriev IP. Targeting of adenovirus serotype 5 pseudotyped with short fiber from serotype 41 to c-erbB2-positive cells using

- bispecific single-chain diabody. *J Mol Biol.* 2009;388(3):443-61. doi: 10.1016/j.jmb.2009.03.016. PubMed PMID: 19285990; PMCID: PMC2696239.
217. Maizel JV, Jr., White DO, Scharff MD. The polypeptides of adenovirus. I. Evidence for multiple protein components in the virion and a comparison of types 2, 7A, and 12. *Virology.* 1968;36(1):115-25. PubMed PMID: 5669982.
218. Caro-Aguilar I, Lapp S, Pohl J, Galinski MR, Moreno A. Chimeric epitopes delivered by polymeric synthetic linear peptides induce protective immunity to malaria. *Microbes Infect.* 2005;7(13):1324-37. doi: 10.1016/j.micinf.2005.04.020. PubMed PMID: 16253535.
219. Ferreira MU, Katzin AM. The assessment of antibody affinity distribution by thiocyanate elution: a simple dose-response approach. *Journal of immunological methods.* 1995;187(2):297-305. PubMed PMID: 7499889.
220. Caro-Aguilar I, Rodriguez A, Calvo-Calle JM, Guzman F, De la Vega P, Patarroyo ME, Galinski MR, Moreno A. Plasmodium vivax promiscuous T-helper epitopes defined and evaluated as linear peptide chimera immunogens. *Infect Immun.* 2002;70(7):3479-92. Epub 2002/06/18. PubMed PMID: 12065487; PMCID: PMC128085.
221. Perciani CT, Peixoto PS, Dias WO, Kubrusly FS, Tanizaki MM. Improved method to calculate the antibody avidity index. *J Clin Lab Anal.* 2007;21(3):201-6. Epub 2007/05/18. doi: 10.1002/jcla.20172. PubMed PMID: 17506479.
222. Butler NS, Moebius J, Pewe LL, Traore B, Doumbo OK, Tygrett LT, Waldschmidt TJ, Crompton PD, Harty JT. Therapeutic blockade of PD-L1 and LAG-3 rapidly clears established blood-stage Plasmodium infection. *Nat Immunol.* 2012;13(2):188-95. doi: 10.1038/ni.2180. PubMed PMID: 22157630; PMCID: 3262959.

223. Roederer M, Nozzi JL, Nason MC. SPICE: exploration and analysis of post-cytometric complex multivariate datasets. *Cytometry A*. 2011;79(2):167-74. doi: 10.1002/cyto.a.21015. PubMed PMID: 21265010; PMCID: PMC3072288.
224. Bewley MC, Springer K, Zhang YB, Freimuth P, Flanagan JM. Structural analysis of the mechanism of adenovirus binding to its human cellular receptor, CAR. *Science*. 1999;286(5444):1579-83. PubMed PMID: 10567268.
225. Cohen CJ, Xiang ZQ, Gao GP, Ertl HC, Wilson JM, Bergelson JM. Chimpanzee adenovirus CV-68 adapted as a gene delivery vector interacts with the coxsackievirus and adenovirus receptor. *The Journal of general virology*. 2002;83(Pt 1):151-5. doi: 10.1099/0022-1317-83-1-151. PubMed PMID: 11752711.
226. Stanistic DI, Richards JS, McCallum FJ, Michon P, King CL, Schoepflin S, Gilson PR, Murphy VJ, Anders RF, Mueller I, Beeson JG. Immunoglobulin G subclass-specific responses against *Plasmodium falciparum* merozoite antigens are associated with control of parasitemia and protection from symptomatic illness. *Infection and immunity*. 2009;77(3):1165-74. doi: 10.1128/IAI.01129-08. PubMed PMID: 19139189; PMCID: PMC2643653.
227. Schwenk R, DeBot M, Porter M, Nikki J, Rein L, Spaccapelo R, Crisanti A, Wightman PD, Ockenhouse CF, Dutta S. IgG2 antibodies against a clinical grade *Plasmodium falciparum* CSP vaccine antigen associate with protection against transgenic sporozoite challenge in mice. *PLoS One*. 2014;9(10):e111020. doi: 10.1371/journal.pone.0111020. PubMed PMID: 25343487; PMCID: PMC4208815.
228. Sun P, Schwenk R, White K, Stoute JA, Cohen J, Ballou WR, Voss G, Kester KE, Heppner DG, Krzych U. Protective immunity induced with malaria vaccine, RTS,S, is linked to

Plasmodium falciparum circumsporozoite protein-specific CD4⁺ and CD8⁺ T cells producing IFN-gamma. *J Immunol.* 2003;171(12):6961-7. PubMed PMID: 14662904.

229. Pombo DJ, Lawrence G, Hirunpetcharat C, Rzepczyk C, Bryden M, Cloonan N, Anderson K, Mahakunkijcharoen Y, Martin LB, Wilson D, Elliott S, Elliott S, Eisen DP, Weinberg JB, Saul A, Good MF. Immunity to malaria after administration of ultra-low doses of red cells infected with *Plasmodium falciparum*. *Lancet.* 2002;360(9333):610-7. Epub 2002/09/21. doi: 10.1016/S0140-6736(02)09784-2. PubMed PMID: 12241933.

230. Roestenberg M, McCall M, Hopman J, Wiersma J, Luty AJ, van Gemert GJ, van de Vegte-Bolmer M, van Schaijk B, Teelen K, Arens T, Spaarman L, de Mast Q, Roeffen W, Snounou G, Renia L, van der Ven A, Hermsen CC, Sauerwein R. Protection against a malaria challenge by sporozoite inoculation. *N Engl J Med.* 2009;361(5):468-77. Epub 2009/07/31. doi: 10.1056/NEJMoa0805832. PubMed PMID: 19641203.

231. Schuldt NJ, Amalfitano A. Malaria vaccines: focus on adenovirus based vectors. *Vaccine.* 2012;30(35):5191-8. doi: 10.1016/j.vaccine.2012.05.048. PubMed PMID: 22683663.

232. Tatsis N, Fitzgerald JC, Reyes-Sandoval A, Harris-McCoy KC, Hensley SE, Zhou D, Lin SW, Bian A, Xiang ZQ, Iparraguirre A, Lopez-Camacho C, Wherry EJ, Ertl HC. Adenoviral vectors persist in vivo and maintain activated CD8⁺ T cells: implications for their use as vaccines. *Blood.* 2007;110(6):1916-23. doi: 10.1182/blood-2007-02-062117. PubMed PMID: 17510320; PMCID: PMC1976365.

233. Butterfield LH, Comin-Anduix B, Vujanovic L, Lee Y, Dissette VB, Yang JQ, Vu HT, Seja E, Oseguera DK, Potter DM, Glaspy JA, Economou JS, Ribas A. Adenovirus MART-1-engineered autologous dendritic cell vaccine for metastatic melanoma. *J Immunother.* 2008;31(3):294-309. Epub 2008/03/05. doi: 10.1097/CJI.0b013e31816a8910

00002371-200804000-00008 [pii]. PubMed PMID: 18317358; PMCID: 3651040.

234. Santosuosso M, McCormick S, Xing Z. Adenoviral vectors for mucosal vaccination against infectious diseases. *Viral Immunol.* 2005;18(2):283-91. Epub 2005/07/23. doi: 10.1089/vim.2005.18.283. PubMed PMID: 16035940.

235. Abbink P, Lemckert AA, Ewald BA, Lynch DM, Denholtz M, Smits S, Holterman L, Damen I, Vogels R, Thorner AR, O'Brien KL, Carville A, Mansfield KG, Goudsmit J, Havenga MJ, Barouch DH. Comparative seroprevalence and immunogenicity of six rare serotype recombinant adenovirus vaccine vectors from subgroups B and D. *J Virol.* 2007;81(9):4654-63. doi: 10.1128/JVI.02696-06. PubMed PMID: 17329340; PMCID: 1900173.

236. Porter MD, Nicki J, Pool CD, DeBot M, Illam RM, Brando C, Bozick B, De La Vega P, Angra D, Spaccapelo R, Crisanti A, Murphy JR, Bennett JW, Schwenk RJ, Ockenhouse CF, Dutta S. Transgenic parasites stably expressing full-length *Plasmodium falciparum* circumsporozoite protein as a model for vaccine down-selection in mice using sterile protection as an endpoint. *Clin Vaccine Immunol.* 2013;20(6):803-10. doi: 10.1128/cvi.00066-13. PubMed PMID: 23536694; PMCID: PMC3675977.

237. Penaloza-MacMaster P, Provine NM, Ra J, Borducchi EN, McNally A, Simmons NL, Iampietro MJ, Barouch DH. Alternative serotype adenovirus vaccine vectors elicit memory T cells with enhanced anamnestic capacity compared to Ad5 vectors. *J Virol.* 2013;87(3):1373-84. doi: 10.1128/JVI.02058-12. PubMed PMID: 23152535; PMCID: PMC3554181.

238. Overstreet MG, Cockburn IA, Chen YC, Zavala F. Protective CD8 T cells against *Plasmodium* liver stages: immunobiology of an 'unnatural' immune response. *Immunol Rev.* 2008;225:272-83. doi: 10.1111/j.1600-065X.2008.00671.x. PubMed PMID: 18837788; PMCID: PMC2597001.

239. Douglas AD, de Cassan SC, Dicks MD, Gilbert SC, Hill AV, Draper SJ. Tailoring subunit vaccine immunogenicity: maximizing antibody and T cell responses by using combinations of adenovirus, poxvirus and protein-adjuvant vaccines against *Plasmodium falciparum* MSP1. *Vaccine*. 2010;28(44):7167-78. doi: 10.1016/j.vaccine.2010.08.068. PubMed PMID: 20937436; PMCID: 3404461.
240. Antrobus RD, Coughlan L, Berthoud TK, Dicks MD, Hill AV, Lambe T, Gilbert SC. Clinical assessment of a novel recombinant simian adenovirus ChAdOx1 as a vectored vaccine expressing conserved Influenza A antigens. *Mol Ther*. 2014;22(3):668-74. doi: 10.1038/mt.2013.284. PubMed PMID: 24374965; PMCID: PMC3944330.
241. Vogels R, Zuijdgeest D, van Rijnsoever R, Hartkoorn E, Damen I, de Bethune MP, Kostense S, Penders G, Helmus N, Koudstaal W, Cecchini M, Wetterwald A, Sprangers M, Lemckert A, Ophorst O, Koel B, van Meerendonk M, Quax P, Panitti L, Grimbergen J, Bout A, Goudsmit J, Havenga M. Replication-deficient human adenovirus type 35 vectors for gene transfer and vaccination: efficient human cell infection and bypass of preexisting adenovirus immunity. *J Virol*. 2003;77(15):8263-71. PubMed PMID: 12857895; PMCID: 165227.
242. Shott JP, McGrath SM, Pau MG, Custers JH, Ophorst O, Demoitie MA, Dubois MC, Komisar J, Cobb M, Kester KE, Dubois P, Cohen J, Goudsmit J, Heppner DG, Stewart VA. Adenovirus 5 and 35 vectors expressing *Plasmodium falciparum* circumsporozoite surface protein elicit potent antigen-specific cellular IFN-gamma and antibody responses in mice. *Vaccine*. 2008;26(23):2818-23. doi: 10.1016/j.vaccine.2008.03.080. PubMed PMID: 18455276.
243. McCall MB, Sauerwein RW. Interferon-gamma--central mediator of protective immune responses against the pre-erythrocytic and blood stage of malaria. *J Leukoc Biol*. 2010;88(6):1131-43. Epub 2010/07/09. doi: 10.1189/jlb.0310137. PubMed PMID: 20610802.

244. Cohen S, Mc GI, Carrington S. Gamma-globulin and acquired immunity to human malaria. *Nature*. 1961;192:733-7. Epub 1961/11/25. PubMed PMID: 13880318.
245. Greenwood B, Dicko A, Sagara I, Zongo I, Tinto H, Cairns M, Kuepfer I, Milligan P, Ouedraogo JB, Doumbo O, Chandramohan D. Seasonal vaccination against malaria: a potential use for an imperfect malaria vaccine. *Malar J*. 2017;16(1):182. doi: 10.1186/s12936-017-1841-9. PubMed PMID: 28464937; PMCID: PMC5414195.
246. Coughlan L, Mullarkey C, Gilbert S. Adenoviral vectors as novel vaccines for influenza. *J Pharm Pharmacol*. 2015;67(3):382-99. doi: 10.1111/jphp.12350. PubMed PMID: 25560474.
247. Appaiahgari MB, Vrati S. Adenoviruses as gene/vaccine delivery vectors: promises and pitfalls. *Expert Opin Biol Ther*. 2015;15(3):337-51. doi: 10.1517/14712598.2015.993374. PubMed PMID: 25529044.
248. Majhen D, Calderon H, Chandra N, Fajardo CA, Rajan A, Alemany R, Custers J. Adenovirus-based vaccines for fighting infectious diseases and cancer: progress in the field. *Hum Gene Ther*. 2014;25(4):301-17. doi: 10.1089/hum.2013.235. PubMed PMID: 24580050.
249. Capone S, D'Alise AM, Ammendola V, Colloca S, Cortese R, Nicosia A, Folgori A. Development of chimpanzee adenoviruses as vaccine vectors: challenges and successes emerging from clinical trials. *Expert Rev Vaccines*. 2013;12(4):379-93. doi: 10.1586/erv.13.15. PubMed PMID: 23560919.
250. Fonseca JA, McCaffery JN, Kashentseva E, Singh B, Dmitriev IP, Curiel DT, Moreno A. A prime-boost immunization regimen based on a simian adenovirus 36 vectored multi-stage malaria vaccine induces protective immunity in mice. *Vaccine*. 2017;35(24):3239-48. Epub 2017/05/10. doi: 10.1016/j.vaccine.2017.04.062. PubMed PMID: 28483199; PMCID: PMC5522619.

251. Ewer KJ, O'Hara GA, Duncan CJ, Collins KA, Sheehy SH, Reyes-Sandoval A, Goodman AL, Edwards NJ, Elias SC, Halstead FD, Longley RJ, Rowland R, Poulton ID, Draper SJ, Blagborough AM, Berrie E, Moyle S, Williams N, Siani L, Folgori A, Colloca S, Sinden RE, Lawrie AM, Cortese R, Gilbert SC, Nicosia A, Hill AV. Protective CD8⁺ T-cell immunity to human malaria induced by chimpanzee adenovirus-MVA immunisation. *Nat Commun.* 2013;4:2836. Epub 2013/11/29. doi: 10.1038/ncomms3836. PubMed PMID: 24284865; PMCID: PMC3868203.
252. Lee J, Hashimoto M, Im SJ, Araki K, Jin HT, Davis CW, Konieczny BT, Spies GA, McElrath MJ, Ahmed R. Adenovirus Serotype 5 Vaccination Results in Suboptimal CD4 T Helper 1 Responses in Mice. *J Virol.* 2017;91(5). doi: 10.1128/JVI.01132-16. PubMed PMID: 28003483; PMCID: PMC5309930.
253. Hegde RS, Bernstein HD. The surprising complexity of signal sequences. *Trends Biochem Sci.* 2006;31(10):563-71. doi: 10.1016/j.tibs.2006.08.004. PubMed PMID: 16919958.
254. Guler-Gane G, Kidd S, Sridharan S, Vaughan TJ, Wilkinson TC, Tigue NJ. Overcoming the Refractory Expression of Secreted Recombinant Proteins in Mammalian Cells through Modification of the Signal Peptide and Adjacent Amino Acids. *PLoS One.* 2016;11(5):e0155340. doi: 10.1371/journal.pone.0155340. PubMed PMID: 27195765; PMCID: PMC4873207.
255. Liu H, Zou X, Li T, Wang X, Yuan W, Chen Y, Han W. Enhanced production of secretory glycoprotein VSTM1-v2 with mouse IgGkappa signal peptide in optimized HEK293F transient transfection. *J Biosci Bioeng.* 2016;121(2):133-9. doi: 10.1016/j.jbiosc.2015.05.016. PubMed PMID: 26140918.

256. Wang X, Liu H, Yuan W, Cheng Y, Han W. Efficient production of CYTL1 protein using mouse IgGkappa signal peptide in the CHO cell expression system. *Acta Biochim Biophys Sin (Shanghai)*. 2016;48(4):391-4. doi: 10.1093/abbs/gmw007. PubMed PMID: 26922322; PMCID: PMC4886246.
257. Bair CR, Kotha Lakshmi Narayan P, Kajon AE. The tripartite leader sequence is required for ectopic expression of HAdV-B and HAdV-E E3 CR1 genes. *Virology*. 2017;505:139-47. doi: 10.1016/j.virol.2017.02.021. PubMed PMID: 28259047.
258. Chandra J, Dutton JL, Li B, Woo WP, Xu Y, Tolley LK, Yong M, Wells JW, G RL, Finlayson N, Frazer IH. DNA Vaccine Encoding HPV16 Oncogenes E6 and E7 Induces Potent Cell-mediated and Humoral Immunity Which Protects in Tumor Challenge and Drives E7-expressing Skin Graft Rejection. *J Immunother*. 2017;40(2):62-70. doi: 10.1097/CJI.000000000000156. PubMed PMID: 28166181; PMCID: PMC5293162.
259. Fonseca JA, Cabrera-Mora M, Singh B, Oliveira-Ferreira J, da Costa Lima-Junior J, Calvo-Calle JM, Lozano JM, Moreno A. A chimeric protein-based malaria vaccine candidate induces robust T cell responses against *Plasmodium vivax* MSP119. *Sci Rep*. 2016;6:34527. Epub 2016/10/07. doi: 10.1038/srep34527. PubMed PMID: 27708348; PMCID: PMC5052570.
260. Mills CD, Kincaid K, Alt JM, Heilman MJ, Hill AM. M-1/M-2 macrophages and the Th1/Th2 paradigm. *J Immunol*. 2000;164(12):6166-73. Epub 2000/06/08. PubMed PMID: 10843666.
261. Matheu MP, Parker I, Cahalan MD. Dissection and 2-photon imaging of peripheral lymph nodes in mice. *J Vis Exp*. 2007(7):265. Epub 2008/11/08. doi: 10.3791/265. PubMed PMID: 18989436; PMCID: PMC2565854.

262. Mac-Daniel L, Buckwalter MR, Gueirard P, Menard R. Myeloid Cell Isolation from Mouse Skin and Draining Lymph Node Following Intradermal Immunization with Live Attenuated Plasmodium Sporozoites. *J Vis Exp.* 2016(111). Epub 2016/06/11. doi: 10.3791/53796. PubMed PMID: 27286053.
263. Li Y, Leneghan DB, Miura K, Nikolaeva D, Brian IJ, Dicks MD, Fyfe AJ, Zakutansky SE, de Cassan S, Long CA, Draper SJ, Hill AV, Hill F, Biswas S. Enhancing immunogenicity and transmission-blocking activity of malaria vaccines by fusing Pfs25 to IMX313 multimerization technology. *Sci Rep.* 2016;6:18848. Epub 2016/01/09. doi: 10.1038/srep18848. PubMed PMID: 26743316; PMCID: PMC4705524.
264. McGowan JW, Bidwell GL, 3rd. The Use of Ex Vivo Whole-organ Imaging and Quantitative Tissue Histology to Determine the Bio-distribution of Fluorescently Labeled Molecules. *J Vis Exp.* 2016(118). Epub 2017/01/07. doi: 10.3791/54987. PubMed PMID: 28060286; PMCID: PMC5226456.
265. Espinosa DA, Yadava A, Angov E, Maurizio PL, Ockenhouse CF, Zavala F. Development of a chimeric Plasmodium berghei strain expressing the repeat region of the P. vivax circumsporozoite protein for in vivo evaluation of vaccine efficacy. *Infect Immun.* 2013;81(8):2882-7. doi: 10.1128/IAI.00461-13. PubMed PMID: 23716612; PMCID: PMC3719583.
266. Kazmin D, Nakaya HI, Lee EK, Johnson MJ, van der Most R, van den Berg RA, Ballou WR, Jongert E, Wille-Reece U, Ockenhouse C, Aderem A, Zak DE, Sadoff J, Hendriks J, Wrammert J, Ahmed R, Pulendran B. Systems analysis of protective immune responses to RTS,S malaria vaccination in humans. *Proc Natl Acad Sci U S A.* 2017;114(9):2425-30. doi: 10.1073/pnas.1621489114. PubMed PMID: 28193898; PMCID: PMC5338562.

267. Rodrigues EG, Zavala F, Nussenzweig RS, Wilson JM, Tsuji M. Efficient induction of protective anti-malaria immunity by recombinant adenovirus. *Vaccine*. 1998;16(19):1812-7. PubMed PMID: 9795385.
268. Stewart VA, McGrath SM, Dubois PM, Pau MG, Mettens P, Shott J, Cobb M, Burge JR, Larson D, Ware LA, Demoitie MA, Weverling GJ, Bayat B, Custers JH, Dubois MC, Cohen J, Goudsmit J, Heppner DG, Jr. Priming with an adenovirus 35-circumsporozoite protein (CS) vaccine followed by RTS,S/AS01B boosting significantly improves immunogenicity to *Plasmodium falciparum* CS compared to that with either malaria vaccine alone. *Infect Immun*. 2007;75(5):2283-90. doi: 10.1128/IAI.01879-06. PubMed PMID: 17307942; PMCID: PMC1865796.
269. Rodriguez A, Mintardjo R, Tax D, Gillissen G, Custers J, Pau MG, Klap J, Santra S, Balachandran H, Letvin NL, Goudsmit J, Radosevic K. Evaluation of a prime-boost vaccine schedule with distinct adenovirus vectors against malaria in rhesus monkeys. *Vaccine*. 2009;27(44):6226-33. doi: 10.1016/j.vaccine.2009.07.106. PubMed PMID: 19686691.
270. O'Hara GA, Duncan CJ, Ewer KJ, Collins KA, Elias SC, Halstead FD, Goodman AL, Edwards NJ, Reyes-Sandoval A, Bird P, Rowland R, Sheehy SH, Poulton ID, Hutchings C, Todryk S, Andrews L, Folgori A, Berrie E, Moyle S, Nicosia A, Colloca S, Cortese R, Siani L, Lawrie AM, Gilbert SC, Hill AV. Clinical assessment of a recombinant simian adenovirus ChAd63: a potent new vaccine vector. *J Infect Dis*. 2012;205(5):772-81. doi: 10.1093/infdis/jir850. PubMed PMID: 22275401; PMCID: PMC3274376.
271. Yolitz J, Schwing C, Chang J, Van Ryk D, Nawaz F, Wei D, Cicala C, Arthos J, Fauci AS. Signal peptide of HIV envelope protein impacts glycosylation and antigenicity of gp120.

Proc Natl Acad Sci U S A. 2018;115(10):2443-8. Epub 2018/02/22. doi:

10.1073/pnas.1722627115. PubMed PMID: 29463753.

272. Massa S, Paolini F, Curzio G, Cordeiro MN, Illiano E, Demurtas OC, Franconi R, Venuti A. A plant protein signal sequence improved humoral immune response to HPV prophylactic and therapeutic DNA vaccines. *Hum Vaccin Immunother.* 2017;13(2):271-82. Epub 2017/01/25. doi: 10.1080/21645515.2017.1264766. PubMed PMID: 28118086; PMCID: PMC5328226.

273. Gunn BM, Alter G. Modulating Antibody Functionality in Infectious Disease and Vaccination. *Trends Mol Med.* 2016;22(11):969-82. Epub 2016/10/21. doi: 10.1016/j.molmed.2016.09.002. PubMed PMID: 27756530.

274. Chung AW, Kumar MP, Arnold KB, Yu WH, Schoen MK, Dunphy LJ, Suscovich TJ, Frahm N, Linde C, Mahan AE, Hoffner M, Streeck H, Ackerman ME, McElrath MJ, Schuitemaker H, Pau MG, Baden LR, Kim JH, Michael NL, Barouch DH, Lauffenburger DA, Alter G. Dissecting Polyclonal Vaccine-Induced Humoral Immunity against HIV Using Systems Serology. *Cell.* 2015;163(4):988-98. Epub 2015/11/07. doi: 10.1016/j.cell.2015.10.027. PubMed PMID: 26544943; PMCID: PMC5490491.

275. Mahan AE, Jennewein MF, Suscovich T, Dionne K, Tedesco J, Chung AW, Streeck H, Pau M, Schuitemaker H, Francis D, Fast P, Laufer D, Walker BD, Baden L, Barouch DH, Alter G. Antigen-Specific Antibody Glycosylation Is Regulated via Vaccination. *PLoS Pathog.* 2016;12(3):e1005456. Epub 2016/03/18. doi: 10.1371/journal.ppat.1005456. PubMed PMID: 26982805; PMCID: PMC4794126.

276. Davies J, Jiang L, Pan LZ, LaBarre MJ, Anderson D, Reff M. Expression of GnTIII in a recombinant anti-CD20 CHO production cell line: Expression of antibodies with altered

glycoforms leads to an increase in ADCC through higher affinity for FC gamma RIII. *Biotechnol Bioeng.* 2001;74(4):288-94. Epub 2001/06/19. PubMed PMID: 11410853.

277. Druilhe P, Spertini F, Soesoe D, Corradin G, Mejia P, Singh S, Audran R, Bouzidi A, Oeuvray C, Roussilhon C. A malaria vaccine that elicits in humans antibodies able to kill *Plasmodium falciparum*. *PLoS Med.* 2005;2(11):e344. Epub 2005/11/03. doi: 10.1371/journal.pmed.0020344. PubMed PMID: 16262450; PMCID: PMC1277929.

278. Liao W, Lin JX, Leonard WJ. Interleukin-2 at the crossroads of effector responses, tolerance, and immunotherapy. *Immunity.* 2013;38(1):13-25. doi: 10.1016/j.immuni.2013.01.004. PubMed PMID: 23352221; PMCID: PMC3610532.

279. Figueiredo MM, Costa PAC, Diniz SQ, Henriques PM, Kano FS, Tada MS, Pereira DB, Soares IS, Martins-Filho OA, Jankovic D, Gazzinelli RT, Antonelli L. T follicular helper cells regulate the activation of B lymphocytes and antibody production during *Plasmodium vivax* infection. *PLoS Pathog.* 2017;13(7):e1006484. Epub 2017/07/13. doi: 10.1371/journal.ppat.1006484. PubMed PMID: 28700710; PMCID: PMC5519210.

280. Perez-Mazliah D, Nguyen MP, Hosking C, McLaughlin S, Lewis MD, Tumwine I, Levy P, Langhorne J. Follicular Helper T Cells are Essential for the Elimination of *Plasmodium* Infection. *EBioMedicine.* 2017;24:216-30. Epub 2017/09/11. doi: 10.1016/j.ebiom.2017.08.030. PubMed PMID: 28888925; PMCID: PMC5652023.

281. Perez-Mazliah D, Ng DH, Freitas do Rosario AP, McLaughlin S, Mastelic-Gavillet B, Sodenkamp J, Kushinga G, Langhorne J. Disruption of IL-21 signaling affects T cell-B cell interactions and abrogates protective humoral immunity to malaria. *PLoS Pathog.* 2015;11(3):e1004715. Epub 2015/03/13. doi: 10.1371/journal.ppat.1004715. PubMed PMID: 25763578; PMCID: PMC4370355.

282. Guerra CA, Howes RE, Patil AP, Gething PW, Van Boeckel TP, Temperley WH, Kabaria CW, Tatem AJ, Manh BH, Elyazar IRF, Baird JK, Snow RW, Hay SI. The International Limits and Population at Risk of *Plasmodium vivax* Transmission in 2009. Plos Neglected Tropical Diseases. 2010;4(8):e774. doi: ARTN e774
DOI 10.1371/journal.pntd.0000774. PubMed PMID: WOS:000281443200006.
283. World Health Organization. World malaria report 2014. Geneva: World Health Organization; 2014. 253 p.
284. Krotoski WA, Garnham PC, Bray RS, Krotoski DM, Killick-Kendrick R, Draper CC, Targett GA, Guy MW. Observations on early and late post-sporozoite tissue stages in primate malaria. I. Discovery of a new latent form of *Plasmodium cynomolgi* (the hypnozoite), and failure to detect hepatic forms within the first 24 hours after infection. Am J Trop Med Hyg. 1982;31(1):24-35.
285. Battle KE, Gething PW, Elyazar IR, Moyes CL, Sinka ME, Howes RE, Guerra CA, Price RN, Baird KJ, Hay SI. The global public health significance of *Plasmodium vivax*. Advances in parasitology. 2012;80:1-111. Epub 2012/12/04. doi: 10.1016/B978-0-12-397900-1.00001-3. PubMed PMID: 23199486.
286. Gething PW, Elyazar IR, Moyes CL, Smith DL, Battle KE, Guerra CA, Patil AP, Tatem AJ, Howes RE, Myers MF, George DB, Horby P, Wertheim HF, Price RN, Mueller I, Baird JK, Hay SI. A long neglected world malaria map: *Plasmodium vivax* endemicity in 2010. PLoS Negl Trop Dis. 2012;6(9):e1814. doi: 10.1371/journal.pntd.0001814. PubMed PMID: 22970336; PMCID: 3435256.

287. Mendis K, Rietveld A, Warsame M, Bosman A, Greenwood B, Wernsdorfer WH. From malaria control to eradication: The WHO perspective. *Tropical Medicine & International Health*. 2009;14(7):802-9.
288. Bockarie MJ, Dagoro H. Are insecticide-treated bednets more protective against *Plasmodium falciparum* than *Plasmodium vivax*-infected mosquitoes? *Malar J*. 2006;5:15. doi: 10.1186/1475-2875-5-15. PubMed PMID: 16504027; PMCID: 1388224.
289. Dondorp AM, Nosten F, Yi P, Das D, Phyo AP, Tarning J, Lwin KM, Ariey F, Hanpithakpong W, Lee SJ, Ringwald P, Silamut K, Imwong M, Chotivanich K, Lim P, Herdman T, An SS, Yeung S, Singhasivanon P, Day NP, Lindegardh N, Socheat D, White NJ. Artemisinin resistance in *Plasmodium falciparum* malaria. *N Engl J Med*. 2009;361(5):455-67. Epub 2009/07/31. doi: 10.1056/NEJMoa0808859. PubMed PMID: 19641202; PMCID: 3495232.
290. Corbel V, N'Guessan R, Brengues C, Chandre F, Djogbenou L, Martin T, Akogbeto M, Hougard JM, Rowland M. Multiple insecticide resistance mechanisms in *Anopheles gambiae* and *Culex quinquefasciatus* from Benin, West Africa. *Acta Trop*. 2007;101(3):207-16. Epub 2007/03/16. doi: S0001-706X(07)00051-4 [pii] 10.1016/j.actatropica.2007.01.005. PubMed PMID: 17359927.
291. Haldar K, Bhattacharjee S, Safeukui I. Drug resistance in *Plasmodium*. *Nat Rev Microbiol*. 2018;16(3):156-70. Epub 2018/01/23. doi: 10.1038/nrmicro.2017.161. PubMed PMID: 29355852.
292. Thomas D, Tazerouni H, Sundararaj KG, Cooper JC. Therapeutic failure of primaquine and need for new medicines in radical cure of *Plasmodium vivax*. *Acta Trop*. 2016;160:35-8. Epub 2016/04/26. doi: 10.1016/j.actatropica.2016.04.009. PubMed PMID: 27109040.

293. Tsuboi T, Kaslow DC, Gozar MM, Tachibana M, Cao YM, Torii M. Sequence polymorphism in two novel *Plasmodium vivax* ookinete surface proteins, Pvs25 and Pvs28, that are malaria transmission-blocking vaccine candidates. *Mol Med*. 1998;4(12):772-82. Epub 1999/02/17. PubMed PMID: 9990863; PMCID: PMC2230397.
294. Blagborough AM, Musiychuk K, Bi H, Jones RM, Chichester JA, Streatfield S, Sala KA, Zakutansky SE, Upton LM, Sinden RE, Brian I, Biswas S, Sattabonkot J, Yusibov V. Transmission blocking potency and immunogenicity of a plant-produced Pvs25-based subunit vaccine against *Plasmodium vivax*. *Vaccine*. 2016;34(28):3252-9. Epub 2016/05/15. doi: 10.1016/j.vaccine.2016.05.007. PubMed PMID: 27177945; PMCID: PMC4915602.
295. Radtke AJ, Anderson CF, Riteau N, Rausch K, Scaria P, Kelnhofer ER, Howard RF, Sher A, Germain RN, Duffy P. Adjuvant and carrier protein-dependent T-cell priming promotes a robust antibody response against the *Plasmodium falciparum* Pfs25 vaccine candidate. *Sci Rep*. 2017;7:40312. Epub 2017/01/17. doi: 10.1038/srep40312. PubMed PMID: 28091576; PMCID: PMC5238395.
296. Qian F, Wu Y, Muratova O, Zhou H, Dobrescu G, Duggan P, Lynn L, Song G, Zhang Y, Reiter K, MacDonald N, Narum DL, Long CA, Miller LH, Saul A, Mullen GED. Conjugating recombinant proteins to *Pseudomonas aeruginosa* ExoProtein A: A strategy for enhancing immunogenicity of malaria vaccine candidates. *Vaccine*. 2007;25(20):3923-33. doi: DOI: 10.1016/j.vaccine.2007.02.073.
297. Parzych EM, Miura K, Ramanathan A, Long CA, Burns JM, Jr. Evaluation of a *Plasmodium*-Specific Carrier Protein To Enhance Production of Recombinant Pfs25, a Leading Transmission-Blocking Vaccine Candidate. *Infection and immunity*. 2017;86(1):e00486-17. doi: 10.1128/IAI.00486-17. PubMed PMID: 28993460.

298. Van den Eede P, Soto-Calle VE, Delgado C, Gamboa D, Grande T, Rodriguez H, Llanos-Cuentas A, Anné J, D'Alessandro U, Erhart A. Plasmodium vivax Sub-Patent Infections after Radical Treatment Are Common in Peruvian Patients: Results of a 1-Year Prospective Cohort Study. PLOS ONE. 2011;6(1):e16257. doi: 10.1371/journal.pone.0016257.
299. Singh S, Pandey K, Chattopadhyay R, Yazdani SS, Lynn A, Bharadwaj A, Ranjan A, Chitnis C. Biochemical, Biophysical, and Functional Characterization of Bacterially Expressed and Refolded Receptor Binding Domain of Plasmodium vivax Duffy-binding Protein. Journal of Biological Chemistry. 2001;276(20):17111-6. doi: 10.1074/jbc.M101531200.
300. Janse CJ, Mons B, Rouwenhorst RJ, Van der Klooster PF, Overdulve JP, Van der Kaay HJ. In vitro formation of ookinetes and functional maturity of Plasmodium berghei gametocytes. Parasitology. 1985;91 (Pt 1):19-29. PubMed PMID: 2863802.
301. Arevalo-Herrera M, Solarte Y, Zamora F, Mendez F, Yasnot MF, Rocha L, Long C, Miller LH, Herrera S. Plasmodium vivax: transmission-blocking immunity in a malaria-endemic area of Colombia. Am J Trop Med Hyg. 2005;73(5 Suppl):38-43. PubMed PMID: 16291765.
302. Arevalo-Herrera M, Vallejo AF, Rubiano K, Solarte Y, Marin C, Castellanos A, Cespedes N, Herrera S. Recombinant Pvs48/45 antigen expressed in E. coli generates antibodies that block malaria transmission in Anopheles albimanus mosquitoes. PLoS One. 2015;10(3):e0119335. Epub 2015/03/17. doi: 10.1371/journal.pone.0119335. PubMed PMID: 25775466; PMCID: PMC4361554.
303. Vallejo AF, Rubiano K, Amado A, Krystosik AR, Herrera S, Arevalo-Herrera M. Optimization of a Membrane Feeding Assay for Plasmodium vivax Infection in Anopheles albimanus. PLoS Negl Trop Dis. 2016;10(6):e0004807. Epub 2016/06/30. doi: 10.1371/journal.pntd.0004807. PubMed PMID: 27355210; PMCID: PMC4927173.

304. Fonseca JA, McCaffery JN, Caceres J, Kashentseva E, Singh B, Dmitriev IP, Curiel DT, Moreno A. Inclusion of the murine IgGkappa signal peptide increases the cellular immunogenicity of a simian adenoviral vectored Plasmodium vivax multistage vaccine. *Vaccine*. 2018;36(20):2799-808. Epub 2018/04/17. doi: 10.1016/j.vaccine.2018.03.091. PubMed PMID: 29657070.
305. Hisaeda H, Collins WE, Saul A, Stowers AW. Antibodies to Plasmodium vivax transmission-blocking vaccine candidate antigens Pvs25 and Pvs28 do not show synergism. *Vaccine*. 2001;20(5):763-70. doi: [https://doi.org/10.1016/S0264-410X\(01\)00402-9](https://doi.org/10.1016/S0264-410X(01)00402-9).
306. Saxena AK, Singh K, Su HP, Klein MM, Stowers AW, Saul AJ, Long CA, Garboczi DN. The essential mosquito-stage P25 and P28 proteins from Plasmodium form tile-like triangular prisms. *Nat Struct Mol Biol*. 2006;13(1):90-1. Epub 2005/12/06. doi: nsmb1024 [pii] 10.1038/nsmb1024. PubMed PMID: 16327807.
307. Ramjane S, Robertson JS, Franke-Fayard B, Sinha R, Waters AP, Janse CJ, Wu Y, Blagborough AM, Saul A, Sinden RE. The use of transgenic Plasmodium berghei expressing the Plasmodium vivax antigen P25 to determine the transmission-blocking activity of sera from malaria vaccine trials. *Vaccine*. 2007;25(5):886-94. Epub 2006/10/20. doi: S0264-410X(06)01014-0 [pii] 10.1016/j.vaccine.2006.09.035. PubMed PMID: 17049690.
308. Nunes JK, Woods C, Carter T, Raphael T, Morin MJ, Diallo D, Leboulleux D, Jain S, Loucq C, Kaslow DC, Birkett AJ. Development of a transmission-blocking malaria vaccine: progress, challenges, and the path forward. *Vaccine*. 2014;32(43):5531-9. Epub 2014/08/01. doi: 10.1016/j.vaccine.2014.07.030. PubMed PMID: 25077422.

309. Aucouturier J, Dupuis L, Deville S, Ascarateil S, Ganne V. Montanide ISA 720 and 51: a new generation of water in oil emulsions as adjuvants for human vaccines. *Expert Review of Vaccines*. 2002;1(1):111-8. doi: 10.1586/14760584.1.1.111.
310. Caballero I, Aira LE, Lavastida A, Popa X, Rivero J, González J, Mesa M, González N, Coba K, Lorenzo-Luaces P, Wilkinson B, Santiesteban Y, Santiesteban Y, Troche M, Suarez E, Crombet T, Sánchez B, Casacó A, Macías A, Mazorra Z. Safety and Immunogenicity of a Human Epidermal Growth Factor Receptor 1 (HER1)-Based Vaccine in Prostate Castration-Resistant Carcinoma Patients: A Dose-Escalation Phase I Study Trial. *Frontiers in Pharmacology*. 2017;8(263). doi: 10.3389/fphar.2017.00263.
311. Saavedra D, Crombet T. CIMAvax-EGF: A New Therapeutic Vaccine for Advanced Non-Small Cell Lung Cancer Patients. *Frontiers in Immunology*. 2017;8(269). doi: 10.3389/fimmu.2017.00269.
312. Baumgaertner P, Costa Nunes C, Cachot A, Maby-El Hajjami H, Cagnon L, Braun M, Derré L, Rivals JP, Rimoldi D, Gnjatich S, Abed Maillard S, Marcos Mondéjar P, Protti MP, Romano E, Michielin O, Romero P, Speiser DE, Jandus C. Vaccination of stage III/IV melanoma patients with long NY-ESO-1 peptide and CpG-B elicits robust CD8(+) and CD4(+) T-cell responses with multiple specificities including a novel DR7-restricted epitope. *Oncoimmunology*. 2016;5(10):e1216290-e. doi: 10.1080/2162402X.2016.1216290. PubMed PMID: 27853637.
313. Riteau N, Radtke AJ, Shenderov K, Mittereder L, Oland SD, Hieny S, Jankovic D, Sher A. Water-in-Oil-Only Adjuvants Selectively Promote T Follicular Helper Cell Polarization through a Type I IFN and IL-6-Dependent Pathway. *The Journal of Immunology*. 2016;1600883. doi: 10.4049/jimmunol.1600883.

314. Patra KP, Li F, Carter D, Gregory JA, Baga S, Reed SG, Mayfield SP, Vinetz JM. Alga-produced malaria transmission-blocking vaccine candidate Pfs25 formulated with a human use-compatible potent adjuvant induces high-affinity antibodies that block *Plasmodium falciparum* infection of mosquitoes. *Infect Immun*. 2015;83(5):1799-808. Epub 2015/02/19. doi: 10.1128/IAI.02980-14. PubMed PMID: 25690099; PMCID: PMC4399074.
315. Talaat KR, Ellis RD, Hurd J, Hentrich A, Gabriel E, Hynes NA, Rausch KM, Zhu D, Muratova O, Herrera R, Anderson C, Jones D, Aebig J, Brockley S, MacDonald NJ, Wang X, Fay MP, Healy SA, Durbin AP, Narum DL, Wu Y, Duffy PE. Safety and Immunogenicity of Pfs25-EPA/Alhydrogel(R), a Transmission Blocking Vaccine against *Plasmodium falciparum*: An Open Label Study in Malaria Naive Adults. *PLoS One*. 2016;11(10):e0163144. Epub 2016/10/18. doi: 10.1371/journal.pone.0163144. PubMed PMID: 27749907; PMCID: PMC5066979.
316. Mlambo G, Maciel J, Kumar N. Murine model for assessment of *Plasmodium falciparum* transmission-blocking vaccine using transgenic *Plasmodium berghei* parasites expressing the target antigen Pfs25. *Infect Immun*. 2008;76(5):2018-24. doi: 10.1128/IAI.01409-07. PubMed PMID: 18316385; PMCID: 2346707.
317. Bompard A, Da DF, Yerbanga RS, Biswas S, Kapulu M, Bousema T, Lefevre T, Cohuet A, Churcher TS. Evaluation of two lead malaria transmission blocking vaccine candidate antibodies in natural parasite-vector combinations. *Sci Rep*. 2017;7(1):6766. Epub 2017/07/30. doi: 10.1038/s41598-017-06130-1. PubMed PMID: 28754921; PMCID: PMC5533793.
318. Rappuoli R. Glycoconjugate vaccines: Principles and mechanisms. *Science Translational Medicine*. 2018;10(456):eaat4615. doi: 10.1126/scitranslmed.aat4615.

319. Sagara I, Healy SA, Assadou MH, Gabriel EE, Kone M, Sissoko K, Tembine I, Guindo MA, Doucoure MB, Niaré K, Dolo A, Rausch KM, Narum DL, Jones DL, MacDonald NJ, Zhu D, Mohan R, Muratova O, Baber I, Coulibaly MB, Fay MP, Anderson C, Wu Y, Traore SF, Doumbo OK, Duffy PE. Safety and immunogenicity of Pfs25H-EPA/Alhydrogel, a transmission-blocking vaccine against *Plasmodium falciparum*: a randomised, double-blind, comparator-controlled, dose-escalation study in healthy Malian adults. *The Lancet Infectious Diseases*. 2018;18(9):969-82. doi: [https://doi.org/10.1016/S1473-3099\(18\)30344-X](https://doi.org/10.1016/S1473-3099(18)30344-X).
320. Moorthy VS, Newman RD, Okwo-Bele JM. Malaria vaccine technology roadmap. *Lancet*. 2013;382(9906):1700-1. Epub 2013/11/19. doi: 10.1016/S0140-6736(13)62238-2. PubMed PMID: 24239252.
321. Geiger C, Agustar HK, Compaoré G, Coulibaly B, Sié A, Becher H, Lanzer M, Jänisch T. Declining malaria parasite prevalence and trends of asymptomatic parasitaemia in a seasonal transmission setting in north-western Burkina Faso between 2000 and 2009–2012. *Malaria Journal*. 2013;12(1):27. doi: 10.1186/1475-2875-12-27.
322. Harris I, Sharrock WW, Bain LM, Gray K-A, Bobogare A, Boaz L, Lilley K, Krause D, Vallely A, Johnson M-L, Gatton ML, Shanks GD, Cheng Q. A large proportion of asymptomatic *Plasmodium* infections with low and sub-microscopic parasite densities in the low transmission setting of Temotu Province, Solomon Islands: challenges for malaria diagnostics in an elimination setting. *Malaria Journal*. 2010;9(1):254. doi: 10.1186/1475-2875-9-254.
323. Lindblade KA, Steinhardt L, Samuels A, Kachur SP, Slutsker L. The silent threat: asymptomatic parasitemia and malaria transmission. *Expert Review of Anti-infective Therapy*. 2013;11(6):623-39. doi: 10.1586/eri.13.45.

324. Niang M, Thiam LG, Sane R, Diagne N, Talla C, Doucoure S, Faye J, Diop F, Badiane A, Diouf B, Camara D, Diene-Sarr F, Sokhna C, Richard V, Toure-Balde A. Substantial asymptomatic submicroscopic Plasmodium carriage during dry season in low transmission areas in Senegal: Implications for malaria control and elimination. PLOS ONE. 2017;12(8):e0182189. doi: 10.1371/journal.pone.0182189.
325. Okell LC, Ghani AC, Lyons E, Drakeley CJ. Submicroscopic Infection in *Plasmodium falciparum* Endemic Populations: A Systematic Review and Meta-Analysis. The Journal of Infectious Diseases. 2009;200(10):1509-17.
326. Epelboin L, Boullé C, Ouar-Epelboin S, Hanf M, Dussart P, Djossou F, Nacher M, Carme B. Discriminating Malaria from Dengue Fever in Endemic Areas: Clinical and Biological Criteria, Prognostic Score and Utility of the C-Reactive Protein: A Retrospective Matched-Pair Study in French Guiana. PLOS Neglected Tropical Diseases. 2013;7(9):e2420. doi: 10.1371/journal.pntd.0002420.
327. Sun J-L, Zhou S, Geng Q-B, Zhang Q, Zhang Z-K, Zheng C-J, Hu W-B, Clements ACA, Lai S-J, Li Z-J. Comparative evaluation of the diagnosis, reporting and investigation of malaria cases in China, 2005–2014: transition from control to elimination for the national malaria programme. Infectious Diseases of Poverty. 2016;5(1):65. doi: 10.1186/s40249-016-0163-4.
328. Sagara I, Sangare D, Dolo G, Guindo A, Sissoko M, Sogoba M, Niamebele MB, Yalcoue D, Kaslow DC, Dicko A, Klion AD, Diallo D, Miller LH, Toure Y, Doumbo O. A high malaria reinfection rate in children and young adults living under a low entomological inoculation rate in a periurban area of Bamako, Mali. Am J Trop Med Hyg. 2002;66(3):310-3. Epub 2002/07/26. PubMed PMID: 12139226.

329. Smith T, Killeen G, Lengeler C, Tanner M. Relationships between the outcome of *Plasmodium falciparum* infection and the intensity of transmission in Africa. *Am J Trop Med Hyg.* 2004;71(2 Suppl):80-6. Epub 2004/08/28. PubMed PMID: 15331822.
330. Abba K, Kirkham AJ, Olliaro PL, Deeks JJ, Donegan S, Garner P, Takwoingi Y. Rapid diagnostic tests for diagnosing uncomplicated non-falciparum or *Plasmodium vivax* malaria in endemic countries. *Cochrane Database Syst Rev.* 2014(12):CD011431. Epub 2014/12/19. doi: 10.1002/14651858.CD011431. PubMed PMID: 25519857; PMCID: PMC4453861.
331. Mueller I, Zimmerman PA, Reeder JC. *Plasmodium malariae* and *Plasmodium ovale*--the "bashful" malaria parasites. *Trends Parasitol.* 2007;23(6):278-83. Epub 2007/04/27. doi: 10.1016/j.pt.2007.04.009. PubMed PMID: 17459775; PMCID: PMC3728836.
332. Yman V, White MT, Rono J, Arcà B, Osier FH, Troye-Blomberg M, Boström S, Ronca R, Rooth I, Färnert A. Antibody acquisition models: A new tool for serological surveillance of malaria transmission intensity. *Scientific Reports.* 2016;6:19472. doi: 10.1038/srep19472
<https://www.nature.com/articles/srep19472#supplementary-information>.
333. Simmons RA, Mboera L, Miranda ML, Morris A, Stresman G, Turner EL, Kramer R, Drakeley C, O'Meara WP. A longitudinal cohort study of malaria exposure and changing serostatus in a malaria endemic area of rural Tanzania. *Malaria Journal.* 2017;16(1):309. doi: 10.1186/s12936-017-1945-2.
334. Corran PH, Cook J, Lynch C, Leendertse H, Manjurano A, Griffin J, Cox J, Abeku T, Bousema T, Ghani AC, Drakeley C, Riley E. Dried blood spots as a source of anti-malarial antibodies for epidemiological studies. *Malar J.* 2008;7:195. Epub 2008/10/02. doi: 10.1186/1475-2875-7-195. PubMed PMID: 18826573; PMCID: PMC2567984.

335. Drakeley CJ, Corran PH, Coleman PG, Tongren JE, McDonald SLR, Carneiro I, Malima R, Lusingu J, Manjurano A, Nkya WMM, Lemnge MM, Cox J, Reyburn H, Riley EM. Estimating medium- and long-term trends in malaria transmission by using serological markers of malaria exposure. *Proceedings of the National Academy of Sciences of the United States of America*. 2005;102(14):5108. doi: 10.1073/pnas.0408725102.
336. Priest JW, Plucinski MM, Huber CS, Rogier E, Mao B, Gregory CJ, Candrinho B, Colborn J, Barnwell JW. Specificity of the IgG antibody response to *Plasmodium falciparum*, *Plasmodium vivax*, *Plasmodium malariae*, and *Plasmodium ovale* MSP119 subunit proteins in multiplexed serologic assays. *Malaria Journal*. 2018;17(1):417. doi: 10.1186/s12936-018-2566-0.
337. Yao M-X, Sun X-D, Gao Y-H, Cheng Z-B, Deng W-W, Zhang J-J, Wang H. Multi-epitope chimeric antigen used as a serological marker to estimate *Plasmodium falciparum* transmission intensity in the border area of China-Myanmar. *Infectious Diseases of Poverty*. 2016;5(1):98. doi: 10.1186/s40249-016-0194-x.
338. Cai Q, Peng G, Bu L, Lin Y, Zhang L, Lustigmen S, Wang H. Immunogenicity and in vitro protective efficacy of a polyepitope *Plasmodium falciparum* candidate vaccine constructed by epitope shuffling. *Vaccine*. 2007;25(28):5155-65. doi: <https://doi.org/10.1016/j.vaccine.2007.04.085>.
339. Plucinski MM, Herman C, Jones S, Dimbu R, Fortes F, Ljolje D, Lucchi N, Murphy SC, Smith NT, Cruz KR, Seilie AM, Halsey ES, Udhayakumar V, Aidoo M, Rogier E. Screening for Pfhrrp2/3-Deleted *Plasmodium falciparum*, Non-falciparum, and Low-Density Malaria Infections by a Multiplex Antigen Assay. *J Infect Dis*. 2019;219(3):437-47. Epub 2018/09/12. doi: 10.1093/infdis/jiy525. PubMed PMID: 30202972; PMCID: PMC6325347.

340. Plucinski MM, Candrinho B, Chambe G, Muchanga J, Muguande O, Matsinhe G, Mathe G, Rogier E, Doyle T, Zulliger R, Colborn J, Saifodine A, Lammie P, Priest JW. Multiplex serology for impact evaluation of bed net distribution on burden of lymphatic filariasis and four species of human malaria in northern Mozambique. *PLoS Negl Trop Dis*. 2018;12(2):e0006278. Epub 2018/02/15. doi: 10.1371/journal.pntd.0006278. PubMed PMID: 29444078; PMCID: PMC5854460.
341. Lucchi NW, Ndiaye D, Britton S, Udhayakumar V. Expanding the malaria molecular diagnostic options: opportunities and challenges for loop-mediated isothermal amplification tests for malaria control and elimination. *Expert Rev Mol Diagn*. 2018;18(2):195-203. Epub 2018/01/23. doi: 10.1080/14737159.2018.1431529. PubMed PMID: 29353522.
342. Britton S, Cheng Q, McCarthy JS. Novel molecular diagnostic tools for malaria elimination: a review of options from the point of view of high-throughput and applicability in resource limited settings. *Malar J*. 2016;15:88. Epub 2016/02/18. doi: 10.1186/s12936-016-1158-0. PubMed PMID: 26879936; PMCID: PMC4754967.
343. Snow RW, Guerra CA, Noor AM, Myint HY, Hay SI. The global distribution of clinical episodes of *Plasmodium falciparum* malaria. *Nature*. 2005;434(7030):214-7. doi: 10.1038/nature03342.
344. Alaro JR, Partridge A, Miura K, Diouf A, Lopez AM, Angov E, Long CA, Burns JM, Jr. A chimeric *Plasmodium falciparum* merozoite surface protein vaccine induces high titers of parasite growth inhibitory antibodies. *Infect Immun*. 2013;81(10):3843-54. Epub 2013/07/31. doi: 10.1128/IAI.00522-13. PubMed PMID: 23897613; PMCID: PMC3811772.
345. Burns JM, Jr., Miura K, Sullivan J, Long CA, Barnwell JW. Immunogenicity of a chimeric *Plasmodium falciparum* merozoite surface protein vaccine in *Aotus* monkeys. *Malar J*.

2016;15:159. Epub 2016/03/16. doi: 10.1186/s12936-016-1226-5. PubMed PMID: 26975721; PMCID: PMC4791798.

346. Egan AF, Chappel JA, Burghaus PA, Morris JS, McBride JS, Holder AA, Kaslow DC, Riley EM. Serum antibodies from malaria-exposed people recognize conserved epitopes formed by the two epidermal growth factor motifs of MSP1(19), the carboxy-terminal fragment of the major merozoite surface protein of *Plasmodium falciparum*. *Infect Immun*. 1995;63(2):456-66. Epub 1995/02/01. PubMed PMID: 7822010; PMCID: PMC173017.

347. Pizarro JC, Chitarra V, Verger D, Holm I, Petres S, Darteville S, Nato F, Longacre S, Bentley GA. Crystal structure of a Fab complex formed with PfMSP1-19, the C-terminal fragment of merozoite surface protein 1 from *Plasmodium falciparum*: a malaria vaccine candidate. *J Mol Biol*. 2003;328(5):1091-103. Epub 2003/05/06. doi: 10.1016/s0022-2836(03)00376-0. PubMed PMID: 12729744.

348. Carter KH, Singh P, Mujica OJ, Escalada RP, Ade MP, Castellanos LG, Espinal MA. Malaria in the Americas: trends from 1959 to 2011. *Am J Trop Med Hyg*. 2015;92(2):302-16. Epub 2014/12/31. doi: 10.4269/ajtmh.14-0368. PubMed PMID: 25548378; PMCID: PMC4347333.

349. van den Hoogen LL, Walk J, Oulton T, Reuling IJ, Reiling L, Beeson JG, Coppel RL, Singh SK, Draper SJ, Bousema T, Drakeley C, Sauerwein R, Tetteh KKA. Antibody Responses to Antigenic Targets of Recent Exposure Are Associated With Low-Density Parasitemia in Controlled Human *Plasmodium falciparum* Infections. *Front Microbiol*. 2018;9:3300. Epub 2019/02/01. doi: 10.3389/fmicb.2018.03300. PubMed PMID: 30700984; PMCID: PMC6343524.

350. Helb DA, Tetteh KK, Felgner PL, Skinner J, Hubbard A, Arinaitwe E, Mayanja-Kizza H, Ssewanyana I, Kanya MR, Beeson JG, Tappero J, Smith DL, Crompton PD, Rosenthal PJ,

Dorsey G, Drakeley CJ, Greenhouse B. Novel serologic biomarkers provide accurate estimates of recent *Plasmodium falciparum* exposure for individuals and communities. *Proc Natl Acad Sci U S A*. 2015;112(32):E4438-47. Epub 2015/07/29. doi: 10.1073/pnas.1501705112. PubMed PMID: 26216993; PMCID: PMC4538641.

351. McCaffery JN, Fonseca JA, Singh B, Cabrera-Mora M, Bohannon C, Jacob J, Arévalo-Herrera M, Moreno A. A Multi-Stage *Plasmodium vivax* Malaria Vaccine Candidate Able to Induce Long-Lived Antibody Responses Against Blood Stage Parasites and Robust Transmission-Blocking Activity. *Frontiers in Cellular and Infection Microbiology*. 2019;9(135). doi: 10.3389/fcimb.2019.00135.

352. Venkatraman N, Anagnostou N, Bliss C, Bowyer G, Wright D, Lövgren-Bengtsson K, Roberts R, Poulton I, Lawrie A, Ewer K, V. S. Hill A. Safety and immunogenicity of heterologous prime-boost immunization with viral-vectored malaria vaccines adjuvanted with Matrix-M™. *Vaccine*. 2017;35(45):6208-17. doi: <https://doi.org/10.1016/j.vaccine.2017.09.028>.

353. Rampling T, Ewer KJ, Bowyer G, Edwards NJ, Wright D, Sridhar S, Payne R, Powlson J, Bliss C, Venkatraman N, Poulton ID, de Graaf H, Gbesemete D, Grobbelaar A, Davies H, Roberts R, Angus B, Ivinson K, Weltzin R, Rajkumar B-Y, Wille-Reece U, Lee C, Ockenhouse C, Sinden RE, Gerry SC, Lawrie AM, Vekemans J, Morelle D, Lievens M, Ballou RW, Lewis DJM, Cooke GS, Faust SN, Gilbert S, Hill AVS. Safety and efficacy of novel malaria vaccine regimens of RTS,S/AS01B alone, or with concomitant ChAd63-MVA-vectored vaccines expressing ME-TRAP. *NPJ Vaccines*. 2018;3:49-. doi: 10.1038/s41541-018-0084-2. PubMed PMID: 30323956.

354. Payne RO, Silk SE, Elias SC, Miura K, Diouf A, Galaway F, de Graaf H, Brendish NJ, Poulton ID, Griffiths OJ, Edwards NJ, Jin J, Labbé GM, Alanine DG, Siani L, Di Marco S,

Roberts R, Green N, Berrie E, Ishizuka AS, Nielsen CM, Bardelli M, Partey FD, Ofori MF, Barfod L, Wambua J, Murungi LM, Osier FH, Biswas S, McCarthy JS, Minassian AM, Ashfield R, Viebig NK, Nugent FL, Douglas AD, Vekemans J, Wright GJ, Faust SN, Hill AV, Long CA, Lawrie AM, Draper SJ. Human vaccination against RH5 induces neutralizing antimalarial antibodies that inhibit RH5 invasion complex interactions. *JCI Insight*. 2017;2(21):e96381. doi: 10.1172/jci.insight.96381. PubMed PMID: 29093263.

355. de Camargo TM, de Freitas EO, Gimenez AM, Lima LC, de Almeida Caramico K, Franoso KS, Bruna-Romero O, Andolina C, Nosten F, R nia L, Ertl HCJ, Nussenzweig RS, Nussenzweig V, Rodrigues MM, Reyes-Sandoval A, Soares IS. Prime-boost vaccination with recombinant protein and adenovirus-vector expressing *Plasmodium vivax* circumsporozoite protein (CSP) partially protects mice against Pb/Pv sporozoite challenge. *Scientific Reports*. 2018;8(1):1118. doi: 10.1038/s41598-017-19063-6.

356. Karyolaimos A, Ampah-Korsah H, Hillenaar T, Mestre Borr s A, Dolata KM, Sievers S, Riedel K, Daniels R, de Gier J-W. Enhancing Recombinant Protein Yields in the *E. coli* Periplasm by Combining Signal Peptide and Production Rate Screening. *Frontiers in Microbiology*. 2019;10(1511). doi: 10.3389/fmicb.2019.01511.

357. Fougereux C, Turner L, Bojesen AM, Lavstsen T, Holst PJ. Modified MHC Class II-Associated Invariant Chain Induces Increased Antibody Responses against *Plasmodium falciparum* Antigen after Adenoviral Vaccination. *The Journal of Immunology*. 2019;202(8):2320. doi: 10.4049/jimmunol.1801210.

358. Scaria PV, Rowe CG, Chen BB, Muratova OV, Fischer ER, Barnafo EK, Anderson CF, Zaidi IU, Lambert LE, Lucas BJ, Nahas DD, Narum DL, Duffy PE. Outer membrane protein

complex as a carrier for malaria transmission blocking antigen Pfs230. *NPJ Vaccines*. 2019;4:24-. doi: 10.1038/s41541-019-0121-9. PubMed PMID: 31312527.

359. Acquah FK, Adjah J, Williamson KC, Amoah LE. Transmission-Blocking Vaccines: Old Friends and New Prospects. *Infection and Immunity*. 2019;87(6):e00775-18. doi: 10.1128/IAI.00775-18.

360. Smith RC, Vega-Rodríguez J, Jacobs-Lorena M. The Plasmodium bottleneck: malaria parasite losses in the mosquito vector. *Memórias do Instituto Oswaldo Cruz*. 2014;109:644-61.

361. Coelho CH, Rappuoli R, Hotez PJ, Duffy PE. Transmission-Blocking Vaccines for Malaria: Time to Talk about Vaccine Introduction. *Trends in Parasitology*. 2019;35(7):483-6. doi: 10.1016/j.pt.2019.04.008.

362. White SE, Harvey SA, Meza G, Llanos A, Guzman M, Gamboa D, Vinetz JM. Acceptability of a herd immunity-focused, transmission-blocking malaria vaccine in malaria-endemic communities in the Peruvian Amazon: an exploratory study. *Malaria journal*. 2018;17(1):179-. doi: 10.1186/s12936-018-2328-z. PubMed PMID: 29703192.

363. Miguel RB, Albuquerque HG, Sanchez MCA, Coura JR, Santos SdS, Silva Sd, Moreira CJdC, Suárez-Mutis MC. Asymptomatic Plasmodium infection in a residual malaria transmission area in the Atlantic Forest region: Implications for elimination. *Revista da Sociedade Brasileira de Medicina Tropical*. 2019;52.

364. Surendra H, Wijayanti MA, Murhandarwati EH, Irnawati, Yuniarti T, Mardiaty, Herdiana, Sumiwi ME, Hawley WA, Lobo NF, Cook J, Drakeley C, Supargiyono. Analysis of serological data to investigate heterogeneity of malaria transmission: a community-based cross-sectional study in an area conducting elimination in Indonesia. *Malaria Journal*. 2019;18(1):227. doi: 10.1186/s12936-019-2866-z.

365. Keffale M, Shumie G, Behaksra SW, Chali W, Hoogen LLvd, Hailemeskel E, Mekonnen D, Chanyalew M, Damte D, Fanta T, Ashine T, Chali S, Tetteh KKA, Birhanu DD, Balcha TT, Aseffa A, Drakeley C, Tessema TS, Adamu H, Bousema T, Gadisa E, Tadesse FG. Serological evidence for a decline in malaria transmission following major scale-up of control efforts in a setting selected for *Plasmodium vivax* and *Plasmodium falciparum* malaria elimination in Babile district, Oromia, Ethiopia. *Trans R Soc Trop Med Hyg.* 2019;113(6):305-11. doi: 10.1093/trstmh/trz005. PubMed PMID: 30927007.
366. Kobayashi T, Jain A, Liang L, Obiero JM, Hamapumbu H, Stevenson JC, Thuma PE, Lupiya J, Chaponda M, Mulenga M, Mamini E, Mharakurwa S, Gwanzura L, Munyati S, Mutambu S, Felgner P, Davies DH, Moss WJ. Distinct Antibody Signatures Associated with Different Malaria Transmission Intensities in Zambia and Zimbabwe. *mSphere.* 2019;4(2):e00061-19. doi: 10.1128/mSphereDirect.00061-19. PubMed PMID: 30918058.
367. Achan J, Reuling I, Yap XZ, Dabira E, Ahmad A, Cox M, Nwakanma D, Tetteh K, Wu L, Bastiaens GJH, Abebe Y, Manoj A, Kaur H, Miura K, Long C, Billingsley PF, Sim BKL, Hoffman SL, Drakeley C, Bousema T, D'Alessandro U. Serologic markers of previous malaria exposure and functional antibodies inhibiting parasite growth are associated with parasite kinetics following a *Plasmodium falciparum* controlled human infection. *Clinical Infectious Diseases.* 2019. doi: 10.1093/cid/ciz740.
368. Tiono AB, Nébié I, Anagnostou N, Coulibaly AS, Bowyer G, Lam E, Bougouma EC, Ouedraogo A, Yaro JBB, Barry A, Roberts R, Rampling T, Bliss C, Hodgson S, Lawrie A, Ouedraogo A, Imoukhuede EB, Ewer KJ, Viebig NK, Diarra A, Leroy O, Bejon P, Hill AVS, Sirima SB. First field efficacy trial of the ChAd63 MVA ME-TRAP vectored malaria vaccine

candidate in 5-17 months old infants and children. PLOS ONE. 2018;13(12):e0208328. doi:
10.1371/journal.pone.0208328.